Title

Production of Bioplastic Polyhydroxyalkanoates (PHA) Utilizing Cheese Processing Byproducts by Halophilic Microbes

Author

Hobby, Alexander Michael

Publication Date

2023

Peer reviewed|Thesis/dissertation

Production of Bioplastic Polyhydroxyalkanoates (PHA) Utilizing Cheese Processing Byproducts by Halophilic Microbes

By

ALEXANDER HOBBY

DISSERTATION

Submitted in partial satisfaction of the requirements for the degree of

DOCTOR OF PHILOSOPHY

in

Biological Systems Engineering

in the

OFFICE OF GRADUATE STUDIES

of the

UNIVERSITY OF CALIFORNIA

DAVIS

Approved:

_____

Ruihong Zhang, Chair

_____

Zhiliang Fan

_____

Md Shamim Ahamed

Committee in Charge

2023

Abstract

Plastic products have become indispensable in various industrial sectors and everyday life worldwide. However, conventional plastics present significant sustainability challenges due to their reliance on unsustainable petroleum sources, contribution to greenhouse gas emissions, and their resistance to biodegradation, which leads to environmental waste accumulation. In response to these issues and the need to decrease carbon emissions, there has been a growing interest in bioplastics. One promising family of bioplastics is polyhydroxyalkanoate (PHA), a group of natural polyesters that can serve as a sustainable alternative to traditional plastics in numerous applications. PHA stands out among bioplastics for several reasons, including production from organic waste substrates. The polyester can be produced from various organic waste materials, reducing the demand for costly virgin resources and providing an environmentally friendly solution for waste management. PHA additionally possesses high biodegradability compared to other bioplastics on the market, allowing it to break down more efficiently in the environment and minimize long-term pollution. PHA can replace several families of petroleum-based plastics, making it a versatile option for a wide range of products and applications. However, despite these promising attributes, the high production cost of PHA remains a significant barrier to its widespread adoption. The expensive carbon sources utilized in microbial fermentation are the primary factor contributing to this cost, limiting the growth of the PHA market. There is a critical need to develop an efficient bioprocessing system that can produce high-quality PHA at a significantly lower cost. To address this imperative, the primary goal of this study was to create an integrated PHA production system that utilizes inexpensive cheese byproducts feedstock, making PHA production more economically viable while maximizing resource efficiency and minimizing waste.

Whey and whey byproducts generated from cheese production offer a promising source for bioplastic production. Researchers estimate that approximately half of this whey produced from cheese

making is processed into useful forms for human or animal consumption, with the rest ending up as waste material, contributing to high carbon emissions. While some cheese manufacturers can convert whey byproducts into valuable food ingredients, like whey protein concentrates and lactose powder, additional byproducts continue to be generated. Whey permeate is produced after concentrating the liquid whey with membrane filtration, containing most of the lactose and minerals. The whey permeate can be further processed into lactose powder with evaporation and drying systems creating byproduct delactosed permeate (DLP). Crystallization limitations prevent the complete recovery of lactose for food products. As a result, approximately one-third of the lactose remains as delactosed permeate (DLP), which is either sold as low-value animal feed or disposed of as waste. DLP is the main cheese byproduct without a widespread commercial application, which presents an opportunity for biomaterial production. Therefore, this study aimed to convert low-value cheese byproducts DLP into high-value bioplastic PHA.

The PHA producer *Haloferax mediterranei* (*H. mediterranei*) appears to be a suitable candidate for utilizing cheese byproducts as feedstock. This fit is due to the archaea's unique ability to thrive in extreme halophilic conditions, tolerating salinity levels of up to 20%. The presence of high salt-containing cheese byproducts provides a compatible source of nutrients for *H. mediterranei*, compared to other PHA producers and common contaminant organisms that can become inhibited from such high salt concentrations. The high salt environment removes the need for an expensive sterility unit operation, such as high-temperature exposure or antibiotics, reducing production costs. Moreover, the intracellular PHA extraction from *H. mediterranei* can be achieved through a straightforward process of water addition, causing osmotic shock and cell lysis. High salt-containing cheese byproducts provide Another advantage of *H. mediterranei* is its ability to produce a higher-value PHA polyester, poly(3-hydroxybutyrate-co-3-hydroxyvalerate) (PHBV). This PHA polyester exhibits enhanced properties compared to the more commonly produced polyhydroxybutyrate (PHB). The presence of 3-hydroxyvalerate units in PHBV

enhances its flexibility, making it suitable for various applications, especially in the food industry. The potential applications of PHBV in food packaging, such as films, bags, containers, or cutlery, align with the circular economy principles. By utilizing cheese byproducts and producing high-value PHBV, the cheese industry can take significant steps toward sustainability and waste reduction.

A pretreatment method of the DLP was developed and optimized utilizing centrifugation and enzymatic lactase hydrolysis. The centrifugation pretreatment was shown to increase lactase hydrolysis efficiency and *H. mediterranei* cell growth. The optimal lactase enzyme conditions with the centrifuged DLP to achieve a lactose hydrolysis efficiency of 92.5% were determined to be a loading of 0.025 g lactase/g lactose and shaking incubation at 40 ℃ for 12 hours. The effects of hydrolyzed DLP on *H. mediterranei* cell growth and PHA production were studied. The hydrolyzed DLP achieved high PHA yields of 0.33 ± 0.01 g VS/g total sugar that surpassed yields obtained with glucose feedstock. However, lower galactose consumption by *H. mediterranei* was observed to limit PHA production with this substrate. After demonstrating that hydrolyzed DLP could result in effective *H. mediterranei* growth and PHA production, nitrogen source optimization was conducted to devise a cost-effective feedstock for *H. mediterranei* growth on hydrolyzed DLP substrate. Three nitrogen sources were tested at equivalent C/N ratios of 8, yeast extract, ammonium chloride, and an equal nitrogen loading of yeast extract and ammonium chloride. Supplementation of ammonium chloride resulted in the highest PHA yield, reaching 0.34 ± 0.03 g VS/g total sugar. Furthermore, the media supplemented with ammonium chloride nitrogen source gave the lowest PHA production of the feedstocks investigated. These cost savings make ammonium chloride an economically favorable choice for PHA production compared to other nitrogen sources containing yeast extract. The results of these studies demonstrated that cheese byproduct DLP could be used as an effective feedstock for PHA production, helping to create a circular economy for the cheese industry.

The hydrolyzed DLP supplemented with ammonium chloride nitrogen source was studied as feedstock for *H. mediterranei* cultivation with three feeding strategies; batch, fed-batch, and continuous feeding. With batch feeding, four different hydrolyzed DLP and whey permeate loadings of 10, 20, 30, and 40 g total sugar/l were studied. The loading of 10 g total sugar/l was determined to be the maximum loading of hydrolyzed DLP, as higher loadings resulted in considerable inhibition. However, hydrolyzed whey permeate resulted in a higher maximum loading of 30 g total sugar/l. This difference in maximum loading between the two hydrolyzed cheese byproduct feedstocks indicated that inhibitory constituents were present in DLP that were not in whey permeate. High-heat reaction products that form during whey permeate processing to lactose powder and DLP, such as Maillard products that are inhibitory to other microorganisms, could be the source of increased inhibition with DLP. The PHA yields of the hydrolyzed DLP and whey permeate were similar at 0.30 ± 0.03 and 0.27 ± 0.02 g VS/g total sugar, respectively. These yields were on the higher end of those reported for glucose feedstock of 0.07-0.33 g PHA/g sugar, demonstrating that hydrolyzed cheese byproducts are an effective substrate for PHA production. The maximum specific growth rates of *H. mediterranei* growth with hydrolyzed DLP and whey permeate were estimated with batch feeding and found to be similar for the two byproducts. These results can assist in developing large-scale PHA production facilities utilizing the cheese byproduct substrates.

Based on the batch operation findings, a 6 L fed-batch bioreactor with an initial working volume of 3 L was operated to attempt to decrease substrate inhibition with the hydrolyzed DLP. Hydrolyzed DLP and whey permeate feedstocks were fed every four days at a loading of 10 g total sugar/l. A 50% increase in the final PHA concentration of the hydrolyzed DLP was achieved with the fed-batch operation and two feedings than with the single batch loading of 10 g total sugar/l. This increase in PHA production with fed-batch operation was due to the additional loading of 10 g total sugar/l that was able to be fed without inhibition occurring. However, the culture became inhibited and unstable past the third feeding of

hydrolyzed DLP. For the whey permeate, the PHA concentration increased with the first three feedings, and a stable culture was maintained after three additional feedings. These results confirmed that increased inhibition occurs with hydrolyzed DLP compared to hydrolyzed whey permeate feedstock. The results indicated that fed-batch bioreactor operation with hydrolyzed DLP and hydrolyzed whey permeate feedstocks can improve PHA production compared to batch cultivation.

Since fed-batch feeding only increased PHA production with hydrolyzed DLP marginally, a continuous stirred tank reactor (CSTR) with hydrolyzed DLP feedstock was studied to try to reduce substrate inhibition further and increase PHA production. The CSTR was operated at a hydraulic retention time of 10 days with an organic loading rate (OLR) of 2.5 g total sugar/l/day, and a hydraulic retention time of 20 days with various OLRs of 1.25-2 g total sugar/l/day. The 10-day HRT CSTR resulted in a PHA yield of 0.18 g VS/g total sugar, comparable to that achieved with the fed-batch bioreactors. However, the 10-day CSTR became unstable after 22 days of continuous feeding, potentially due to hydrolyzed DLP substrate inhibition. Although the 20-day HRT CSTR was able to maintain a stable culture for 130 days, considerably lower PHA yields were achieved of < 0.10 g VS/g total sugar. Therefore, continuous feeding at the applied HRTs and OLRs was not recommended for PHA production with hydrolyzed DLP.

Lower galactose consumption was observed for the batch and fed-batch studies than for glucose. Therefore, a galactose acclimation study was conducted to determine if growing *H. mediterranei* on successive batches of galactose could increase consumption and PHA production with the sugar. The archaea was cultivated on galactose for five consecutive batches. The final cell dry mass (CDM) concentration of *H. mediterranei* significantly increased with three batches, the specific growth rate with four batches, the final PHA concentration with five batches, and the galactose consumption with three batches (total galactose consumption), demonstrating effective galactose acclimation had occurred. The

research can potentially lead to improved PHA yields with galactose-containing feedstocks such as hydrolyzed cheese byproducts. Overall, the study demonstrated that cheese byproduct delactosed permeate could successfully be utilized as feedstock for PHA bioplastic production with *H. mediterranei*. The results of the study should be used to further scale the proposed process leading to commercialization.

To my wife,

Gabrielle

And my parents,

Dennis and Caroline

Whose love and support made this journey possible.

Acknowledgements

I would like to express my heartfelt gratitude to my major professor, Professor Ruihong Zhang, for her invaluable guidance, support, and mentorship throughout my research pursuit. I would also like to thank Professor Zhiliang Fan and Professor Md Shamim Ahamed for serving on my dissertation committee and for their critical review. I am thankful for Professor Tina Jeoh, Professor Bryan Jenkins, and Professor Thomas Young for serving on my qualifying exam. Thank you, Dr. Hamed El-Mashad, for your careful review and insightful feedback that played a crucial role in enhancing the quality and rigor of this work. I am grateful for Kameron Chun and Victor Duraj for maintaining a safe working environment. A special thank you to Dr. Ke Wang for teaching me about the bioprocess and support in developing my research skills, and to Kelly Graff whose laboratory assistance was vital and for helping me keep high spirits. I am grateful for all my Zhang lab colleagues Allan Chio, Lin Cao, Dr. Yike Chen, Cody Yothers, Emily Sechrist, and Dr. Tyler Barzee. I was able to learn so much from everyone. To the undergraduates that worked in the lab, Rachael Trinh, Melanie Siu, Steven Nguyen, Joud Alamri, Derron Ma, Raymond Doan, and Hayeon Park, thank you for all the help you provided. Thank you, Nicole Lonergan, for helping me to improve my writing and quality of work, and Hector Scott for providing lactase enzyme for the study.

I want to acknowledge the assistance of Dairy Management Inc., the National Dairy Council, and Hilmar Cheese Co. who made this project possible. I am also appreciative of the Jastro-Shields Research Award that helped support the research.

Lastly, thank you to my wife Gabrielle Gunter, without your love and encouragement, none of this would have been possible, and to my parents Dennis Hobby and Caroline Low-Hobby for always believing in me and pushing me to strive for excellence.

Table of Contents

List of Figures

List of Tables

Chapter 1. Introduction

1.1 Global environmental problems of traditional plastics

Plastic products are used worldwide in seemingly limitless applications across industrial sectors and everyday life. Global plastic production is estimated to be 390 million metric tons (MT) per year, of which approximately 50% is for single-use items (European Bioplastics, 2023; Geyer et al., 2017). In 2015, only 20% of plastics were recycled, with 50% ending in landfills (Geyer et al., 2017). Similarly, in 2018, the United States produced nearly 35.6 MT of plastic; roughly only 3.0 MT were recycled, with 5.6 MT combusted with associated greenhouse gas emissions and 27.0 MT landfilled, accounting for 18.5% of all municipal solid wastes landfilled (Geyer et al., 2017; US EPA, 2017). Researchers estimated that between 4.8 to 12.7 MT of plastic enters the ocean each year (Jambeck et al., 2015). Plastic debris accumulates in the ocean, threatens aquatic wildlife and ecosystems, and is a potential risk to human health and food safety (Carbery et al., 2018; Cózar et al., 2014). Plastics can fragment over time resulting in microplastic particles that are difficult to remove from the open ocean and are untraceable back to their source (Dilkes-Hoffman et al., 2018). Due to these waste management issues, there is a need to design plastic materials to decrease the impact of improperly discarded plastics on the marine environment.

Plastics are also a major contributor to greenhouse gases. Researchers estimated that globally plastics emitted 1.7 gigatons (GT) of CO_2-eq in 2015, or 3.8% of all CO_2-eq emissions. It was also projected that if similar plastic growth trends continue by 2050, plastics will emit 6.5 GT of CO_2-eq or 15% of all CO_2-eq emissions worldwide (Zheng & Suh, 2019). Due to the environmental issues associated with traditional plastics, there has been an international trend towards alternative plastics that are bioderived (from sustainable biological sources) and are biodegradable (decompose in a short amount of time by living organisms), rather than plastics that are petroleum based. However, in 2022 bioplastics only represented less than 1% of the total plastics produced, with greater than 99% of plastics derived from unsustainable

petroleum sources. Bioplastic production was 2.22 MT in 2022, and analysts expect the bioplastic market to grow to approximately 6.30 MT by 2027 (European Bioplastics, 2023). Further research is needed to develop more cost-effective production methods and to create the materials at scale (Dietrich et al., 2017; Roland-Holst, 2013).

1.2 Alternative biodegradable bioplastic polyhydroxyalkanoates

1.2.1 Overview and classification

Numerous bioderived and biodegradable alternatives to traditional plastics exist on the market (European Bioplastics, 2023), and considerable research is being conducted globally on this topic (Dietrich et al., 2017; Roland-Holst, 2013). Polyhydroxyalkanoates (PHA) are one of the alternatives (Figure 1.1a). PHA is a bioplastic with properties similar to thermoplastics (Bugnicourt et al., 2014) that can degrade at ambient temperatures in terrestrial and ocean environments in less than six months (Meereboer et al., 2020). PHA can also break down in both aerobic and anaerobic conditions (Hegde et al., 2021). PHA can be produced from renewable resources and are biocompatible (not harmful to living tissue) (Rivera-Briso & Serrano-Aroca, 2018). Over 75 genera of microorganisms can synthesize PHA intracellularly, acting as a stored energy source (Figure 1.1b) (Reddy et al., 2003). Typically, unfavorable growth conditions, e.g., lack of essential nutrients, trigger PHA synthesis and accumulation (Bernard, 2014; Smet, 1983). However, researchers have demonstrated that some PHA producers can accumulate the polymer under normal growth conditions with adequate carbon, nitrogen, and phosphorus concentrations present (Cui, Shi, et al., 2017; Reddy et al., 2003; Wang & Zhang, 2021). Since the PHA family consists of over 150 monomers with variable characteristics, they can be used to create numerous products (Reddy et al., 2003). Poly(3-hydroxybutyrate-co-3-hydroxyvalerate) (PHBV) is one type of PHA (Figure 1.1c). PHBV exhibits desirable thermal and mechanical properties that make it a suitable replacement for high-density polyethylene

(HDPE), low-density polyethylene (LDPE), and polypropylene (PP) (Dietrich et al., 2017; Guo & Crittenden, 2011; Joyce, 2018).

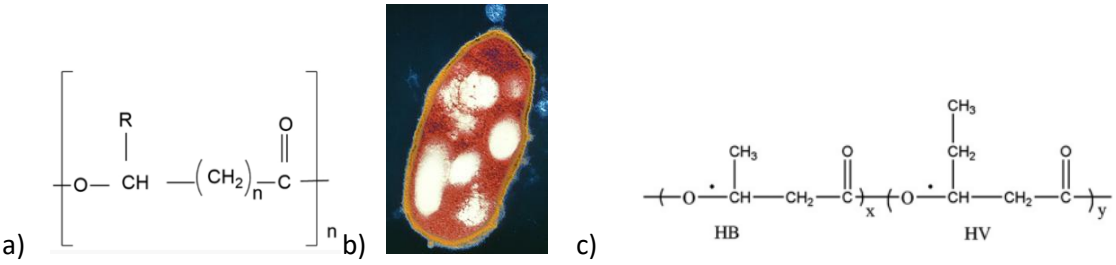

Figure 1.1 a) PHA chemical composition (Mudenur et al., 2019); b) Intracellular PHA granules in white (Naor et al., 2012); c) PHBV chemical structure (Calil et al., 2021).

1.2.2 Market and application

Polyhydroxyalkanoates can be used in a wide range of applications, including plastic bags, packaging film, food containers, disposable cutlery, 3D printing material, and medical sutures (Bugnicourt et al., 2014; Joyce, 2018; Raza et al., 2018). Figure 1.2 displays various PHA products on the market, most for single-use items. Approximately 87 thousand metric tons of PHA are produced annually, or 3.9% of the global bioplastic market (European Bioplastics, 2023). However, PHA is the fastest-growing biodegradable bioplastic due to its unique characteristics, such as excellent biodegradability, application for numerous products, and favorable thermal and mechanical properties (European Bioplastics, 2023; Raza et al., 2018; Reddy et al., 2003). Bioplastic market analysts expect the global PHA production capacity to more than double by 2027 and its global bioplastic market share to expand to 8.9% (Figure 1.3) (European Bioplastics, 2023). Likewise, analysts valued the 2021 PHA market at $57.8 million and expect the PHA market to increase to $98.5 million by 2026 with a CAGR of 11.8% (Market Data Forecast, 2022). This market growth is related to the increased awareness of sustainability, reducing greenhouse gas emissions, circular economies, regulatory framework, and the biodegradability and wide range of

applications of PHA (Dietrich et al., 2017; Market Data Forecast, 2022; Raza et al., 2018). Table 1.1 shows notable global PHA production companies at the commercial and laboratory scale. It can be observed from the table that there is no dominant manufacturer of PHA leading to market opportunities (Joyce, 2018; Kourmentza et al., 2017; Mango Materials, 2022; Shieber, 2020; TianAn Biopolyme, 2022; Yield10 Bio, 2022).

a)  b) 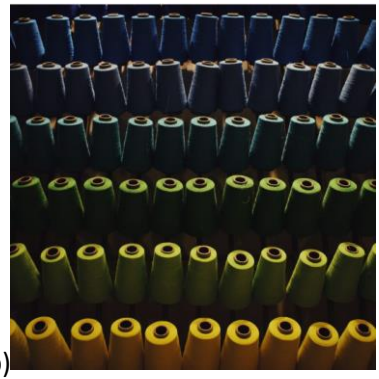 c) 

d)  e) 

Figure 1.2 Various PHA products; top) different types of PHA products created from different processing; a) injection molding; b) fibers; c) films; bottom) single-use products; d) shavers, cups, and cosmetic packaging; e) food service products (Bomgardner, 2012; Joyce, 2018; Mango Materials, 2022).

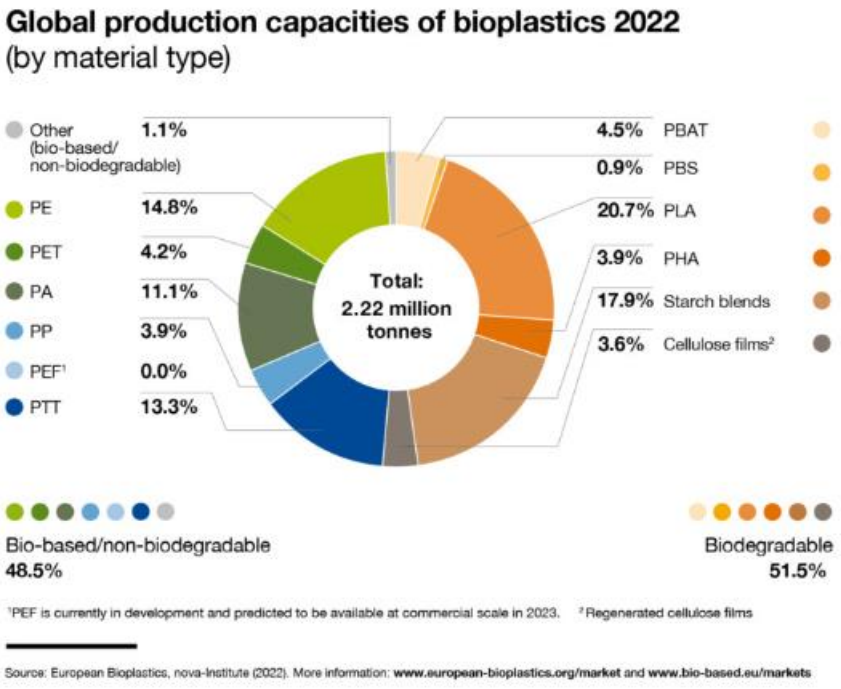

Figure 1.3 Global bioplastic production capacities in 2022 (European Bioplastics, 2023).

Table 1.1 Notable pilot and industrial-scale PHA manufacturers active worldwide (Joyce, 2018; Kourmentza et al., 2017; Mango Materials, 2022; Shieber, 2020; TianAn Biopolyme, 2022; Yield10 Bio, 2022).

Company	**Country**	**Product/Trademark**	**Renewable raw materials**	**Biocatalyst**	**Capacity (metric tons /year)**
Biomatera	Canada	PHA resins (Biomatera)	Sugar (sucrose)	Non-pathogenic, non-transgenic bacteria isolated from soil	-

Biomer	Germany	PHB pellets (Biomer®)	Sugar beets	-	-
Bio-On Srl.	Italy	PHB, PHBV spheres (minerv®-PHA)	-	*Cupriavidus necator*	10,000
BluePHA	China	Customized PHBVHHx, PHV, P3HP3HB, P3HP4HB, P3HP, P4HB synthesis	-	Development of microbial strains via synthetic biology	
Danimer Scientific	USA	MCL-PHA (Nodax® PHA)	Cold-pressed canola oil	-	29,000
Full Cycle Bioplastics	USA	PHBV	Organic food waste	Non-GMO bacterial strain	Research
Genecis Bioindustries Inc	Canada	PHBV	Organic food waste	Bacterial strain	3-4
Kaneka Corporation	Japan	PHB-PHHx (AONILEX®)	Plant oils	-	3,200
Mango Materials	USA	P3HB	Wastewater	Non-GMO methanotrophs	0.5
Newlight Technologies LLC	USA	PHA resins (AirCarbonTM)	Oxygen from the air and carbon from captured methane emissions	Newlight's 9X biocatalyst	-
PHB Industrial S.A.	Brazil	PHB, PHBV (BIOCYCLE®)	Saccharose	Alcaligenes sp	3,000

PolyFerm	Canada	mcl-PHA (VersaMerTM PHA)	Sugars, vegetable oils	Naturally selected microorganisms	-
Shenzhen Ecomann Biotechnology Co. Ltd.	China	PHA pellets, resins, microbeads (AmBio®)	Sugar or glucose	-	5,000
SIRIM Bioplastics Pilot Plant	Malaysia	Various types of PHA	Palm oil mill effluent (POME), crude palm kernel oil	-	2,000
Tepha	USA	*T*ephaFLEX® P3HB, P(3HB-co-4HB), P4HB, P(3HB-co-3HV), P(3HO-3HH)	-	-	Pilot
TianAn Biologic Materials Co. Ltd.	China	PHB, PHBV (ENMATTM)	Dextrose deriving from corn of cassava grown in China	*Ralstonia eutropha*	10,000-50,000
Tianjin GreenBio Material Co.	China	P (3, 4HB) films, pellets/foam pellets (Sogreen®)	Sugar	-	10,000

1.2.3 PHA production opportunities and challenges

PHA's selling price is typically in the range of $5-10/kg, depending on the type and quality of the polymer produced. However, researchers have suggested that the price should be $3-5/kg to be commercially competitive with traditional plastics The PHA production cost can be compared to similar conventional plastic high-density polyethylene (HDPE) at $1.1/kg and the highest produced bioplastic polylactic acid (PLA) at $2/kg (European Bioplastics, 2023; Roland-Holst, 2013). Since PHA and PLA have similar properties, PHA could replace many PLA applications if it became cost-competitive. PHA is also more heat stable than PLA, enabling it to be used in high-temperature applications, such as hot beverage cups, which unblended PLA cannot (Meereboer et al., 2020; Obuchi & Ogawa, 2010). Another benefit of PHA compared with PLA is that it can biodegrade in more diverse settings compared with PLA. PLA can biodegrade within three months in high temperature (140°F) controlled environments with specific cultures. However, PLA cannot degrade in natural environments, taking up to 100 years to degrade in landfills (Meereboer et al., 2020; Rossi et al., 2015). Consequently, some researchers have shown PLA can possess higher greenhouse gas emissions associated with its biodegradation when composted or landfilled compared to traditional plastics HDPE and LDPE (Benavides et al., 2020). Alternatively, PHA can biodegrade in ambient environments, both terrestrial and aquatic (Hegde et al., 2021). PHA is the only class of bioplastics with efficient marine biodegradation, while PLA does not possess this capability (Meereboer et al., 2020). Additionally, PHA can degrade in anaerobic digesters where the biogas captured can replace natural gas with associated carbon credits (Hegde et al., 2021). Therefore, PHA is an ideal replacement for traditional plastics and offers benefits over other bioplastic options since it will more rapidly break down in the natural environment and standard waste management systems.

The high production cost of PHA is a major limiting factor for further market expansion. The production cost of PHA varies greatly depending on the production process and is in the range of $4-16/kg

(Roland-Holst, 2013). The substrate used as a carbon source for PHA fermentation is often recognized as the main cost of PHA production (Nielsen et al., 2017). Even commonly studied substrates for large-scale PHA production, such as glycerol at $0.50/kg and glucose at $1.50/kg, add appreciable costs (Alibaba a., 2023; Yoong Kit et al., 2017). Therefore, it would be economically beneficial to utilize low-value carbon sources that result in high yields of PHA. High PHA substrate costs have led to considerable research on PHA production utilizing low-value carbon sources such as agricultural and food wastes (Alsafadi, Ibrahim, et al., 2020; Koller, 2015a; Liu et al., 2021; Wang & Zhang, 2021).

1.2.4 Dairy byproducts as PHA feedstock

Cheese and whey byproducts are food wastes that could be used as bioplastic feedstock (Amaro et al., 2019). The cheese industry has transformed former waste byproducts into valuable co-products (Oliveira et al., 2019). Cheese manufacturers created valuable whey protein products from the liquid whey produced during cheese-making, which was once considered a major waste product. Similarly, cheese manufacturers created a valuable co-product, lactose powder, from the byproduct of whey powder, whey permeate (Byylund, 2015; Oliveira et al., 2019). However, there has not been a widely accepted commercial use for the byproduct of lactose powder, delactosed permeate (DLP), which contains approximately one-third of the lactose present in whey permeate and most of the original milk minerals (Byylund, 2015; Liang et al., 2009; Oliveira et al., 2019). This lack of valuable use for DLP has led to most byproducts being sold as low-value animal feed or disposed of as waste (Liang et al., 2009). Figure 1.4 illustrates the different processing functions involved in creating these co- and byproducts of cheese (Byylund, 2015).

Whey permeate and delactosed permeate have been studied as mineral-enriched salt substitutes, lactose-enriched food streams, lactic acid for food or biomaterial applications, and as a substrate for

bioethanol. However, the commercial success of these applications is meager as these proposed products require high capital and operating costs that do not offset the revenue streams generated (Oliveira et al., 2019). Alternatively, the lactose contained in the DLP could be converted to bioplastics through a fermentation process with a biological catalyst (Amaro et al., 2019). DLP cost per pound of sugar is in the range of $0.09-0.18/kg, making the carbon source economically competitive with other frequently studied substrates such as glycerol and sugar (Dietrich et al., 2017; Roland-Holst, 2013; Wang et al., 2021; Yoong Kit et al., 2017). Additionally, economic modeling has demonstrated that utilizing DLP as a PHA substrate could result in economically competitive production costs of less than $4.0/kg. A large cheese processing plant could produce ~10,000 MT PHA/year, over a tenth of the global PHA market (Wang et al., 2021). Therefore, large-scale production of PHA derived from cheese byproducts appears economical and scalable.

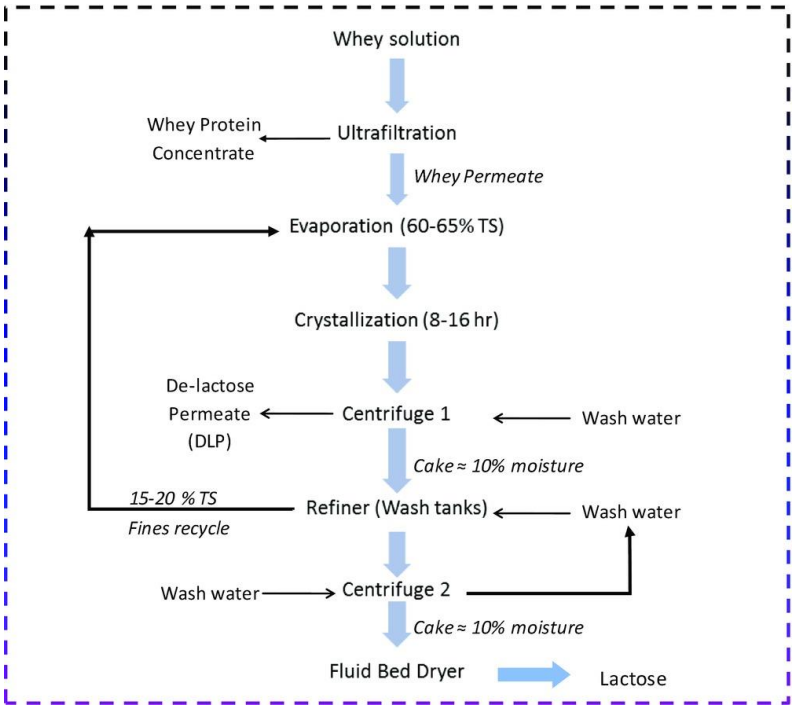

Figure 1.4 Process flow diagram for the production of DLP and from whey solution (Byylund, 2015).

1.2.5 PHA production with extreme halophiles and dairy byproducts.

Researchers have studied numerous microorganisms to produce PHA commercially (Amaro et al., 2019; Koller, 2018; Kourmentza et al., 2017; Raza et al., 2018). Careful considerations must be made for proper microbial selection depending on the target PHA substrate (Amaro et al., 2019; Koller, 2018). One organism, *Haloferax mediterranei* (*H. mediterranei)*, appears to be an excellent fit with cheese byproducts. This fit is due to *H. mediterranei* being an extreme halophile that grows in high-salinity environments with up to 20% salts (Ferre-Guell & Winterburn, 2018). The high-salinity environment allows simple integration of waste or byproducts since frequent contaminants, such as *Bacillus cereus*, cannot endure the severe salt environment. Therefore, an expensive sterilization pretreatment step is not required before PHA production, like for many other PHA producers (Amaro et al., 2019; Koller et al., 2011). Straightforward utilization of high salt-containing cheese byproducts can be incorporated as *H. mediterranei* nutrients for cell growth unsuitable for some commercial PHA producers (Amaro et al., 2019; Koller, 2018). Lastly, PHA extraction can be conducted with simple water addition that results in cell lysis and exposure of intracellular PHA from osmotic shock rather than applying costly chemicals that are typically harmful to the environment (Ghosh et al., 2019; Yoong Kit et al., 2017). *H. mediterranei* also naturally produces a more valuable form of PHA, poly(3-hydroxybutyrate-co-3-hydroxyvalerate) (PHBV) rather than common polyhydroxybutyrate (PHB), that has more desirable thermal and mechanical properties allowing it to be used for food packaging film, bags, and containers (Amaro et al., 2019; Joyce, 2018; Koller, 2018).

1.3 Research goals and objectives

There is a dearth of information about the utilization of DLP as a feedstock for producing PHA using *H. mediterranei.* There is also a need to estimate the kinetics, optimize the cultivation conditions of *H. mediterranei* growth in DLP, and design production systems for producing and harvesting PHA.

The overall goal of this research was to further develop a cost-efficient system to produce PHA from inexpensive feedstock cheese byproduct DLP. The specific objectives of this study included: 1) characterize DLP produced at an industrial scale cheese factory; 2) determine a pretreatment method to allow effective consumption of the DLP feedstock; 3) further optimize the *H. mediterranei* media with DLP feedstock; 4) develop an effective feeding strategy for *H. mediterranei* cultivation with DLP feedstock; and 5) improve the understanding of *H. mediterranei* galactose consumption and utilization.

The proposed PHA process utilizes novel low-value substrate DLP, decreases energy and downstream processing costs by eliminating a sterilization step, and simplifies PHA extraction and purification versus conventional commercial PHA production methods. This research directs efforts to create a value-added product and increase the dairy industry's sustainability while addressing global plastic waste disposal issues and climate change.

Chapter 2. Literature Review

2.1 Introduction

Bioplastics are an emerging market due to consumer interest and governmental regulations that seek to solve plastic and organic waste issues and decrease carbon emissions (Bernard, 2014; European Bioplastics, 2023). Bioplastic production was 2.7 MT (million metric tons) in 2021 and is expected to grow to approximately 8.4 MT by 2026 (European Bioplastics, 2023). PHA is the fastest-growing biodegradable bioplastic due to its unique attributes (European Bioplastics, 2023), including production from organic waste substrates, considerably higher biodegradability compared to other bioplastics on the market, and versatile range of applications and replacement to several families of traditional petroleum-based plastics (Bernard, 2014; Meereboer et al., 2020). The high production cost of PHA is the primary impedance to further market growth. The expensive carbon sources used for microbial fermentation are the main factor affecting the production cost (Nielsen et al., 2017). Researchers have proposed numerous organic waste streams to lower substrate costs of PHA production while also addressing the disposal of these problematic waste streams (Bernard, 2014; Koller, 2017; Reddy et al., 2003). However, organic waste streams pose challenges due to pretreatments, such as sterilization, separation, and fermentation steps that are often needed (Amaro et al., 2019; Koller, 2017; Wang & Zhang, 2021). These pretreatment methods are often numerous and complex and can offset the savings from using low-value wastes (Amaro et al., 2019; Koller, 2017; Wang, 2021). One industrial organic waste suggested for PHA production is cheese byproducts. However, their use is hindered by suitable microorganism selection and the requirement of extensive pretreatment practices (Amaro et al., 2019; Bernard, 2014). This review compared the advantages of applying cheese byproducts versus other organic wastes, explored PHA producers that best-fit cheese byproduct feedstocks, identified methods to overcome potential challenges associated with the use of cheese byproducts for PHA production, and determined PHA fermentation conditions and parameters for following experiments.

2.2 Polyhydroxyalkanoate

Polyhydroxyalkanoate (PHA) is a naturally produced, water-insoluble, lipid-like linear polyester. The polymer is typically between 1,000 -10,000 monomer subunits in size, 0.2-0.5 mm in length (Bernard, 2014), and 50,000-1,000,000 Daltons in molecular weight (Madison & Huisman, 1999). PHA is composed of 3-hydroxy fatty monomers, with the carboxyl group of one monomer forming an ester bond with the hydroxyl group of the adjacent monomer (Figure 2.1). An R functional group is present at the C-3 position of the monomer that can be an alkyl group ranging from C1 (methyl) to C13 (tridecyl) or another functional group, such as an unsaturated, aromatic, halogenated, epoxidized, or branched monomer (Madison & Huisman, 1999). This variation in the side chain, besides PHAs possessing variable lengths, is the basis for the PHA polymer family having a wide range of properties and use for numerous applications (Madison & Huisman, 1999; Reddy et al., 2003). PHA is naturally synthesized, recovered with simple downstream processing, and can be produced from inexpensive feedstocks, making it an attractive material (Bernard, 2014; Koller, 2017; Reddy et al., 2003). Over 75 genera of microorganisms synthesize PHA intracellularly, characteristically accumulating the PHA as granules inside the cells (Figure 2.2) (Bernard, 2014; Simó-Cabrera et al., 2021). PHA can act as a stored energy source, or play a role in non-storage uses in the cytoplasm and cytoplasm membrane with presumed functions in calcium channels, DNA transport, and protection of macromolecules (Anderson & Dawes, 1990). Non-storage PHA is cited as polyhydroxybutyrate (PHB) with low molecular weight (<15,000 Da) (Reddy et al., 2003). Unfavorable growth conditions, e.g., lack of essential nutrients, such as nitrogen or phosphorus with excess carbon, generally trigger storage PHA synthesis and accumulation (Bernard, 2014; Korkakaki et al., 2017). However, some microorganisms can produce PHA under normal growth conditions with adequate nitrogen and phosphorus present (Cui, Shi, et al., 2017; Wang & Zhang, 2021).

PHB is the most commonly produced PHA polymer that is highly crystalline and possesses properties similar to traditional plastics such as polypropylene (Li et al., 2017; Ten et al., 2015). PHB has a melting temperature of 173–180°C and a glass transition temperature of 5°C, which leads to the homopolymer having a narrow processability window. Another disadvantage of PHB is that it is characteristically brittle with impaired mechanical properties due to low nucleation density, which causes large spherulite formation and secondary crystallization (Reddy et al., 2003). Poly(3-hydroxybutyrate-co-3-hydroxyvalerate) (PHBV) is another type of PHA polymer. PHBV has a melting temperature near 150 °C, a decreased melting temperature with increasing HV content, and a glass transition temperature of -1°C (Qian et al., 2007; Rivera-Briso & Serrano-Aroca, 2018). PHBV possesses advantages compared to PHB of higher ductility and can be processed at lower temperatures, considerably reducing thermal degradation and processing costs (Ten et al., 2015). Although some cited applications for PHB and PHBV are often similar, including films, packaging, and medial materials, PHBV, compared to PHB, is less crystalline and is, therefore, more flexible with greater impact resistance and toughness, leading PHBV to be better suited than PHB for flexible packaging (Abbasi et al., 2022; Holmes, 1985; Meereboer et al., 2020). Also, PHBV is an ideal PHA polymer for food containers and disposable cutlery due to its mechanical and thermal properties (Joyce, 2018). PHB must often be blended with other PHA polymers, such as PHBV, to improve mechanical and thermal qualities (Ten et al., 2015). Therefore, PHBV typically has a higher value than PHB due to these more desirable properties (Reddy et al., 2003; Roland-Holst et al., 2013).

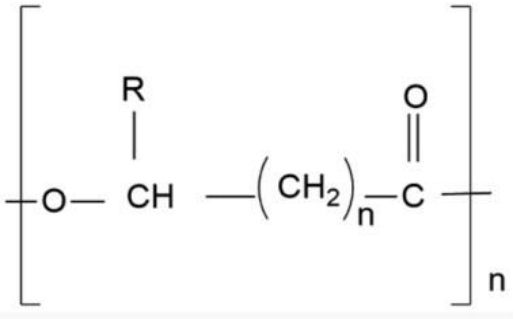

Figure 2.1 Polyhydroxyalkanoate (PHA) chemical composition (Mudenur et al., 2019).

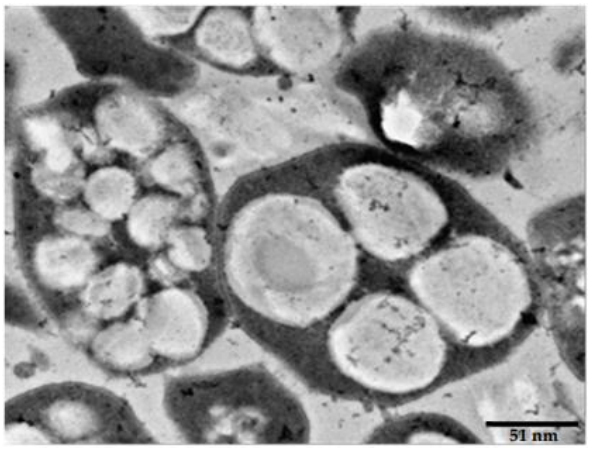

Figure 2.2 Electronic microscopy image of *Haloferax mediterranei* cells showing intracellular PHA granules (Simó-Cabrera et al., 2021).

2.3 Polyhydroxyalkanoate from waste-derived nutrients

Governments, industries, and consumers are interested in utilizing waste-derived carbon sources and nutrients for PHA production to reduce substrate costs and build a circular economy (Sharifzadeh et al., 2010; Yadav et al., 2020). PHA can be produced from numerous organic waste feedstocks with varying carbon sources, including fats or other long carbon chains, such as, palm oil mill effluent (Md. Din et al., 2012), olive oil mill effluent (Dionisi et al., 2005), waste cooking oil (Kamilah et al., 2013), and biodiesel

production wastewater (Dobroth et al., 2011); sugars, starches, and plant-derived polysaccharides, such as sugar cane (Albuquerque et al., 2007), sugar beets (Kiselev et al., 2022), industrial apple waste (Liu et al., 2021), coffee grounds (Kovalcik et al., 2018), corn starch wastes (Tian et al., 2022), vegetable processing wastes (Poli et al., 2011), paper mill waste (Munir et al., 2015), lignocellulosic biomass (Al-Battashi et al., 2019) and pea shells (Kumar et al., 2016); and volatile fatty acids derived from fermented food wastes (J. C. Fradinho et al., 2014; Wang & Zhang, 2021). Although many organic waste streams have been tested for PHA production, applying these feedstocks has several difficulties, such as the high possibility of contamination by non-PHA producing microorganisms that can compete with the desired PHA producers and cause low production yields. A sterility step can be added to address this issue, such as thermal pasteurization, antibiotics, or ultraviolet radiation. However, these processes can add appreciable costs and, in the case of heat treatments, can result in unwanted precipitants and other physical/chemical changes to the substrate (Amaro et al., 2019; Koller, 2017). A frequently used method to avoid this sterility issue, without introducing a major unit operation, is to employ mixed microbial cultures (MMCs). The most common MMC strategy to select for a PHA accumulating culture is applying feast and famine (FF) regimes. In this method, in the feast phase, intermittent feeding of substrate occurs and external carbon is consumed and stored as PHA, followed by the famine phase where periods without substrate addition that favors cell growth on stored products. This FF regime creates selective pressure for PHA-producing organisms. However, the technique limits the rate at which PHA can be produced over time due to the periods of the famine phase where no substrate is fed, and can cause erratic product quality (J. Fradinho et al., 2016; Reis et al., 2003).

Another challenge of using food waste (e.g., mixed food waste separated from municipal solid waste) for PHA production is that numerous pretreatment methods are often needed for PHA producers to utilize the waste feedstocks. First, equipment, such as a grinder, must break down the food waste into

smaller particles. Initial anaerobic digestion can convert the ground feedstock containing complex organic polymers into volatile fatty acids (VFAs) that some PHA producers can consume. Then the biomass solids from the resultant anaerobic digester effluent must be removed by a screw press or centrifugation system. Lastly, the resulting liquid must be concentrated with a membrane system, potentially multiple in series, to remove suspended solids and concentrate the nutrient solids. The desired PHA producers can then convert the concentrated food waste feedstock into bioplastic (Szacherska et al., 2021; Wang & Zhang, 2021). Each pretreatment step adds additional capital and operating costs for the proposed process, reducing the PHA product's economic return (Szacherska et al., 2021). Anaerobic digesters can commonly become inhibited by overloading or toxicants, which could slow or completely halt large-scale PHA production. Additionally, some of the carbon can be lost to biomass or gas production in the anaerobic digestion process, lowering overall PHA yields (Y. Chen et al., 2008; Szacherska et al., 2021). Using municipal food waste and anaerobic digestion could cause inconsistent substrate quality and composition leading to varying PHA product quality (Szacherska et al., 2021; Wang, 2022). Another food waste that researchers have investigated is cheese byproduct whey. Although PHA producers can utilize whey without complex anaerobic digestion and contains a more consistent composition than municipal food wastes, expensive pretreatment methods are still often required, such as membrane filtration, and the salts contained in the substrate can be inhibitory to some PHA producers (Amaro et al., 2019). Therefore, inexpensive substrates coupled with a synergistic PHA producer that best fits the specific feedstock should be explored for producing PHA more efficiently.

2.4 Potential polyhydroxyalkanoate feedstocks whey permeate and delactosed permeate

In cheese and whey powder production, liquid whey is separated from the cheese curds and concentrated utilizing membrane filtration. The fluid that fluxes through the membranes containing most of the lactose and minerals is the byproduct whey permeate (Byylund, 2015). Cheese makers can use

evaporator and crystallizer technologies to process the whey permeate further into lactose powder. Around two-thirds of the lactose crystallizes and is removed from the liquid whey permeate. The resultant lactose crystals are washed, dried, and milled to produce the final lactose powder. Delactosed permeate (DLP), or mother liquor, is the remaining liquid after lactose crystallization of the whey permeate (Oliveira et al., 2019). Since DLP results from the concentration of whey permeate, it contains around three times more mineral salts than whey permeate (Koller et al., 2007a; Liang et al., 2009). DLP can also possess low levels of organic acids, fats, protein-derived nitrogen sources, and vitamins (Liang et al., 2009; Oliveira et al., 2019). Mother liquor composition can vary from plant to plant and depends on starting source material and processing operations (Liang et al., 2009). Liang et al. (2009) demonstrated that DLP from different dairy processors' total solids can vary from 36-26% (wet basis), lactose 41-68% (dry basis), protein from 1.4-2.4% (dry basis), phosphorus from 1.6-2.3% (dry basis), and potassium from 4-8% (dry basis).

DLP is challenging to incorporate into food products due to its high-water content (60-75%). Its tendency to adhere and high hygroscopicity leads to most being either sold as low-value animal feed or disposed of as waste, which is environmentally malign (Liang et al., 2009). When sold as animal feed, DLP has a considerably lower value than whey permeate per total mass and mass of sugar since DLP has a lower fraction of lactose than whey permeate (Oliveira et al., 2019; Wang & Zhang, 2021). DLP contains approximately 20% of the original milk solids; for every 1.0 kg of milk used for cheese, whey, and lactose production, 0.5 kg of DLP is produced (Liang et al., 2009). Therefore, DLP appears to be a major opportunity to create value-added products since it is produced in large quantities at industrial-scale cheese factories, contains high concentrations of fermentable sugars, is of low value, and has no widespread use (Liang et al., 2009; Oliveira et al., 2019). However, limited research exists to create valuable co-products from DLP. As seen in Figure 2.3, some DLP opportunities proposed or explored are mineral-enriched salt substitutes, lactose-enriched food streams, extracting oligosaccharides for an infant

formula ingredient, separating compounds with prebiotic characteristics, and as a substrate for bioethanol. However, the commercial success of these applications is meager, and these proposed products require further processing from membrane filtration, evaporation, drying, enzymatic treatment, and fermentation processes, which can be costly (Oliveira et al., 2019). Thus, future research is needed to capitalize on the potential opportunities for DLP. Bioplastic production from delactosed permeate has been proposed through lactic acid fermentation to produce polylactic acid (PLA), but limited research exists, with most focusing on upstream cheese byproducts whey and whey permeate (Dosuky et al., 2019; Oliveira et al., 2019). Dosuky et al. (2019) achieved 60-80% efficiency conversion of lactose sugar derived from whey and whey permeate to lactic acid that could be further processed into PLA bioplastic. PHA, however, has advantages over PLA that have led to the PHA market growing at a faster rate than the PLA market, including superior biodegradability and more product applications (European Bioplastics, 2023; Meereboer et al., 2020; Obuchi & Ogawa, 2010).

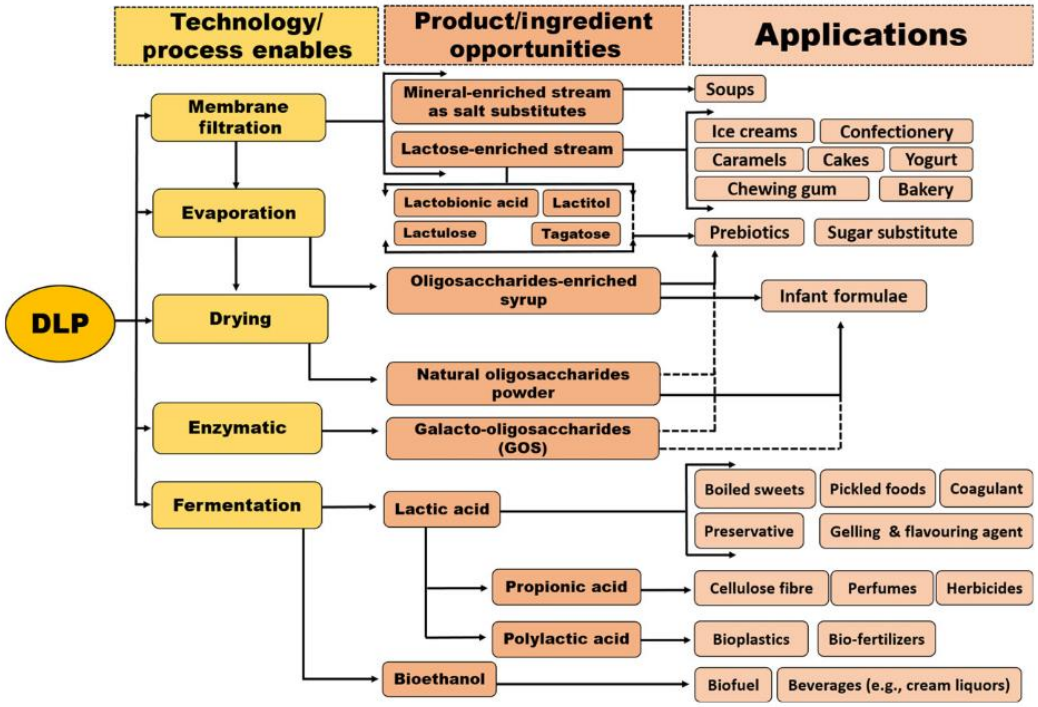

Figure 2.3 Potential applications for delactosed permeate (Oliveira et al., 2019).

Although cheese byproducts are rich in nutrients, finding suitable PHA-producing organisms has been noted to be problematic by researchers. Few naturally occurring PHA producers are able to consume lactose directly, and no PHBV producers have been demonstrated to consume lactose at high rates (Amaro et al., 2019; Koller, 2017; Rodriguez-Valera et al., 1983). Hence, to effectively convert lactose-containing substrates, such as cheese byproducts for PHA production, microbial genetic engineering or hydrolysis of the lactose appears to be needed, with the former raising ethical and environmental contamination concerns (Amaro et al., 2019). Various microorganisms have been studied for their ability to produce PHA from hydrolyzed lactose powder or lactose derived from pretreated whey and whey permeate with varying success (Amaro et al., 2019; Koller et al., 2007b). Some studied organisms required salt removal from pretreatment processes, which is not ideal since cheese byproducts can contain up to 5% salts (Amaro et al., 2019; Oliveira et al., 2019).

Another common problem with using cheese processing byproducts for PHA substrate is that they are unsterile (Amaro et al., 2019). Thus, some method to keep unwanted microorganisms from growing is often first applied to these byproducts, such as heat treatment, UV, or antibiotics (Ghaly & Kamal, 2004; Koller et al., 2011). Mixed microbial cultures can be applied instead of a sterilization step to convert cheese byproducts into PHA, decreasing operating costs and increasing flexibility (Colombo et al., 2016; Valentino et al., 2015)., However, MMCs typically result in considerably lower yields than monoclonal cultures and raise questions regarding production efficiency, consistency of the PHA product, and production control (Amaro et al., 2019). Additionally, research has yet to examine DLP as a substrate for PHA production. Most research on hydrolyzed cheese byproducts conversion to PHA utilized synthetic or highly pretreated cheese byproducts. These feedstock choices have led researchers to conclude that more studies are needed on raw dairy byproducts to commercialize the process. (Amaro et al., 2019)

2.5 Polyhydroxyalkanoate production with *Haloferax mediterranei*

2.5.1 *Haloferax mediterranei* cultivation with cheese byproducts

Microorganism selection for PHA production from cheese byproducts has issues such as low PHA yields, salt tolerance, contamination, and downstream processing costs (Amaro et al., 2019). PHA producer *Pseudomonas hydrogenovora* grown with hydrolyzed whey permeate resulted in a low yield of 0.08 g PHA/g sugar and a low PHA content of 12% (% PHA of cell dry mass) (Koller et al., 2007b). Similarly, thermophilic PHA producer *Thermus thermophilus* was grown with highly pretreated (acid removal of proteins, centrifugation, and filtration applied) whey supernatant, resulting in low PHA production of 0.57 g/l compared to 12 g/l of lactose sugar fed (Chavan et al., 2021; Pantazaki et al., 2009). Commercial PHA producer *Ralstonia eutropha* can accumulate up to 90% of its weight with PHA but typically grows in media containing a salinity of around 0.5%, considerably lower than what is found in many cheese byproducts (Khanna & Srivastava, 2005; Suriyamongkol et al., 2007). Koller et al. (2008) found that PHA productivity by *Hydrogenophaga pseudoflava* with hydrolyzed whey feedstock could be reduced by more than half without applying expensive antibiotic vancomycin to kill common *Bacillus cereus* contaminants. Intracellular PHA extraction from most PHA producers involves the use of solvents such as chloroform and methanol that are expensive and environmentally malign (Byrom, 1987) or enzymes and detergents that are also costly and can result in low PHA recovery (Suriyamongkol et al., 2007). Therefore, having a PHA producer more suitable for cheese byproducts would be beneficial.

In particular, *Haloferax mediterranei (H. mediterranei)* appears to be an ideal fit with cheese byproducts (Amaro et al., 2019; Koller, 2017). *H. mediterranei* is an archaea originally cultivated in Alicante, Spain (Rodriguez-Valera et al., 1980). The microorganism is a notably pink color (Figure 2.4) due to C40 and C50 carotenoids that provide ultraviolet (UV) protection in the wild (Calo et al., 1995; Fang et al., 2010). Researchers have demonstrated that the organism can convert organic waste streams,

including date palm waste, food waste, olive mill wastewater, and cheese byproducts whey and whey permeate byproducts efficiently into PHA (Alsafadi, Ibrahim, et al., 2020; Dionisi et al., 2005; Koller et al., 2007a; Koller, 2017; Pais et al., 2016; Wang & Zhang, 2021). Table 2.1 shows the experimental results of *H. mediterranei* cultured with various substrates. This potential synergy between the microorganism and cheese byproducts is due to *H. mediterranei* being an extreme halophile that grows in up to 20% high salinity environments (Ferre-Guell & Winterburn, 2018). Scientists have identified 17 genera of microorganisms that are extreme halophiles capable of producing PHA, with *H. mediterranei* cited as one of the best PHA producers of those halophiles studied (Mitra et al., 2020). A high saline environment suitable for *H. mediterranei* allows easy incorporation of cheese waste or byproducts since common contaminants present cannot survive in these conditions. Thus, a costly sterility step before fermentation, typical for several other PHA producers studied with hydrolyzed cheese byproducts, is not required. Direct inclusion of cheese byproducts, which contain high concentrations of up to 5% salts, can also occur with *H. mediterranei*. The salts, which several other PHA producers cannot tolerate and require removal, can act as beneficial *H. mediterranei* nutrients for growth (Amaro et al., 2019; Koller, 2017). Additionally, intracellular PHA extraction can occur via simple water addition, causing cell lysis from osmotic shock (Ghosh et al., 2019). This method contrasts with other commonly applied PHA extraction techniques that use expensive chemicals, often chlorine-based and environmentally malign (Ghosh et al., 2019; Yoong Kit et al., 2017). Lastly, *H. mediterranei* produces a more valuable form of PHA, PHBV (Figure 2.5), without the need to add precursors such as propionate that many other PHBV producers require (Albuquerque et al., 2007; Yoong Kit et al., 2017). PHBV is cited for having more desirable mechanical properties than PHB, which is characteristically brittle, and can be used to create a wide range of applications, to replace traditional plastics, such as cutlery, food packaging film, bags, or containers (Joyce, 2018; Reddy et al., 2003).

Wang et al. (2021) conducted a techno-economic study of *H. mediterranei* PHA production with cheese byproducts lactose powder, whey permeate, and DLP. The DLP was the most economical of the three feedstocks studied, with a breakeven price of less than $4/kg PHA. This breakeven price was less than the breakeven price Yoong Kit et al. (2017) found with glycerol feedstock of $5.7/kg PHA (Wang et al., 2021; Yoong Kit et al., 2017). DLP's breakeven price was less compared to the other cheese byproducts, whey permeate at $5-6/kg PHA and lactose powder at $6-10/kg PHA (Wang et al., 2021), demonstrating that DLP offers the best economic return for PHA production with cheese byproducts.

Table 2.1 PHA production via *H. mediterranei* with various substrates.

Substrate	**Culture method**	**Cell dry mass (CDM) (g VS/l)**	**PHA yield (g PHA/g substrate)**	**PHA content (% CDM dry basis)**	**Reference**
Hydrolyzed whey and yeast extract	Batch	7.5	0.78	53	(Pais et al., 2016)
Hydrolyzed whey permeate and yeast extract	Batch	11.0	0.33	50	(Koller et al., 2007b)
Glucose + galactose and yeast extract	Batch	3.6-6.8	0.66-0.82	29-46	(Pais et al., 2016)
Glucose	Batch	2.3-6.1	0.07-0.10	13-28	(Melanie et al., 2018)
Glucose	Continuous	3.6	0.18	42	(Lillo & Rodriguez-Valera, 1990)

Volatile fatty acids	Fed-batch	3.7-7.7	0.31-0.36 (per g C)	10-27	(Ferre-Guell & Winterburn, 2018)
Food waste derived VFAs	Batch	0.3-3.0	0.41-0.54	43-57	(Wang & Zhang, 2021)

Figure 2.4 *H. mediterranei* cells cultivated with hydrolyzed whey (Koller, 2017).

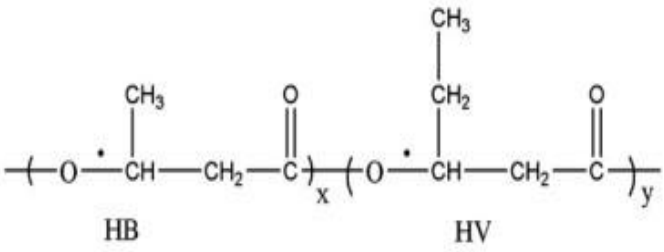

Figure 2.5 Poly(3-hydroxybutyrate-co-3-hydroxyvalerate) PHBV chemical structure

(Calil et al., 2021).

2.5.2 Enzymatic hydrolysis of lactose for *H. mediterranei* consumption

The lactose contained in DLP must first be hydrolyzed into glucose and galactose since *H. mediterranei* cannot use the disaccharide directly (Koller et al., 2007a; Pais et al., 2016). Enzymatic hydrolysis is the most common method to convert lactose into monosaccharide hexoses. Lactase enzymes (β-D-galactosidase; β-D-galactoside galactohydrolase) are extensively found in nature, including animals organs such as the stomachs of cows and sheep, yeast, fungi, bacteria, in addition to plants, particularly in apples, almonds, apricots, and peaches (Richmond et al., 1981). Lactase enzymes were first proposed for industrial dairy applications in the 1950s and have been commercially available since the 1970s (Dam et al., 1950; Panesar et al., 2006). Lactase enzymes are widespread in food applications due to their straightforward use that does not require additional equipment for dairy processors. The most common application for commercial lactase enzymes is lactose-free milk, and dairy processors in the cheese, whey, and yogurt industries also use the enzyme (Harju et al., 2012). Although lactases are one of the most important enzymes used in food processing, minimal research has been conducted both in academia and by prominent commercial lactase vendors on delactosed permeate since it is typically land spread or fed directly to animal livestock (Harju et al., 2012; Oliveira et al., 2019; H. Scott, personal communication, October 15, 2020). DLP could pose lactase hydrolysis issues due to large concentrations of mineral salts such as calcium and sodium, which were demonstrated to be ionic inhibitors for some lactase enzymes (Fox, 1997; Liang et al., 2009). However, minerals are also needed for effective hydrolysis by several lactases, including sodium, potassium, magnesium, and manganese (Fox, 1997). Additionally, DLP can contain suspended solids that could pose mass transfer issues when utilizing lactase enzymes (Oliveira et al., 2019; H. Scott, personal communication, October 15, 2020). Therefore, research is needed to determine if commercial lactase enzymes can lead to effective DLP hydrolysis.

Numerous lactases, typically derived from microbial sources, are commercially produced. The chemical reaction of lactose and lactase depends on pH, time, loading, and temperature (Harju et al., 2012; H. Scott, personal communication, October 15, 2020). Different microorganism lactase enzymes function optimally at varying pH ranges in the acidic or neutral range. For example, *Aspergillus niger* lactase's pH optimum range is very acidic at 3.0-4.0, *Bacillus stearothermophilus* lactase's pH optimum range is slightly acidic at 5.8-6.4, and *Streptococcus thermophilus* lactase's optimal pH is near neutral at 7.1. These different optimal pH values allow effective hydrolysis with the direct use of lactases for numerous dairy products with pH values in the acidic to neutral range (Harju et al., 2012). A wide range of temperatures and loadings can also be employed with lactase enzymes depending on the specific lactase used, financial impacts, and sensitivity of the product to become contaminated or change flavors if kept at high temperatures for prolonged periods (Dahlqvist et al., 1977; Harju et al., 2012; Popescu et al., 2021). Dahlqvist (1997) tested the enzymatic hydrolysis of milk containing 5% lactose at a room temperature of 20 ℃ with a pH of 7 with minute loadings (1-30 mg/l of lactase) of lactase enzyme (*Saccharomyces lactis*) for extended incubation times up to 40 days. The researchers determined that 10-30 mg/l lactase loadings could result in over 90% hydrolysis with a 10-day incubation time. Dahlqvist (1997) also tested a demineralized whey solution with 8.5% lactose at room temperature of 20 ℃ with a pH near 7.0 and found that a minute loading of 10 mg/l of lactase with a hydrolysis time of 5 days could result in greater than 80% hydrolysis. Popescu et al. (2021) demonstrated that a higher temperature of 20 ℃ and enzyme loading of 0.15 g/l (*B. licheniformis*) for the hydrolysis of milk containing 4.75% lactose could give a hydrolysis extent of >90% with a very short 2-hour incubation time.

Lactase pretreatment poses associated problems for PHA production, the most notable being increased capital costs from purchasing lactase enzyme (Wang et al., 2021). However, several methods have been proposed to reduce enzyme costs (Dahlqvist et al., 1977; Finocchiaro et al., 1980; Miller &

Brand, 1980). The most straightforward and effective method was adding smaller amounts of lactase to the product and extending the chemical reaction time (Dahlqvist et al., 1977). Lactase immobilization allows repeated use of the enzyme and is recognized as a viable option for decreasing production costs with over 50 years of research (Finocchiaro et al., 1980; Mai et al., 2013; Richmond et al., 1981). Lactase recovery using membrane systems has also been demonstrated to be an effective technique for reusing the enzyme (Almutairi et al., 2022; Gänzle et al., 2008; Miller & Brand, 1980). Furthermore, through techno-economic modeling, Wang et al. (2021) demonstrated that by utilizing membrane lactase recovery with cheese byproduct-derived PHA production, the lower production costs from enzyme reuse can outweigh the downsides of increased capital and operating costs from an additional unit operation. Other alternatives to lactase enzymatic hydrolysis include acid hydrolysis. In this method, a strong acid is typically added to the lactose-containing stream, dropping the pH very low to 1.2 at 150 °C for a short period. However, this method is only viable for protein-free streams. The technique can also be costly due to the acid needed to decrease the pH, extensive heat requirements for the high temperatures of hydrolysis, and caustic required to increase the pH for ideal fermentation conditions (Zadow, 1984).

2.5.3 *H. mediterranei* growth with hydrolyzed lactose substrate

Hydrolyzed lactose streams contain glucose and galactose sugar; therefore, both sugars need to be effectively consumed and utilized by *H. mediterranei* to maximize PHA production. *H. mediterranei* can effectively grow and produce PHA with glucose substrate with reported PHA yields of 0.07-0.33 g PHA/g glucose consumed and PHA contents of 17-60% of total residual cell dry mass (Don et al., 2006; Lillo & Rodriguez-Valera, 1990; Melanie et al., 2018). However, there are mixed conclusions if galactose is an effective substrate. Several researchers demonstrated that *H. mediterranei* less effectively utilizes galactose than glucose (Bonete et al., 1996; Pais et al., 2016; Rodriguez-Valera et al., 1980). Pais et al. (2016) noted that glucose is the more favorable substrate and is consumed first by *H. mediterranei* when

grown in glucose and galactose mixtures. Additionally, some researchers have demonstrated that for sugar mixtures of glucose and galactose, galactose may not result in cell growth, but only PHA production or maintenance energy, and the archaea may not consume all of the available galactose (Koller et al., 2007a; Pais et al., 2016). Other studies have shown contradicting results that *H. mediterranei* can consume galactose concurrently with glucose, galactose can result in cell growth, and galactose can be consumed entirely in glucose and galactose-containing feedstocks (Raho et al., 2020). Furthermore, no detailed published data exist regarding *H. mediterranei* PHA production with galactose as a sole carbon source (Bonete et al., 1996; Rodriguez-Valera et al., 1980).

2.5.4 *H. mediterranei* metabolic pathways

In the first step of PHBV production, *H. mediterranei* uses the semi-phosphorylative Entner-Dourdoroff (ED) metabolic pathway to convert glucose into pyruvate catabolically. Figure 2.6 displays the sugar catabolic pathways for halophilic archaea such as *H. mediterranei*. The organism can utilize numerous sugars including sucrose, fructose, and glucose. Figure 2.6 shows that the first step in the semi-phosphorylative ED pathway for glucose catabolism is the use of glucose dehydrogenase to produce gluconate (Williams et al., 2019). The glucose dehydrogenase of *H. mediterranei* has been cited to be promiscuous as it can catalyze the oxidation of several aldose sugars, including, D-Galactose, D-Xylose, D-Mannose, D-Fructose, D-Fucose, D-Glucosamine, and D-Ribose. However, the relative rates of glucose dehydrogenase enzymatic activity for these sugars can vary compared to glucose when using $NADP^+$ as a coenzyme. For example, after defining glucose as a 100% reference, Bonete et al. (1996) found that although the relative enzyme rate of D-Xylose was near glucose at 88%, D-Fucose and D-Galactose were considerably lower at 18% and 13%, respectively. Therefore, from a biokinetics perspective, galactose is metabolized substantially slower than glucose, which agrees with the lower galactose consumption

compared to glucose consumption when *H. mediterranei* was fed both sugar substrates by Koller et al. (2007a) and Pais et al. (2016).

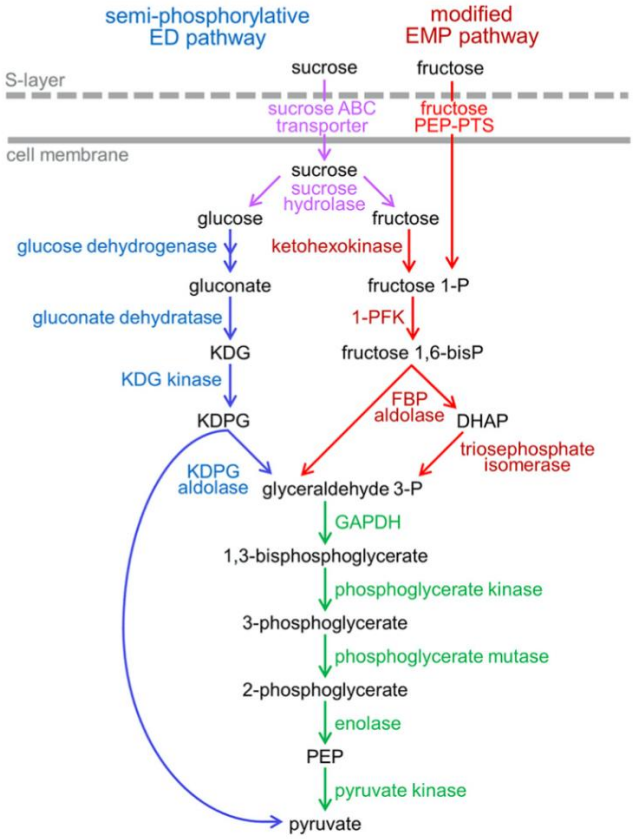

Figure 2.6 Sugar catabolism pathways in haloarchaea (Williams et al., 2019).

Pais et al. (2016) showed that the availability of micronutrients could be a critical factor in *H. mediterranei's* ability to metabolize galactose. Pais et al. (2016) studied the effects of loading SL-6, a general microorganism micronutrient recipe containing zinc, manganese, boron, cobalt, copper, nickel, and molybdenum, at 0%, 0.1%, and 1.0% v/v on *H. mediterranei* cell growth, PHA production, and sugar consumption with synthetic glucose and galactose media. Pais et al. (2016) found increased glucose and galactose consumption rates by adding SL-6 trace elements. The highest final cell mass and PHA

concentrations occurred with the highest 1% v/v loading of SL-6. *H. mediterranei* consumed little glucose (~25%) and almost no galactose with the 0% v/v SL-6 loading after 120 hours; all the glucose after 20 hours and around one-third of the galactose after 120 hours with the 0.1% v/v loading; and all the glucose after 20 hours, and approximately two-thirds of the galactose with the 1.0% loading. This experiment demonstrated the potential importance of micronutrients for *H. mediterranei* culturing (Pais et al., 2016). Pire et al. (2000) found that *H. mediterranei*'s glucose dehydrogenase enzyme contains two zinc ions per subunit and suggested that one zinc ion plays a role in the catalytic activity, with the other being part of the enzyme structure. Additionally, Bonete et al. (1996) demonstrated that divalent cations Mn^{2+}, Mg^{2+}, and Ni^{2+} can increase glucose dehydrogenase activity with manganese, resulting in the highest increase in enzyme activity and nickel with the lowest increase in enzyme activity. The absence of all divalent ions resulted in the lowest enzyme activities observed (Bonete et al., 1996). These results pose theoretical reasons for the observation of Pais et al. (2016) that trace elements appear to play an essential role in glucose dehydrogenase activity that can affect *H. mediterranei* cell mass growth.

Figure 2.7 presents the *H. mediterranei* biochemical pathways for PHBV production utilizing pyruvate. *H. mediterranei* synthesizes PHBV through propionyl-CoA, a precursor of the 3HV monomer, which many other PHA producers lack. The use of propionyl-CoA is why many halophilic archaea, including *H. mediterranei,* can accumulate PHBV from various carbon sources compared with other PHBV producers that require propionyl-CoA precursors, e.g., propionate. Researchers have found evidence suggesting that at least four metabolic pathways can convert glucose to propionyl Co-A. The paths, as observed in Figure 2.7, are the citramalate/2-oxobutyrate pathway (Path I), the aspartate/2-oxobutyrate pathway (Path II), the methylmalonyl-CoA pathway (Path III), and the 3-hydroxypropionate pathway (Path IV). Paths II and III are common in many PHA-producing organisms and lead to carbon storage from TCA intermediates. Paths I and IV are unique to *H. mediterranei* (and other haloarchaea) and cause direct carbon storage from

pyruvate and acetyl-CoA as PHA granules. The absence of Paths 1 and IV by other PHBV producers could be another reason why many other PHPV producers cannot directly generate PHBV without adding a precursor. Han et al. (2013) found that *H. mediterranei* is the only organism to have the ability to simultaneously utilize four pathways for propionyl-CoA generation. The use of the four pathways allows the extreme halophile to produce PHBV with a high HV molar fraction from unrelated carbon sources (Han et al., 2013), which is beneficial from a commercial mechanical and thermal properties aspect as these PHA polymers typically possess higher value (Reddy et al., 2003). It is also important to note from Figure 2.7 that all paths except IV lead to the generation of carbon dioxide. This diversion of carbon flow from PHA production can potentially reduce yields compared to other non-sugar substrates.

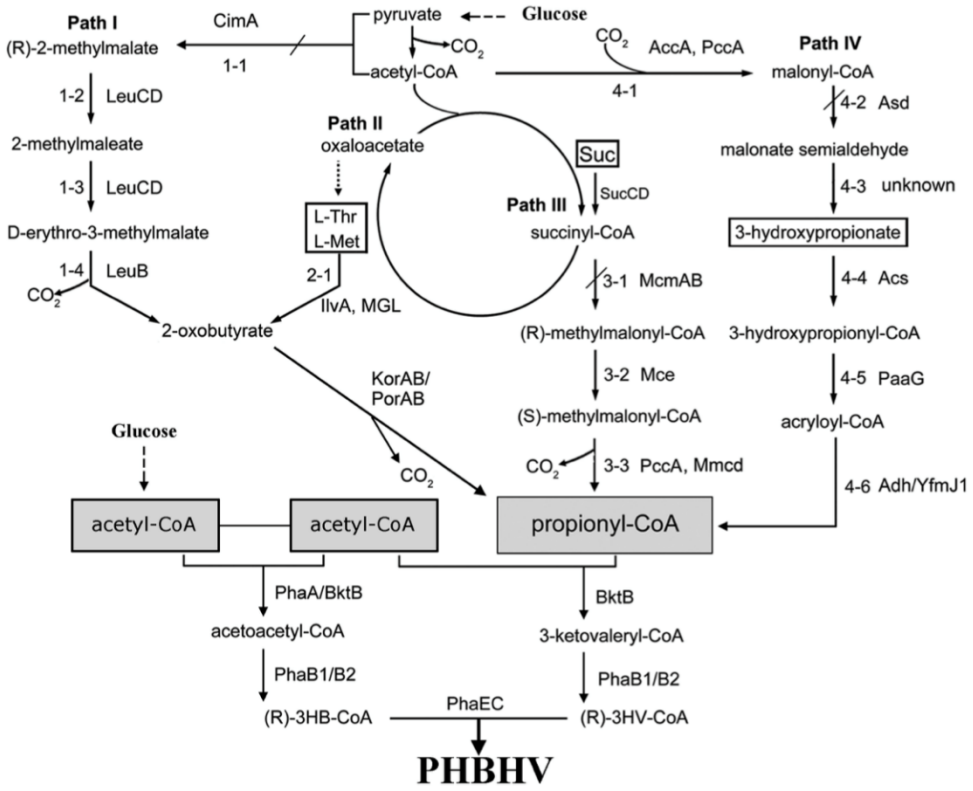

Figure 2.7 Four proposed pathways for propionyl-CoA synthesis in *H. mediterranei* (Han et al., 2013).

2.6 PHA production with various feeding strategies

Most studies of PHA production with *H. mediterranei* utilized batch systems, with some employing fed-batch systems (Alsafadi, Ibrahim, et al., 2020; Alsafadi & Al-Mashaqbeh, 2017; Cui, 2017; Cui, Shi, et al., 2017; Huang et al., 2006; Koller, 2015b; Pais et al., 2016; Wang & Zhang, 2021). Little research, however, has been conducted utilizing continuous systems. Lillo and Rodriguez-Valera (1990) demonstrated the viability of continuous culturing for 3 months with glucose substrate and a dilution rate of 0.02 hr^{-1} giving the best results. Lillo and Rodriguez-Valera (1990) were able to obtain a steady-state biomass concentration of 3.6 g/l and PHA concentration of 1.5 g/l, but with low PHA yields of 0.10 g/g of sugar fed. Although Lilo and Rodriguez-Valera (1990) had success with continuous cultures minimal follow-up research on continuous system has been conducted. Likewise for hydrolyzed dairy feedstocks, most research has been conducted with batch cultures, some with fed-batch, and none with continuous systems (Amaro et al., 2019; Koller et al., 2007b, 2007a; Pais et al., 2016; Raho et al., 2020). Drawbacks exist for batch systems, including potentially lower productivity due to downtime between batches and less control over product consistency from the varying fermentation conditions (Braunegg et al., 1995; Koller & Muhr, 2014). A common benefit of selecting batch versus continuous systems is reducing contamination risk, as continuous systems are more likely to introduce foreign microorganisms. However, using *H. mediterranei* for PHA production should limit contaminants from growing in high-salinity environments. Therefore, reducing this frequent downside of continuous systems (Koller & Muhr, 2014). Additionally, cheese co-products are continuously produced at large-scale. The co-product streams can contain abnormally high concentrations of constituents if upsets occur in upstream processing, which could lead to inhibitory conditions, especially in batch systems (Byylund, 2015; Koller & Muhr, 2014). A continuous system can help lower possible substrate inhibition due to the dilution of the feed with the bioreactor volume (Koller & Muhr, 2014). Consequently, more research is needed to compare the

performance of continuous, batch, and fed-batch systems for *H. mediterranei* PHA production from cheese co-products.

2.7 *Haloferax mediterranei* culturing parameters

H. mediterranei requires a high saline environment containing numerous macro and micronutrients. The culturing media must contain carbon, nitrogen, phosphorus, mineral salts, and trace elements for optimal growth. Other operating parameters such as temperature, pH, and dissolved oxygen require control for ideal cell growth.

2.7.1 Nutrient conditions

H. mediterranei is unique compared to many other PHA producers because it can accumulate PHA under normal growth conditions (Cui, Shi, et al., 2017; Wang & Zhang, 2021). Nevertheless, essential nutrients nitrogen and phosphorus can affect the rate at which the halophile stores PHA (Cui, Shi, et al., 2017; Lillo & Rodriguez-Valera, 1990). Cui et al. (2017) studied the impacts of carbon to nitrogen ratio (C/N) on *H. mediterranei* growth and PHA production. Cui et al. (2017) tested four C/N ratios of 5, 15, 35, and 65 with organic nitrogen sources casamino and yeast extract. Cui et al. (2017) found that a very high C/N ratio of 65 can severely inhibit cell growth and PHA production, but a more moderately high C/N ratio of 35 could lead to improved PHA accumulation. However, although the lower C/N ratios of 5 and 15 saw slightly lower PHA contents of approximately 10-15% less than the C/N ratio of 35, overall PHA production was higher for these lower C/N ratios. This result was most likely due to improved overall cell growth with the lower C/N ratios as nitrogen was in excess. Therefore, although higher C/N ratios may increase PHA accumulation potentially due to nitrogen limitation leading to excess carbon stored as PHA, *H. mediterranei*'s growth associated PHA production can outweigh these potential benefits (Cui, Shi, et al., 2017). Cheese byproducts can contain nitrogen due to milk proteins present (Oliveira et al., 2019).

However, Pais et al. (2016), who studied hydrolyzed whey substrate, utilized complex nutrient source yeast extract as a nitrogen source, potentially due to the uncertainty of the bioavailability and the amount of nitrogen present. Pais et al. (2016) did not state what their target C/N was, but it could be estimated from their stated media composition to be approximately 10 without including the nitrogen contained in the whey. Based on these findings, this study applied a low C/N ratio of approximately 8 to allow for high cell growth that can lead to increased PHA production.

Besides organic nitrogen source yeast extract, *H. mediterranei* can utilize other nitrogen sources, including ammonia and nitrate. Ammonia was found to be the preferred inorganic nitrogen source resulting in improved cell growth (Ferre-Guell and Winterburn, 2017). Researchers have studied ammonium chloride with *H. mediterranei* cultivation since the 1990s, and its use as an effective nitrogen source with sugar-containing feedstocks is well established (Alsafadi & Al-Mashaqbeh, 2017; Cui, Shi, et al., 2017; Lillo & Rodriguez-Valera, 1990; Pire et al., 2014). Varying results exist if organic or inorganic nitrogen sources lead to improved PHA production (Alsafadi, Al-Mashaqbeh, et al., 2020; Cui, Shi, et al., 2017). Using glucose substrate, Cui et al. (2017) stated that inorganic nitrogen sources improve PHA production compared with organic sources since inorganic nitrogen sources are better utilized in *H. mediterranei* metabolic pathways than organic sources by the archaea. In contrast, Alsafadi et al. (2017), who also applied glucose substrate, studied three nitrogen sources: organic yeast extract, inorganic ammonia chloride, and an equal mixture of yeast extract and ammonium chloride. Alsafadi et al. (2017) determined that the combined organic and inorganic nitrogen source resulted in the highest PHA production, followed by the organic yeast extract, and the least for inorganic ammonium chloride. These researchers hypothesized that organic nitrogen sources improved PHA production due to the amino acids and peptides present that *H. mediterranei* can directly incorporate rather than needing to be anabolized from inorganic sources (Alsafadi & Al-Mashaqbeh, 2017). This PHA study applied inorganic ammonium

chloride and organic yeast extract as nitrogen sources. Yeast extract was also supplemented fermentation media as a complex nutrient source since numerous other researchers have used it for this purpose (Koller et al., 2007b; Lillo & Rodriguez-Valera, 1990; Melanie et al., 2018; Pais et al., 2016).

Phosphorus is another essential nutrient for *H. mediterranei* growth that, like nitrogen, some researchers have reported increased PHA accumulation when there are deficiencies. However, researchers have mixed conclusions about the optimal phosphorus loading. Lillo Rodriguez-Valera (1990) examined varying concentrations of KH_2PO_4 loadings at 0.03, 0.015, 0.0075, 0.00375, and 0.0009375% with glucose substrate. The researchers found that phosphorus limitation improved PHA production and PHA yields, with 0.00375% obtaining the best results for these parameters and 0.0009375% with the following best (Lillo & Rodriguez-Valera, 1990). Alternatively, Melanie et al. (2018) had different conclusions from their experiment when testing three phosphorus KH_2PO_4 loadings of 0.5, 0.25, and 0.00375 g/l. The highest loading of 0.5 g/l, with a C/P ratio of 35 and excess phosphorus available, resulted in the highest specific growth rate, final cell mass concentration, and final PHA concentration. The lowest loading of 0.00375 g/l resulted in notably lower values for these parameters but did result in a higher PHA content of more than 10% versus the higher loadings (Melanie et al., 2018). Delactosed permeate contains very high phosphorus concentrations from the original milk derived from. The C/P ratio of DLP is ~10 (Liang et al., 2009). Therefore, excess phosphorus is present in DLP-containing media even if dilution is applied. Melanie et al. (2018) demonstrated that excess phosphorus could benefit *H. mediterranei* growth and PHA production. Removing the phosphorus to decrease the C/P would also add a unit operation, increasing capital and operating costs to the proposed PHA production process. Therefore, DLP without phosphorus removal was used in the fermentation studies.

2.7.2 Minimum salt media and micronutrients

High saline (HS) minimum salt media (MSM) with 15-25% salinity is typically applied for *H. mediterranei* cultivation (Ferre-Guell & Winterburn, 2018; Rodriguez-Valera et al., 1980). The MSM replicates artificial seawater with higher concentrations of sodium and chloride (Lillo & Rodriguez-Valera, 1990; Rodriguez-Valera et al., 1980). Early research by Rodriguez-Valera et al. (1980) studied the effects of MSM concentration on *H. mediterranei* growth and found that a 20% salinity resulted in the highest growth rate. More recent research by Matarredona (2021) also demonstrated that increased *H. mediterranei* final cell mass concentration and specific growth rate could occur with 20% salinity. Studies utilizing hydrolyzed dairy byproducts to culture *H. mediterranei* have successfully employed HS MSM based on media with 20% salinity containing: NaCl, 156 g/L; $MgCl_2.6H_2O$, 13 g/L; $MgSO_4.7H_2O$, 20 g/L; $CaCl_2.6H_2O$, 1 g/L; KCl, 4 g/L; NaBr, 0.5 g/L (Koller et al., 2007a; Pais et al., 2016). Therefore, MSM at 20% salinity was applied in this study for optimal *H. mediterranei* cell growth.

Koller et al. (2005) utilized SL-6 trace elements for *Wautersia eutropha* cultivation on green grass and silage juice substrate with a loading of 0.1 v/v. Based on Koller et al. (2005) use of SL-6 trace elements for PHA production, Pais et al. (2016) studied the effects of SL-6 on *H. mediterranei* cell growth, PHA production, and sugar consumption. Pais et al. (2016) found that higher loadings of SL-6 up to 1.0% (v/v) could improve these parameters. Other researchers who studied *H. mediterranei* PHA production with other non-dairy sugar substrates, such as glucose, have also utilized SL-6 in their media (Alsafadi, Ibrahim, et al., 2020; Ferre-Guell & Winterburn, 2018). Therefore, in these studies, 1.0% v/v SL-6 micronutrients were provided to the media containing: $ZnSO_4.7H2O$, 100 mg/L; $MnCl_2.4H_2O$, 30 mg/L; H_3BO_3, 300 mg/L; $CoCl_2.6H_2O$, 200 mg/L; $CuCl_2.2H_2O$, 10 mg/L; $NiCl_2.6H_20$, 20 mg/L; $Na_2MoO_4.H_2O$, 30 mg/L (Koller et al., 2005; Pais et al., 2016).

2.8.2 Culturing conditions

2.8.2.1 Temperature

Like numerous other microorganisms, extreme halophile growth follows the Arrhenius equation for cell growth rate versus temperature (Robinson et al., 2005). Robinson et al. (2005) determined that many extreme halophiles, including *H. mediterranei,* exhibited nearly identical slopes in the Arrhenius portions of their temperature growth curves. *H. mediterranei* can grow successfully in a wide temperature range of 32-52˚C. Lillo and Rodriguez-Valera et al. (1990) first studied the effects of temperature on *H. mediterranei* growth with glucose substrate. Lillo and Rodriguez-Valera et al. (1990) reported that the archaea's maximum growth occurred at 45°C. Robinson et al. (2015) found no significant differences in final cell mass for the 37, 42, and 47°C temperatures tested for *H. mediterranei* growth. However, the highest cell mass growth rate was obtained at 42˚C. Although a temperature near 45˚C may be optimal for *H. mediterranei* cell growth, Lillo and Rodriguez-Valera et al. (1990) showed that maximal PHA content occurred at 37˚C (Rodriguez-Valera et al., 1980). Alsafadi and Al-Mashaqbeh et al. (2017) also demonstrated improved PHA content at 37˚C compared with 45˚C, and similar PHA productions could result with 37˚C and 45˚C with olive mill wastewater substrate. Many researchers, including those studying sugar and hydrolyzed cheese byproduct feedstocks, have applied a lower temperature of 37°C versus 45°C to save energy costs for fermentation while maximizing PHA production (Huang et al., 2006; Koller et al., 2007a, 2007a; Pais et al., 2016). Therefore, a temperature of 37°C was applied in this study to benefit PHA production and energy savings.

2.8.2.2 pH

H. mediterranei is typically cultivated at a pH near neutral of 7.0 (Abbott, 2010; Koller et al., 2007a; Lillo & Rodriguez-Valera, 1990). Mattarredona et al. (2021) found that the halophile archaea can grow in a wide pH range of 5.75-8.75, with the optimal pH for final cell mass and specific growth rate around

neutral at 7.20. With sugar media, researchers have shown that *H. mediterranei* can accumulate organic acid metabolites over time during cell growth, dropping the pH as low as 5.0, which can inhibit the archaea (Bhattacharyya et al., 2014; Ghosh et al., 2019). Sodium bicarbonate has been applied as a buffer to maintain pH with *H. mediterranei* cultivation, including in media with cheese byproduct substrate (Byylund, 2015; Koller, 2015b; Pais et al., 2016). According to these results, this study maintained a neutral pH near 7.0 and sodium bicarbonate buffer was added to the media to prevent pH swings.

2.8.2.3 Dissolved oxygen

H. mediterranei is an aerobic respiring organism that needs adequate oxygen levels for ideal cell growth and PHA production. High salinity media oxygen saturation is considerably lower than fresh and salt water (3.5% total salts). With the selected salt concentration of 20% and temperature of 37 ˚C (at atmospheric pressure) for fermentation experiments, the saturated oxygen is approximately 2.5 mg/l. In comparison, the saturated oxygen for fresh water is appreciably higher at approximately 6.7 mg/l. A consensus control target for dissolved oxygen (DO) does not exist like for temperature and pH for *H. mediterranei* cultivation (Koller et al., 2005; Lillo & Rodriguez-Valera, 1990; Matarredona et al., 2021; Pais et al., 2016; Rodriguez-Valera et al., 1991). Researchers that employed shaker incubators used an agitation of 150-200 rpm for mixing and aeration (Cui, 2017; Pais et al., 2016). Wang (2021) studied the effects of having constant aeration of 2.5 volume of air sparged per unit volume of growth medium per minute (vvm) compared with controlling the DO above a 50% saturation level with forced aeration in batch experiments. Wang (2021) concluded that a higher PHA production rate could occur with the 2.5 vvm aeration control strategy compared to keeping the DO above 50%, but keeping the DO above 50% led to an increased cell growth rate. Koller et al. (2007b) also examined PHA production with hydrolyzed whey permeate substrate with three different PHA producers, including *H. mediterranei,* maintained a DO near 20% saturation level for the study.

2.9 Conclusions

This literature review detailed the feasibility and benefits of utilizing cheese byproducts such as delactosed permeate (DLP) for PHA production. Areas of additional research needed to improve this proposed process include studies with real-world cheese byproducts, nutrient optimization, and feeding strategy. After the production of PHA with cheese byproducts is better known then, further investigation of energy use and environmental impacts of the proposed process should also be studied. The identification of *H. mediterranei* as a PHA producer appropriate to use with hydrolyzed cheese byproducts, including DLP, was made with supporting rationale. To convert DLP into valuable PHA with *H. mediterranei,* pretreatment methods such as enzymatic hydrolysis were explored. The necessary nutrients and operating parameters for *H. mediterranei* growth and PHA production for subsequent fermentation experiments were determined.

Chapter 3. Polyhydroxyalkanoate Production by Extreme Halophile Archaea *Haloferax mediterranei* Using Hydrolyzed Delactosed Permeate and Synthetic Sugar Media

3.1 Abstract

Haloferax mediterranei (H. mediterranei) can consume monosaccharides, glucose and galactose. This chapter examined hydrolyzed cheese byproduct delactosed permeate (DLP) for *H. mediterranei* cell mass growth and PHA production. Glucose, galactose, and an artificial hydrolyzed lactose media, containing equal concentrations of glucose and galactose, were also studied to better understand the variance between these sugar-containing synthetic media and hydrolyzed real-world byproduct DLP. Enzymatic hydrolysis of DLP using commercially available acidic lactase enzyme was optimized. A centrifugation pretreatment step of the DLP resulted in improved enzymatic hydrolysis and cell growth of *H. mediterranei*. Hydrolyzed delactosed permeate was determined to produce higher final cell mass and PHA concentrations at an equal loading of 10 g/l of total sugars than the other three sugar media. The study demonstrated proof of concept that hydrolyzed DLP could be an effective, low-cost substrate for PHA production by *H. mediterranei*. The research also led to a better understanding and quantification of the differences between hexose glucose and galactose, and the benefits of utilizing cheese byproducts compared with synthetic sugar feedstocks for *H. mediterranei* growth and PHA production. The findings can help promote alternative uses for cheese byproducts such as DLP, producing more environmentally friendly materials and increasing sustainability in the dairy industry.

Key Words

Polyhydroxyalkanoates, *Haloferax mediterranei*, cheese byproduct, delactosed permeate

3.2 Introduction

Polyhydroxyalkanoates (PHA) are a family of high-value bioplastic materials that can replace traditional plastics in an environmentally friendly manner (Bernard, 2014). Although PHA is one of the fastest-growing bioplastics, production costs, including expensive feedstocks, limit its market growth (European Bioplastics, 2021; Nielsen et al., 2017). Several food wastes and byproducts have been studied to reduce the costs, including those from dairy processors (Alsafadi, Ibrahim, et al., 2020; Amaro et al., 2019; Koller, 2015b; Wang & Zhang, 2021). Recent studies that explored PHA production with cheese byproduct feedstocks with various PHA producers have utilized whey protein derivatives that have often gone through several pretreatment methods (Berwig et al., 2016; Valentino et al., 2015). These pretreatment steps can include costly ultrafiltration to remove proteins and spray-drying into powder products (Berwig et al., 2016; Pantazaki et al., 2009). Other research studies applied synthetic media containing either pure glucose and galactose or expensive hydrolyzed lactose powder that may not represent cheese byproducts (Koller et al., 2011; Wallner et al., 2001). Therefore, minimally processed real-world cheese byproducts should be studied for PHA production to understand the potential benefits for industry application (Amaro et al., 2019). Two such cheese byproducts are whey permeate and delactosed permeate (DLP). Cheese and whey processors generate whey permeate after the liquid whey separated from the cheese curds is concentrated with membrane filtration to produce whey protein powder (Oliveira et al., 2019). The whey permeate is the liquid that fluxes through the membrane systems containing most of the original lactose and minerals (Byylund, 2015). Some cheesemakers process the whey permeate into lactose powder with evaporator and dryer systems. The byproduct of the lactose powder, delactosed permeate or mother liquor, contains approximately one-third of the lactose and most of the minerals (Liang et al., 2009). Although some researchers studied producing PHA from whey permeate, no research exists for PHA production with DLP feedstock (Amaro et al., 2019; Koller et al., 2007a). Many cheesemakers sell the cheese byproducts as low-value animal feed, with DLP having a value

up to less than 10 times that of whey permeate (Liang et al., 2009; Wang et al., 2021). This difference in value between the cheese byproducts is due to DLP containing lower sugar concentrations than whey permeate and limitations for feeding DLP to livestock from its considerably higher mineral content (Liang et al., 2009; Oliveira et al., 2019). An economic analysis by Wang et al. (2021) demonstrated that DLP could result in the lowest breakeven cost of common cheese byproducts of less than $4/kg compared to whey permeate at $5-6/kg and lactose powder of $6-10/kg. Additionally, DLP does not have a widespread application to yield a value-added product like for other cheese byproducts, whey, and whey permeate (Oliveira et al., 2019; Smith et al., 2016). Therefore, DLP was selected for this study to observe if it could be an effective substrate for PHA production.

Researchers have studied numerous PHA producers with real-world, pretreated, and synthetic cheese byproducts. One organism, *Haloferax mediterranei (H. mediterranei)*, fits well with DLP. This ideal pairing is because *H. mediterranei* is an extreme halophile that grows in up to 20% salts and can tolerate DLP's high salt content that many other PHA producers cannot thrive in (Amaro et al., 2019; Ferre-Guell & Winterburn, 2018). Additionally, the archaea being an extreme halophile allows it to maintain a stable culture without an expensive sterility pretreatment step, and permits simple extraction of intracellular PHA with water addition causing cell lysis (Ghaly & Kamal, 2004). *H. mediterranei* cannot consume the lactose contained in cheese byproducts directly, like nearly all PHA producers, but can consume glucose and galactose present with the hydrolysis of the lactose. Therefore, hydrolysis of cheese byproducts such as DLP must first occur to convert the lactose into monosaccharide sugars glucose and galactose (Amaro et al., 2019). Limited DLP hydrolysis research has been conducted academically and in industry since there is no widespread use of the byproduct that requires hydrolysis pretreatment (Liang et al., 2009; Oliveira et al., 2019; H. Scott, personal communication, October 15, 2020). DLP contains high salt and suspended solids concentrations that could interfere with lactase enzyme activity (Oliveira et al., 2019; H. Scott,

personal communication, October 15, 2020). Therefore, testing of enzymatic hydrolysis of DLP with commercially available lactase enzyme should occur before applying the byproduct for PHA production. Centrifugation is one potential option to remove suspended solids from DLP if enzymatic hydrolysis issues occur (Byylund, 2015). The effects of this centrifugation pretreatment of hydrolyzed DLP on the fermentation of *H. mediterranei* should also be studied to assess the potential differences with and without the pretreatment.

Researchers have studied glucose extensively with reported PHA yields stated in the range of 0.07-0.33 g PHA/g glucose consumed and PHA contents of 17%-60% of total residual cell dry mass (Don et al., 2006; Lillo & Rodriguez-Valera, 1990; Melanie et al., 2018; Rodriguez-Valera et al., 1991). However, limited research exists for galactose substrate (Bonete et al., 1996; Rodriguez-Valera et al., 1980). Rodriguez-Valera et al. (1980) and Bonete et al. (1996) studied galactose consumption by *H. mediterranei* and concluded that the extreme halophile could utilize galactose, but at considerably slower rates than glucose. However, Rodriguez-Valera et al. (1980) and Bonete et al. (1996) did not measure growth kinetics or report standard parameters such as specific growth rate, final cell mass concentration, final PHA concentration, cell mass yield, PHA yield, and PHA content. Additionally, hydrolyzed cheese byproducts and synthetic hydrolyzed lactose media containing equal concentrations of glucose and galactose have been researched, but it is difficult to observe what impacts each sugar contributed independently from many of these studies (Amaro et al., 2019; Pais et al., 2016; Wallner et al., 2001). Pais et al. (2016) concluded that *H. mediterranei* could not use galactose for cell growth but could for polymer accumulation with the galactose contained in glucose and galactose mixtures. Since galactose represents 50% of the substrate of hydrolyzed dairy byproducts, further research is needed to understand galactose utilization to maximize PHA production.

The tasks of this research were to: 1) determine the best method to hydrolyze the lactose contained in DLP; 2) investigate hydrolyzed DLP as an effective substrate for *H. mediterranei* and PHA production and determine the sugar conversion efficiencies; 3) better understand the differences that exist between glucose and galactose for *H. mediterranei* growth and PHA accumulation. The study can help find more valuable uses for DLP that could be applied in industry to deliver a new value-added product for cheese makers and increase the global bioplastic production capacity.

3.3 Materials and methods

3.3.1 Culture medium and inoculum preparation

H. mediterranei (ATCC 33500) was cultivated in the highly saline (HS) minimum salt medium (MSM) as described by Fang et al. (2010), with the composition: NaCl, 156 g/L; $MgCl_2.6H_2O$, 13 g/L; $MgSO_4.7H_20$, 20 g/L; $CaCl_2.6H_20$, 1 g/L; KCl, 4 g/L; NaBr, 0.5 g/L. The cells were grown at a pH of 7.0 ± 0.2 and a temperature of 37 ℃. A micronutrient solution, SL-6, as described by Koller et al. (2005), was shown by Pais et al. (2016) to improve glucose consumption up to 0.1% and galactose consumption up to a 1.0% v/v loading. Therefore, SL-6 was provided at a loading of 1% v/v with the composition: $ZnSO_4.7H_20$, 100 mg/L; $MnCl_2.4H_2O$, 30 mg/L; H_3BO_3, 300 mg/L; $CoCl_2.6H_20$, 200 mg/L; $CuCl_2.2H_20$, 10 mg/L; $NiCl_2.6H_20$, 20 mg/L; $Na_2MoO_4.H_20$, 30 mg/L. Cells for inoculation were cultured in ATCC 1176 medium (ATCC, 2022) at 37℃. At the late exponential growth phase, the cells were harvested with centrifugation, resuspended in the HS media with SL-6 nutrients, as described above, and used in the following experiments.

3.3.2 PHA production using pure sugars glucose and galactose

Batch flask bioreactors were used for *H. mediterranei* PHA production. The flasks were operated with a working volume of 130 ml in a shaker incubator (New Brunswick Scientific, C24KC refrigerated incubator shaker, Edison, New Jersey, United States) controlled to a temperature of 37℃ and agitation at

180 rpm (Figure 3.1). *H. mediterranei* was cultured until the stationary phase was achieved after 240 hours. Glucose and galactose were utilized each at an initial concentration of 10 g total sugar/l and a combination of both (5 g/l of each sugar, named glucose + galactose) for the cultivation of *H. mediterranei*. The three sugar media were studied to better understand the differences between the two sugars present in hydrolyzed cheese byproducts and the difference between synthetic sugar media, and real-world cheese byproduct DLP. Ammonium chloride was added as the primary nitrogen source to give a C/N ratio of 8, which provided nitrogen at a loading shown by several researchers to be in the optimal range for *H. mediterranei* cell growth and PHA production (Cui, Shi, et al., 2017; Ferre-Guell & Winterburn, 2018; Lillo & Rodriguez-Valera, 1990). KH_2PO_4 was added as the primary phosphorus source to obtain a C/P ratio of 35, which provided an excess of phosphorus. Melanie et al. (2018) demonstrated that excess phosphorus was optimal for *H. mediterranei* cell growth and PHA production. Additionally, 1 g/l yeast extract was added as a complex nutrient source. Although some researchers have applied 5 g/l of yeast extract with comparable sugar loadings, a lower loading was selected to observe the effect of the sugars better since yeast extract contains nearly the same percent carbon as glucose and galactose (Alsafadi & Al-Mashaqbeh, 2017; Koller et al., 2007a; Lillo & Rodriguez-Valera, 1990; Melanie et al., 2018; Pais et al., 2016). The base for all sugar media contained HS MSM and SL-6 trace elements described above. Sodium bicarbonate was added as a buffer at a concentration of 2.5 g/l. The pH of the flask bioreactors was maintained at 7.0 ± 0.2 by adjusting the pH twice per day using 3M NaOH or 3M HCl.

Figure 3.1 Shaker incubator utilized for flask fermentation experiments.

3.3.3 PHA production with hydrolyzed cheese byproduct delactosed permeate

3.3.3.1 Delactosed permeate collection and characterization

The DLP was collected in the lactose plant of Hilmar Cheese Company, Hilmar, California. Enough DLP was collected from the same batch tank to use throughout all experiments. Two hundred milliliters of DLP samples were collected before and after centrifugation for characterization. The centrifugation pretreatment was facilitated with a bench-top centrifuge (Heraeus Multifuge X1R Thermo Scientific, Waltham, Massachusetts) at 5,000 rpm with a swinging bucket rotor for 30 minutes. The DLP with and without centrifugation were characterized for dry matter, moisture, ash, lactose, total nitrogen (TN), phosphorus, and soluble chemical oxygen demand (sCOD). The DLP lactose sugar was measured with high performance liquid chromatography (HPLC) equipped with a refractive index detector (RID) and photodiode array detector (PDA). The sugar analysis was conducted following an analytical method described by Sluiter (2008). A Biorad Aminex HPX-87H column (Hercules, California, United States) was used as the analytical column. A 5 mM H_2SO_4 solution was prepared and used as the mobile phase with a 0.6 ml/min flow rate. The oven temperature was controlled to 60 ℃ during HPLC analysis. Standard

chemical kits were used to measure sCOD and TN (COD digestion vials high range plus, TNTplus Vial Test, Hach Corp., Loveland, Colorado, United States). The total solids (TS), ash, and moisture were measured as described in the standard methods (American Public Health Association, 2012). Additionally, minerals sodium, magnesium, potassium, calcium, bromide, sulfur, chloride, and micronutrients zinc, manganese, cobalt, copper, nickel, and molybdenum were measured with inductively coupled plasma-mass spectrometry (ICP) following standard methods (US EPA, 1996).

3.3.3.2 Hydrolysis centrifugation pretreatment

H. mediterranei, like most PHA producers, cannot utilize lactose directly. Therefore, a hydrolysis pretreatment step is required to convert lactose in the DLP into monosaccharides glucose and galactose (Amaro et al., 2019). However, the DLP collected from Hilmar Cheese Company contained suspended particles, primarily from the feedstock's minerals and organic sources such as insoluble proteins (Oliveira et al., 2019). Divalent calcium and magnesium cations and phosphorus and carbonates anions can precipitate out of the solution, and potentially adsorb the lactase during enzymatic hydrolysis of DLP (Cao & Harris, 2008; Liang et al., 2009). The solids can also introduce impurities in PHA's downstream extraction and purification process. A preliminary hydrolysis experiment with centrifugation pretreatment was conducted to test the effects of suspended solids removal on enzymatic lactose hydrolysis.

The centrifuge operates by principles of Stoke's law which states that the separation of the suspended particles from the liquid occurs due to differences in density (Axelsson, 2010). The suspended solids settled to the bottom of the buckets during the process. The supernatant, free from most suspended solids, was decanted for hydrolysis (Figure 3.2). Acidic lactase enzyme Nola Fit 5550 (Chris Hansen, Hoersholm, Denmark) was kindly provided by Chris Hansen for DLP hydrolysis. The pH of the DLP with and without centrifugation was increased to 5.5 with 3 M NaOH to the optimal range stated by the

vendor. Thirty milliliters of the DLP sample were placed in 50 ml tubes for hydrolysis. Two enzyme loadings, 0.025 and 0.25 g of lactase enzyme per g of lactose, were applied to the DLP samples with the target of converting at least 92.5% of the lactose into glucose and galactose. The DLP with and without centrifugation containing the added lactase were placed in a shaker incubator for hydrolysis with a temperature of 40 ℃ and continuous agitation at 180 rpm. Samples of 0.5 ml were taken at 12 and 20 hours for sugar measurement. The lactose, glucose, and galactose were measured by HPLC, as described previously.

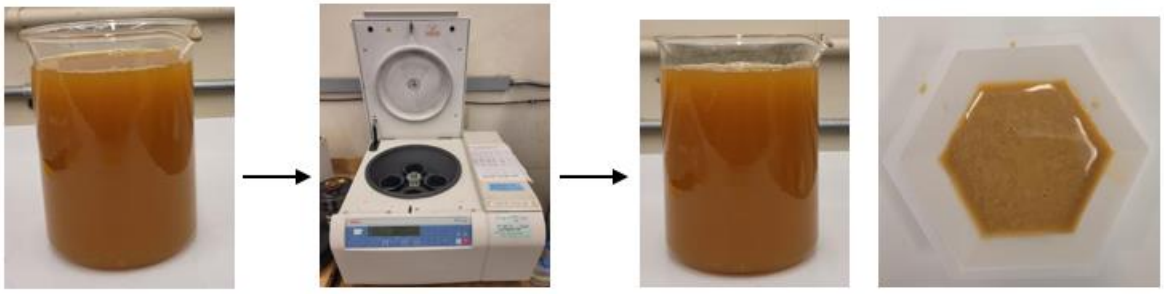

Figure 3.2 Centrifugation of DLP left) before centrifugation right) after centrifugation supernatant and solids.

3.3.3.3 Centrifugation pretreatment of hydrolyzed DLP for *H. mediterranei* PHA production

The suspended particles in the DLP could cause similar issues as hydrolysis, such as mass transfer limitations during *H. mediterranei* PHA production (Harju et al., 2012; H. Scott, personal communication, October 15, 2020). Therefore, a preliminary fermentation experiment with hydrolyzed DLP (HDLP) feedstock was conducted to determine if there were also benefits for *H. mediterranei* growth with centrifugation pretreatment of the hydrolyzed DLP. Hydrolyzed DLP, with and without centrifugation pretreatment, was used as *H. mediterranei* feedstock. The hydrolyzed DLP was loaded to give an initial

total sugar concentration of 10 g total sugar/l. Complex nutrient source yeast extract was loaded at 5 g/l as described by Pais et al. (2016) and Koller (2007a) to give a C/N ratio of 8. Salt nutrients were added to achieve the concentrations of the HS MSM stated and were determined by considering the concentrations of sodium, magnesium, potassium, bromide, calcium, and phosphorus already contained in the DLP. Similar amounts of sodium, magnesium, bromide, and chloride were added compared to the sugar media. However, less potassium and calcium, and no phosphorus, were added compared to the sugar media since DLP is rich in these mineral nutrients. Like the sugar media, a 1.0% v/v SL-6 micronutrient loading was added to the hydrolyzed DLP media. The pH of the flasks was corrected twice a day using 3 M HCl and 3 M NaOH. The optical density OD of the flasks was measured every other day, as described in the following sections. The final cell dry mass concentration, final PHA concentration, and PHA content were measured when the stationary phase was achieved after 408 hours, following methods described in the following sections.

3.3.3.4 Comparison of PHA production with hydrolyzed DLP and glucose and galactose feedstocks

In addition to the previously described glucose, galactose, and glucose+galactose feedstocks, the study investigated hydrolyzed DLP (HDLP) as a potential PHA feedstock. The centrifugation pretreatment was applied to the hydrolyzed DLP as described previously. The hydrolyzed DLP was added to the flasks to give an equivalent loading of 10 g total sugar/l. Salt nutrients were added to achieve the concentrations of the HS MSM stated and were determined by considering the concentrations of sodium, magnesium, potassium, bromide, calcium, and phosphorus already contained in the DLP, like for the centrifugation hydrolyzed DLP experiments. Like for the sugar media, 1.0% v/v loading SL-6 micronutrients was added to the hydrolyzed DLP media. Ammonium chloride was added as a supplementary nitrogen source, and a loading of 1 g/l of yeast extract was included in the hydrolyzed DLP media to achieve a C/N ratio of 8 and consistency across the different substrates tested. The same pH of 7.0 ± 0.2, incubator temperature of

37℃, and agitation of 180 rpm for the sugar feedstocks was also applied to the hydrolyzed DLP feedstock. *H. mediterranei* was cultured until reaching the stationary phase, which took approximately 240 hours.

3.3.4 Determination of cell dry mass and growth kinetics

Cell growth was monitored daily without disturbing the culture by sampling 1 ml of the fermentation broth daily. The optical density (OD) was measured for the samples at a wavelength of 520 nm in the red region of the visible light spectrum with a spectrophotometer (Hach, DR 2700 Loveland, Colorado, United States) as described by Huang et al. (2006). The final cell dry mass (CDM) after 240 hours of fermentation was measured as the fermentation broth volatile solids (VS). The VS was measured by collecting a 20 ml sample of the fermentation broth and applying centrifugation at 8,000 rpm for 30 minutes to separate the cells. The cell mass was washed with MSM solution twice. The washed cell mass was dried in an oven at 105 ℃ for 4 hours for total solids (TS) measurement and burned in a furnace at 550 ℃ for 2 hours to measure the volatile solids (VS) following standard methods (American Public Health Association, 2012).

3.3.5 Extraction, purification, and quantification of PHA

H. mediterranei accumulates PHA intracellularly, and lysis of the cells needs to occur to separate the PHA from the residual cell mass for quantification (Escalona et al., 1996). PHA extraction followed the methods outlined in the United States patent by Escalona et al. (1996), with modifications. A 20 ml fermentation broth sample was collected and centrifuged at 8,000 rpm for 30 minutes to separate the cell mass. The cell mass was then washed with a 0.1% sodium dodecyl-sulfate (SDS) and deionized water solution and subjected to vigorous vortexing for 2 minutes. The solution was incubated with the 0.1% SDS solution in a shaker incubator at 40℃ and continuous agitation at 180 rpm for 12 hours. The sample was centrifuged again at the same rotation speed and time as before, and the cell pellet was washed twice

with deionized water. The washed PHA was dried in an oven at 105 ℃ for 4 hours for total solids (TS) measurement and then burned in a furnace at 550 ℃ for 2 hours to measure the volatile solids (VS) following the same standard methods for cell dry mass (American Public Health Association, 2012). The PHA concentration was reported as VS (g VS/l).

The resultant PHA pellets from the extraction method were determined to be poly(3-hydroxybutyrate-co-3- hydroxyvalerate) (PHBV), typical of the archaea, using gas chromatography (GC) and a method developed by Wang and Zhang (2021) (Figure 3.3). A gas chromatograph (GC, Agilent 6890N, Santa Clara) equipped with a flame ionization detector (FID) was employed, and an HP-5 capillary column was used with helium carrier gas. Parameters of this method were: inlet temperature and pressure: 230℃, 16 psi; total flow rate: 30 mL/min; split ratio: 8:1; oven temperature: initial 100℃ for 2 mins; ramping from 100 to 124℃, with a rate of 8℃/min; holding 124℃ for 1 min. FID temperature was 240℃, with 40 mL/min of H_2 flow and 450 mL/min of airflow. Additionally, three PHBV standard granules containing 12% mol/mol of hydroxyvalerate HV (Sigma-Aldrich, 403105, St. Louis, United States) were measured as TS and VS following standard methods stated previously to confirm PBHV contained majorly VS (American Public Health Association, 2012). The PHBV granules were confirmed to be nearly all volatile solids (Table 3.1), with an average difference between the TS and VS of 1.2% ± 0.4%. Although TS was used to report PHA by Wang and Zhang (2021) and Wang (2022), VS was selected in the subsequent studies if the PHA wash step left residual salts from the high salinity media contributing to TS.

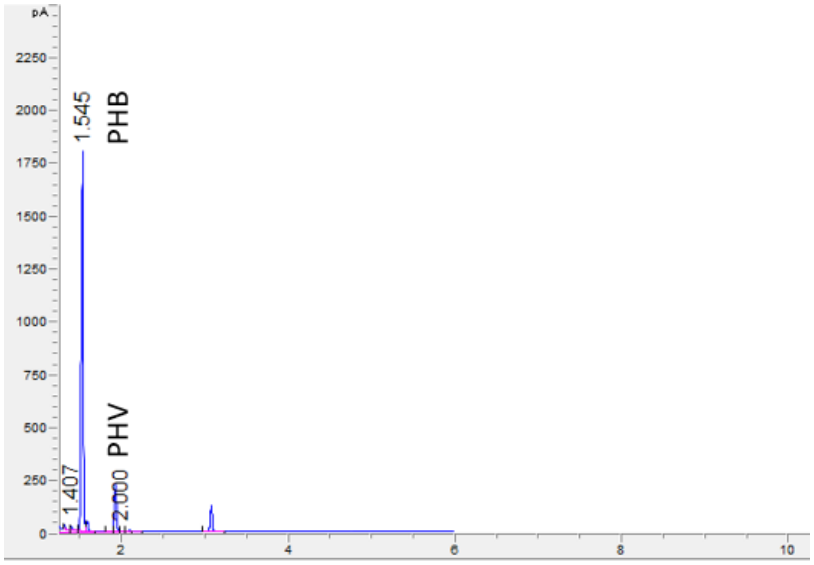

Figure 3.3 Poly(3-hydroxybutyrate-co-3- hydroxyvalerate) (PHBV) derived from *H. mediterranei* on delactosed permeate substrate gas chromatogram. Peaks are hydroxybutyrate (PHB) and hydroxyvalerate (PHV).

Table 3.1 Measured total solids (TS) and volatile solids (VS) of poly(3-hydroxybutyrate-co-3-hydroxyvalerate) (PHBV) standards.

PHBV standard sample	**Total solids (TS) (g)**	**Volatile solids (VS) (g)**	**% Difference between TS & VS**
1	0.0312	0.0307	1.6
2	0.0340	0.0337	0.9
3	0.0367	0.0357	2.7

3.3.6 Measurements of sugars lactose, glucose, and galactose

Lactose, glucose, and galactose were measured to monitor the consumption of the sugars during the fermentation experiment. One milliliter of fermentation broth was collected daily from the flask bioreactors for the sugar analysis. The samples were centrifuged at 12,000 rpm for 20 minutes to remove suspended solids and cell debris, and the supernatant was filtered through 0.22 µm membranes. The supernatant's lactose, glucose, and galactose were measured using high-performance liquid chromatography (HPLC). Characterization of the sugars was conducted using the method described by Sluiter (2008) as described previously for DLP sugar measurement.

3.3.7 Determination of cell dry mass yield, and PHA yield and content

From the cell dry mass (CDM) and HPLC sugar measured results, the CDM yield was determined as the mass of CDM grown divided by the mass of total sugars consumed as reported as g VS/g sugar consumed (Equation 3.1).

$$Y_{CDM} = \frac{\Delta m_{CDM}}{\Delta m_{total\ sugars}} \tag{3.1}$$

Based on the measured PHA results, the PHA yield was calculated as the mass of PHA accumulated divided by the mass of total sugars consumed reported as g VS/g sugar (Equation 3.2).

$$Y_{PHA} = \frac{\Delta m_{PHA}}{\Delta m_{total\ sugars}} \tag{3.2}$$

The cell PHA content was calculated as the percentage of PHA of the total CDM, reported as g VS/g VS (Equation 3.3).

$$PHA\ (\%) = \frac{m_{PHA}}{m_{CDM}} \times 100\% \tag{3.3}$$

3.3.8 Statistical analysis

The centrifugation pretreatment enzymatic hydrolysis and PHA fermentation experiments were duplicated, while the sugar fermentation experiments were conducted in triplicate. Each tests' mean and standard deviation (SD) were computed based on the respective duplicates or triplicates. The measured parameters were stated as the mean ± standard deviation. Pairwise comparisons of the final CDM concentration, final PHA concentration, and PHA content were conducted with t-tests for the hydrolyzed DLP centrifugation pretreatment fermentation study. One-way Analysis of Variance (ANOVA) and the Tukey test with pairwise comparisons were applied to determine the significant levels of the factors measured for the four sugar feedstocks. GraphPad Prism 10 software was used for experimental data analysis.

3.4 Results and discussion

3.4.1 Delactosed permeate characterization

Table 3.2 lists the main nutrient profile of delactosed permeate with and without centrifugation. Both forms of DLP contained high levels of lactose of around 15%, even though cheesemakers generate DLP after removing lactose from whey permeate to produce lactose powder (Liang et al., 2009). The lactose concentrations were similar in both samples since lactose is a soluble nutrient. Both samples also contained high ash levels due to DLP containing most of the salts initially present in milk after producing cheese, whey powder, and lactose powder (Smith et al., 2016). As shown in Figure 3.2, the DLP before and after centrifugation visually appeared similar. However, as observed at the bottom of the centrifuge bottles, notable solids were removed from the liquid. The removal of solids was confirmed with the total solids (w.b.) measurement, as the DLP with centrifugation contained about 5% less than the DLP. Both DLP with and without centrifugation also possessed nitrogen and high phosphorus levels. The DLP with and without centrifugation contained similar C/N ratios of ~24 and ~20, respectively. Therefore, more

nitrogen is needed for these feedstocks to obtain an optimal C/N ratio of <10 (Cui, Shi, et al., 2017; Ferre-Guell & Winterburn, 2018; Lillo & Rodriguez-Valera, 1990). The C/P ratios were also comparable for the DLP with and without centrifugation at ~10 and ~12, respectively. This phosphorous concentration provided an excess amount for *H. mediterranei* growth, which other researchers demonstrated can lead to improved cell growth and PHA production (Melanie et al., 2018). Therefore, sufficient phosphorus levels were already present in the DLP, and it was unnecessary to provide additional phosphorus salts when utilizing DLP as a feedstock at any dilution. Removal of insoluble phosphorus by centrifugation is the most likely reason for the lower phosphorus content in the DLP with centrifugation than without centrifugation (Leentvaar & Rebhun, 1982).

The mineral nutrients and micronutrients contained in MSM and SL-6 micronutrients were measured with ICP. Table 3.2 shows the measured nutrient concentrations of the DLP with and without centrifugation. Although the DLP, with and without centrifugation, contained high levels of minerals, considerably more salts must be added for *H. mediterranei* cultivation. For example, the DLP with and without centrifugation contained around 1% sodium and 0.05% magnesium, but around six and seven times more nutrients are required for MSM media, respectively. Also, no MSM constituent bromide was detected in the DLP with and without centrifugation. However, some nutrients such as potassium and calcium were present at higher concentrations in the DLP with and without centrifugation than required for MSM, around five times more for both elements. Therefore, even if diluted DLP is used for media preparation, these nutrients may be in adequate amounts. The DLP with centrifugation resulted in slightly lower mineral contents than the DLP with centrifugation, most likely due to inorganic solids being removed by centrifugation. The most notable micronutrients measured in the DLP feedstocks were zinc, manganese, boron, and copper. There is around 12 times more zinc, 11 times more boron, 4 times more manganese, and 30 times more copper in DLP, with and without centrifugation than what is provided with

1% v/v SL-6 media (Pais et al., 2016). However, the elevated levels of some of these micronutrients are not high enough to inhibit *H. mediterranei,* as reported by Nieto et al. (1987), who studied metal toxicity. *H. mediterranei* has a high tolerance to heavy metals compared to other halobacteria, where inhibition typically occurs in the 0.5-20 mM range depending on the specific element, considerably higher than the amounts contained in DLP (Matarredona et al., 2021; Nieto et al., 1987). There were also notable levels of micronutrients cobalt (about 20% of the cobalt contained in 1% v/v SL-6 solution) and molybdenum (similar in concentration to the molybdenum contained in a 1% v/v SL-6 solution) present in the DLP with and without centrifugation. The only major micronutrient that was not detected was nickel. Thus, DLP is also rich in micronutrients for *H. mediterranei* growth.

Table 3.2 Main nutrients of delactosed permeate (DLP) with and without centrifugation.

DLP without centrifugation		**DLP with centrifugation**	
Total solids	34.4*	Total solids	29.8*
Moisture	65.6*	Moisture	70.2*
Lactose	14.8*	Lactose	15.0*
Ash	9.5*	Ash	8.2*
Total C	6.0*	Total C	6.1*
Total N	0.25*	Total N	0.30*
Phosphorus	0.6*	Phosphorus	0.5*
SCOD	157**	SCOD	166**

* % (w.b.)

** unit for SCOD is g/l

Table 3.3 Minerals and micronutrients of delactosed permeate (DLP) with and without centrifugation.

DLP without centrifugation		**DLP with centrifugation**	
Sodium	0.96*	Sodium	0.78*
Magnesium	0.06*	Magnesium	0.05*
Potassium	1.11*	Potassium	0.80*
Calcium	0.11*	Calcium	0.09*
Bromide	0.00*	Bromide	0.00*
Sulfur	0.08*	Sulfur	0.06*
Chloride	1.02*	Chloride	0.83*
Zinc	2.87**	Zinc	2.41**
Boron	7.45**	Boron	5.77**
Manganese	0.21**	Manganese	0.30**
Cobalt	0.08**	Cobalt	0.12**
Copper	0.42**	Copper	0.50**
Nickel	0.00**	Nickel	0.00**
Molybdenum	0.07**	Molybdenum	0.11**

* % (w.b.)

** unit for micronutrients is mg/l

3.4.2 Centrifugation pretreatment of DLP

3.4.2.1 Effects of centrifugation pretreatment of DLP on enzymatic hydrolysis

Most PHA-producing microorganisms cannot directly convert lactose into PHA. Therefore, lactose contained in the DLP must first be hydrolyzed into monosaccharides glucose and galactose for *H.*

mediterranei consumption (Amaro et al., 2019). DLP with and without centrifugation were enzymatically hydrolyzed to observe if centrifugation pretreatment was necessary for effective lactose hydrolysis. Two levels of enzyme loading, 0.025 and 0.25 g lactase/g lactose, and time points, 12 and 20 hours, were tested to determine the appropriate levels of these two parameters to achieve a target conversion of > 92.5% lactose to glucose and galactose. Figure 3.4 presents the hydrolysis efficiency versus time for the DLP with and without centrifugation. With the loading of 0.025 g lactase/g lactose, the DLP with centrifugation resulted in a hydrolysis efficiency of 93.3% ± 3.5% and 94.3% ± 2.8% after 12 and 20 hours, respectively. The DLP without centrifugation hydrolysis efficiency was considerably lower at 38.3% ± 3.4% and 53.4% ± 7.6% at 12 and 20 hours, respectively. Extending the hydrolysis time by an extra 8 hours at this level of enzyme loading had a minimal impact on the hydrolysis efficiency for the DLP with centrifugation, resulting in a mere 1.0% increase. In contrast, the DLP without centrifugation showed a considerable improvement, with a 15% increase in hydrolysis efficiency. For the higher loading of 0.25 g lactase/g lactose after 12 hours, the DLP with centrifugation resulted in a hydrolysis efficiency of 95.0% ± 0.7%, over double that of the DLP without centrifugation at 40.2% ± 6.1%. Like the lower enzyme loading, an additional 8 hours of hydrolysis time for the DLP with centrifugation resulted in only a 2% increase in hydrolysis efficiency. However, 8 additional hours of hydrolysis time for the DLP without centrifugation resulted in a hydrolysis efficiency that was more than 30% greater, reaching 72.2 ± 0.7%. The hydrolysis efficiency of the DLP without centrifugation with the loading of 0.25 g lactase/g lactose was nearly 20% more than that found with the loading of 0.025 g lactase/g lactose. Based on the observed difference in lactose hydrolysis efficiency between the two loadings and reaction time for the DLP without centrifugation, it can be inferred that the decrease in hydrolysis efficiency for the DLP without centrifugation can be compensated by increasing both the lactase enzyme loading and the duration of the reaction. Nevertheless, the DLP without centrifugation hydrolysis efficiency with the 0.25 g lactase/g

lactose loading and 20-hour incubation time was approximately 20% more than the hydrolysis efficiency of the DLP with centrifugation and the same conditions.

Since the experiment aimed to achieve at least 92.5% hydrolysis of lactose, the DLP centrifugation pretreatment was conducted in experiments moving forward. Additionally, the loading of 0.025 g lactase/g lactose for 12 hours was applied to future experiments given that these parameters resulted in the hydrolysis goal with only marginal improvements observed for the 20 hours of hydrolysis time and increased loading of 0.25 g lactase/g lactose. The lower loading would require less enzyme and reduce production costs than the ten-fold more 0.25 g lactase/g lactose loadings. The two tested enzyme loadings resulting in similar hydrolysis efficiencies suggest that a lower enzyme loading could be applied while still achieving a hydrolysis efficiency of >92.5%. This additional enzyme loading optimization could further reduce enzyme costs.

a)

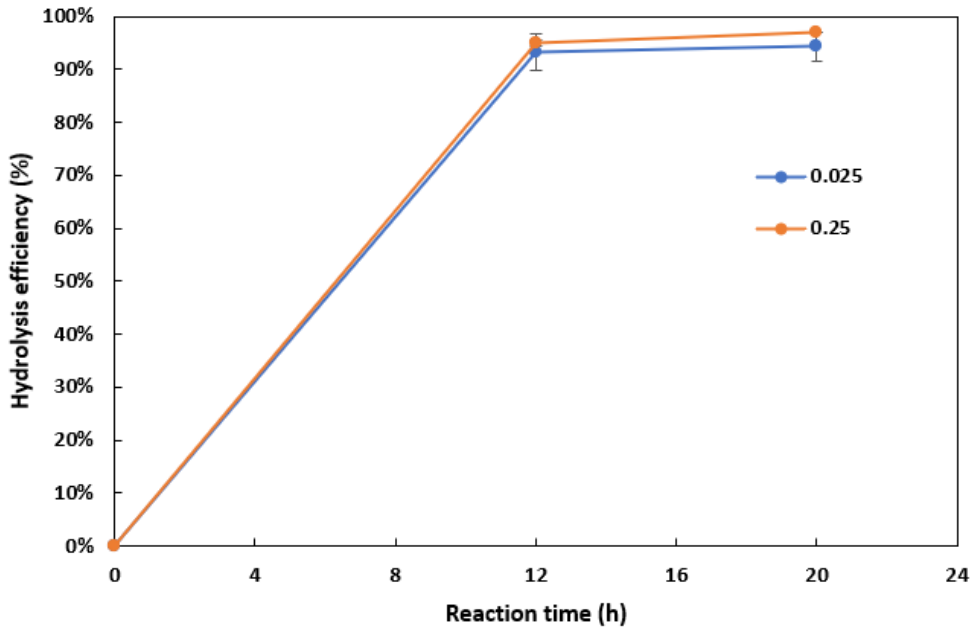

b)

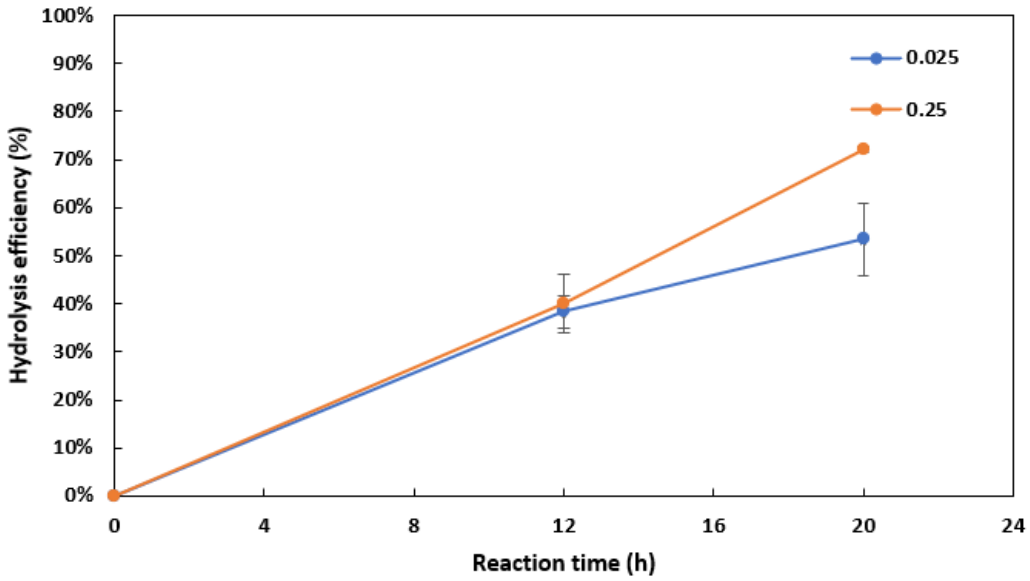

Figure 3.4 Lactose hydrolysis efficiency with different enzyme loadings (0.025 and 0.25 g lactase/g lactose): a) for DLP with centrifugation, and b) DLP without centrifugation. Y-error bars are standard deviations.

3.4.2.2 Effects of centrifugation of hydrolyzed DLP on cell growth and PHA production

Figure 3.5 presents the *H. mediterranei* cell growth time profile or optical density (OD) versus time utilizing hydrolyzed DLP (HDLP) with and without centrifugation feedstock. The OD was measured on days 0 and 1 and then every 48 hours. Both feedstocks exhibited a lag phase of 24 hours. Between hours 24 and 72, the HDLP with centrifugation OD increased at a greater rate than the HDLP without centrifugation. After 72 hours, both feedstocks entered the exponential phase of growth, potentially due to the archaea acclimating to the complex feedstock. The HDLP with centrifugation measured ODs were only slightly greater than the HDLP without centrifugation for all values up to 168 hours. Then, after 168 hours of growth, the HDLP with centrifugation ODs started to be considerably greater than the HDLP without centrifugation. The final OD for the HDLP without centrifugation was 9.5 ± 0.2, and the HDLP with

centrifugation was greater at 12.0 ± 0.5. The HDLP with centrifugation reached the stationary phase faster than the HDLP without centrifugation after 312 hours of growth compared to 360 hours.

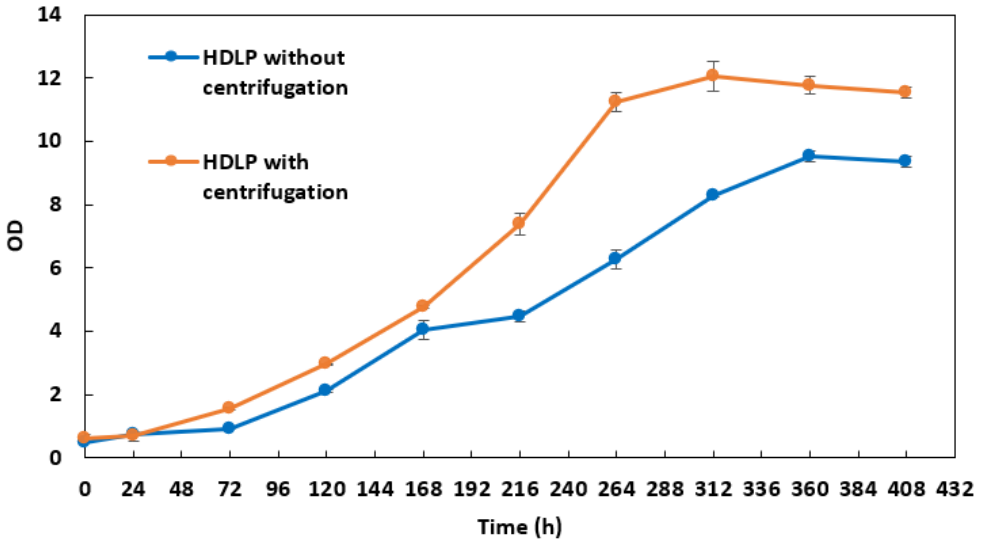

Figure 3.5 *H. mediterranei* cell growth over time with hydrolyzed DLP (HDLP) with and without centrifugation pretreatment. Y-error bars are standard deviations.

Figure 3.6 displays the two hydrolyzed DLP (HDLP) feedstock's final cell dry mass concentration, final PHA concentration, and PHA content. The final cell dry mass (CDM) concentration of the HDLP was 5.9 ± 0.2 g VS/l, significantly greater (p-value = 0.0152) than the HDLP without centrifugation at 5.0 ± 0.1 g VS/l. The final CDM concentration agreed with the final ODs of the two feedstocks. Similarly, the final PHA concentration of the HDLP with centrifugation was 2.9 ± 0.2, significantly greater (p-value = 0.0371) than the HDLP without centrifugation at 2.3 ± 0.1. The PHA content of the HDLP with centrifugation was 45% ± 2%, and the HDLP without centrifugation was marginally greater at 49% ± 1%. The PHA contents of the two feedstocks were not significantly different (p-value= 0.1982). These increases in cell growth and

PHA production with the HDLP with centrifugation compared to without confirmed using the centrifugation pretreatment of the DLP before hydrolysis and PHA fermentation.

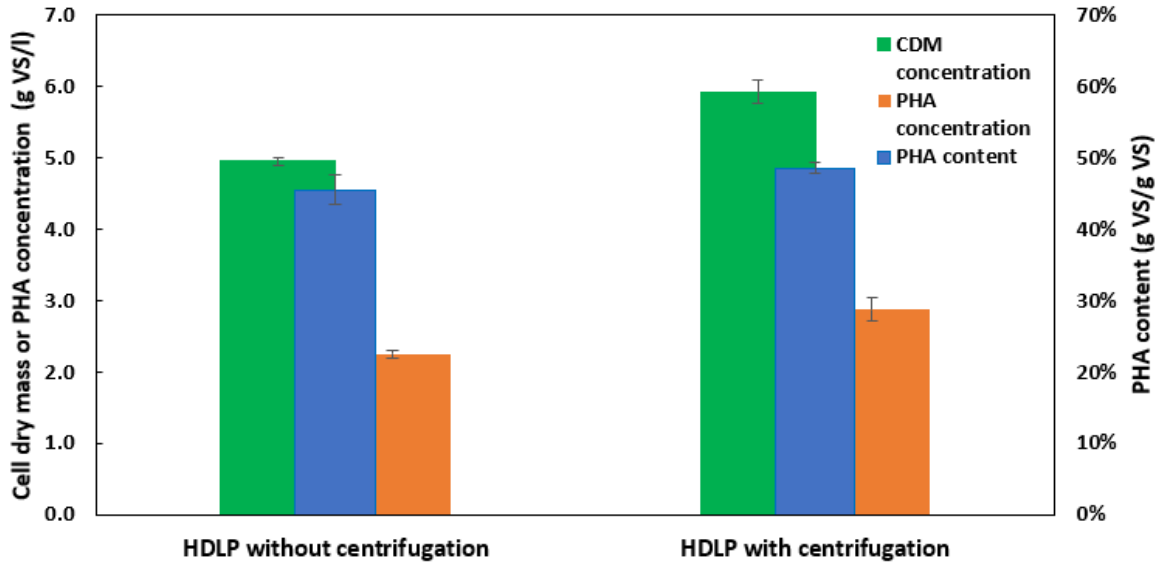

Figure 3.6 *H. mediterranei* final cell dry mass (CDM) concentration, final PHA concentration, and PHA content with hydrolyzed DLP (HDLP) substrate with and without centrifugation pretreatment. Y-error bars are standard deviations.

3.4.3 Cell growth and PHA production by *H. mediterranei* with various sugar substrates

3.4.3.1 Effects of sugar source on cell growth

H. mediterranei successfully grew with all four feedstocks: glucose, galactose, glucose + galactose, and hydrolyzed DLP (with centrifugation pretreatment) (HDLP). Figure 3.7 shows the flasks at the fermentation's start and end. All four feedstocks resulted in pink cultures being present at the end of the fermentation signaling effective growth of the archaea. The pink color is due to carotenoids naturally produced by *H. mediterranei* that, in the wild, provide UV protection from sunlight (Kushwaha et al., 1974). Different shades of pink were present for the different substrates. The glucose and glucose +

galactose feedstocks resulted in a similar dense pink color typically observed for the halophile (Figure 3.8a and c) compared to the HDLP which resulted in a darker color (Figure 3.8d). Other compounds in the DLP can most likely explain this color difference that the other sugar media did not possess. Initially, the glucose and galactose-loaded media were colorless since all nutrients added were white except for the yeast extract (straw in color) loaded at a low enough level that only a minor color change occurred (Figures 3.8a-c). In comparison, the HDLP possessed a yellow-brown color, initially, due to the inherent constituents that DLP contains. Delactosed permeate is a yellow-brown color due to Maillard reaction products produced during high-heat evaporation steps that occur during lactose crystallization (Smith et al., 2016; Zadow, 2012). Additionally, carotenoids such as beta-carotene are present in DLP from the milk it originally derives from, also contributes to its yellow color (Lappa et al., 2019). Although the sole galactose flasks turned pink, it was a noticeably fainter shade of pink (Figure 3.6b). This lighter shade of pink implied that less cell mass growth occurred with galactose substrate, and *H. mediterranei* may not prefer galactose substrate. This result agreed with Rodriguez-Valera et al. (1980), who noted that 22 halophiles grew more slowly on galactose than glucose sugar.

Figure 3.8 shows the cell growth time profile or OD versus time for the different sugar feedstocks. The HDLP feedstock's final OD was 9.3 ± 0.2, the highest of the four feedstocks tested. The glucose and glucose + galactose feedstocks had similar final ODs of 6.0 ± 0.0 and 5.9 ±0.1, respectively. The galactose feedstock's final OD was 2.8 ± 0.3, considerably lower than the three other feedstocks that contained glucose. The galactose and HDLP substrate exhibited a lag phase of 24 hours, but the glucose and glucose + galactose flasks did not show a lag phase as indicated by the nearly doubling of the OD in the first 24 hours. The glucose and glucose + galactose had nearly identical increases in OD throughout the length of the fermentation. The HDLP flasks had comparable ODs to the other glucose-containing media after 72 hours of growth, with ODs near a value of 3.0. The lower OD observed for the HDLP in the first 72 hours

of growth compared to the other glucose-containing feedstocks may be due to limitations from the complexity of the substrate, such as other non-sugar constituents that are present. However, after hour 72, the HDLP substrate continued its high growth rate during the exponential growth phase, while the glucose and glucose + galactose flasks continued at a more moderate growth rate. Conversely, the galactose flasks had considerably lower growth rates than the other sugar media, which only slightly increased to an OD of 1.8 ± 0.2 by hour 96. The galactose flasks also reached the stationary phase much faster after 144 hours of growth, while the glucose-containing feedstocks continued to grow for an extended period, reaching the stationary phase after 240 hours of growth.

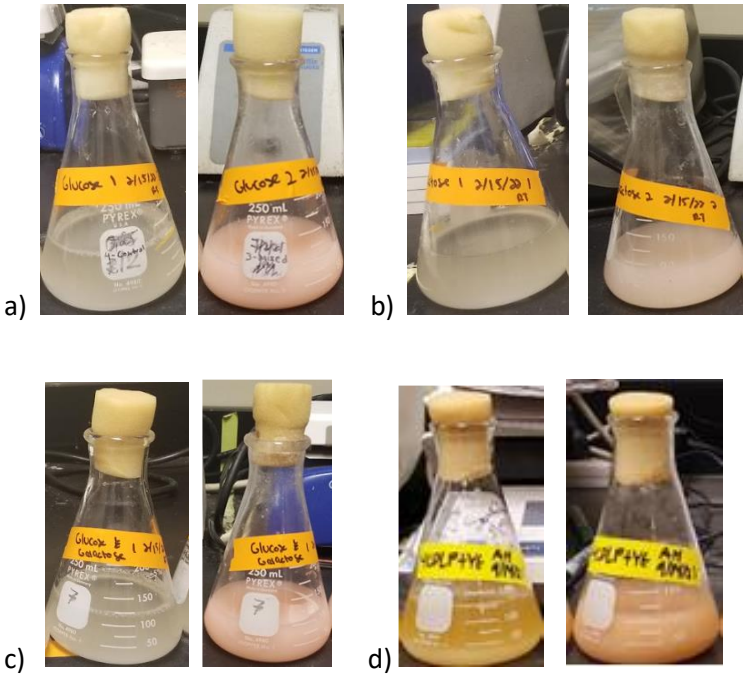

Figure 3.7 Fermentation flasks with various sugar substrates. For the flask pairs, left is day 0, and right is the end of the fermentation; a) glucose; b) galactose; c) glucose and galactose; d) hydrolyzed DLP.

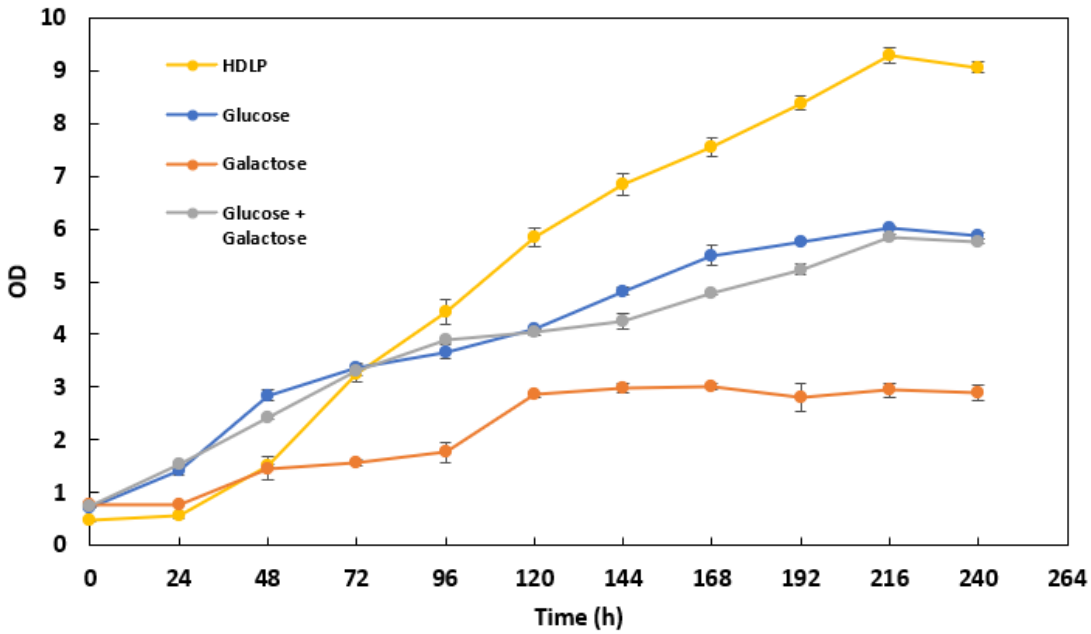

Figure 3.8 *H. mediterranei* cell growth curves with sugar feedstocks hydrolyzed DLP (HDLP), glucose, galactose, glucose and galactose. Y-error bars are standard deviations.

Figure 3.9 presents the analogous final cell dry mass (CDM) concentrations and yields for the four sugar substrates (glucose, galactose, glucose + galactose, and hydrolyzed DLP). As expected, the final CDM concentrations followed similar trends as the observed final ODs. One-way ANOVA demonstrated that the final CDM concentrations and CDM yields of the four feedstocks were significantly different (final CDM concentration p-value < 0.0001) (CDM yield p-value < 0.0001), and a pairwise comparison with the Tukey test was performed. The HDLP final CDM concentration was 3.9 ± 0.0 g VS/l, the highest of the four feedstocks tested. The glucose and glucose + galactose final CDM concentrations were similar at 3.3 ± 0.1 and 3.2 ± 0.1 g VS/l, respectively. The galactose final CDM concentration was 1.3 ± 0.1 g VS/l, the lowest of the feedstocks and approximately one-third of that of the HDLP. The glucose final CDM concentration was significantly greater than the final galactose CDM concentration (p-value < 0.0001). This difference between the two monosaccharides further supported that *H. mediterranei* utilizes glucose more

effectively than galactose, with more than double the CDM obtained with glucose than galactose. *H. mediterranei*'s glucose dehydrogenase enzyme can metabolize both glucose and galactose. However, the glucose dehydrogenase enzyme has an appreciably higher affinity for glucose than sugars with different C2, C3, and C4 configurations, such as the orientation of the hydroxyl group (OH) in galactose at C4 (Bonete et al., 1996). The glucose final CDM concentration was not significantly greater than the glucose + galactose (p-value = 0.2917). However, the HDLP final CDM concentration was significantly greater than all the other three feedstocks (HDLP and glucose p-value < 0.0001) (HDLP and galactose p-value < 0.0001) (HDLP and glucose + galactose < 0.0001). Therefore, HDLP appears to be an effective substrate for *H. mediterranei* growth.

The cell dry mass yield followed a different trend than the final ODs and cell dry mass concentrations of the four different sugar substrates. The glucose + galactose CDM yield was 0.52 ± 0.01 g VS/g total sugar, the highest of the four feedstocks. The HDLP CDM yield was 0.49 ± 0.00 g VS/g total sugar, and the galactose CDM yield was 0.34 ± 0.01 g VS/g total sugar. The glucose CDM yield was 0.32 ± 0.00 g VS/g total sugar, the lowest of the feedstocks. Although the galactose final CDM concentration was significantly less than the glucose final CDM concentration, the galactose CDM yield was not significantly different (p-value = 0.6263) than the glucose CDM yield. Thus, it appears galactose, when consumed by *H. mediterranei,* can effectively produce cell mass, but at considerably slower rates than glucose. The HDLP and glucose + galactose CDM yields were significantly greater than the glucose CDM yield (HDLP and glucose p-value < 0.0001) (glucose and glucose + galactose p-value < 0.0001). Therefore, for the dual sugar feedstocks, a greater percentage of carbon consumed by *H. mediterranei* appears to have been diverted toward *H. mediterranei* growth compared with the pure glucose feedstock.

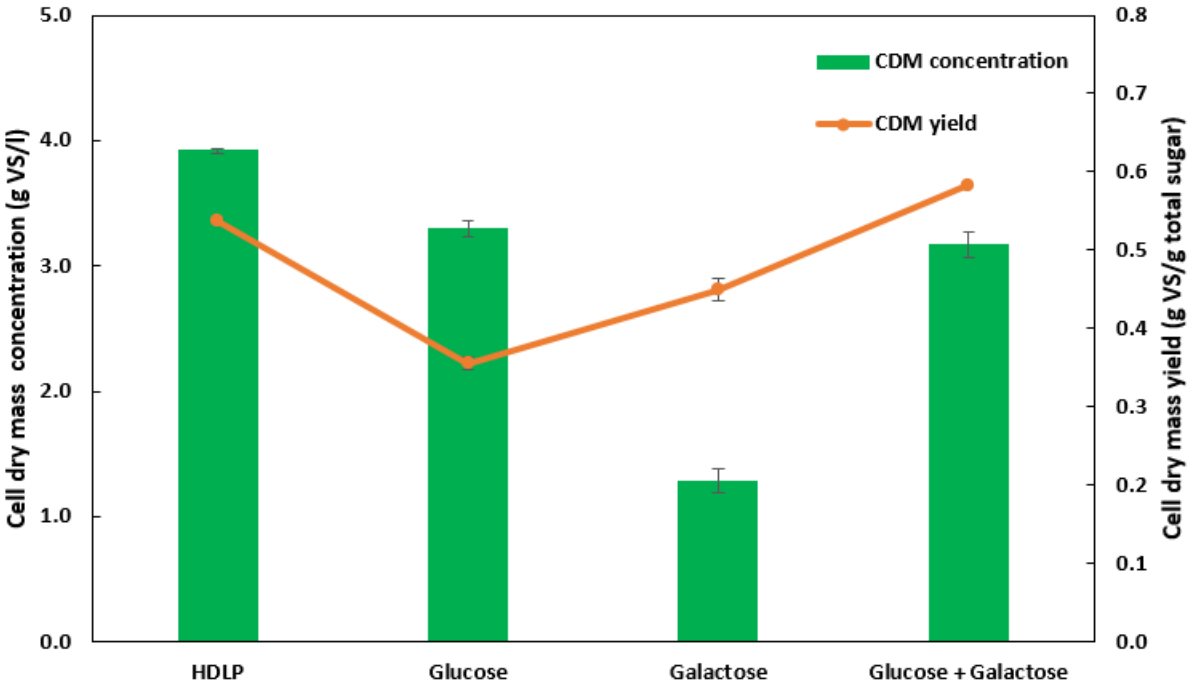

Figure 3.9 Final *H. mediterranei* cell dry mass (CDM) concentration and yield with sugar feedstocks, hydrolyzed DLP (HDLP), glucose, galactose, and glucose and galactose. Y-error bars are standard deviations.

3.4.3.2 Effects of sugar substrate on PHA production

Figure 3.10 displays the corresponding final PHA concentrations and PHA yields for the four sugar feedstocks. One-way ANOVA demonstrated that the final PHA concentrations and PHA yields of the four feedstocks were significantly different (final PHA concentration p-value < 0.0001) (PHA yield p-value < 0.0001), and a pairwise comparison with the Tukey test was performed. The final PHA concentration exhibited a similar trend to the final cell dry mass concentration. Like the final CDM concentration, the final PHA concentration was the highest for HDLP at 2.6 ± 0.1 g VS/l, followed by similar measurements for the glucose and the glucose + galactose at 2.3 ± 0.1 and 2.2 ± 0.1 g VS/l, respectively. The galactose final PHA concentration was 0.7 ± 0.1 g VS/l, significantly less than the glucose (p-value < 0.0001). The

glucose-containing feedstocks resulting in greater final PHA concentrations demonstrate that glucose may be more effective for PHA production than galactose. Also, like for the final CDM concentration, the final PHA concentration of the glucose was not significantly different than the glucose + galactose (p-value = 0.3881). The HDLP final PHA concentration was significantly greater than the three other feedstocks (HDLP and glucose p-value = 0.0229) (HDLP and galactose p-value < 0.001) (HDLP and glucose + galactose p-value = 0.0027). The higher PHA concentrations achieved by the HDLP feedstock compared with the synthetic sugar feedstocks demonstrate that hydrolyzed DLP is an effective substrate for *H. mediterranei* PHA production. The similarities between the final CDM and PHA concentration results can most likely be explained by *H. mediterranei* PHA production is growth or partially growth-associated (Cui, Shi, et al., 2017; Wang & Zhang, 2021). Therefore, the PHA trends should generally follow the CDM trends, given that other factors are nearly constant.

The PHA yields followed a different trend than the final PHA concentrations but were comparable to the CDM yield trend. The glucose + galactose PHA yield was 0.40 ± 0.05 g VS/g total sugar, the highest PHA yield of the feedstocks tested. The HDLP PHA yield was 0.33 ± 0.01 g VS/g total sugar. The glucose and galactose PHA yields were similar at 0.24 ± 0.01 and 0.21 ± 0.01 g VS/g total sugar, respectively. The PHA yield of the glucose and HDLP was within the range reported by other researchers who studied glucose feedstocks of 0.07-0.33 g PHA/g glucose consumed, demonstrating HDLP could lead to effective PHA production compared to commonly applied glucose (Don et al., 2006; Lillo & Rodriguez-Valera, 1990; Melanie et al., 2018; Rodriguez-Valera et al., 1980, 1991). The PHA yields of the glucose and the galactose were determined not to be significantly different from each other (p-value = 0.5481). This result differed from what was established for the final PHA concentration of the two hexoses. Although less galactose appears to have been consumed by *H. mediterranei,* causing a lower final PHA concentration than glucose, the galactose consumed by *H. mediterranei* appears to lead to a similar PHA accumulation. Other

researchers who studied *H. mediterranei* growth with galactose substrate source did not determine the amount and yield of PHA that could be obtained with galactose (Bonete et al., 1996; Rodriguez-Valera et al., 1980). Both multi-sugar feedstocks, HDLP and glucose + galactose, had significantly higher PHA yields than glucose (HDLP and glucose p-value = 0.0048) (glucose + galactose and glucose p-value = 0.0363).

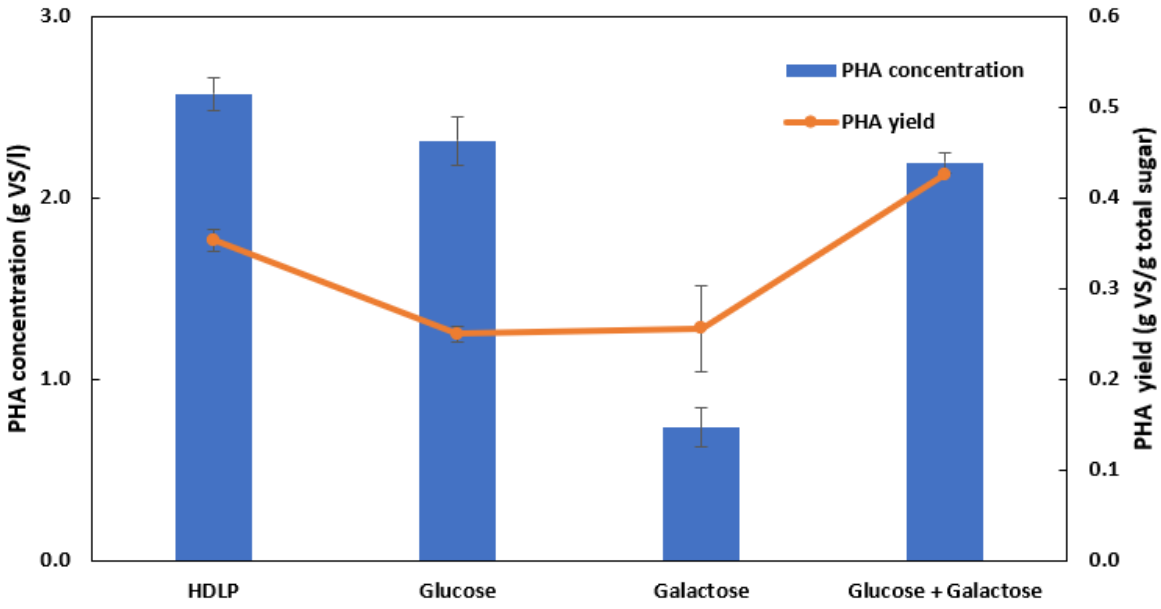

Figure 3.10 Final PHA concentration and PHA yield by *H. mediterranei* with sugar feedstocks, hydrolyzed DLP (HDLP), glucose, galactose, and glucose and galactose. Y-error bars are standard deviations.

3.4.3.3 Effects of sugar substrate on PHA content

PHA content is the amount of the total cell dry mass that is PHA product. Higher values indicate a greater diversion of carbon to the desired PHA product than waste residual cell mass. Figure 3.11 displays the PHA contents of the four sugar substrates. One-way ANOVA demonstrated that the PHA contents of the four feedstocks were significantly different (p-value < 0.0064). All glucose-containing feedstocks possessed similarly high PHA contents. The glucose PHA content was 0.70 ± 0.04 g VS/g VS, the glucose +

galactose was 0.69 ± 0.02 g VS/g VS, and the HDLP was 0.66 ± 0.02 g VS/g VS. The HDLP was not significantly different from the glucose or glucose + galactose (HDLP and glucose p-value = 0.4219) (HDLP and glucose + galactose p-value = 0.6043). These PHA contents were on the higher end of the range of PHA contents reported by other researchers with sugar-containing substrates 0.18-0.88 g PHA/g CDM (Koller et al., 2007a, 2007b; Lillo & Rodriguez-Valera, 1990; Melanie et al., 2018; Pais et al., 2016). The galactose possessed the lowest PHA content of 0.57 ± 0.06 g VS/g VS but was still within the normal range of PHA contents stated by others. The galactose PHA content was significantly less than the glucose (p-value = 0.0074). Therefore, less PHA accumulation may occur with galactose than with glucose.

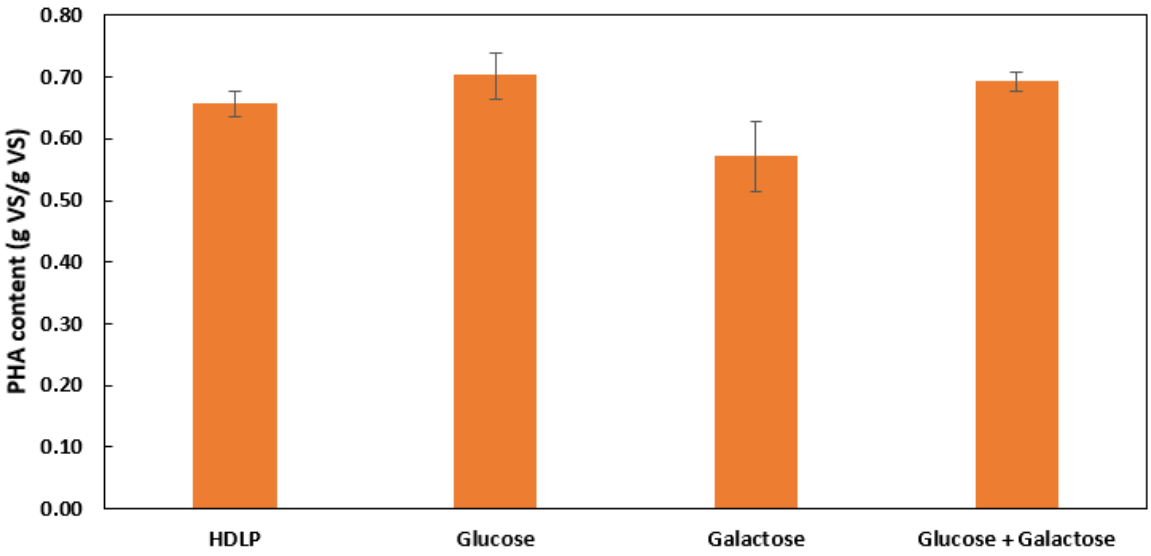

Figure 3.11 Final PHA content by *H. mediterranei* with various sugar feedstocks, hydrolyzed DLP (HDLP), glucose, galactose, glucose and galactose. Y-error bars are standard deviations.

3.4.3.4 Effects of sugar substrate on monosaccharide consumption

Figure 3.12 displays the total sugar consumption at the end of the fermentation of the four sugar-containing feedstocks. The total sugar consumption is the sum of glucose and galactose consumption for

the multi-substrate sugar feedstocks. The glucose had a sugar consumption of 93% ± 2%, the greatest of the sugar feedstocks. This result was expected since *H. mediterranei's* glucose dehydrogenase enzyme has the greatest affinity for glucose of the numerous sugars it can metabolize (Bonete et al., 1996). The HDLP resulted in a sugar consumption of 73% ± 1%. This total sugar consumption was slightly higher than what Pais et al. (2016) found using hydrolyzed cheese byproduct whey at 33%-66%. The glucose + galactose resulted in a total sugar consumption of 53% ± 1%. Since the HDLP and glucose + galactose contained the same initial concentrations of glucose and galactose, it appears that the other constituents contained in DLP may improve sugar consumption. This result agreed with Pais et al. (2016), who found that hydrolyzed whey resulted in greater sugar consumption than synthetic hydrolyzed dairy feedstocks containing glucose and galactose at similar initial concentrations. This improvement in sugar consumption by hydrolyzed cheese byproducts may be due to other nutrients in whey-derived byproducts, such as trace minerals, vitamins, and other co-factors (Oliveira et al., 2019; Pais et al., 2016). The galactose possessed the lowest total sugar consumption at 28% ± 3 %. This result further illustrated that sole galactose is not an effective substrate for *H. mediterranei* PHA production.

Figures 3.13 and 3.14 present the glucose and galactose consumption for the relevant feedstocks that contained these respective sugars. Glucose consumption was high for all feedstocks that contained the sugar at > 93%. Galactose consumption was considerably lower than glucose consumption for the galactose-containing feedstocks. The galactose consumption of HDLP was 46% ± 3 %, the highest of the three galactose-containing feedstocks. The galactose consumption of the sole galactose feedstock was 28% ± 3%, and 13% ± 2% for glucose + galactose feedstock. Therefore, some differences between the glucose + galactose and HDLP final CDM and PHA concentrations may be linked to the improved galactose consumption with the HDLP. Additionally, with the glucose + galactose feedstock, although galactose was present that the culture could have continued to consume for further cell growth, the culture instead

reached the stationary phase consuming a minimal amount of the available galactose. It appears *H. mediterranei* will only consume galactose if certain environmental conditions are present.

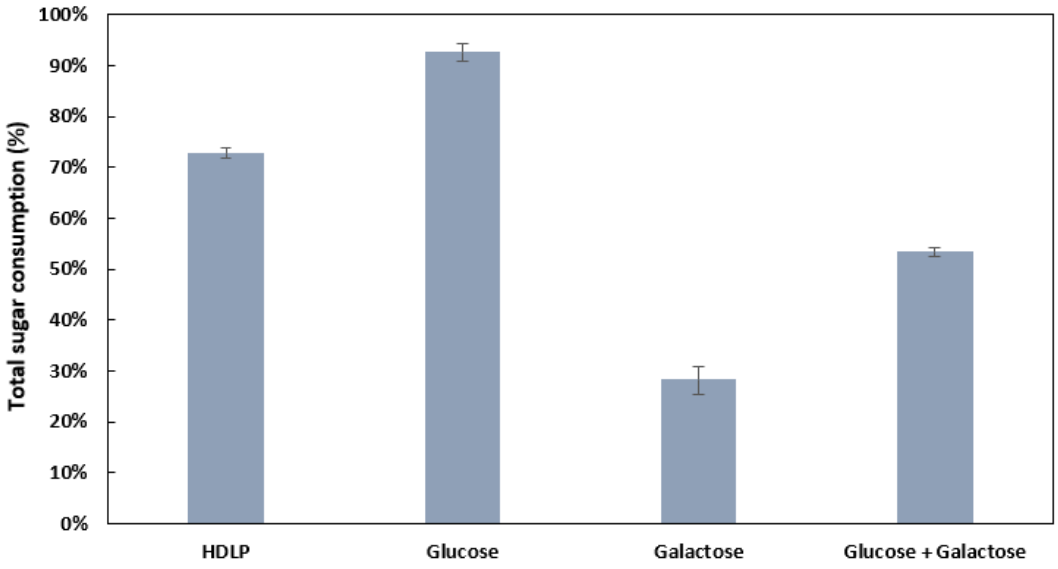

Figure 3.12 *H. mediterranei* total sugar consumption with various sugar feedstocks, hydrolyzed DLP (HDLP), glucose, galactose, and glucose and galactose. Standard deviation error bars are shown.

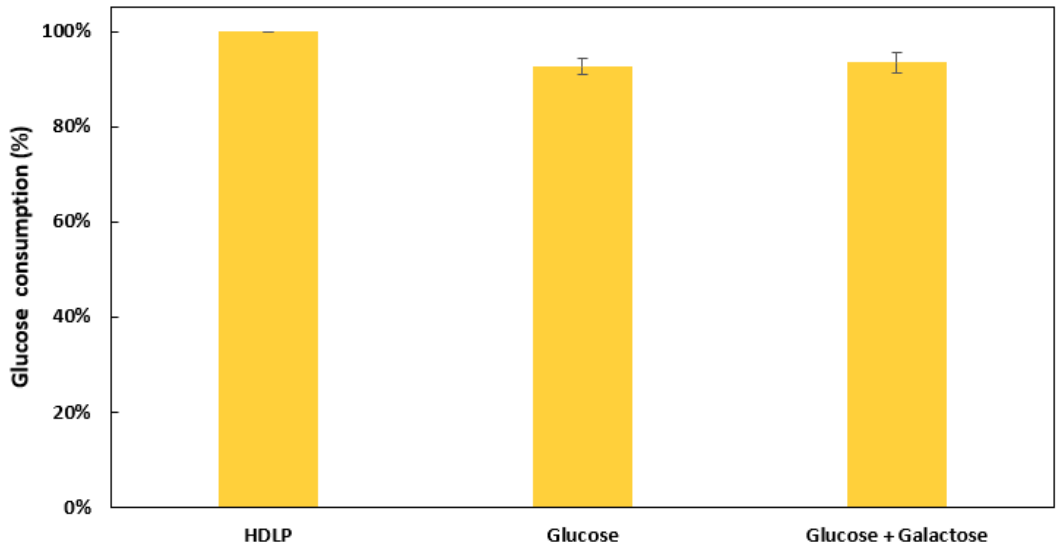

Figure 3.13 *H. mediterranei* glucose consumption with glucose-containing feedstocks, hydrolyzed DLP (HDLP), glucose, and glucose and galactose. Y-error bars are standard deviations.

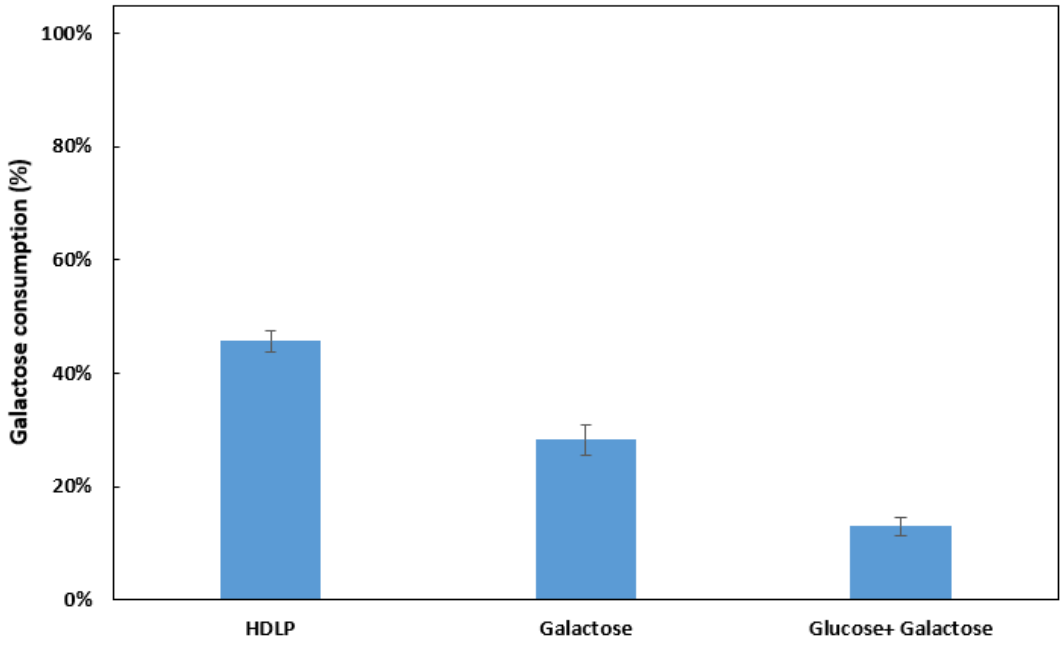

Figure 3.14 *H. mediterranei* galactose consumption with galactose-containing feedstocks, hydrolyzed DLP (HDLP), galactose, and glucose and galactose. Y-error bars are standard deviations.

The sugar concentration time profiles for the single sugar feedstocks containing either glucose or galactose are shown in Figure 3.15. For the sole glucose feedstock, the glucose consumption corresponded well with when OD was increasing, e.g., the first 192 hours resulted in nearly linear increases in OD and decreases in glucose concentration. However, in the last 48 hours, the OD increased minimally while some glucose consumption continued to be observed. This result indicated that the sugar consumed at the end of the fermentation was not primarily going toward cell growth as at the beginning. The stationary phase was achieved for the glucose when nearly all had been consumed, with < 1.2 g/l remaining. The galactose feedsock also had similar OD and substrate consumption trends as expected. In

the first 72 hours for the sole galactose feedstock, the OD increased marginally, while the galactose consumption was also low. However, from hours 72 to 120, a considerable OD increase was observed, with over half of the total galactose consumed during fermentation occurring in these 48 hours. This change in galactose consumption rate may have been caused by *H. mediterranei* acclimating to the galactose present in the environment. A further experiment was conducted to explore this observed phenomenon. The galactose OD reached the stationary phase after 120 hours. Less than 0.5 g/l galactose consumption occurred during the last 120 hours of the fermentation.

Figure 3.18 shows the sugar concentration time profile for the multi-sugar glucose + galactose and HDLP feedstocks where both changes in glucose and galactose can be observed. For both multi-sugar feedstocks, the glucose was first consumed, and the galactose was consumed after the glucose had been depleted. This result agreed with what Pais et al. (2016) found when glucose and galactose substrates were present together. However, for the HDLP, the glucose was consumed faster, with nearly all the glucose being consumed after 96 hours for the HDLP versus 168 hours for the glucose + galactose. Additionally, for glucose + galactose, the steady increase in OD for the first 168 hours appears to align with when *H. mediterranei* was consuming glucose. Then after hour 168, only a small amount of galactose was consumed (< 0.5 g/l), and the OD minimally increased correspondingly. However, for the HDLP, although the greatest increases in OD occurred while the glucose was consumed, the OD continued to increase while the galactose was consumed from hours 96 to 216. The increase in galactose consumption appears to have contributed to the higher final cell mass and final PHA concentrations that were found for the HDLP than the glucose + galactose. Since the major difference between the HDLP and glucose + galactose is other nutrients present in the cheese coproduct compared to the synthetic media, these nutrients may aid galactose consumption.

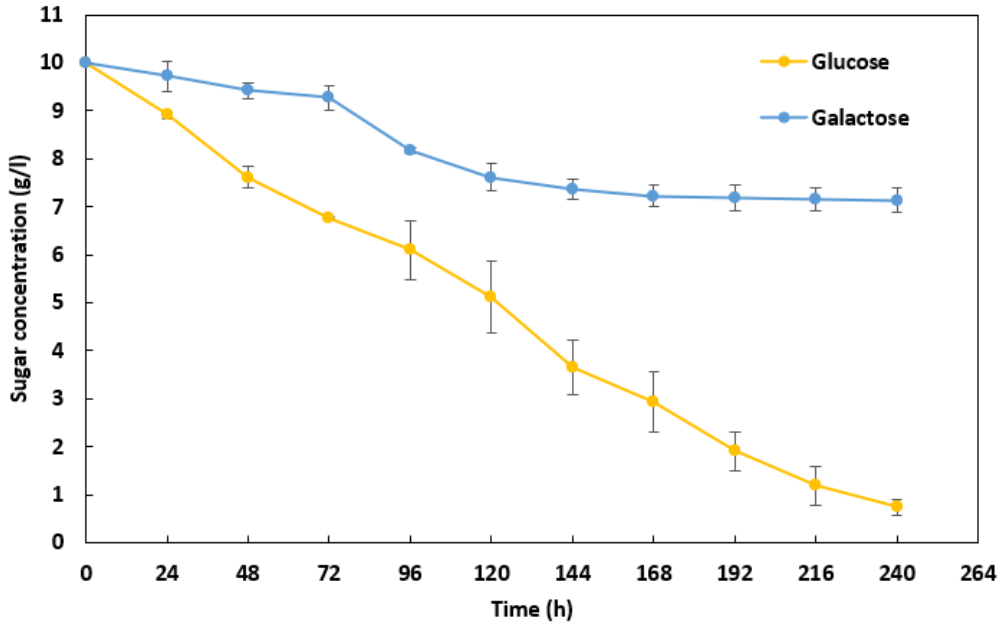

Figure 3.15 *H. mediterranei* sugar concentration time profiles for glucose and galactose feedstocks. Y-error bars are standard deviations.

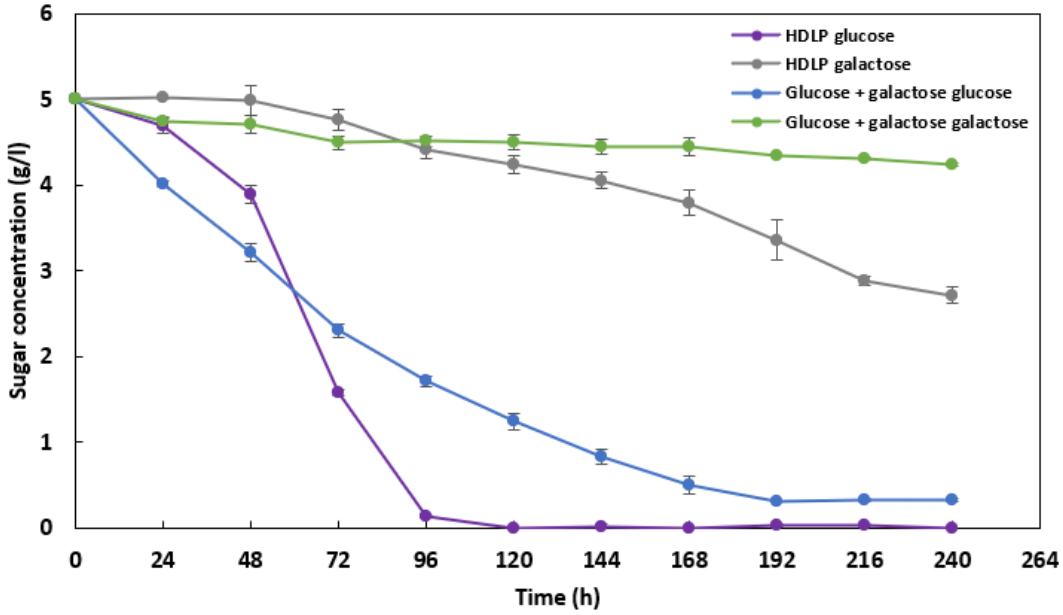

Figure 3.16 *H. mediterranei* sugar concentration time profiles for hydrolyzed DLP (HDLP), and glucose and galactose feedstocks. Y-error bars are standard deviations.

3.5 Conclusions

Lactase enzyme Nola Fit 5550 could be applied to hydrolysis cheese byproduct delactosed permeate (DLP). It was determined that the lactase enzyme could effectively hydrolyze the lactose contained in DLP with centrifugation pretreatment at a loading of 0.025 g lactase/g lactose and shaking incubation at 40 ℃ for 12 hours. *H. mediterranei* successfully grew on all four sugar-containing feedstocks (hydrolyzed DLP, glucose, galactose, an equal glucose and galactose combination) with hydrolyzed DLP, resulting in significantly greater final cell mass and PHA concentrations than the three other sugar feedstocks and comparative cell mass and PHA yields. Glucose was the preferred substrate over galactose by *H. mediterranei*. Glucose consumption was considerably higher than galactose consumption in all cases ranging from 93%-100% versus 11%-46% for galactose. Further research is needed to increase galactose consumption and utilization by *H. mediterranei* to PHA to improve PHA yields from hydrolyzed dairy substrates. This study provided proof of concept that hydrolyzed delactosed permeate could effectively be employed with *H. mediterranei* to obtain high PHA concentrations, PHA yields, and sugar consumption. PHA production from low-value cheese byproducts could lead to an additional revenue stream by cheesemakers growing the dairy market and expanding the PHA bioplastic market, leading to sustainable and more environmentally benign materials. The results of the experiments could be applied to other dairy byproducts through further research.

Chapter 4. Effect of Organic and Inorganic Nitrogen Source on Polyhydroxyalkanoates Yields Using Delactosed Permeate by Extreme Halophile Archaea *Haloferax mediterranei*

4.1 Abstract

From the previous chapter, it was demonstrated that synthetic hydrolyzed dairy media containing glucose and galactose, in addition to real-world cheese byproduct delactosed permeate (DLP), were viable carbon sources to grow *Haloferax mediterranei* (*H. mediterranei*) with high PHA yields. The tasks of this study were to explore the effect of incorporating yeast extract and ammonium chloride on the *H. mediterranei* media for improving the PHA yields using hydrolyzed DLP as the main carbon source. DLP was pretreated with centrifugation before the hydrolysis of the lactose into monosaccharides glucose and galactose via lactase enzyme. Three hydrolyzed DLP media were tested with equal loadings of 10 g total sugar/l total and were supplemented with different nitrogen sources at equivalent C/N ratios of 8. The first tested media contained 5 g/l of yeast extract, the second ammonium chloride, and the last an equal nitrogen loading of yeast extract and ammonium chloride. The production costs of the hydrolyzed DLP feedstocks were compared to determine which was the most economical. The results demonstrated that similar cell dry mass and PHA yields could be obtained with hydrolyzed DLP supplemented with inorganic ammonium chloride nitrogen source compared to yeast extract. The hydrolyzed DLP supplemented with ammonium chloride also resulted in the lowest feedstock costs. Therefore, ammonium chloride could be more favorable as a nitrogen source. The results of the study can help create economic PHA production with cheese byproducts by reducing feedstock costs growing the dairy industry and creating a circular economy.

Keywords: Polyhydroxyalkanoates, delactosed permeate, yeast extract, *Haloferax mediterranei*

4.2 Introduction

Plastic production, an integral part of the global economy, primarily depends on fossil fuel feedstocks. Most traditional plastic products end up in landfills or the ocean, further causing environmental issues (Geyer et al., 2017). These environmental problems associated with conventional plastics have led to considerable growth in the bioplastic market with production expected to increase from 2.4 million tons in 2022 to 6.9 million in 2027 (European Bioplastics, 2023). One of the fastest-growing bioplastics is polyhydroxyalkanoates (PHA) due to its unique characteristics of being a tunable plastic that can be used for numerous applications, having the ability to biodegrade in terrestrial and ocean environments at ambient temperatures, and is more heat stable than many other bioplastics (Bugnicourt et al., 2014; Raza et al., 2018). PHA have a high value of $5-10/kg, and their production is expected to more than double by 2027 (European Bioplastics, 2023; Roland-Holst et al., 2013). PHA production occurs by microbial fermentation of organic matter into bioplastic compounds that are naturally used by the organism as an energy source. The PHA can then be extracted from the cells and purified to yield a powder or granules for additional processing into commercial products. The high production cost of PHA is the main constraint for further market expansion with expensive substrate accounting for up to 40% of total operational costs (Nielsen et al., 2017). Therefore, there has been substantial research to reduce PHA production costs by utilizing low-value food byproducts and wastes to lower substrate costs (Alsafadi, Ibrahim, et al., 2020; Amaro et al., 2019; Koller, 2015b).

Whey and whey byproducts from cheese makers can be used to produce bioplastic. Worldwide, it is estimated that 120 million tons of whey are produced per year. Only about half of the whey is processed into a useful form for human or animal consumption, with the rest ending up as waste material contributing to high carbon emissions (Nikodinovic-Runic et al., 2013). Although some cheese manufacturers can create food ingredients, such as whey protein concentrates and lactose powder from

these byproducts (Figure 4.1) (Byylund, 2015), market limitations and capital cost investments prevent all cheese manufacturer byproducts from being utilized for animal or human consumption (Oliveira et al., 2019). Additionally, for cheese manufacturers who produce whey and lactose products, there are crystallization limitations to how much lactose can be recovered for food products leading to one-third of the lactose remaining as delactosed permeate (DLP) still being sold as low-value animal feed or disposed of as waste (Liang et al., 2009). DLP is the only cheese byproduct without a widespread commercial application and therefore, represents an opportunity for biomaterial production (Oliveira et al., 2019). Several microorganisms have been studied to attempt to convert cheese byproducts into PHA, but one organism, *H. mediterranei,* appears to be a good fit with cheese byproducts (Amaro et al., 2019). This pairing is due to *H. mediterranei* being an extreme halophile that grows in high-salinity environments with up to 20% salts (Ferre-Guell & Winterburn, 2018). The high saline environment allows straightforward incorporation of waste or byproducts, since many common contaminants present cannot survive these harsh conditions (Amaro et al., 2019; Lillo & Rodriguez-Valera, 1990). Therefore, a costly sterility step, common for food wastes and byproducts, is not required before fermentation (Amaro et al., 2019; Koller et al., 2011). The straightforward inclusion of high salt-containing cheese byproducts can also occur as these salt nutrients are needed for *H. mediterranei* growth (Amaro et al., 2019; Lillo & Rodriguez-Valera, 1990). Lastly, intracellular PHA extraction can occur via simple water addition, causing cell lysis from osmotic shock rather than using expensive chemicals that are often environmentally malign (Byrom, 1987; Ghosh et al., 2019).

Most PHA production research with *H. mediterranei* and cheese byproducts has been focused on lactose powder and pretreated whey, with little research on raw byproducts, whey and whey permeate, and no research to my knowledge on DLP (Amaro et al., 2019; Koller, 2018). Although delactosed permeate contains nitrogen from whey protein-derived sources, its C/N ratio is moderately high at

approximately 20. DLP's C/N ratio contrasts with the ideal C/N ratio that other researchers have found with glucose sugar substrate at <10 (Cui, Shi, et al., 2017; Ferre-Guell & Winterburn, 2018; Wang, 2021). Likewise, for PHA production from similar upstream cheese byproduct whey, researchers often add supplementary nitrogen sources (Amaro et al., 2019; Pais et al., 2016) even though whey contains a low C/N ratio of approximately 9 (Byylund, 2015). It appears that *H. mediterranei* media with cheese byproducts should contain additional nitrogen to obtain a low C/N ratio <10. Few studies have been conducted with *H. mediterranei* with hydrolyzed cheese byproducts. For those studies that have been conducted with cheese byproducts, whey and whey permeate, yeast extract was applied as a nitrogen source at high rates of up to 5 g/l yeast extract per 8-12 g total sugar/l provided by hydrolyzed cheese byproducts. High PHA yields of 0.29-0.78 g PHA/g of sugar consumed were obtained with these hydrolyzed cheese byproduct feedstocks supplemented with yeast extract (Koller, 2015a; Koller et al., 2007b; Pais et al., 2016). Additionally, Alsafadi et al. (2020a) studied the effect of three nitrogen sources: yeast extract, ammonia chloride, and an equal mixture of yeast extract and ammonium chloride, on the PHA yield from *H. mediterranei* media using glucose as a substrate. The authors showed that the media with yeast extract and ammonium chloride, and solely yeast extract yielded the greatest PHA production compared to the ammonium chloride counterpart. However, yeast extract is expensive and can cost up to $3.85/kg (Maddipati et al., 2011). Therefore, its use in commercial PHA production should be avoided.

Besides organic nitrogen source yeast extract, other nitrogen sources that *H. mediterranei* can utilize are inorganic ammonium and nitrate (Esclapez et al., 2014; Ferre-Guell & Winterburn, 2018). Esclapez et al. (2014) found nearly triple the specific growth rate with *H. mediterranei* using ammonium compared to nitrate nitrogen source with 5 g/l glucose as a substrate. Ammonium chloride has been well studied as a nitrogen source for the cultivation of *H. mediterranei* since early research in the 1990s with sugar-containing carbon sources (Alsafadi & Al-Mashaqbeh, 2017; Cui, Shi, et al., 2017; Lillo & Rodriguez-

Valera, 1990; Pire et al., 2014). The chloride ions in ammonium chloride are also required in high concentrations for the halophile media (Koller et al., 2007a). Alternatively, ammonium sulfate contains slightly less nitrogen at 21% compared to ammonium chloride at 24%. Ammonium sulfate is comparable in cost and is less studied than ammonium chloride. Consequently, ammonium sulfate does not appear to offer benefits over ammonium chloride. Similarly, alternatives organic urea and inorganic ammonium nitrate are not well studied and are more costly (Alibaba a., 2023; Alibaba b., 2023; Esclapez et al., 2014; Lillo & Rodriguez-Valera, 1990; USDA, 2023). Therefore, ammonium chloride was the main nitrogen source utilized in this study to compare against yeast extract that has been demonstrated to result in effective PHA production via *H. mediterranei* in hydrolyzed cheese byproduct feedstocks.

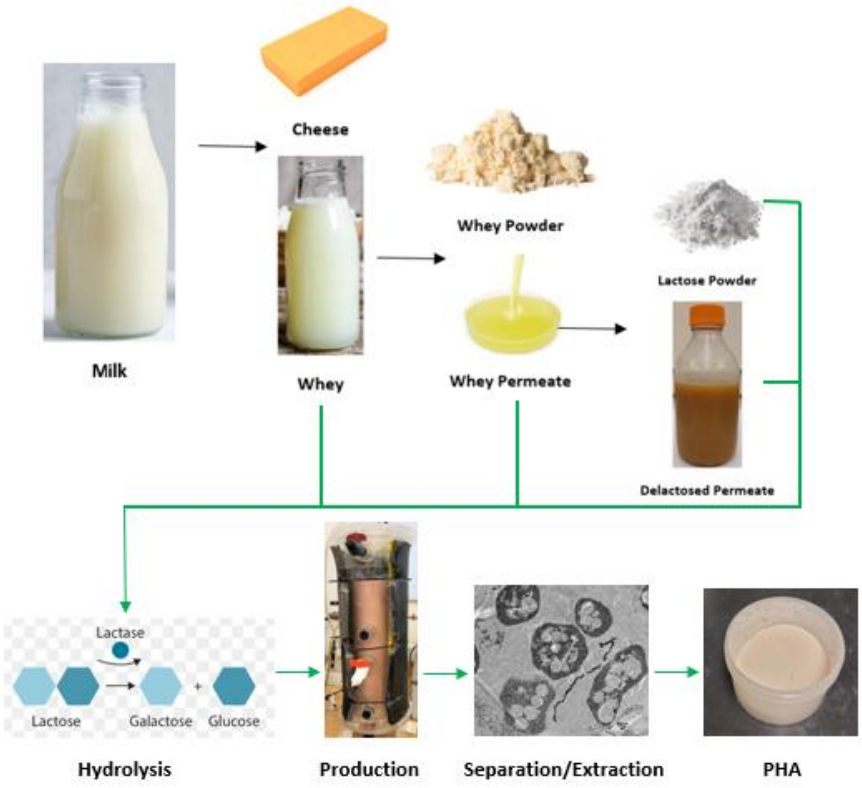

Figure 4.1 Cheese production from milk input with associated byproducts proposed for *H. mediterranei* PHA production.

The tasks of this study were to: 1) evaluate the effects of yeast extract and ammonium chloride as nitrogen supplement on *H. mediterranei* and PHA production; 2) assess the feedstock cost of DLP supplemented with yeast extract and ammonium chloride.

4.3 Materials and methods

4.3.1 Delactosed permeate collection

The DLP was collected in the lactose plant of Hilmar Cheese Company, Hilmar, California. DLP was the stream generated after whey permeate, a byproduct of whey powder, has been processed to create lactose powder. The whey permeate is concentrated with evaporator processes to crystallize the lactose, which is then further dried and milled to produce a high-purity lactose powder product. However, due to solubility limits, not all the lactose can be crystallized out of the whey permeate (Byylund, 2015; Oliveira et al., 2019). This crystallization limitation leads to the remaining liquid, DLP, containing high levels of lactose in addition to most of the minerals initially present in the whey permeate. Therefore, lactose is the main nutrient in DLP, and the byproduct also contains some organic nitrogen and minerals, including phosphorus, sodium, and potassium (Liang et al., 2009). The DLP composition was previously characterized in Chapter 3 for main nutrients, minerals, and trace elements.

4.3.2 Delactosed permeate pretreatment

Centrifugation, shown in Chapter 3, was demonstrated to assist with both lactase hydrolysis and improve *H. mediterranei* cell growth with delactosed permeate substrate. The separation process was again applied in this study and was facilitated with a bench-top centrifuge (Heraeus Multifuge X1R Thermo Scientific, Waltham, Massachusetts) at 5,000 rpm with a swinging bucket rotor for 30 minutes. The liquid on the top of the bottles was decanted from the solids that settled for further use. The centrifuged DLP was then hydrolyzed with lactase enzyme Nola Fit 5550 (Chris Hansen, Hoersholm, Denmark) with a 0.025

g lactase/g lactose loading. The centrifuged DLP containing the lactase enzyme was placed in an incubator shaker with a temperature of 40 ℃ and continuous agitation at 180 rpm for 12 hours, as described in Chapter 3. The resultant centrifuged hydrolyzed DLP was utilized as the main substrate for *H. mediterranei*.

4.3.3 Measurement of yeast extract properties and fermentation substrate consumption

Similar methods that were used to characterize the main nutrient profile for DLP in Chapter 3 were applied to yeast extract. The dry matter, moisture, and ash were measured by following standard methods (American Public Health Association, 2012). Total organic carbon (TC) and total nitrogen (TN) were measured with the standard test kits (High Range Test 'N Tube method, Hach Corp., Loveland, Colorado) (TNTplus Vial Test, Hach Corp., Loveland, Colorado, United States). The phosphorus was measured with inductively coupled plasma-mass spectrometry (ICP). The soluble chemical oxygen demand (sCOD) for a 5 g/l loading of yeast extract; and the fermentation broth at the start and the end of the experiment were also measured with standard test kits (COD digestion vials high range plus, Hach Corp., Loveland, Colorado, United States). Before using the kits, 2 ml of samples were collected and then centrifuged for 10 minutes at 12,000 rpm to remove cell debris. Glucose and galactose were also measured for the fermentation broth at the start and end of the experiment, with high-performance liquid chromatography (HPLC) equipped with a refractive index detector (RID) and photodiode array detector (PDA). An analytical method described by Sluiter (2008) was followed for the HPLC sugar analysis. A Biorad Aminex HPX-87H column (Hercules, California, United States) was used as the analytical column. A 5 mM H_2SO_4 solution was prepared and used as the mobile phase with a flow rate of 0.6 ml/min. The oven temperature was controlled to 60 ℃ during HPLC analysis.

4.3.4 Microbial culturing and PHA production

The wild-type strain *H. mediterranei* (ATCC 33500) was grown with highly saline (HS) minimum salt medium (MSM) as outlined by Fang et al. (2010), with the composition: NaCl, 156 g/L; $MgCl_2.6H_2O$, 13 g/L; $MgSO_4.7H_2O$, 20 g/L; $CaCl_2.6H_2O$, 1 g/L; KCl, 4 g/L; NaBr, 0.5 g/L. The cells were grown at a neutral pH of 7.0 ± 0.2 and a temperature controlled at 37 ℃. A micronutrient solution, SL-6, as described by Koller et al. (2005), was also provided at a loading of 1% v/v, demonstrated by Pais et al. (2016) to lead to improved sugar consumption with synthetic media and hydrolyzed cheese byproducts. The composition of the SL-6 was as follows: $ZnSO_4.7\ H_20$, 100 mg/L; $MnCl_2.4H_2O$, 30 mg/L; H_3BO_3, 300 mg/L; $CoCl_2.6H_20$, 200 mg/L; $CuCl_2.2H_20$, 10 mg/L; $NiCl_2.6H_20$, 20 mg/L; $Na_2MoO_4.H_20$, 30 mg/L. For inoculum preparation, the cells were cultured in ATCC 1176 medium (ATCC, 2022) at 37℃, as described in Chapter 3.

Centrifuged and hydrolyzed delactosed permeate, also named hydrolyzed DLP, was used as feedstock to culture *H. mediterranei* for PHA production. The hydrolyzed DLP was equally loaded at 10 g total sugar/l for all media containing the hydrolyzed cheese byproduct. Three nitrogen sources were tested for the DLP feedstocks: yeast extract (HDLP+YE), an equal mass yeast extract and ammonium chloride mixture (HDLP+YE+NH_4Cl), and ammonium chloride (HDLP+NH_4Cl). Yeast extract was loaded at 5 g/l to give a C/N ratio of 8 when used as the sole nitrogen source based on media utilized by Koller et al. (2007b) and Pais et al. (2016) with *H. mediterranei* and hydrolyzed cheese byproducts. The other nitrogen sources were loaded to give a constant C/N ratio of 8 for all hydrolyzed DLP-containing media. Glucose (Glucose+YE) and galactose (Galactose+YE) controls with equivalent sugar loadings of 10 g/l were also prepared with 5 g/l yeast extract nitrogen source in addition to an exclusively 5 g/l yeast extract media (YE) for comparison.

Glucose was compared to the hydrolyzed cheese byproducts, as it is well-studied as a sugar carbon source (Alsafadi, Al-Mashaqbeh, et al., 2020; Bonete et al., 1996; Lillo & Rodriguez-Valera, 1990). Pais et al. (2016) found increased galactose consumption with glucose and galactose-containing media with the application of yeast extract and SL-6, and therefore, the nutrients were included to observe if galactose consumption could be improved from what was observed in Chapter 3 (Pais et al., 2016). Yeast extract was studied by itself as a control and compared to the sugars supplied. Equivalent concentrations of minimum salt medium (MSM) and 1% SL-6 trace elements, as described previously were added to the media to provide nutrients and sufficient salinity for *H. mediterranei* growth. No additional phosphorus was needed since the hydrolyzed DLP contained adequate phosphorus levels even with dilution. For similar reasons, other salts, such as calcium and potassium, required less addition for the hydrolyzed DLP-containing media. Sodium bicarbonate was added as a buffer at a concentration of 2.5 g/l to aid in controlling the pH. The pH was measured and corrected twice daily with a pH meter (Fisher Scientific, accumet excel XL15 pH/mV/temperature meter, Hampton, New Hampshire, United States) and diluted 3 M HCl and 3 M NaOH to maintain a neutral pH of 7.0 ± 0.2. The archaea were cultured in 250 ml Erlenmeyer flasks with 130 ml of working volume that were placed in a shaker incubator (New Brunswick Scientific, C24KC refrigerated incubator shaker, Edison, New Jersey United States) with an agitation of 180 rpm and a temperature controlled to 37℃. Cells were harvested during a stationary phase after 288 hours of fermentation.

4.3.5 Determination of cell mass concentration and PHA extraction and quantification

The cell growth in the batch flask experiments was measured by sampling 1 ml of fermentation broth daily throughout the fermentation. The optical density (OD) was measured for the samples at a wavelength of 520 nm in the red region of the visible light spectrum, as described by Huang et al. (2016). The cell dry mass (CDM) was measured as the fermentation broth's volatile solids (VS) at the end of the

fermentation. To determine the concentration of VS, 20 ml of cell broth were sampled and centrifuged at 8,000 rpm for 30 minutes. The resultant cell pellet was then washed with MSM solution twice, and the VS were measured using an oven and furnace following standard methods (American Public Health Association, 2012).

From the CDM measured results, the CDM yield was determined as the mass of CDM divided by the mass of soluble chemical oxygen demand (sCOD) that was consumed and reported as g VS/g sCOD (Equation 4.1):

$$Y_{CDM} = \frac{\Delta m_{CDM}}{\Delta m_{sCOD\ consumed}} \quad (4.1)$$

PHA was extracted by employing the method described by Escalona et al. (1996) with modifications. As for cell dry mass, 20 ml of cell broth were sampled at the end of the fermentation to determine the VS, and the samples were centrifuged at 8,000 rpm for 30 minutes. The cell pellet was then washed with a 0.1% sodium dodecyl sulfate (SDS) solution and deionized (DI) water, causing cell lysis and the residual cell mass to be solubilized with the SDS surfactant. The cell pellet was incubated with the 0.1% SDS solution for 12 hours in a shaker incubator at 40℃ and agitation of 180 rpm. The pellet was then washed with DI water twice and dried in an oven at 105 ℃ for 12 hours. The VS of the dried pellet was then determined using a furnace at 550 ℃ following standard methods (American Public Health Association, 2012). The measured VS was considered as PHA.

Based on the measured results, the PHA yield was calculated as the mass of PHA accumulated divided by the mass of sCOD that was consumed and reported as g VS/g sCOD (Equation 4.2):

$$Y_{PHA=} \frac{\Delta m_{PHA}}{\Delta m_{sCOD\ consumed}} \quad (4.2)$$

The cell PHA content was calculated from the measured cell dry mass and PHA concentrations as the percentage of PHA of the total cell dry mass, and reported as g VS/g VS (Equation 4.3):

$$PHA\ \% = \frac{m_{PHA}}{m_{CDM}} \times 100\% \quad (4.3)$$

4.3.6. Carbon and nitrogen source cost evaluation

The feedstock costs of employing hydrolyzed DLP as a primary carbon source, yeast extract as a complex organic nitrogen source, and ammonium chloride as an inorganic nitrogen source were evaluated to determine the most economical feedstock. The costs of feeding these nutrients were compared to the obtained PHA yields for each hydrolyzed DLP feedstock. The value of lactose present in the DLP was considered as the market cost for DLP sold for low-value animal feed of $0.14/kg lactose in the cost evaluation (Liang et al., 2009; Wang et al., 2021). The price of the commercially available bulk yeast extract and ammonium chloride was $3.85/kg and $0.20/kg, respectively (Tejayadi & Cheryan, 1995; Wang et al., 2021).

4.3.7 Statistical analysis

Experiments were conducted in duplicates with the mean and standard deviation (SD) of each assay calculated for the duplicates. The values were reported as the mean ± standard deviation. One-way Analysis of Variance (ANOVA) and the Tukey test with pairwise comparisons were performed on the hydrolyzed DLP feedstocks and glucose control to determine the significance of the differences among the studied parameters. Graphpad Prism 10 software was used for the data analysis of the experiments.

4.4 Results and discussion

4.4.1 Yeast extract characterization

Table 4.1 shows the characterized composition of yeast extract. Although yeast extract is often referenced as a nitrogen and/or phosphorus source for *H. mediterranei* cultivation, it was measured to be approximately 40% carbon, 10% nitrogen, and 0.2% phosphorus. Therefore, the yeast extract used in the experiment contained nearly the same mass of carbon per gram compared to the sugars. Several researchers who studied *H. mediterranei* growth with hydrolyzed cheese byproduct derived sugars supplemented with yeast extract did not consider the carbon contained in the yeast extract for their reported yields and only considered the cheese byproduct sugar consumed (Koller et al., 2007a; Pais et al., 2016). Therefore, it would be beneficial to evaluate yield values considering the carbon present in the yeast extract, or the cited numbers may be elevated. In this study sCOD consumed that included the carbon present in the yeast extract was used for yield calculations for this reason. The yeast extract contained approximately 2.5 times less nitrogen per unit mass when compared to ammonium chloride. Therefore, more mass of yeast extract is required compared to ammonium chloride to obtain the same concentration of nitrogen in the media.

Table 4.1 Main nutrients of yeast extract.

Yeast Extract % (w.b)						
Dry matter	Moisture	Ash	Total C	Total N	Phosphorus	sCOD***
95.2*	4.8*	8.2*	40.1*	10.8*	0.2*	106**

* % (w.b.)

** unit for sCOD is g/l

*** For 5 g yeast extract dissolved in 1 liter of water

4.4.2 Cell growth and PHA production of *H. mediterranei* and hydrolyzed DLP supplemented with yeast extract and ammonium chloride

4.4.2.1 Effects of hydrolyzed DLP feedstock and nitrogen source on cell growth

H. mediterranei was able to grow with all four substrates and nitrogen sources. The bioreactor flasks at the start and end of the fermentation can be seen in Figure 4.2. The coloring and shade varied for the initial feedstocks. All the flasks containing hydrolyzed DLP appeared brown, while the sugar and yeast extract flasks exhibited a light-yellow hue. This color difference can be attributed to innate soluble constituents that are present in the feedstocks. For example, the brownish color that is present in hydrolyzed DLP feedstocks may result from Maillard reaction products that occur during lactose powder processing (Smith et al., 2016). After reaching the stationary phase for the varying feedstocks, the color of the fermentation broth for all flasks changed to various shades of pink. This color change was due to *H. mediterranei* cells after considerable growth had occurred. The pink pigment of the cells, characteristic of many extreme salinity archaeal halophiles, is due to C40 and C50 carotenoids such as 3-hydroxy-echinenone that function as UV protection in the wild (Calo et al., 1995; Kushwaha et al., 1974).

The cell growth time profile or OD versus time for the various feedstocks can be observed in Figures 4.3 and 4.4. All hydrolyzed DLP-containing feedstocks reached the stationary phase after 288 hours. The highest final ODs of the hydrolyzed DLP-containing feedstocks occurred for the HDLP+YE and the HDLP+YE+NH_4Cl at 11.8 ± 0.2 and 11.5 ± 0.1, respectively. The HDLP+YE possessed the highest sCOD loading of the hydrolyzed DLP feedstocks tested followed by the DLP+YE+NH_4Cl, since an equivalent sCOD loading was provided by the hydrolyzed DLP and the yeast extract contained additional sCOD loading. The HDLP+NH_4Cl contained approximately one-third and one-fifth less sCOD loading than the HDLP+YE and HDLP+YE+NH_4Cl, respectively for this reason. The HDLP+YE and HDLP+YE+NH_4Cl final ODs were 22% and 19% higher, respectively than HDLP+NH_4Cl. Therefore, the increase in the final OD of the HDLP+YE+NH_4Cl

compared to the HDLP+NH_4Cl was nearly proportional to the increased loading of sCOD. However, the increase in final OD for the HDLP+YE compared to the HDLP+NH_4Cl was not proportional to the increase in sCOD loading as a corresponding 33% increase in OD would have been expected. This nonproportional increase in OD compared to sCOD loaded suggested that the HDLP+NH_4Cl grew more cell mass per initial sCOD loaded than the HDLP+YE. This notion was further explored.

For the glucose and galactose supplemented with yeast extract and solely yeast extract feedstocks, the stationary phase was achieved after 240 hours. The Glucose+YE resulted in the highest final OD of all feedstocks at 12.1 ± 0.2, comparable to the HDLP+YE and HDLP+YE+NH_4Cl final ODs. Therefore, it appears hydrolyzed DLP leads to similar cell mass growth for *H. mediterranei* compared to standard glucose substrate with yeast extract as a complex nitrogen source. The Galactose+YE final OD was around 50% less than Glucose+YE even though a similar initial sCOD loading was present. The Galactose+YE final OD was comparable to the YE even though it contained approximately triple the sCOD loading. These results suggested that a considerable amount of the cell mass growth for Galactose+YE may have occurred due to yeast extract consumption rather than galactose consumption.

To better compare the cell growth of the different loadings of the feedstocks, the cell dry mass (CDM) yield versus time was calculated by converting the OD to cell dry mass following the conversion described by Huang et al. (2013) and dividing by the initial sCOD loaded for each of the feedstocks. The results can be observed in Figures 4.5 and 4.6 below for the hydrolyzed DLP, individual monosaccharide sugars, and yeast extract feedstocks. The HDLP+YE+NH_4Cl and HDLP+NH_4Cl had the highest final CDM yields for the hydrolyzed DLP feedstocks at 0.37 ± 0.2 and 0.38 ± 0.01 g CDM/g sCOD, respectively. The HDLP+YE final CDM yield was approximately 16% and 18% less than the HDLP+YE+NH_4Cl and HDLP+NH_4Cl, respectively. These higher yields, observed for the ammonium chloride supplemented feedstocks, may be

caused by inorganic ammonium can be utilized through more *H. mediterranei* central pathways for cell growth compared with organic nitrogen sources such as amino acids and peptides (Alsafadi, Al-Mashaqbeh, et al., 2020; Cui, Shi, et al., 2017).

The YE final CDM yield of 0.48 ± 0.01 g CDM/g sCOD was the highest of all the feedstocks tested. This demonstrated that solely yeast extract is an effective carbon and nitrogen source for *H. mediterranei* growth. Yeast extract contains complex carbohydrates and simple carbon sources such as trehalose, both of which have been shown to result in high cell mass yields with the archaea (Lillo & Rodriguez-Valera, 1990; Zhang et al., 2003). The Glucose+YE resulted in a final CDM yield of 0.32 ± 0.0 g CDM/g sCOD loaded, similar to the yield of HDLP+YE. These similar yield values demonstrated that the sugars contained in the hydrolyzed DLP can lead to similar *H. mediterranei* growth compared to commonly studied glucose. The Galactose+YE resulted in the lowest final CDM yield of all the feedstocks tested at 0.18 ± 0.01 g CDM/g sCOD loaded. This demonstrated the difficulties of *H. mediterranei's* utilization of galactose substrate.

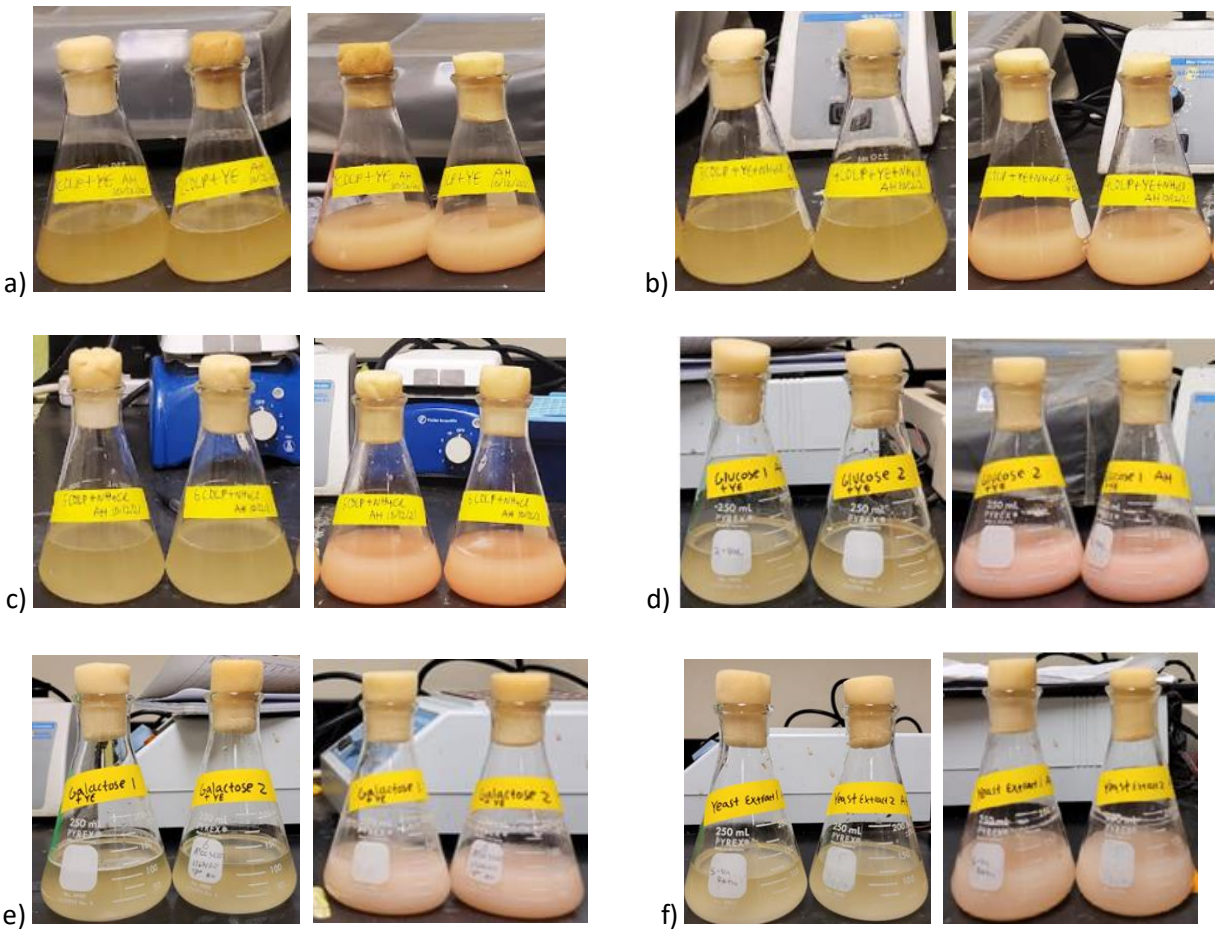

Figure 4.2 Initial fermentation media and final cell broth with hydrolyzed DLP (HDLP), glucose, galactose, and yeast extract supplemented with yeast extract and ammonium chloride: a) HDLP and yeast extract; b) HDLP, yeast extract, and ammonium chloride; c) HDLP and ammonium chloride; d) glucose and yeast extract; e) galactose and yeast extract; f) yeast extract.

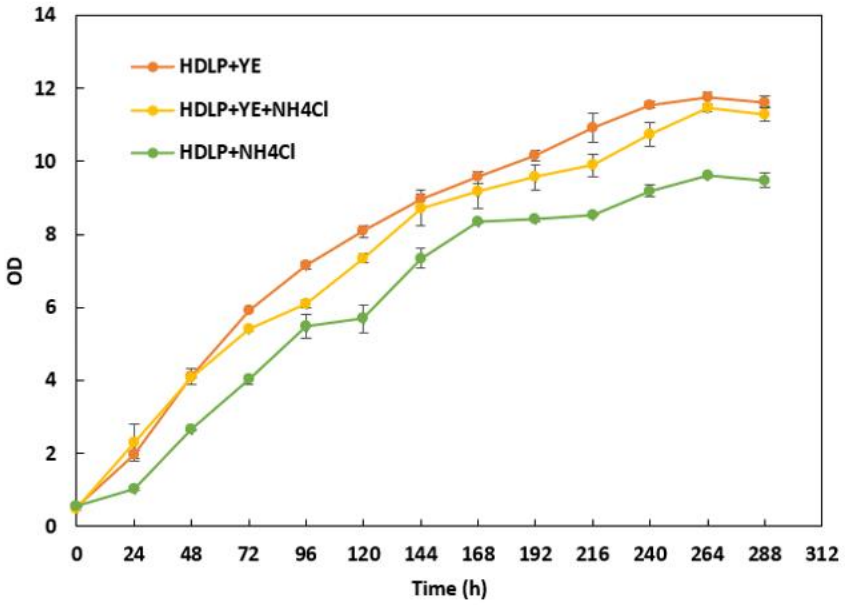

Figure 4.3 *H. mediterranei* cell growth over time with hydrolyzed DLP supplemented with yeast extract (YE) and ammonium chloride (NH_4Cl). Y-error bars are standard deviations.

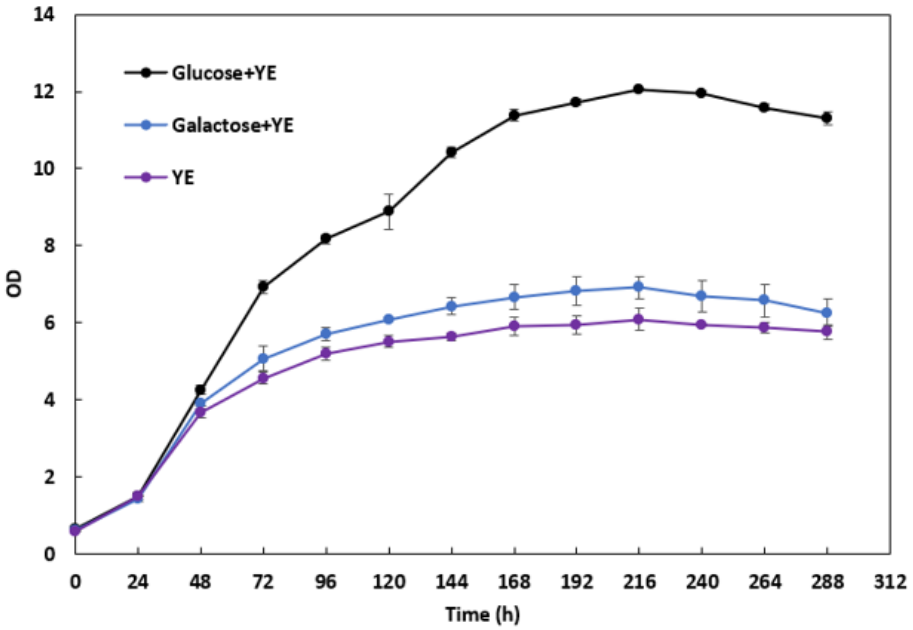

Figure 4.4 *H. mediterranei* cell growth curves over time with glucose and galactose supplemented with yeast extract (YE) and solely yeast extract. Y-error bars are standard deviations.

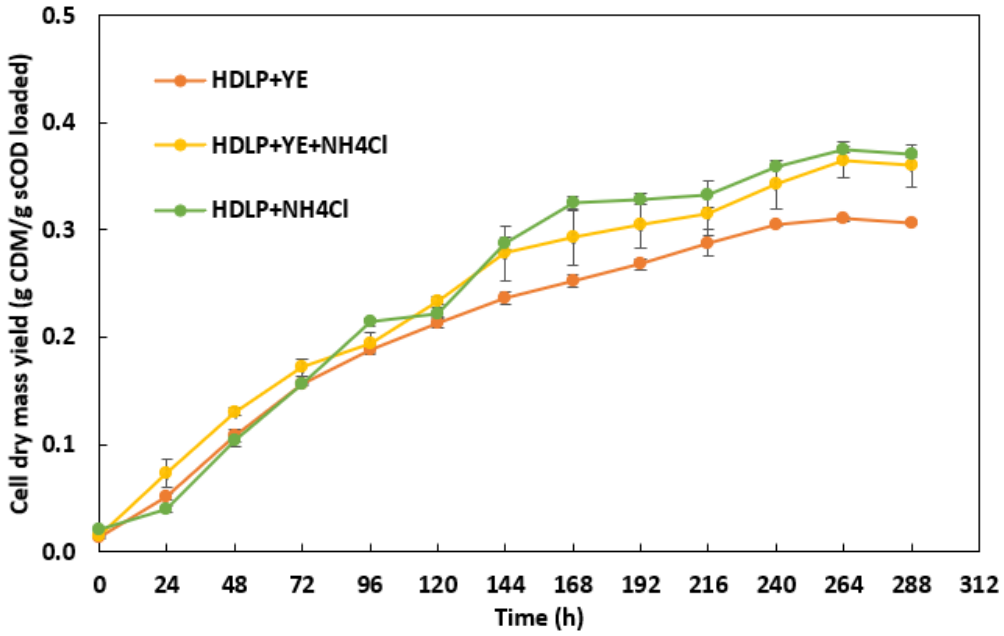

Figure 4.5 *H. mediterranei* cell dry mass yield over time with hydrolyzed DLP supplemented with yeast extract (YE) and ammonium chloride (NH_4Cl). Y-error bars are standard deviations.

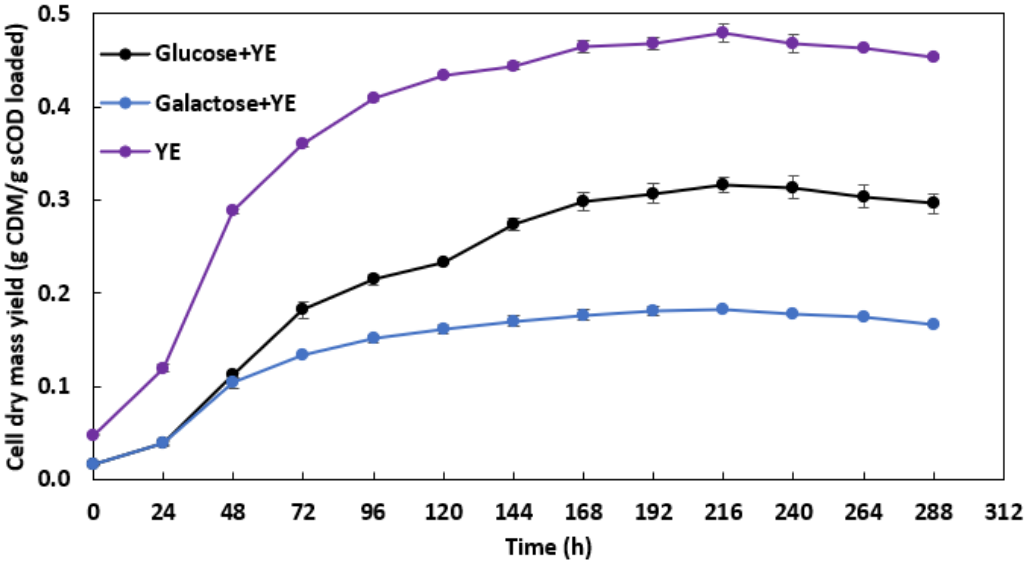

Figure 4.6 *H. mediterranei* cell mass yield over time with glucose and galactose supplemented with yeast extract (YE) and solely yeast extract. Y-error bars are standard deviations.

Figure 4.7 shows the corresponding final cell dry mass (CDM) concentrations and cell dry mass yields for the various feedstocks. One-way ANOVA demonstrated that the final CDM concentrations and CDM yields of the hydrolyzed DLP and glucose feedstocks were significantly different (final CDM concentration p-value = 0.0054) (CDM yield p-value = 0.0009), and the Tukey test was performed for pairwise comparisons. The final CDM concentrations aligned well with the cell growth curves of the measured OD. The HDLP+YE resulted in the highest final CDM concentration among all feedstocks studied at 6.0 ± 0.1 g VS/l. The Glucose+YE final CDM concentration was 5.7 ± 0.1 g VS/l, and the HDLP+YE+NH_4Cl final CDM concentration was 5.4 ± 0.2 g VS/l, both similar to the HDLP+YE. The HDLP+YE and Glucose+YE were not significantly different (p-value 0.5871). Therefore, hydrolyzed DLP appears to result in comparable *H. mediterranei* cell mass growth as commonly applied glucose when supplemented with yeast extract as a nitrogen source. The HDLP+NH_4Cl resulted in a final CDM concentration of 4.7 ± 0.2 g VS/l, significantly less than HDLP+YE (p-value 0.0500). The HDLP+NH_4Cl final CDM concentration was also significantly less than the HDLP+YE+NH_4Cl (p-value 0.0403). The yeast extract resulted in the lowest final CDM at 2.7 ± 0.1 g VS/l, which was expected since it had the lowest sCOD loaded. The galactose final CDM was 3.6 ± 0.2 g VS/l, the lowest of the sugar-containing substrates. It appears galactose is not as effective as a substrate as glucose and hydrolyzed DLP for *H. mediterranei* growth. These results for galactose may be due to low enzyme affinity for galactose compared to glucose (Bonete et al., 1996).

The results for the final CDM concentration contrast with the CDM yield values obtained for the feedstocks. When considering this parameter for the hydrolyzed DLP feedstocks, the HDLP+NH_4Cl resulted in the greatest CDM yield of 0.63 ± 0.03 g VS/g sCOD, the HDLP+YE resulted in the lowest CDM yield of 0.42 ± 0.02 g VS/g sCOD, and the HDLP+YE+NH_4Cl in between at 0.48 ± 0.01 g VS/g sCOD. The HDLP+NH_4Cl CDM yield was significantly greater than HDLP+YE (p-value = 0.0016). Additionally, the HDLP+NH_4Cl CDM yield was significantly greater than the HDLP+YE+NH_4Cl (p-value = 0.0052). Therefore, solely ammonium

chloride appears to be an effective nitrogen source for *H. mediterranei* growth with hydrolyzed DLP substrate, as it resulted in greater CDM yields than the yeast extract containing feedstocks. The hydrolyzed DLP CDM yields were comparable to those found by other researchers with hydrolyzed whey permeate at 0.66 g CDM/g sugar and hydrolyzed whey at 0.40 g CDM/g sugar (Koller et al., 2007b, 2007a). The Glucose+YE had a comparable CDM yield to the HDLP+YE at 0.39 ± 0.00 g VS/g sCOD and were not significantly different from each other (p-value 0.4911). The YE resulted in the second highest CDM yield of the substrates studied of 0.56 ± 0.03 g VS/g sCOD supporting the notion that yeast extract is an effective substrate for *H. mediterranei* growth. The Glucose+YE and Galactose+YE CDM yields were similar at approximately 0.40 g VS/g sCOD. These results may be due to the use of yeast extract in both cases, which was shown to result in high CDM yields.

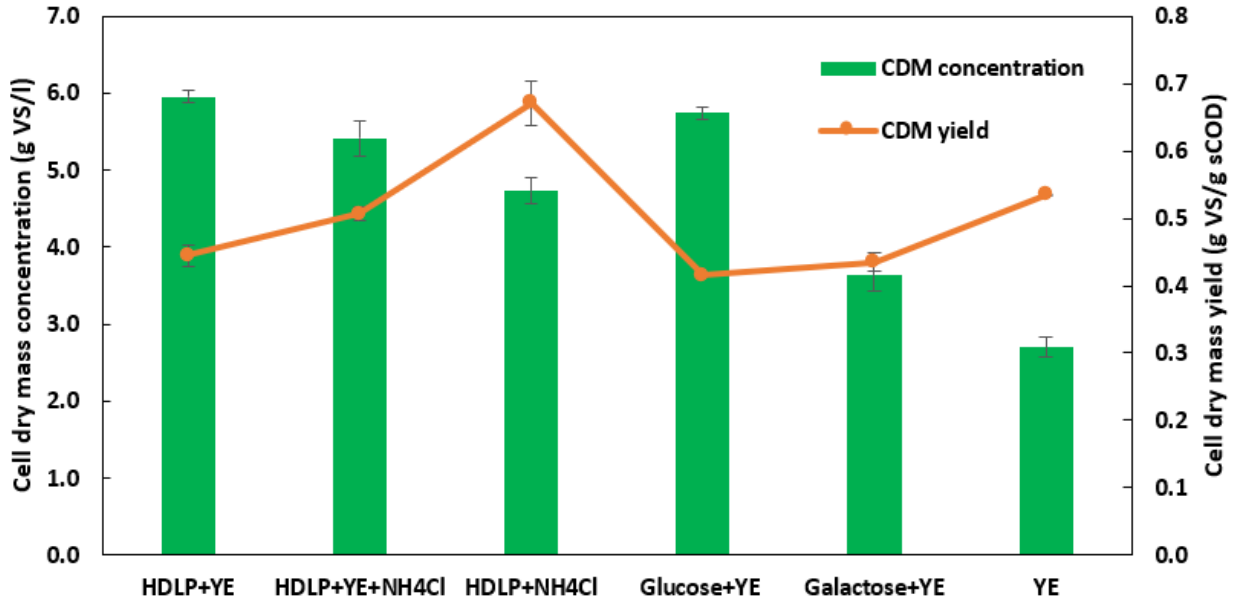

Figure 4.7 Final *H. mediterranei* cell dry mass (CDM) concentration and yield with hydrolyzed DLP supplemented with yeast extract (YE) and ammonium chloride (NH_4Cl), glucose and galactose

supplemented with yeast extract, and solely yeast extract after 288 hours. Y-error bars are standard deviations.

4.4.2.2 Effects of hydrolyzed DLP feedstock and nitrogen source on PHA production

Figure 4.8 shows the final PHA concentrations and PHA yields for the different feedstocks studied. One-way ANOVA demonstrated that the final PHA concentrations and PHA yields of the hydrolyzed DLP and glucose feedstocks were significantly different (final PHA concentration p-value = 0.0090) (PHA yield p-value = 0.0019), and the Tukey test was performed for pairwise comparisons. For the hydrolyzed DLP feedstocks, the final PHA concentration trend was the same as for the final CDM concentration with the HDLP+YE at 3.4 ± 0.2 g VS/l being the highest, the HDLP+NH_4Cl at 2.5 ± 0.2 g VS/l being the lowest, and the HDLP+YE+NH_4Cl at 3.3 ± 0.2 g VS/l, slightly less than the HDLP+YE. Although the Glucose+YE had the second highest final CDM concentration of all the feedstocks, its final PHA concentration was less than all the studied hydrolyzed DLP feedstocks. The Glucose+YE final PHA concentration was significantly less than HDLP+YE and HDLP+YE+NH_4Cl (HDLP+YE and Glucose+YE p-value 0.0146) (HDLP+YE+NH_4Cl and Glucose+YE 0.0286). These results demonstrate that hydrolyzed DLP may improve PHA production in *H. mediterranei* compared to glucose substrate when complex nutrient source yeast extract is provided. The Glucose+YE resulted in nearly double the final PHA concentration compared to the Galactose+YE. This difference between the monosaccharides suggested that the addition of galactose led to a negligible difference in PHA accumulation by the microbe when also supplied yeast extract at the same concentration.

Like CDM yield, the greatest PHA yield for the hydrolyzed DLP feedstocks occurred with the HDLP+NH_4Cl at 0.34 ± 0.03 g VS/g sCOD, followed by HDLP+YE+NH_4Cl at 0.29 ± 0.01 g VS/g sCOD, and the lowest for HDLP+YE at 0.25 ± 0.01 g VS/g sCOD. The PHA yield of the HDLP+NH_4Cl was significantly greater than the HDLP+YE (p-value = 0.0157) but not significantly different from the HDLP+YE+NH_4Cl (p-value =

0.1227). These results demonstrated that hydrolyzed DLP supplemented with ammonium chloride can lead to similar or greater PHA yields compared to applying yeast extract. The PHA yields for all the hydrolyzed DLP feedstocks were comparable to those reported by Koller et al. (2007a and 2007b) with hydrolyzed cheese byproducts whey and whey permeate. The authors reported PHA yields of 0.33 g VS/g sugars for hydrolyzed whey permeate and 0.29 g VS/g sugars with hydrolyzed whey. However, Pais et al. (2016) reported considerably higher PHA yields of 0.78 g VS/g sugars. This discrepancy in PHA yields may be because Pais et al. (2016) did not consider the PHA yielded from yeast extract in their study. Based on the results from this experiment, the PHA yielded from 5 g/l yeast extract could have contributed up to nearly one-third of the total PHA reported by the researchers. The Glucose+YE yield was 0.17 g VS/g sCOD, comparable to what other researchers have found with equivalent glucose and yeast extract loadings (Alsafadi, Al-Mashaqbeh, et al., 2020). The Glucose+YE yield was determined to be significantly less than the HDLP+YE (p-value = 0.0285). This difference between the feedstocks' yields again established that hydrolyzed DLP is more effective for *H. mediterranei* PHA production than glucose substrate. The Glucose+YE PHA yield was also nearly equivalent to the Galactose+YE like for CDM yield. The YE PHA yield was 0.53 g VS/g sCOD, between the hydrolyzed DLP and sugar feedstocks. The high YE CDM and PHA yields demonstrated the need to include the yeast extract fed in the reported yields.

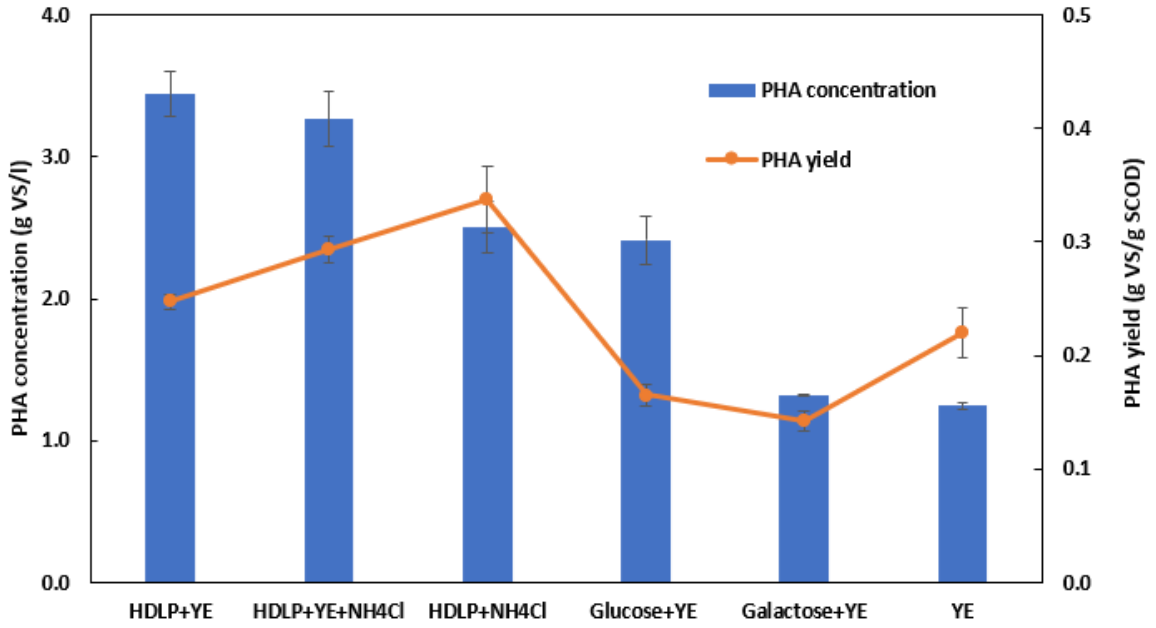

Figure 4.8 Final *H. mediterranei* PHA concentration and yield with hydrolyzed DLP supplemented with yeast extract (YE) and ammonium chloride (NH_4Cl), glucose and galactose supplemented with yeast extract, and solely yeast extract after 288 hours. Standard deviation error bars are shown.

4.4.2.3 Effects of hydrolyzed DLP feedstock and nitrogen source on PHA content

An important parameter to gauge the ability of PHA to accumulate in *H. mediterranei* cells is PHA content, which defines the portion of the total cell dry mass that is PHA, compared to the residual cell mass. Figure 4.9 shows the PHA content of the cell dry mass produced with the different feedstocks. One-way ANOVA demonstrated that the final PHA contents of the hydrolyzed DLP and glucose feedstocks were significantly different (p-value = 0.0056), and the Tukey test was performed for pairwise comparisons. The HDLP+YE+NH_4Cl PHA content was 60 ± 4 %, the highest PHA content of the feedstocks studied. In contrast, the Galactose+YE PHA content was 36 ± 1%, the lowest of the feedstocks studied. None of the PHA contents of the three different hydrolyzed feedstocks were significantly different from each other

(HDLP+YE and HDLP+YE+NH_4Cl p-value 0.6325) (HDLP+YE and HDLP+NH_4Cl p-value = 0.3623) (HDLP+YE+NH_4Cl and HDLP+NH_4Cl p-value = 0.1108). This result may be due to the main carbon source for the three feedstocks is glucose and galactose sugars provided from the hydrolyzed DLP that are metabolized through the same pathways for PHA synthesis (Han et al., 2013; Williams et al., 2019). The similar PHA contents achieved by the HDLP+YE+NH_4Cl and the HDLP+NH_4Cl feedstocks compared to the HDLP+YE demonstrated that hydrolyzed DLP supplemented with ammonium chloride can lead to effective *H. mediterranei* PHA accumulation. The hydrolyzed DLP feedstocks' PHA contents were similar to what has been found with hydrolyzed whey and whey permeate feedstocks supplemented with yeast extract at 50-73% (Koller, 2015a; Koller et al., 2007a, 2007b; Pais et al., 2016). Additionally, the HDLP+YE PHA content was significantly greater than the Glucose+YE (P-value 0.0101). Other researchers have also found that hydrolyzed cheese byproducts produce greater PHA yields than synthetic sugar media. The difference in PHA yields by the two feedstocks may be caused by other nutrient and growth factors present in cheese byproducts that have been suggested can lead to higher polymer production (Pais et al., 2016).

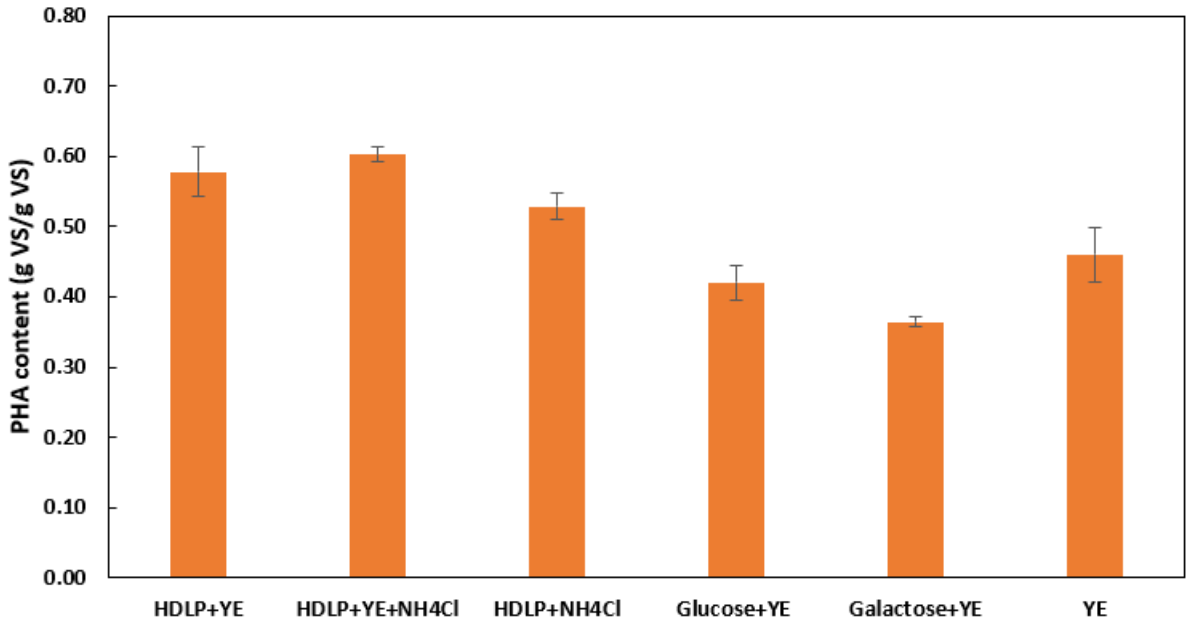

Figure 4.9 *H. mediterranei* PHA content of cell dry mass with hydrolyzed DLP supplemented with yeast extract (YE) and ammonium chloride (NH_4Cl), glucose and galactose supplemented with yeast extract, and solely yeast extract after 288 hours. Y-error bars are standard deviations.

4.4.2.4 Effects of hydrolyzed DLP feedstock and nitrogen source on sCOD and sugar consumption

The sCOD consumption and glucose and galactose sugar consumption can be seen in Figures 4.10 and 4.11, respectively. Greater than 65% sCOD consumption was observed for all feedstocks besides the Galactose+YE. It appears that *H. mediterranei* can consume glucose and yeast extract at high rates compared with galactose which is not as readily consumed. The HDLP+NH_4Cl sCOD consumption was 66% ± 0%, less than the HDLP+YE at 84% ± 1% and HDLP+YE+NH_4Cl at 81% ± 1%. The HDLP+NH_4Cl lack of yeast extract may have led to this difference in sCOD consumption. For sugar consumption, no glucose was detected at the end of the fermentations for all feedstocks that contained glucose, and therefore 100% glucose consumption was observed in all cases. In contrast, the galactose consumption ranged from 32 ± 5 % for Galactose+YE to 70 ± 1 % for the HDLP+YE. The difference between glucose and galactose consumption may be attributed to the glucose dehydrogenase enzyme that has been found to be able to metabolize both glucose and galactose, in addition to other sugars, but at considerably greater rates for glucose than galactose (Bonete et al., 1996; Zhang et al., 2003). *H. mediterranei*'s preference for glucose and limited galactose consumption was comparable to results obtained by other researchers who studied glucose and galactose-containing feedstocks, including synthetic sugar media and hydrolyzed cheese byproducts (Koller et al., 2007a; Pais et al., 2016). The galactose consumption of the hydrolyzed DLP feedstocks was near what Pais et al. (2016) found with hydrolyzed whey supplemented with yeast extract between approximately 33%-66%. Although the HDLP+YE galactose consumption was greater than the other feedstocks that possessed galactose, as previously stated, similar or greater CDM and PHA yields

were found with the DLP+YE+NH_4Cl and the DLP+NH_4Cl. These results suggested that the additional galactose that *H. mediterranei* consumed with the DLP+YE was not going towards further cell mass growth or PHA production. The hydrolyzed DLP feedstocks' galactose consumptions were more than two to three times greater than the Galactose+YE, indicating that hydrolyzed DLP itself may improve galactose consumption compared to synthetic sugar media. The Galactose+YE galactose consumption was comparable to the galactose consumption (28% ± 3%) found in Chapter 3. Therefore, it does not appear that the additional yeast extract resulted in greater galactose consumption.

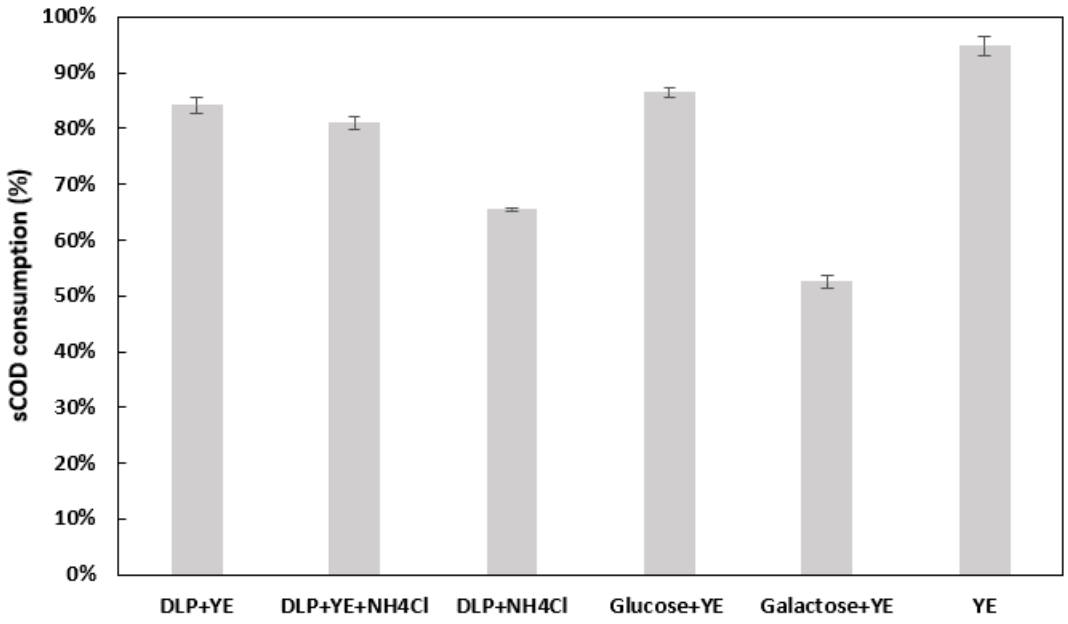

Figure 4.10 sCOD consumption by *H. mediterranei* with hydrolyzed DLP supplemented with yeast extract (YE) and ammonium chloride (NH_4Cl), glucose and galactose supplemented with yeast extract, and solely yeast extract after 288 hours. Y-error bars are standard deviations.

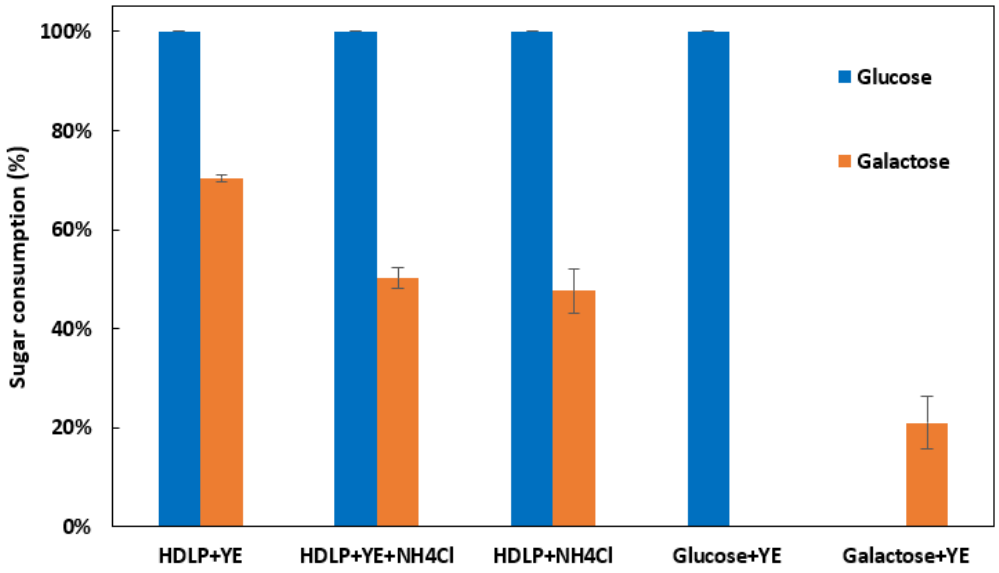

Figure 4.11 Glucose and galactose consumption by *H. mediterranei* with hydrolyzed DLP supplemented with yeast extract (YE) and ammonium chloride (NH_4Cl), and glucose and galactose supplemented with yeast extract after 288 hours. Y-error bars are standard deviations.

4.4.3 Feedstock cost analysis

Cost analysis was conducted for the three hydrolyzed DLP feedstocks supplemented with yeast extract and ammonium chloride, considering the costs of lactose provided by the DLP, yeast extract, and ammonium chloride to determine the most economical. The costs of the feedstock sources per kilogram of PHA produced can be observed in Figure 4.12. The HDLP+YE cost per kg of PHA produced was \$6.00 ± \$0.28, the highest of the three feedstocks. The high cost can be attributed to HDLP containing the greatest yeast extract concentration. Even by reducing the yeast extract by half in the HDLP+YE+NH_4Cl, the feedstock cost per kg of PHA produced was still \$3.50 ± \$0.38. The HDLP+NH_4Cl resulted in the lowest feedstock cost per kg of PHA produced at \$0.73 ± \$0.05. The considerably lower cost can be attributed to using less expensive hydrolyzed DLP as the sole carbon source and ammonium chloride as the sole

nitrogen source. Yeast extract contains a similar percent carbon to the lactose contained in delactosed permeate and less than half the percent nitrogen of ammonium chloride. However, it is approximately 28 and 20 times more expensive per kilogram, respectively (Tejayadi & Cheryan, 1995; Wang et al., 2021). Therefore, it is a considerably more expensive feedstock to use for *H. mediterranei* cultivation. Although *H. mediterranei* was shown to result in high cell mass and PHA yields with yeast extract, it does not appear to be economical to use as a complex nutrient source at any loading at an industrial scale. Ammonium chloride was used in future studies that utilized hydrolyzed DLP as substrate since the HDLP+NH_4Cl resulted in similar or improved PHA yields compared to the hydrolyzed DLP feedstocks that were supplemented with yeast extract and the cost analysis demonstrated substantial savings with the use of ammonium chloride compared to yeast extract. Yoong Kit et al. (2017) created a *H. mediterranei* PHA production economic model with glycerol substrate. The authors found that feedstock cost per kg of PHA produced (without considering a nitrogen source) was around $1.39/kg (Yoong Kit et al., 2017). Therefore, the proposed use of hydrolyzed delactosed permeate feedstock supplemented with ammonium chloride nitrogen source for *H. mediterranei* PHA production appears to be economically competitive.

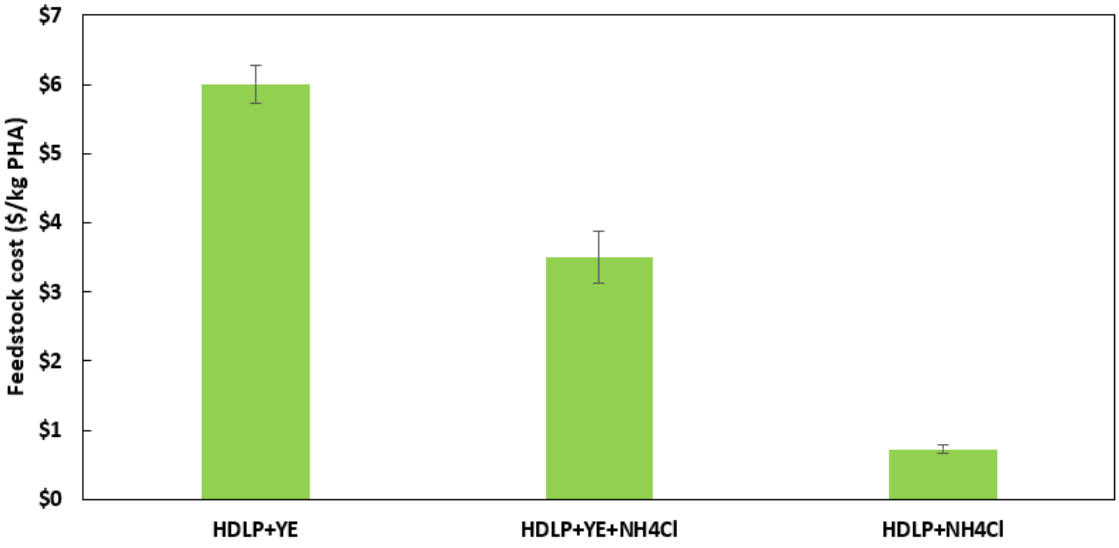

Figure 4.12 Feedstock cost per kg of PHA produced with hydrolyzed DLP supplemented with yeast extract (YE) and ammonium chloride (NH_4Cl). Y-error bars are standard deviations.

4.5 Conclusions

Hydrolyzed DLP supplemented with three different nitrogen sources were tested to determine the effects of organic nitrogen source yeast extract and inorganic nitrogen source ammonium chloride on *H. mediterranei* growth and PHA production. Glucose and galactose supplemented with yeast extract were also studied and compared with a control containing merely yeast extract. All feedstocks were successful in culturing *H. mediterranei*. The hydrolyzed DLP feedstock supplemented with ammonium chloride nitrogen source (HDLP+NH_4Cl) resulted in significantly greater or no difference in CDM and PHA yields than the hydrolyzed DLP feedstocks supplemented with yeast extract. Therefore, inorganic ammonium chloride is as effective as a nitrogen source as yeast extract with hydrolyzed DLP feedstock. Although complex nutrient source yeast extract was shown to result in high CDM and PHA yields, yeast extract was demonstrated to be considerably more expensive to use as feedstock compared with hydrolyzed DLP supplemented with ammonium chloride to produce PHA, adding over $5/kg of PHA produced with a 5 g/l loading. Therefore, ammonium chloride was selected as the sole nitrogen source in future studies since it gave similar yields of PHA and cost substantially less than yeast extract. It is important to note that some researchers have not included the carbon contributed by yeast extract in CDM or PHA yield calculations when using it as a nitrogen source with hydrolyzed dairy byproducts. However, since yeast extract gave high CDM and PHA yields when applied as substrate, it should be included in yield calculations, or the reported yields will be appreciably higher. The hydrolyzed cheese byproduct feedstocks demonstrated in this study could be applied to industrial-scale PHA production,

creating a new revenue stream for cheese makers. The research can lead to lower production costs for PHA to expand its market and mitigate the environmental impacts of traditional plastics.

Chapter 5. Batch *H. mediterranei* and PHA production with Hydrolyzed DLP and Whey Permeate

5.1 Abstract

Polyhydroxyalkanoates (PHA) are the fastest-growing bioplastic derived from organic sources. However, the further market expansion of PHA is limited by the use of expensive feedstocks such as glucose and glycerol. This study explored reducing PHA production costs by incorporating low-value cheese byproducts, delactosed permeate (DLP) and whey permeate, that were first hydrolyzed by lactase enzyme. PHA producer *Haloferax mediterranei* (*H. mediterranei*) was employed in batch bioreactors with a total and working volumes of 250 and 200 ml, respectively. The effect of four different loadings (10, 20, 30, and 40 g total sugar/l) of the feedstocks on PHA yield was determined and compared with glucose as a control. The maximum loading of hydrolyzed DLP that could produce a high yield of PHA was determined to be 10 g total sugar/l. Higher loadings resulted in significantly less *H. mediterranei* cell dry mass and PHA due to potential substrate inhibition. The maximum loading of hydrolyzed whey permeate was determined to be 30 g total sugar/l, and the maximum loading of glucose was 20 g total sugar/l. The differences between hydrolyzed DLP and whey permeate might be attributed to the presence of inhibitory compounds, such as Maillard reaction products formed during the processing of whey permeate into lactose powder and DLP. The performance of a 6 L batch bioreactor with a working volume of 5 L was also tested. Results showed that the bioreactor could also be operated at a maximum loading of 10 g total sugar/l using hydrolyzed DLP as a feedstock. The maximum specific growth rates for the two hydrolyzed cheese byproducts were estimated to be equivalent with $\mu_{max} = 0.02\ h^{-1}$. These findings could assist in developing large-scale PHA production facilities utilizing cheese byproduct substrate. This cheese byproduct-derived PHA production would help grow the dairy industry from an additional revenue stream, support the industry targets of net-zero emissions, and obtain a circular economy.

Keywords: *Haloferax mediterranei*, delactosed permeate, whey permeate, polyhydroxyalkanoates, batch

5.2 Introduction

Governments, industries, and consumers are interested in utilizing waste-derived carbon sources and nutrients for bioplastic production to reduce the environmental impacts of traditional plastics and build a circular economy (Sharifzadeh et al., 2010; Yadav et al., 2020). Polyhydroxyalkanoates (PHA) are one bioplastic of interest to replace traditional plastics (Bugnicourt et al., 2014). PHA is a naturally occurring polymer with properties similar to thermoplastics with high biodegradability. They can degrade at ambient temperatures in terrestrial and ocean environments (Bernard, 2014; Meereboer et al., 2020). PHA can be used in applications to replace traditional plastics, such as food packaging film, cutlery, bags, or containers (Joyce, 2018; Reddy et al., 2003). These benefits of PHA have led its market to be expected to more than double from 2022 to 2027 (European Bioplastics, 2021). Although PHA is the fastest-growing bioplastic, further market growth is limited by the high cost of feedstocks such as glucose and glycerol (European Bioplastics, 2021; Lim et al., 2023; Nielsen et al., 2017).

To reduce the feedstock costs, many waste and byproduct feedstocks for PHA production have been studied, including olive mill wastes (Dionisi et al., 2005), date palm crop waste (Alsafadi, Ibrahim, et al., 2020) , waste cooking oil (Kamilah et al., 2013), municipal food waste (Wang & Zhang, 2021), and dairy wastewater (Sharifzadeh et al., 2010). Cheese byproducts, whey permeate and delactosed permeate (DLP), are another potential source of low-value organic feedstock for PHA production (Amaro et al., 2019; Oliveira et al., 2019). Whey permeate is the byproduct of whey powder generated when the liquid whey from cheese making is concentrated with membrane filtration. The retentate from the filtration process is further concentrated and dried into whey protein powder, while the liquid that passes through the filter is the byproduct whey permeate (Byylund, 2015). The whey permeate can be further concentrated with evaporator systems to produce lactose powder with the remaining liquid byproduct DLP (Oliveira et al., 2019). Figure 5.1 shows the sources of these cheese byproducts starting from milk. Cheese byproducts,

whey permeate and delactosed permeate (DLP), contain high concentrations of sugars, are produced in large quantities, and are often sold as a low-value animal feed or field spread (Liang et al., 2009; Oliveira et al., 2019). Therefore, these byproducts present an opportunity for conversion into higher-value products such as PHA bioplastic. Wang et al. (2021) demonstrated that DLP and whey permeate could result in PHA breakeven costs of $4/kg and $5/kg, respectively, which is on the lower end of reported values of $4-16/kg (Roland-Holst, 2013). Limited research has been conducted on the conversion of whey permeate into PHA (Koller et al., 2007). To my knowledge, no research has been conducted with DLP (Amaro et al., 2019; Koller, 2018; Koller et al., 2007a). Therefore, there is a need to study the parameters affecting the production of PHA using these cheese byproducts as a feedstock.

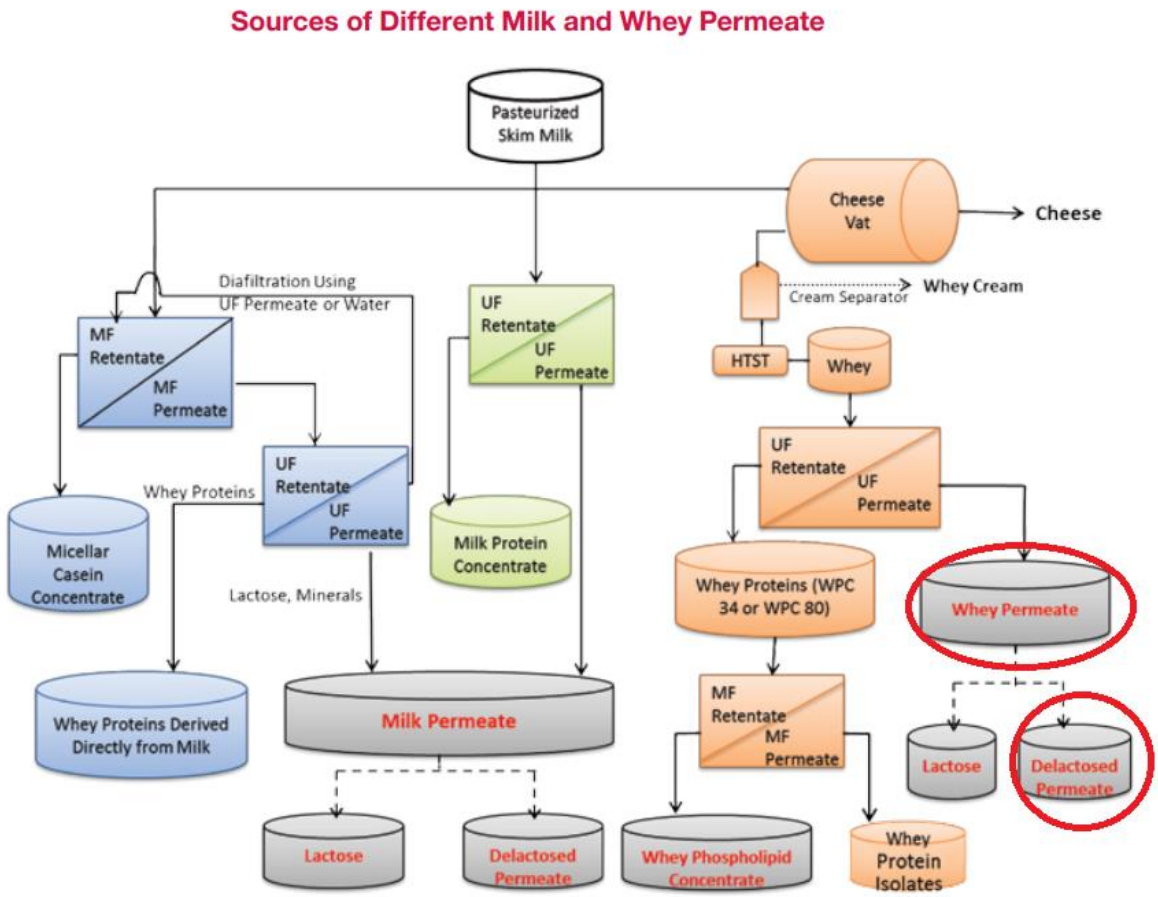

Figure 5.1 Sources of cheese byproducts whey permeate and delactosed permeate (DLP) circled in red (Burrington et al., 2014).

The results presented in Chapters 3 and 4 showed that H. *mediterranei* could successfully grow and produce PHA at high yields with hydrolyzed DLP at a loading of 10 g total sugars/l. The loading of 10 g total sugar/l was similar in concentration to other studies that explored PHA production with *H. mediterranei* and hydrolyzed cheese byproducts in the range of 8-12 total sugars/l (Koller, 2015b; Pais et al., 2016). It would be beneficial to apply higher loadings of hydrolyzed DLP to increase PHA production and reduce the bioreactor volume needed so that it could be possible to reduce the capital costs of large-scale production systems (Wang et al., 2021). Wang (2021) tested two loadings of hydrolyzed lactose powder, 22.5 and 45 g soluble COD (sCOD)/l, as feedstock for *H. mediterranei* PHA production. Results showed an increased cell dry mass (CDM) and PHA production with higher loadings of hydrolyzed lactose powder. The increase in PHA production was nearly proportional to the increase in loading. However, the increase in cell dry mass was considerably less. Likewise, the cell dry mass yield decreased with the increase in loading, but the PHA yield increased with the increase in loading. These results may have been due to higher concentrations of carbon present in the environment that can trigger PHA accumulation (Anderson & Dawes, 1990). Wang (2022) demonstrated the maximum loading of food waste permeate (FWP), containing volatile fatty acids and lactic acid, feedstock with *H. mediterranei* growth and PHA production. The author tested four loadings (20, 40, 60, and 80 g COD/l) of FWP derived from two different samples of the same anaerobic digester at different times of the year. The two FWP samples' highest CDM and PHA concentrations resulted from different loadings of 40 and 60 g COD/l, respectively. Therefore, similar PHA feedstocks may yield different maximal loadings, potentially due to differences in micronutrients and other constituents that can affect *H. mediterranei* growth (Wang, 2022).

Although whey permeate and DLP are derived from the same cheese whey, as observed in Figure 5.1, the two cheese byproducts contain different compositions of lactose, nitrogen, and mineral nutrients due to the lactose crystallization process (Byylund, 2015; Liang et al., 2009; Oliveira et al., 2019). Whey permeate is upstream of DLP before the lactose crystallization process that involves concentration with high-heat evaporation. The proteins and minerals in whey permeate are further concentrated during this evaporator step, while lactose is crystallized out of the solution (Byylund, 2015). This process results in DLP containing higher concentrations of minerals and protein, but a lower percentage of lactose total solids than whey permeate (Byylund, 2015; Liang et al., 2009). Additionally, DLP can contain high-heat products that form during the lactose crystallization process, such as Maillard reaction products (Byylund, 2015; Kuechel, 2017). Maillard reaction products have been demonstrated to be inhibitory for several microorganisms, and their presence could affect *H. mediterranei* growth (Einarsson et al., 1983; Einarsson & Eklund, 1988). Therefore, studying the maximum loading of hydrolyzed DLP and whey permeate could be beneficial to better understand the differences that exist between them. The growth kinetics of the two hydrolyzed cheese byproducts need to be compared. Therefore, it could be possible to design efficient bioreactors to produce cost-effective PHA.

The tasks of this study were to: 1) characterize whey permeate collected from a large-scale cheese producer; 2) determine the maximum loading of hydrolyzed DLP and whey permeate for *H. mediterranei* growth in batch reactors; 3) estimate the maximum specific growth rate for *H. mediterranei* cultivated on hydrolyzed DLP and whey permeate.

5.3 Materials and methods

5.3.1 Feedstock collection and characterization of whey permeate

The same DLP collected from Hilmar Cheese Company, Hilmar, California, previously used in Chapters 3 and 4, was applied as feedstock for *H. mediterranei* cultivation. Whey permeate was also collected from Hilmar Cheese Company's lactose plant. Whey permeate is upstream of DLP in the processing of lactose powder before the evaporator concentration steps (Byylund, 2015). Therefore, whey permeate contains a higher percent lactose of total solids but lower concentrations of nitrogen and minerals than DLP (Byylund, 2015; Liang et al., 2009). Whey and delactosed permeate appear different despite being produced from the same whey co-product stream (Figure 5.2). Whey permeate is yellow due to milk nutrients and cheese colorings, such as annatto present (Beucler et al., 2005; Byylund, 2015). Although delactosed permeate also contains these constituents, it possesses a brown color due to nonenzymatic browning and Maillard reaction products from exposure to high-heat evaporation systems (Božanić et al., 2014; Kuechel, 2017).

The whey permeate was characterized for total solids (TS), moisture, ash, lactose, total nitrogen (TN), phosphorus, and soluble chemical oxygen demand (sCOD). The DLP lactose sugar was measured with high performance liquid chromatography (HPLC) equipped with a refractive index detector (RID) and photodiode array detector (PDA) following the analytical method described by Sluiter (2008) in previous chapters. Standard chemical kits were used to measure sCOD and TN (COD digestion vials high range plus, TNTplus Vial Test, Hach Corp., Loveland, Colorado, United States). Standard methods were followed for measuring TS, ash, and moisture (American Public Health Association, 2012). Additionally, minerals sodium, magnesium, potassium, calcium, bromide, sulfur, chloride, and micronutrients zinc, manganese, cobalt, copper, nickel, and molybdenum were measured with inductively coupled plasma-mass spectrometry (ICP) to determine the nutrients and micronutrients present in the DLP (US EPA, 1996).

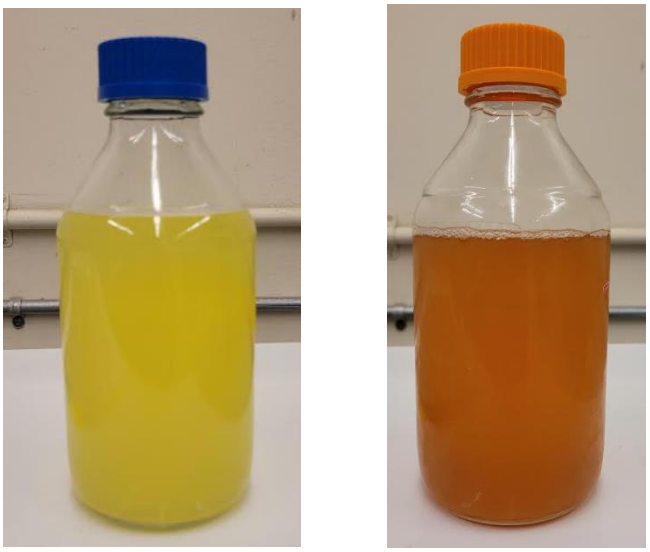

Figure 5.2 Whey permeate (left) and delactosed permeate (right) collected from Hilmar Cheese Company.

5.3.2 Delactosed permeate and whey permeate pretreatment

The DLP was centrifuged before enzymatic hydrolysis as described in Chapter 3. The separation process was facilitated with a bench-top centrifuge (Heraeus Multifuge X1R Thermo Scientific, Waltham, Massachusetts) at 5,000 rpm with a swinging bucket rotor for 30 minutes. The liquid on the top was decanted from the solids that settled on the bottom of the bottles for hydrolysis. However, the whey permeate did not require centrifugation pretreatment since it contained little suspended solids and was visibly clear. The centrifuged DLP and whey permeate were hydrolyzed with lactase enzyme Nola Fit 5550 (Chris Hansen, Hoersholm, Denmark) with a loading of 0.025 g lactase/g lactose. The centrifuged DLP and whey permeate with added lactase enzyme were placed in an incubator shaker at 40 ℃ and agitated at 180 rpm for 12 hours, as described in Chapter 3. The hydrolyzed DLP and whey permeate were used as feedstock for *H. mediterranei* cultivation.

5.3.3 PHA production using hydrolyzed cheese byproducts and glucose feedstocks

This study used halophilic archaeon *H. mediterranei* (ATCC 33500) as the microbial PHA producer. The active inoculum was prepared according to the procedures described in the previous chapters. Three sugar mediums were studied, hydrolyzed DLP, hydrolyzed whey permeate, and glucose at four loadings of 10, 20, 30, and 40 g total sugars/l. The previously described minimum salt media (MSM), and 1% v/v SL-6 trace elements, were used as the base for feedstocks. Ammonium chloride was added as a supplementary nitrogen source to all feedstocks to give a constant C/N ratio of 8, which provided excess nitrogen for cell growth (Cui, Shi, et al., 2017). Likewise, potassium dihydrogen phosphate was added to obtain a C/P ratio of 35, which provided an excess of phosphorous (Melanie et al., 2018). Yeast extract was used as a complex nutrient source at a loading of 1 g/l for glucose control. Sodium bicarbonate was added as a buffer at a loading of 2.5 g/l, and 3 M NaOH and 3 M HCl were added twice daily to control the pH. Two-hundred-and-fifty milliliter bioreactors were operated with a working volume of 200 ml and placed in an incubator (Fisher Scientific, Temperature Incubator, Hampton, New Hampshire, United States) controlled at 37℃ (Figure 5.3). Forced aeration was provided to achieve a 2.5 vvm, which Wang (2022) recommended for *H. mediterranei* cultivation to provide adequate dissolved oxygen for substrate loadings of up to 80 g COD/l. This aeration is higher than what is typically applied in the biotech industry of 0.5-1.5 vvm due to the high salinity of the MSM (Wang, 2022). The fermentation was stopped after the culture had reached the stationary phase after 240-624 days.

Figure 5.3 Batch incubation set-up.

5.3.4 Six-liter batch cultivation of *H. mediterranei* with hydrolyzed DLP

The batch hydrolyzed DLP PHA production was scaled with a 6 L bioreactor with a working volume of 5 L. Two loadings of 10 and 20 g total sugar/l were tested to determine the inhibition of the substrate for *H. mediterranei*. The same media used for the 250 ml bioreactors was applied. Wang (2022) demonstrated that improved cell mass growth could occur with dissolved oxygen (DO) controlled to above 50% saturation. Therefore, the bioreactor DO was controlled to above 50% saturation. The DO of the fermentation broth was monitored daily with a DO meter (YSI ProDSS, Rye Brook, New York, United States). The bioreactor's temperature was controlled to 37 ± 1.0 ℃ using a water bath and jacket that enclosed the bioreactor. The pH was controlled to 7.0 with 3 M NaOH and 3 M HCl and pH controller (Bluelab, Tauranga, Gisborne, New Zealand). The cells were cultured until the cell growth reached the stationary phase at 216 hours.

5.3.5 Determination of cell dry mass concentration and PHA extraction and quantification

The cell growth in the batch experiments was measured by sampling 1 ml of fermentation broth daily throughout the fermentation. The samples' optical density (OD) was measured at 520 nm, as described by Huang et al. (2016). The final cell dry mass (CDM) was measured as the fermentation broth's volatile solids (VS) at the end of cell cultivation. To determine the mass of VS, 20 ml of fermentation broth was sampled and centrifuged at 8,000 rpm for 30 minutes. The resultant cell pellet was then washed with MSM solution twice, and the VS was measured using an oven and furnace following standard methods (American Public Health Association, 2012). Similarly to the CDM, the PHA mass was measured as VS after separating the PHA from the residual cell dry mass. The PHA was extracted following methods stated previously based on a method described by Escalona et al. (1996) with modifications. Twenty milliliters of fermentation broth were sampled at the end of cell cultivation and centrifuged at 8,000 rpm for 30 minutes. A surfactant solution of 0.1% sodium dodecyl-sulfate (SDS) and deionized (DI) water was added to the sample tube causing cell lysis and solubilization of cell mass. The cell pellet with SDS surfactant was placed in a shaker incubation at 40℃ and agitation at 180 rpm for 12 hours. The resultant PHA was then washed with DI water twice. The VS of the washed PHA pellet was then determined following the same standard methods as stated for cell dry mass (American Public Health Association, 2012). The PHA content was calculated as the percentage of PHA of the total CDM, g VS PHA/g VS CDM.

5.3.6 Measurement of sugars and determination of yields

The glucose and galactose were measured at the beginning and end of the fermentation to determine the sugar consumption and CDM and PHA yield. The sugars were measured with high-performance liquid chromatography (HPLC) equipped with a refractive index detector (RID) and photodiode array detector (PDA), and following an analytical method was followed by Sluiter (2008). One milliliter of fermentation broth was sampled daily from the bioreactors. The samples were centrifuged at

12,000 rpm for 20 minutes, and the supernatant was filtered through 0.22 µm membranes to remove suspended solids. A Biorad Aminex HPX-87H column (Hercules, California, United States) was used as the analytical column, and a 5 mM H2SO4 solution as the mobile phase. During the HPLC analysis, the oven temperature was controlled to 60 ℃ and the flow rate at 0.6 ml/min. The cell dry mass yield was determined as the mass of CDM grown divided by the mass of total sugars consumed, g VS/g total sugar. Similarly, the PHA yield was calculated by the mass of PHA accumulated divided by the total sugars consumed, g VS/g total sugar. (Bhattacharyya et al., 2014)

5.3.7 Maximum growth rate estimation

The maximum growth of hydrolyzed DLP was estimated with four loadings of the feedstock, 2.5, 5.0, 7.5, and 10 g total sugar/l. The same MSM media conditions described previously were used in the study. The maximum growth rate of the hydrolyzed whey permeate was estimated from the previous batch fermentation data that applied loadings of 10, 20, 30, and 40 g total sugar/l. The OD was measured daily and was converted to cell dry mass (g/l) (X) following the conversion ratio described by Huang et al. (2013). The specific growth rate (µ) was determined by considering the cell dry mass change during the exponential growth phase from hour 0 to 96 and the solution to first-order growth kinetics (Equations 5.1 and 5.2):

$$\frac{\partial X}{\partial t} = \mu X \qquad (5.1)$$

After integration and applying the initial conditions:

$$\ln(\mathrm{X}) = \mu \mathrm{t} + \ln\,(X_0) \qquad (5.2)$$

By plotting ln(X) against time and using linear regression in Microsoft Excel, the slope was the specific growth rate, and the y-intercept is ln (X_0). The greatest specific growth rate obtained was considered as the maximum specific growth rate, μ_{max}.

5.3.8 Statistical analysis

The 250 ml bioreactor, 6 L bioreactor, and Monod kinetic fermentations were conducted in duplicate. The mean and standard deviation (SD) of each assay were calculated for the duplicates. The values were reported as the mean ± standard deviation. Two-way Analysis of Variance (ANOVA) and Tukey test with pair comparisons were conducted for the batch loading experiment to determine the significant levels of the factors and group comparison with GraphPad Prism 10 software. Two-way ANOVA was conducted since two factors, feedstock type and loading, were studied with the batch loading experiment. The T-test for pairwise comparisons was performed for the 6 L bioreactor study to determine the significance of the differences among the studied parameters.

5.4 Results and discussion

5.4.1 Whey permeate characterization

Table 5.1 shows the main nutrient profile of the whey permeate. The whey permeate's main carbon source was lactose representing 19% of the total mass (wet basis). The whey permeate also contained notable amounts of nitrogen (0.16%) and phosphorus (0.20%), essential nutrients for *H. mediterranei* growth. The hydrolyzed whey permeate lactose concentration was higher than what was measured for DLP in Chapter 3. However, the DLP possessed considerably more ash, and slightly higher nitrogen and phosphorus concentrations. Table 5.2 presents the essential minerals and micronutrients in whey permeate. It contained lower minerals and micronutrients than DLP. Therefore, more MSM salts should be added to whey permeate compared to DLP for optimal *H. mediterranei* growth. Lower mineral

and micronutrients were present in whey permeate than in DLP because whey permeate is upstream of evaporator steps that concentrate the soluble minerals and micronutrients in the byproducts.

Table 5.1 Main nutrients of whey permeate.

Component	Contents
Total solids	28.0*
Moisture	72.0*
Lactose	19.0*
Ash	1.5*
Total C	7.7*
Total N	0.16*
Phosphorus	0.20*
SCOD	207**

* % (w.b.)

*unit for SCOD is g/l

Table 5.2 Minerals and micronutrients of whey permeate.

Element	Concentration
Sodium	0.20*
Magnesium	0.01*
Potassium	0.57*
Calcium	0.01*
Bromide	0.00*

Sulfur	0.01*
Chloride	0.24*
Zinc	0.14*
Boron	0.30**
Manganese	0.00**
Cobalt	0.00**
Copper	0.02**
Nickel	0.00**
Molybdenum	0.00**

* % (w.b.)

**unit for micronutrients is mg/l

5.4.2 Batch loading experiment

5.4.2.1 Effects of hydrolyzed DLP and whey permeate loading on cell growth

Hydrolyzed DLP, hydrolyzed whey permeate, and glucose were loaded at 10, 20, 30, and 40 g total sugars/l to determine the maximum substrate loading before inhibition of *H. mediterranei* occurred. Sugar was the main carbon source for the feedstocks, with the hydrolyzed DLP and whey permeate possessing both glucose and galactose monosaccharides. Figure 5.4 shows the 250 ml bioreactors at the beginning and end of the fermentation experiment. At the beginning of the fermentation, the hydrolyzed DLP bioreactors were brown due to nonenzymatic browning that can occur from the caramelization of sugars and the Maillard reaction, which produce melanoidin browning pigments (Božanić et al., 2014; Kuechel, 2017). The whey permeate flasks were initially yellow due to inherent constituents in the cheese byproduct, including annatto used for coloring cheese, beta carotene, and other vitamins in milk (Beucler et al., 2005; Byylund, 2015). The glucose flasks were opaque white since the yeast extract was the only

nutrient with color added at a low concentration of 1 g/l. After the stationary phase, all loadings of hydrolyzed whey permeate and glucose resulted in dense pink culture demonstrating successful growth. However, for the hydrolyzed DLP, only the loading of 10 g total sugar/l resulted in a pink culture being present. The three higher loadings slightly changed color, resulting in a lighter shade of brown, indicating the minimal growth of *H. mediterranei*. This result was the first indication that inhibition could occur with hydrolyzed DLP loadings greater than 10 g total sugar/l.

a)

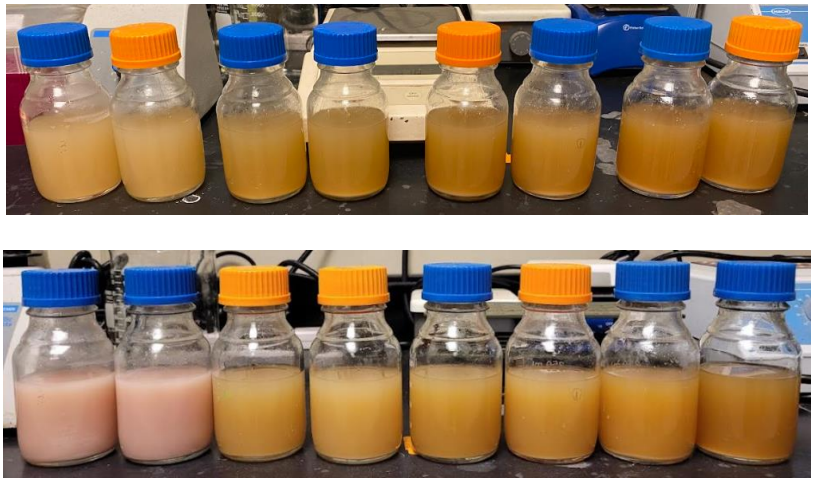

b)

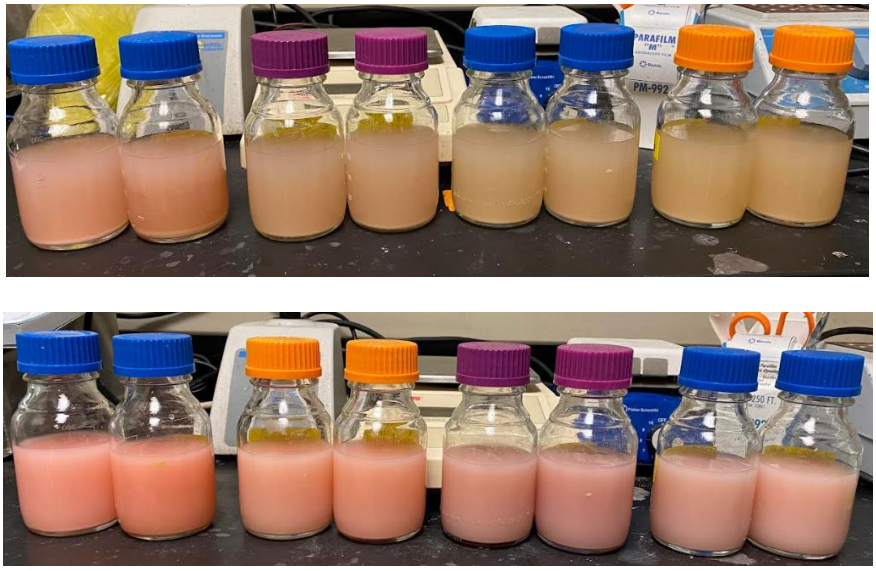

c)

Figure 5.4 Initial fermentation media and final cell broth with three sugar feedstocks at four different loadings: a) hydrolyzed DLP; b) hydrolyzed whey permeate; c) glucose. Loadings for the duplicate bioreactors from left to right: 10, 20, 30, and 40 g total sugar/l.

Figure 5.5 presents the final cell dry mass (CDM) concentration and yields of the three feedstocks at the four loadings tested. From two-way ANOVA, the effects of feedstock (p-value < 0.0001), loading (p-value < 0.0001), and interaction (p-value < 0.0001) on final CDM concentration were statistically significant. The effects of feedstock (p-value < 0.0001), loading (p-value < 0.0001), and interaction (p-value < 0.0001) on CDM yield were also statistically significant. The final CDM concentrations were comparable to the final OD results. The highest final CDM concentrations were obtained with the loadings of hydrolyzed whey permeate of 20, 30, and 40 g total sugar/l and were 4.7 ± 0.2, 6.3 ± 0.4, and 5.2 ± 0.2 g VS/l, respectively. The hydrolyzed whey permeate final CDM concentration increased with an increase in substrate loading up to 30 g total sugar/l. The hydrolyzed whey permeate at a loading of 20 g total sugar/l was significantly greater (p-value = 0.0364) than the 10 g total sugar/l, and the loading of 30 g total sugar/l was significantly greater (p-value = 0.0331) than the loading of 20 g total sugar/l. However, the increase in CDM was not proportional to the increase in substrate concentration. The hydrolyzed whey permeate loading of 40 g total sugar/l resulted in a final CDM that was less than the loading of 30 g total sugar/l, suggesting inhibition may be present above 30 g total sugar/l for this feedstock. The glucose final CDM concentration significantly increased (p-value = 0.0331) for the first two loadings of 10 and 20 g total sugar/l. However, the loadings of 20 and 30 g total sugar/l l were not significantly different (p-value = 0.6619), indicating no increase in CDM concentration occurred with the additional sugar. The glucose loading of 40 g total sugar/l resulted in the lowest final CDM at 1.8 ± 0.2 g VS/l, significantly less (p-value = 0.0000) than the loading of 30 g total sugar/l. These results might suggest substrate or intermediate inhibition may have occurred with the higher loadings of glucose substrate. For the hydrolyzed DLP with the loading of 20 g total sugar/l, the final CDM concentration of 2.0 ± 0.2 g VS/l was significantly less (p-value = 0.0000) than the loading of 10 g total sugar/l of 4.2 ± 0.5 g VS/l. Additionally, at the loadings of 30 and 40 g total sugar/l, the final CDM concentrations were less than 2.1 g VS/l of CDM, demonstrating that the maximum loading of hydrolyzed DLP was 10 g total sugar/l.

Hydrolyzed DLP appears to result in more inhibition than hydrolyzed whey permeate. DLP is downstream from whey permeate in the cheese, whey powder, and lactose powder processing. Constituents present from whey permeate processing into lactose powder and DLP may be a reason for the increased inhibition. DLP has been noted to have Maillard reaction products present due to the high-temperature evaporation steps required for lactose crystallization (Božanić et al., 2014) that can be inhibitory to microorganisms (Einarsson et al., 1983; Einarsson & Eklund, 1988). DLP also contains some of the same constituents as whey permeate, but at higher concentrations, since DLP is produced from concentrating the whey permeate to cause lactose crystallization (Byylund, 2015). Potential inhibitory compounds such as heavy metals could be present in low concentrations in whey permeate but inhibitory levels in DLP. However, ICP analysis demonstrated that the DLP contained concentrations of heavy metals As, Ni, Co, Pb, Cd, Cr, Zn, and Cu were well below inhibitory levels for *H. mediterranei* (Nieto et al., 1987). Additionally, *H. mediterranei* is one of the most tolerant halophilic archaea to heavy metal inhibition (Matarredona et al., 2021; Nieto et al., 1987). Therefore, DLP heavy metal inhibition does not appear to be the cause of lower *H. mediterranei* cell growth at higher substrate loadings.

The hydrolyzed DLP with a loading of 10 g total sugar/l achieved a CDM yield of 0.58 ± 0.06 g VS/g total sugar, and the hydrolyzed whey permeate CDM yield at this loading was 0.44 ± 0.01 g VS/g total sugar. These CDM yield values were the highest of all feedstocks and loadings tested. In comparison, the glucose loading of 10 g total sugar/l CDM yield was 0.32 ± 0.00 g VS/g total sugar. The hydrolyzed DLP and whey permeate CDM yields were significantly greater than the glucose (hydrolyzed DLP and glucose p-value < 0.0001) (hydrolyzed whey permeate and glucose p-value = 0.0006). The hydrolyzed DLP was also significantly greater (p-value = 0.0004) than the whey permeate CDM yield. These effects may be due to other nutrients that the hydrolyzed cheese byproducts possessed, such as milk-derived vitamins and co-factors (Oliveira et al., 2019), that the glucose feedstock did not possess, that the hydrolyzed DLP

contained at higher concentrations than the hydrolyzed whey permeate. The CDM yield for all three feedstocks decreased with increasing loading. This result suggested that less consumed sugar was diverted toward cell mass growth with the higher loadings.

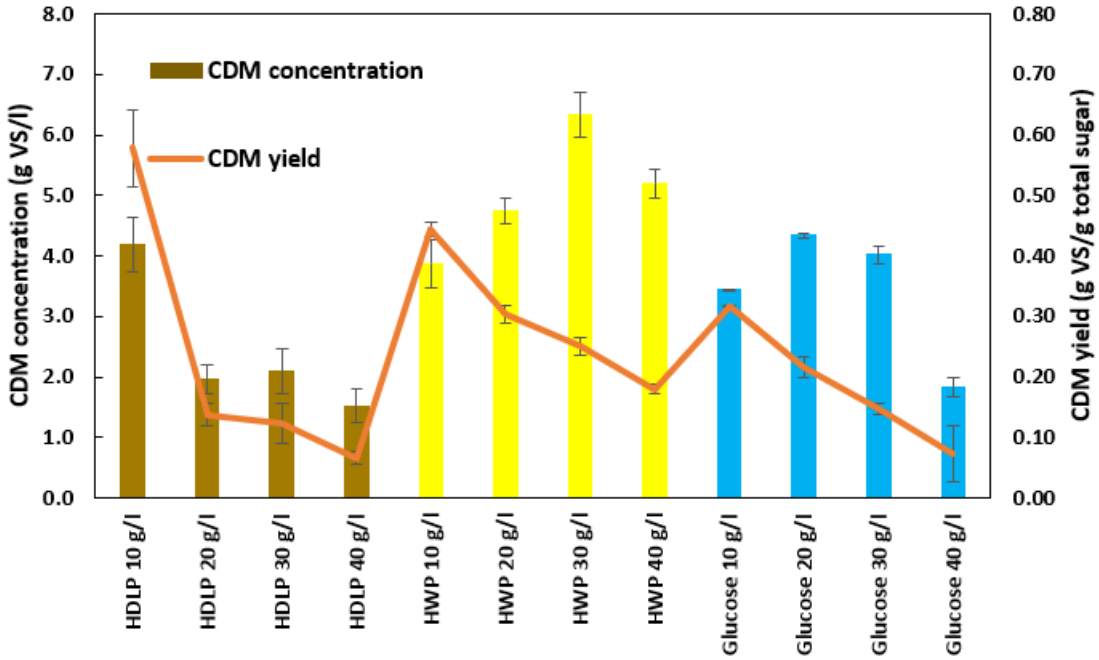

Figure 5.5 Final *H. mediterranei* cell dry mass (CDM) concentration and yield at different loadings of total sugars: a) hydrolyzed DLP (HDLP); b) hydrolyzed whey permeate (HWP); and c) glucose. Y-error bars are standard deviations.

5.4.2.2 Effects of hydrolyzed DLP and whey permeate loading on PHA production, yield, and content

Figure 5.6. displays the final PHA concentration and yields of the three feedstocks at the four different loadings. From two-way ANOVA, the effects of feedstock (p-value < 0.0001), loading (p-value = 0.0013), and interaction (p-value < 0.0001) on final PHA concentration were statistically significant. The effects of feedstock (p-value < 0.0001), loading (p-value < 0.0001), and interaction (p-value < 0.0001) on

PHA yield were also statistically significant. The final PHA concentrations obtained with the hydrolyzed whey permeate loadings of 20, 30, and 40 g total sugar/l were 3.4 ± 0.3, 4.2 ± 0.1, and 3.5 ± 0.0 g VS/l, respectively. These final PHA concentrations were the three highest for all feedstocks and loadings tested, likewise to the final CDM concentration. The final PHA concentrations increased with loading up to 30 g total sugar/l. However, the loading of 40 g/l was significantly less (p-value = 0.0194) than the loading of 30 g total sugar/l. The results demonstrated increased PHA production with higher loadings of hydrolyzed whey permeate up to 30 g total sugar/l. At the glucose loading of 20 g total sugar/l, the final PHA concentration was 1.5 ± 0.2 g VS/l, the highest final PHA concentration for this feedstock. Only the final PHA concentrations at the loadings of 20 g/l and 40 g total sugar/l were significantly different (p-value = 0.0203), indicating that higher sugar loading did not result in appreciable increases in PHA production. The final PHA concentration of the hydrolyzed DLP decreased with increasing loading past the 10 g total sugar/l, like for CDM, demonstrating the maximum loading of hydrolyzed DLP was 10 g total sugar/l. For the low loading of 10 g/l, the hydrolyzed DLP and whey permeate feedstocks resulted in comparable final PHA concentrations of 2.1 ± 0.2 g and 2.3 ± 0.1 g VS/l, respectively. The two hydrolyzed cheese byproducts' final PHA concentrations at this loading were not significantly different (p-value = 0.7455) from each other but were both significantly greater than glucose (hydrolyzed DLP and glucose p-value = 0.0050) (hydrolyzed whey permeate and glucose p-value = 0.0014). These results indicated that the cheese byproducts were more effective for PHA production than glucose.

The PHA yield followed a similar trend to the CDM yield. Using the hydrolyzed DLP and whey permeate with a loading of 10 g total sugar/l, the PHA yields were 0.30 ± 0.03 and 0.27 ± 0.02 g VS/g total sugar, respectively. These PHA yields were the highest for all feedstocks and loadings studied. The PHA yield obtained with the glucose loading of 10 g total sugar/l was 0.13 ± 0.03 g VS/g total sugar. The hydrolyzed DLP and whey permeate PHA yields at this loading were significantly greater than the glucose

(hydrolyzed DLP and glucose p-value < 0.0001) (hydrolyzed whey permeate and glucose p-value < 0.0001). The PHA yields of the hydrolyzed cheese byproducts with a loading of 10 g total sugar/l were not significantly different (p-value = 0.1951). The cheese byproducts' similar PHA yields are likely because both feedstocks' main carbon sources are glucose and galactose monosaccharides and contain other milk nutrients. The hydrolyzed whey permeate with loadings of 10 and 20 g total sugar/l resulted in PHA yields of 0.27 ± 0.02 and 0.22 g ± 0.02 VS/g total sugar, respectively. These yields were comparable to those obtained by Koller et al. (2007a) of 0.29 g PHA/g total sugar with a loading of 10 g total sugar/l of whey permeate supplemented with 5 g/l yeast extract. The PHA yields for all feedstock studied, like CDM yield, decreased with the increase of substrate concentrations. This result signified that the additional sugar consumed with the higher loadings was less efficiently going toward PHA production. Wang (2021) reported low PHA yields with hydrolyzed lactose powder substrate of less than 0.10 g PHA/g sCOD at the loadings of 22.5 and 45.0 g sCOD/l. These hydrolyzed lactose powder PHA yields were significantly less than the PHA yields of pretreated food waste substrates (volatile fatty acids main carbon source) that were greater than 0.10 g/g sCOD. The results obtained by Wang (2021) may be partly caused by the lower PHA yields that appear to occur with higher sugar loadings demonstrated in this study.

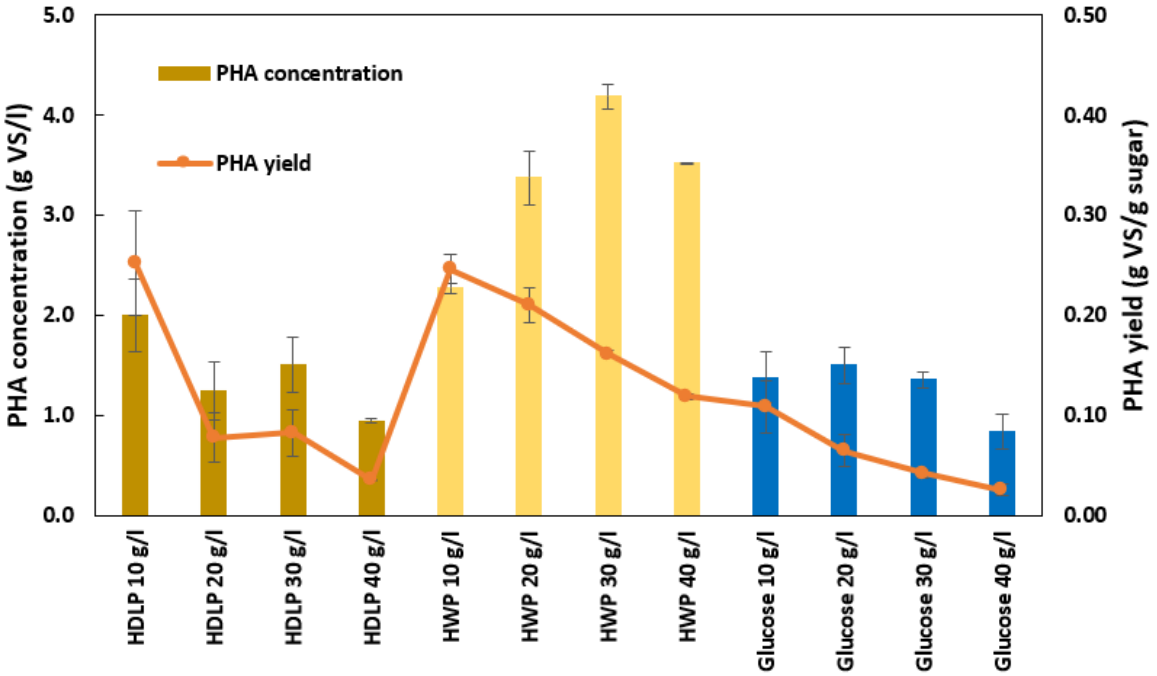

Figure 5.6 Final *H. mediterranei* PHA concentration and yield at different loadings of total sugars with a) hydrolyzed DLP (HDLP); b) hydrolyzed whey permeate (HWP); and c) glucose. Y-error bars are standard deviations.

Figure 5.7 shows the PHA content of the three feedstocks with four different loadings. From two-way ANOVA, the effects of feedstock (p-value < 0.0354), loading (p-value = 0.0463), and interaction (p-value < 0.0001) on final PHA concentration were statistically significant. From the Tukey pairwise comparison, the PHA contents for each feedstock (hydrolyzed DLP, hydrolyzed whey permeate, and glucose) at the various loadings were not significantly different in all cases except for the hydrolyzed DLP with the loadings of 10 and 30 g total sugar/l (p-value = 0.0066). The hydrolyzed DLP PHA contents were 0.51-0.72 g VS/g VS, and the hydrolyzed whey permeate PHA contents were 0.59-0.71 g VS/g VS. These values were on the higher end of PHA contents typically reported in the literature for *H. mediterranei* with sugar substrates of 0.28-0.66 g VS/g VS (Melanie et al., 2018; Pais et al., 2016; Rodriguez-Valera et al., 1991). Other researchers have also demonstrated that *H. mediterranei* PHA contents of 0.60 g VS/g VS or

higher can be achieved with rice-based ethanol stillage (0.71 g VS/g VS) (Bhattacharyya et al., 2014) and VFAs (up to 0.60 g VS/g VS) (Wang & Zhang, 2021). The PHA contents with the loading of the 10 g total sugar/l for the three sugar feedstocks were comparable to each other at 0.51 ± 0.01 g VS/g VS for the HDLP, 0.59 ± 0.05 g VS/g VS for hydrolyzed whey permeate, and 0.40 ± 0.07 g VS/g VS for glucose. Only the hydrolyzed DLP and glucose were significantly different (p-value = 0.0088) at this low loading. The higher PHA contents observed for the hydrolyzed cheese byproducts feedstocks compared to glucose suggests the complex cheese byproducts may improve *H. Mediterranei* PHA accumulation. This result may be due to other nutrients that the cheese byproducts possess in addition to sugars.

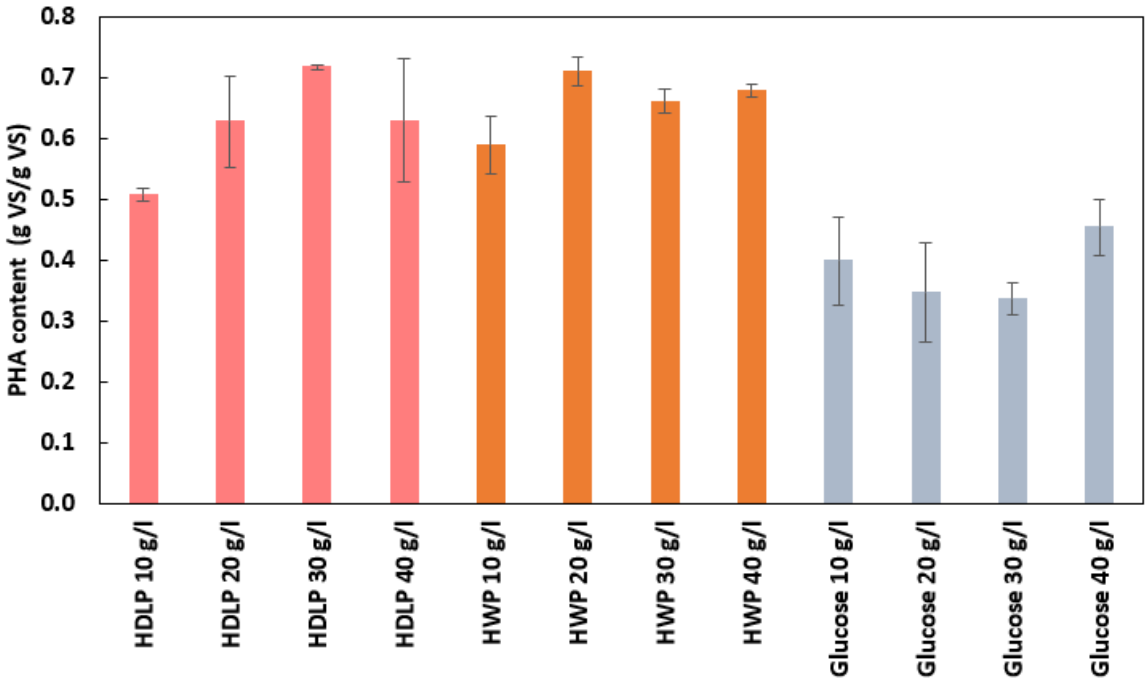

Figure 5.7 *H. mediterranei* PHA content at different loadings of total sugars: a) hydrolyzed DLP (HDLP); b) hydrolyzed whey permeate (HWP); and c) glucose. Y-error bars are standard deviations.

5.4.2.3 Effects of hydrolyzed DLP and whey permeate loading on sugar consumption

Figure 5.8 shows the total sugar consumption with the three feedstocks and four loadings. The glucose, galactose, and total sugar consumptions are shown for the multi-sugar hydrolyzed DLP and whey permeate feedstocks. For the hydrolyzed cheese byproducts, high glucose consumption of > 83% was observed for all the loadings, and > 90% glucose consumption occurred for all the hydrolyzed whey permeate loadings and the two lower loadings of hydrolyzed DLP. Galactose consumption was considerably lower for all the hydrolyzed cheese byproduct loadings, 3%-35% for the hydrolyzed DLP and 45%-63% for the hydrolyzed whey permeate. The higher glucose consumption compared with galactose agreed with Pais et al. (2016) and results obtained in previous Chapters 3 and 4 that *H. mediterranei* prefers glucose over galactose. Greater than 60% galactose consumption occurred with the hydrolyzed whey permeate with the loadings of 10 and 30 g total sugar/l. For the glucose feedstock, high sugar consumption of > 94% occurred with the loading of 10 and 20 g total sugar/l. Additionally, the loading of 30 g/l resulted in a high glucose consumption of 84 ± 3%. However, less glucose consumption occurred with the glucose loading of 40 g/l at 52 ± 5%. The low sugar consumption of the glucose loading of 40 g total sugar/l aligned with the low final CDM and PHA concentrations results for this feedstock and loading.

a)

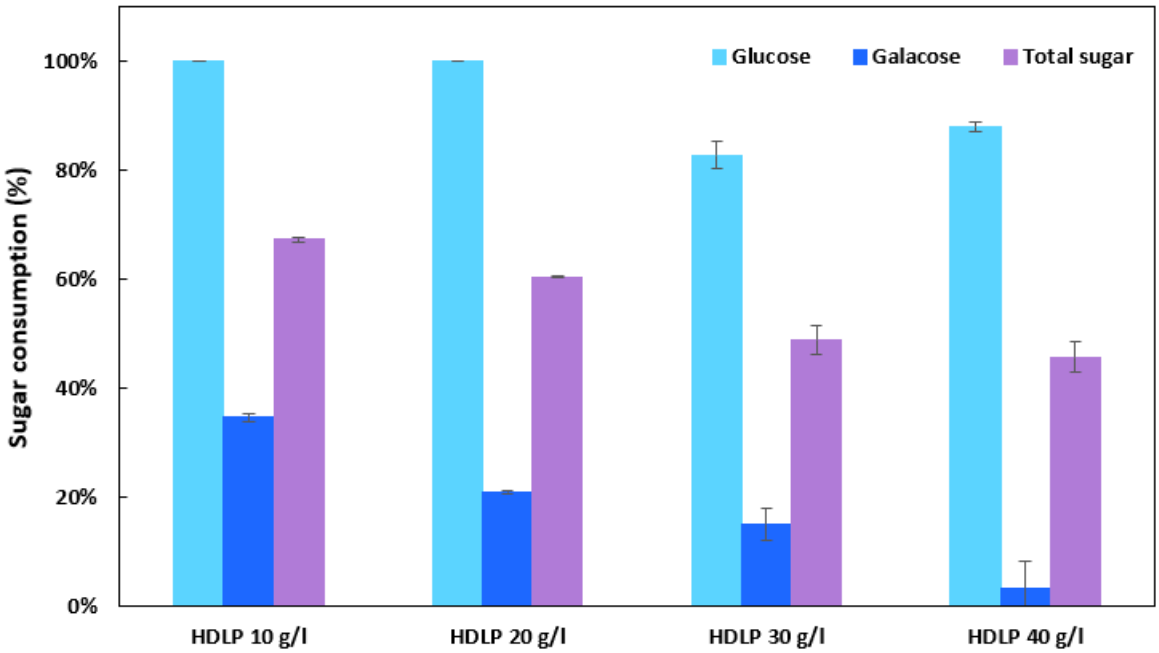
Glucose
Galacose
Total sugar
Sugar consumption (%)
100%
80%
60%
40%
20%
0%
HDLP 10 g/l
HDLP 20 g/l
HDLP 30 g/l
HDLP 40 g/l

b)

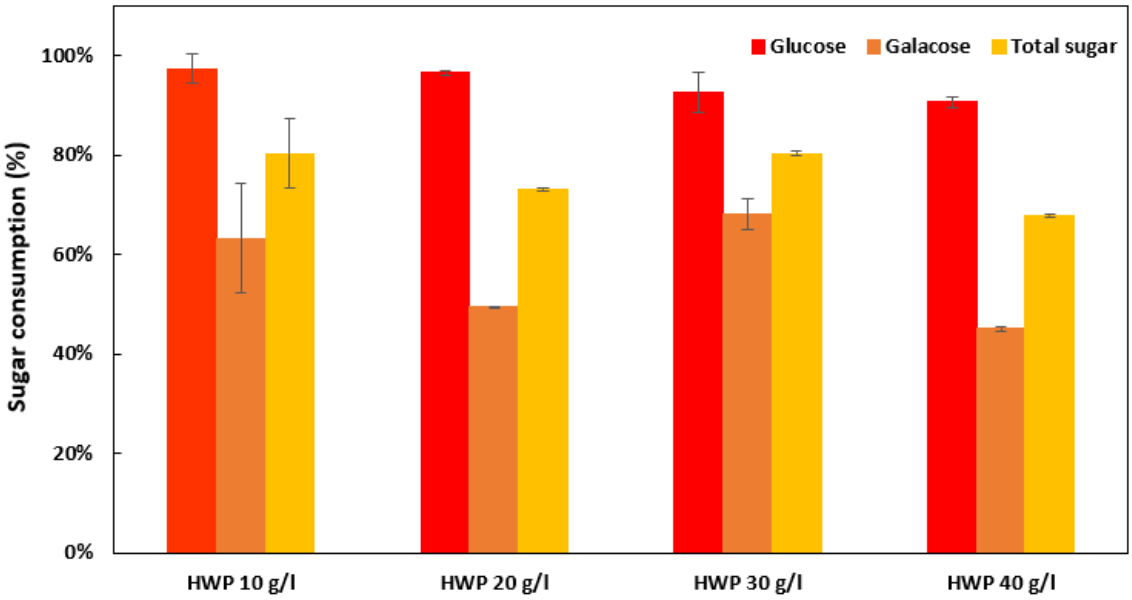
Glucose
Galacose
Total sugar
Sugar consumption (%)
100%
80%
60%
40%
20%
0%
HWP 10 g/l
HWP 20 g/l
HWP 30 g/l
HWP 40 g/l

c)

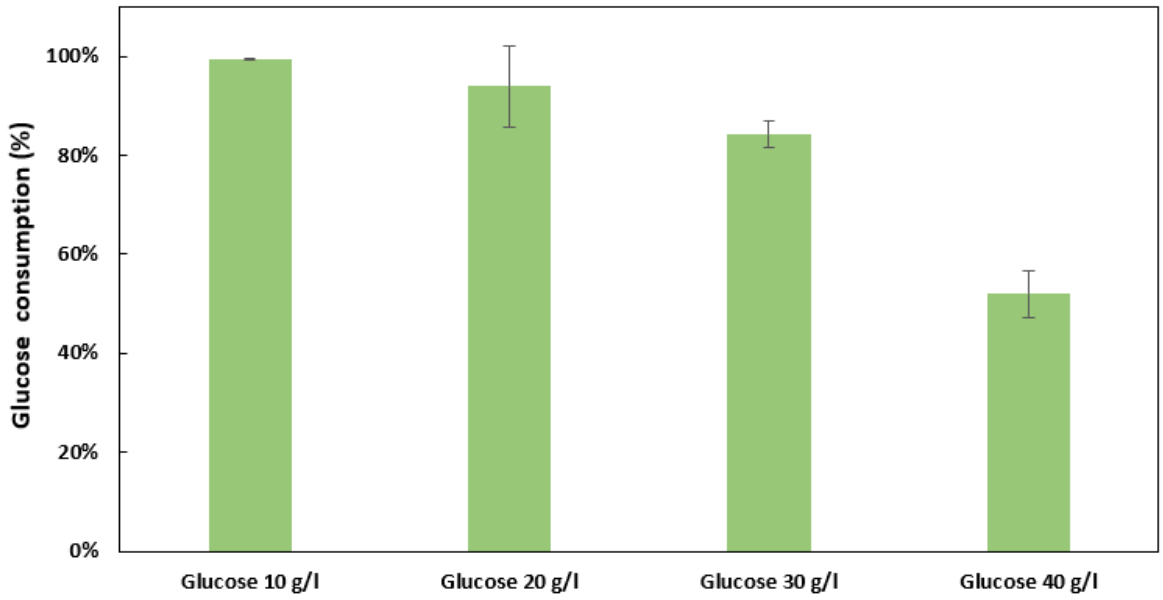

Figure 5.8 *H. mediterranei* sugar consumption at different loadings of total sugars: a) hydrolyzed DLP (HDLP); b) hydrolyzed whey permeate (HWP); and c) glucose. Y-error bars are standard deviations.

5.4.3 Hydrolyzed DLP batch loading with 6 L bioreactor

Cell growth decreased with hydrolyzed DLP loadings above 10 g total sugar/l in the batch 250 ml bioreactors. Wang (2022) demonstrated that a DO of greater than 50% could improve cell mass growth. A 6 L reactor with a 5 L working volume was operated with the DO controlled over 50% saturation to confirm that hydrolyzed DLP inhibition occurred for loadings over 10 g total sugar/l and to scale the process. The 6 L bioreactor was initially loaded with hydrolyzed DLP at 10 and 20 g total sugar/l. Figure 5.9 shows the bioreactor at the start and the end of fermentation after 192 hours. At the beginning of the fermentation, the loading of 10 g total sugar/l was yellow-pink due to the low loading levels of the hydrolyzed DLP combined with the pink *H. mediterranei* inoculum. The loading of 20 g total sugar/l had a considerably darker brown color due to the previously noted constituents of DLP. After 192 hours, the

loading of 10 g total sugar/l resulted in a dense pink color, indicating the growth of the archaea. Therefore, a successful scale-up appeared to have occurred at this hydrolyzed DLP loading. In contrast, although the loading of 20 g total sugar/l changed color to a lighter yellow shade suggesting some biomass growth, the reactor did not turn the same vibrant pink color as the loading of 10 g total sugar/l, indicating minimal cell growth. Inhibition appeared to have occurred again, potentially due to compounds formed during the high-heat processing of whey permeate, like for the 250 ml bioreactors with hydrolyzed DLP loadings above 10 g total sugar/l.

Figure 5.10 shows the cell growth curves of the two loadings. No appreciable lag phase was observed for the loading of 10 g total sugar/l as the OD increased in the first 24 hours of growth. The cell growth rapidly increased in the exponential growth phase for the first 96 hours before decelerating in the next 72 hours and reaching the stationary phase after 168 hours. A final OD of 9.0 ± 0.2 was measured for the loading of 10 g total sugar/l, comparable to what was observed with the 250 ml bioreactors. A lag phase was present for the loading of 20 g total sugar/l for the first 24 hours, followed by a cell growth rate comparable to the loading of 10 g/l for the next 48 hours. However, a stationary phase was achieved after 96 hours, considerably sooner than the loading of 10 g total sugar/l. Negligible cell growth occurred during the next 120 hours of fermentation, demonstrating inhibition. The final OD value at 20 g total sugar/l was 3.4 ± 0.1, appreciably less than that was measured with the loading of 10 g total sugar/l.

a) b)

Figure 5.9 Initial fermentation media and final cell broth with hydrolyzed DLP at two different loadings: a) 10 g total sugar/l; b) 20 g total sugar/l; left) 0 hour; right) 192 hours.

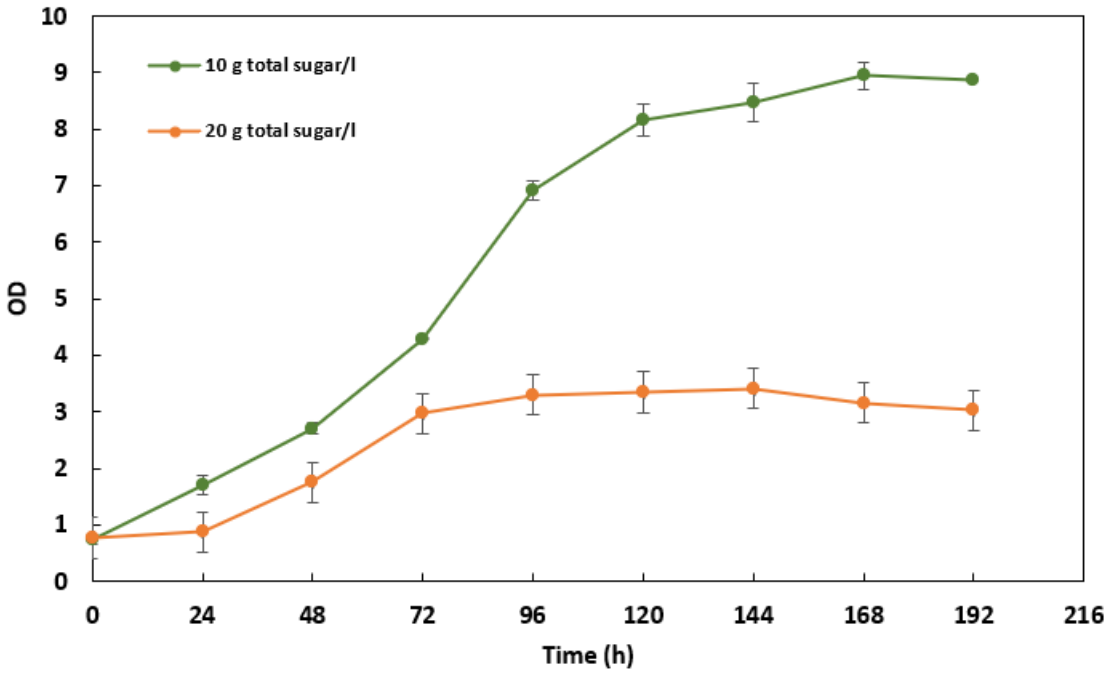

Figure 5.10 Cell growth of *H. mediterranei* over time with hydrolyzed DLP at two total sugar loadings. Y-error bars are standard deviations.

Figure 5.11 displays the corresponding final CDM and PHA concentrations of the 6 L reactor operation with the two substrate loadings. The final CDM concentration obtained with the loading of 10 g total sugar/l was 4.4 ± 0.0 g VS/l compared to 2.3 ± 0.2 g VSS/l that was obtained with the loading of 20 g total sugar/l. At the loading of 10 g total sugar/l, the final CDM concentration was significantly greater than that obtained with the loading of 20 g total sugar/l (p-value = 0.0057). This result confirmed that cell mass growth inhibition occurred at higher loadings of hydrolyzed DLP above 10 g total sugars/l. The final PHA concentration of the 10 g total sugar/l loading was also significantly greater than the 20 g total sugar/l loading (p-value = 0.0169) and was at 1.8 ± 0.1 g VS/l compared to 1.2 ± 0.1 g VS/l. Effective scale-up from 0.2 to 5 L for the loading of 10 g total sugar/l was achieved since similar CDM and PHA production occurred at the larger 6 L scale compared to the 250 ml bioreactors. If batch production is utilized with hydrolyzed DLP, a loading of 10 g total sugar/l should be applied to minimize substrate inhibition.

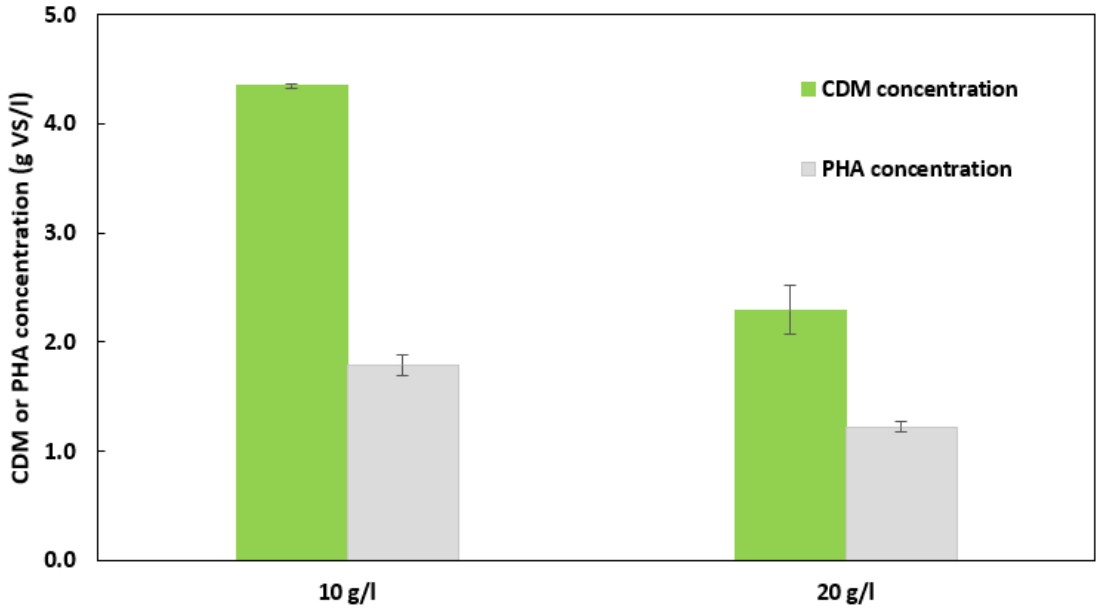

Figure 5.11 Final *H. mediterranei* cell dry mass (CDM) and PHA concentration with hydrolyzed DLP at two total sugar loadings. Y-error bars are standard deviations.

Figure 5.12 shows the CDM yield, PHA yield, and PHA content of the 6 L reactor operation with hydrolyzed DLP at the two loadings. The measured values of the parameters were similar to those with the 250 ml bioreactor experiments at equivalent loadings. The CDM yield of the loading of 10 g total sugar/l was 0.61 ± 0.02 g VS/g total sugar, significantly greater (p-value = 0.0028) than the loading of 20 g total sugar/l at 0.19 ± 0.02 g VS/g total sugar. Likewise, the PHA yield was significantly greater for the loading of 10 g total sugar/l at 0.25 ± 0.01 g VS/g sugar than the loading of 20 g total sugar/l at 0.10 ± 0.01 g VS/g total sugar (p-value = 0.0012). The PHA content of 0.54 g VS/g VS that was obtained with the loading of 20 g total sugar/l was significantly greater (p-value = 0.0434) than that obtained at the loading of 10 g total sugar/l of 0.41 g VS/g VS.

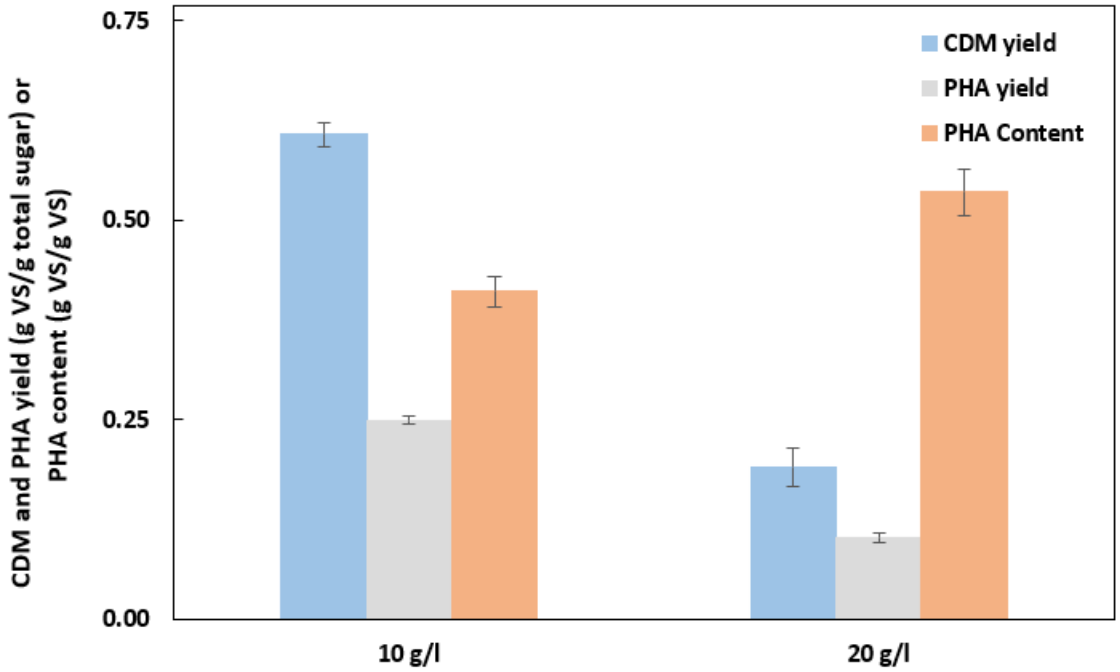

Figure 5.12 *H. mediterranei* cell dry mass (CDM) yield, PHA yield, and PHA content with hydrolyzed DLP at two total sugar loadings. Y-error bars are standard deviations.

5.4.4 Maximum specific growth rate determination of hydrolyzed DLP and whey permeate

Since the hydrolyzed DLP resulted in apparent substrate inhibition above loadings of 10 g total sugar/l, lower loadings of the feedstock were studied to confirm the maximum specific growth rate. Figure 5.13a shows the cell growth curves of the four hydrolyzed DLP feedstock loadings of less than 10 g total sugar/l, and Figure 5.13b displays the cell growth curves of the four hydrolyzed whey permeate feedstock loadings between 10 and 40 g total sugar/l from the previous batch study after 240 hours. The specific growth rates, μ, with hydrolyzed DLP, were estimated to be in the range of 0.01 to 0.02 h^{-1}. All hydrolyzed whey permeate loadings studied resulted in a specific growth rate of 0.02 h^{-1}. Therefore, both hydrolyzed cheese byproducts' maximum specific growth rates, μ_{max}, were 0.02 h^{-1}. The equivalent maximum specific growth rates for the hydrolyzed cheese byproducts may be due to both feedstocks' main carbon sources being glucose and galactose monosaccharides.

a)

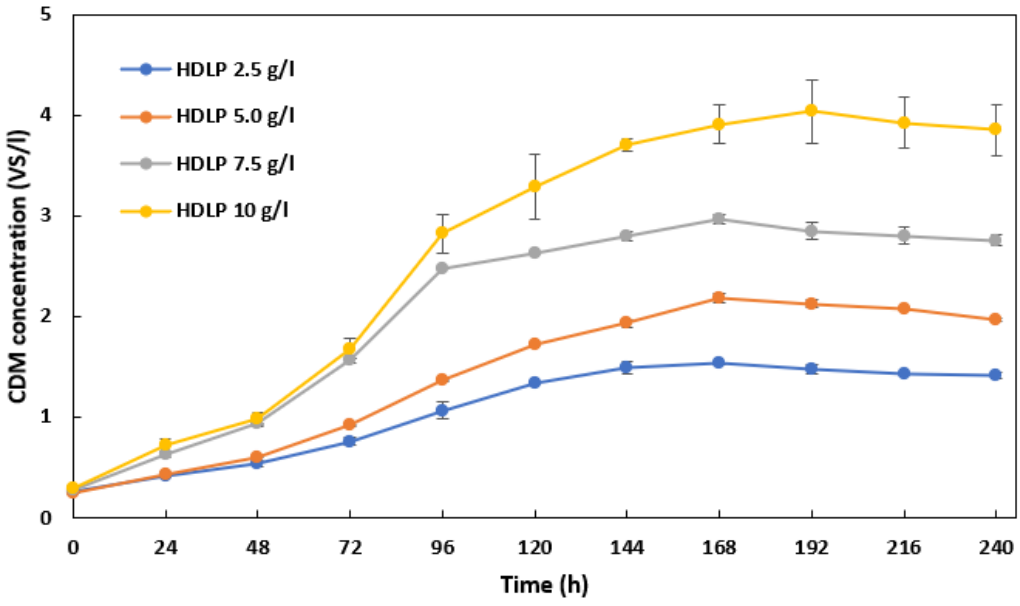

b)

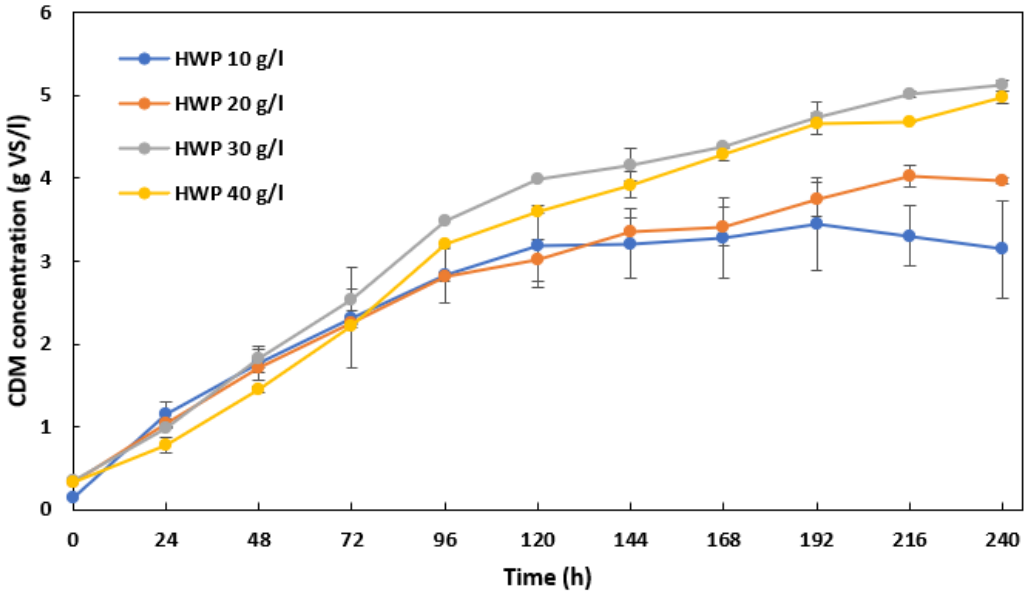

Figure 5.13 Cell growth of *H. mediterranei* over time at different loadings of substrates: a) hydrolyzed DLP; and b) hydrolyzed whey permeate. Y-error bars are standard deviations.

Table 5.3 Hydrolyzed DLP specific growth rate estimation.

Substrate Loading (g/l)	Specific growth rate (u)	X_0	R^2
2.5	0.015	-1.295	0.990
2.5	0.014	-1.299	0.993
5	0.018	-1.345	0.992
5	0.017	-1.314	0.998
7.5	0.022	-1.156	0.987
7.5	0.022	-1.151	0.982
10	0.021	-1.079	0.985
10	0.023	-1.049	0.971

Table 5.4 Hydrolyzed whey permeate specific growth rate estimation.

Substrate loading (g/l)	Specific growth rate (u)	X_0	R^2
10	0.019	-0.707	0.872
10	0.021	-0.610	0.854
20	0.021	-0.751	0.880
20	0.021	-0.736	0.879
30	0.023	-0.750	0.939
30	0.023	-0.734	0.926
40	0.023	-0.858	0.963
40	0.024	-0.986	0.972

5.5 Conclusions

The maximum loading of three sugar feedstocks (hydrolyzed DLP, hydrolyzed whey permeate, and glucose) were determined for the batch growth of *H. mediterranei*. The cell dry mass and PHA production with hydrolyzed DLP decreased with the increase of the loading above 10 g total sugar/l. The cell dry mass and PHA production increased with increasing the loadings of hydrolyzed whey permeate up to a loading of 30 g total sugar/l. The cell dry mass increased with the increase of glucose loading up to 20 g total sugar/l. It is recommended to load hydrolyzed DLP with less than 10 g total sugar/l and hydrolyzed whey permeate up to a 30 g total sugar/l for the batch cultivation and PHA production of *H. mediterranei*. The maximum growth rates of the two cheese byproducts were estimated and determined to be comparable. The kinetic parameters can be used to help in designing industrial-scale production facilities. The results of this study can assist in developing commercial cheese byproduct PHA production by providing the maximum loading of the feedstocks and reaction kinetics. Cheese byproduct-derived PHA production can

add revenue for milk producers and cheese manufacturers and increase the sustainability of the global economy.

Chapter 6. Fed-batch *H. mediterranei* and PHA production Using Hydrolyzed Delactosed Permeate (DLP) and Whey Permeate

6.1 Abstract

The high production cost of bioplastic PHA has limited its market growth, mainly due to expensive feedstocks that are commonly utilized. This study aimed to reduce PHA production costs by using low-value cheese byproducts, delactosed permeate (DLP) and whey permeate, and PHA producer *Haloferax mediterranei (H. mediterranei)*. In Chapter 5, hydrolyzed DLP was demonstrated to result in substrate inhibition at low loadings greater than 10 g total sugar/l. This inhibition result could pose challenges for the commercialization of the PHA process due to increased capital and operating costs required for larger fermentation and downstream processing equipment. Fed-batch operation is one common technique to reduce substrate inhibition by decreasing the maximum substrate loading of a bioreactor. A fed-batch 6 L reactor with an initial working volume of 3 L was tested, feeding an equivalent loading of 10 g total sugar/l of hydrolyzed DLP or whey permeate every four days. Improved PHA production was achieved for hydrolyzed DLP with two feedings. A final PHA concentration of 3.0 ± 0.4 g VS/l, a 50% increase in the final PHA produced with one batch feeding of hydrolyzed DLP in Chapter 5, was obtained due to the input of additional sugars. Hydrolyzed whey permeate fed-batch feeding increased PHA production with up to three feedings, achieving a final PHA concentration of 5.0 g VS/l. Therefore, the fed-batch operation could improve PHA production with hydrolyzed cheese byproduct substrates. These results could assist in developing commercial PHA production from cheese byproducts, growing the dairy industry's sustainability.

Keywords: *Haloferax mediterranei*, delactosed permeate, whey permeate, fed-batch, polyhydroxyalkanoates

6.2 Introduction

Plastics are a valued commodity on the global market and are used across virtually all industrial sectors. Worldwide plastic production is approximately 390 million metric tons (MT) per year (European Bioplastics, 2023), with approximately 50% utilized to create single-use items that are used once before being discarded (Geyer et al., 2017). In 2015, nearly 50% of plastics worldwide were landfilled, with only approximately 20% of plastics being recycled (Geyer et al., 2017). Additionally, it is estimated that up to 12.7 MT of plastic enters the ocean each year (Jambeck et al., 2015), threatening aquatic ecosystems and endangering human health and food safety (Carbery et al., 2018; Cózar et al., 2014). Nearly all plastics on the market are derived from unsustainable fossil fuel feedstocks (European Bioplastics, 2023) and contribute considerably to global greenhouse gas emissions (Zheng & Suh, 2019). Therefore, further attention is needed for plastic product design to decrease the environmental impacts of traditional plastics (Dilkes-Hoffman et al., 2018).

One alternative material to alleviate these issues associated with conventional plastics is bioplastic polyhydroxyalkanoates (PHA). PHA is a family of high-value polyesters with similar properties to common thermoplastics that can be produced from renewable organic feedstocks (Reddy et al., 2003). PHA can biodegrade at ambient temperatures in terrestrial and oceanic environments in less than 6 months (Meereboer et al., 2020) and in aerobic and anaerobic environments (Bugnicourt et al., 2014). This excellent biodegradability permits inadequately discarded PHA products to have considerably reduced environmental impacts. PHAs can be used in numerous applications, including plastic bags, packaging film, food containers, disposable cutlery, 3D printing material, and medical sutures (Joyce, 2018; Reddy et al., 2003). However, even though PHA has been commercialized since the early 1990s (G.-Q. Chen, 2009), its production only accounts for a minimal fraction of the global plastic market (European Bioplastics, 2023). This is mainly due to high production costs from expensive feedstocks commonly

applied, such as sugars, starches, and oils (Bugnicourt et al., 2014; Yoong Kit et al., 2017). Therefore, many researchers have focused on studying low-cost organic substrates to improve the economics of PHA production (Amaro et al., 2019; Koller, 2018; Wang & Zhang, 2021).

One low-value carbon source that could be applied for PHA production is cheese byproducts generated after milk has been processed into cheese (Figure 6.1). The main byproduct of the cheese-making process is liquid whey. Although the cheese industry has been able to transform this costly effluent stream into an innovative range of over 100 high-value products (Tolhurst, 2016), approximately 50% of whey produced globally is not utilized for commercial products due to economic restrictions for smaller scale-operations and market limitations (Nikodinovic-Runic et al., 2013). When the liquid whey is concentrated and dried into protein products, byproduct whey permeate is generated, containing most of the original lactose sugars and minerals (Byylund, 2015). The whey permeate can likewise be further concentrated with crystallization processes to create lactose powder products (Oliveira et al., 2019). The byproduct of this lactose powder process is delactosed permeate (DLP) which again contains most of the milk minerals and still contains approximately one-third of the original lactose due to crystallization limitations (Liang et al., 2009). These various byproduct streams are either sold as low-value animal feed, processed as wastes, or landfilled, causing associated environmental impacts (Liang et al., 2009; Oliveira et al., 2019; Tolhurst, 2016). Therefore, these low-value cheese byproducts that contain high sugar contents represent an attractive potential substrate for PHA production.

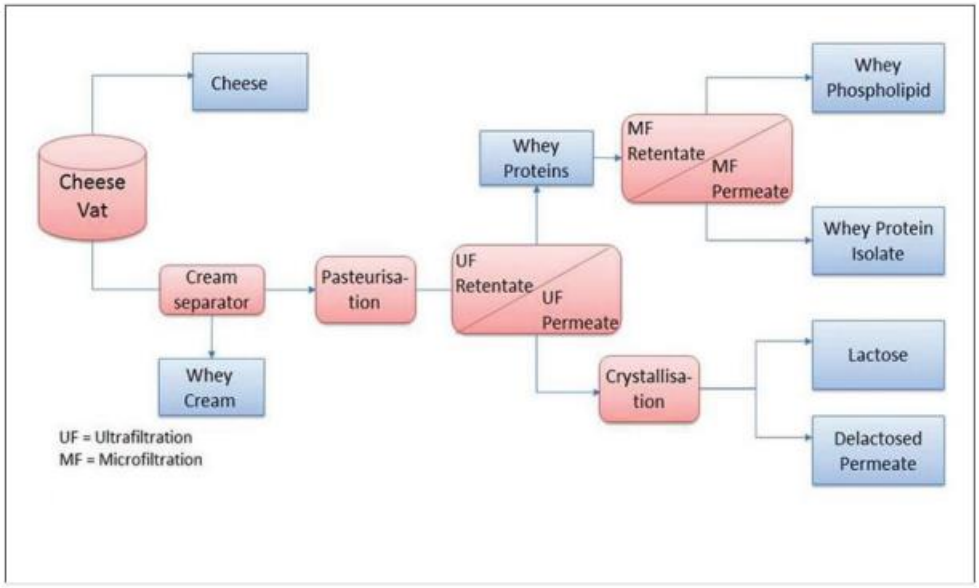

Figure 6.1 Cheese and whey processing unit operations and co-products (Tolhurst, 2016).

Several microorganisms can produce PHA, typically intracellularly stored as an energy reserve (Bernard, 2014). Careful considerations should be made when selecting which PHA producer to pair with a specific waste or byproduct. These substrates can contain a wide range of carbon sources, can possess other constituents that cause inhibition, and are more prone to contaminant organisms (Amaro et al., 2019; Nielsen et al., 2017; Wang, 2022). PHA producer *Haloferax mediterranei* (*H. mediterranei*) seems to be an ideal fit with cheese byproducts. This pairing is because *H. mediterranei* is an extreme halophile that grows up to 20% salinity (Ferre-Guell & Winterburn, 2018). The high saline environment permits straightforward integration of high salt-containing cheese byproducts (Byylund, 2015; Liang et al., 2009) since *H. mediterranei* requires these salts as nutrients that some other PHA producers and common contaminant organisms cannot tolerate (Amaro et al., 2019). The high salt environment also does not necessitate an expensive sterility unit operation, such as high-temperature exposure or antibiotics before fermentation (Amaro et al., 2019; Koller et al., 2011; Wang & Zhang, 2021). Intracellular PHA extraction can transpire through simple water addition causing osmotic shock cell lysis compared with costly

chemicals frequently detrimental to the environment (Byrom, 1987; Ghosh et al., 2019). *H. mediterranei* produces a higher value PHA polyester, poly(3-hydroxybutyrate-co-3-hydroxyvalerate) (PHBV) compared to most commonly produced PHA polyester polyhydroxybutyrate (PHB) (Reddy et al., 2003). PHBV can be used for many applications, such as food packaging film, bags, containers, or cutlery, helping to close the food industry's circular economy (Bugnicourt et al., 2014; Joyce, 2018; Reddy et al., 2003).

Previous chapters 3-5 determined that *H. mediterranei* could successfully grow and produce PHA at high yields using hydrolyzed DLP at low substrate loadings of 10 g total sugar/l with hydrolyzed DLP. However, the study in Chapter 5 showed that inhibition could occur with hydrolyzed DLP above the loading of 10 g total sugar/l. This substrate inhibition that was experienced is a common disadvantage of batch feeding (Koller & Muhr, 2014). Alternatively, fed-batch cultivation can be applied to decrease substrate inhibition or end-product inhibition, shorten fermentation times, and achieve high cell concentrations (Poontawee & Limtong, 2020). Some researchers have studied PHA production with various PHB producers, including genetically modified *E.coli* and natural *Methylobacterium* sp. ZP24, utilizing hydrolyzed cheese byproducts or synthetic dairy media and applying fed-batch feeding strategies. Varying degrees of success were achieved with PHA productivities of 0.08 - 4.6 g/l/h (Ahn et al., 2001; Nath et al., 2008; Wong & Lee, 1998). Using *H. mediterranei*, Koller et al. (2007a) studied the production of PHBV with a fed-batch feeding of hydrolyzed cheese byproduct whey. Koller et al. (2007a) achieved a maximum PHA concentration of 12.2 g/l, PHA productivity of 0.09 g/l/h, and a PHA yield of 0.29 g PHA/g whey sugars consumed. Research is needed to understand the performance of fed-batch reactor operation using *H. mediterranei* and hydrolyzed DLP.

The tasks of this study were to: 1) determine the yield of PHA production using *H. mediterranei* and fed-batch bioreactor operation with hydrolyzed DLP; and 2) compare the *H. mediterranei* PHA yields of fed-batch feeding of hydrolyzed DLP and whey permeate.

6.3 Materials and methods

6.3.1 Feedstock collection

The same DLP and whey permeate collected from Hilmar Cheese Company, Hilmar, California, used in previous Chapter 5, were used as feedstock for *H. mediterranei* cultivation. The DLP and whey permeate were collected from Hilmar Cheese Company's lactose plant. Whey permeate is derived from cheese whey processing with membrane filtration. The whey proteins are concentrated before drying into whey powder, while the liquid that fluxes through the membranes is whey permeate (Byylund, 2015). The whey permeate can then be further concentrated with evaporator systems to crystallize the lactose for drying and milling into lactose powder products (Oliveira et al., 2019). The remaining liquid is DLP, which contains around one-third of the original lactose and most of the original milk minerals (Liang et al., 2009). Therefore, DLP contains a lower percent lactose of total solids but higher levels of nitrogen and minerals than whey permeate.

6.3.2 Delactosed permeate and whey permeate pretreatment

The study used *H. mediterranei* (ATCC 33500) as the microbial PHA producer. The active inoculum was prepared according to the procedures stated in Chapter 3. DLP and whey permeate were studied as feedstocks for the fed-batch cultivation of *H. mediterranei*. The DLP was pretreated with centrifugation as described in Chapter 3. The centrifuged DLP and whey permeate were hydrolyzed with lactase enzyme Nola Fit 5550 (Chris Hansen, Hoersholm, Denmark) with a 0.025 g lactase/g lactose loading, 12 hours of incubation, and a temperature of 40 ℃ as outlined in Chapter 3. The hydrolyzed DLP and whey permeate

were used as feedstock for *H. mediterranei* cultivation. The previously described minimum salt media (MSM) and 1% v/v SL-6 trace elements were used as the base for the two feedstocks. Ammonium chloride was added as a supplementary nitrogen source to all feedstocks to give a constant C/N ratio of 8, which provided excess nitrogen for cell growth (Cui, Shi, et al., 2017). Potassium dihydrogen phosphate was added as a supplementary phosphorus source for the hydrolyzed whey permeate to obtain a C/P ratio of 35, which provided an excess of phosphorous (Melanie et al., 2018). Sodium bicarbonate was added as a buffer at a 2.5 g/l loading. The initial media was loaded with 10 g total sugar/l for the two cheese byproduct feedstocks. The media used for fed-batch feeding were made up using undiluted hydrolyzed DLP and whey permeate and adding equivalent salts to obtain the concentrations in MSM and a 1% v/v loading of SL-6. Ammonium chloride was added as a supplementary nitrogen source to achieve a C/N ratio of 8. The bioreactor was fed an equivalent loading of 10 g total sugar/l every four days, which was demonstrated in previous chapters to be when *H. mediterranei* growth began to reach the deceleration phase, complete glucose consumption occurred, and galactose consumption began. A 6 L bioreactor with an initial working volume of 3 L was operated for the study. The pH was controlled to 7.0 with 3 M NaOH and 3 M HCl and pH controller (Bluelab, Tauranga, Gisborne, New Zealand). The temperature was controlled to 37 ± 1.0 ℃ using a water bath and jacket that enclosed the bioreactor. Forced aeration was provided to achieve dissolved oxygen (DO) of 20%-40% saturation, as shown by Wang (2022), to provide adequate oxygen for *H. mediterranei* cultivation. The bioreactor was operated for 16 days with hydrolyzed DLP and 24 days with hydrolyzed whey permeate.

6.3.3 Determination of cell mass and PHA concentration

The cell growth was measured by sampling 1 ml of fermentation broth from the 6 L bioreactor daily throughout the fermentation. The samples' optical density (OD) was measured at 520 nm, as described by Huang et al. (2016). Additionally, 50 ml of cell broth sample was collected every four days

before feeding to measure the changes in the CDM and PHA concentrations with time. The cell dry mass (CDM) was measured as the fermentation broth's volatile solids (VS). Twenty milliliters of the fermentation broth was sampled and centrifuged at 8,000 rpm for 30 minutes. The resultant cell pellet was washed with MSM solution twice, and the VS was measured using an oven and furnace following standard methods (American Public Health Association, 2012). The PHA mass was also measured as VS after separating the PHA from the residual cell mass. The PHA was extracted following a method described by Escalona et al. (1996) with modifications described in previous chapters. Twenty milliliters of fermentation broth was sampled and centrifuged at 8,000 rpm for 30 minutes, like for CDM. A surfactant solution of 0.1% sodium dodecyl-sulfate (SDS) and deionized (DI) water was added to the cell pellet, causing cell lysis and solubilization of the cell mass. The cell pellet with SDS surfactant was placed in a shaker incubation at 40℃ and agitation at 180 rpm for 12 hours. The extracted PHA was then washed twice with DI water. The VS of the washed PHA pellet was determined following the standard methods as stated for CDM (American Public Health Association, 2012). With the measured CDM and PHA concentrations, the PHA content was calculated as the percentage of PHA of the total CDM, g VS PHA/g VS CDM.

6.3.4 Measurement of sugars and determination of yields

The glucose and galactose were measured with high-performance liquid chromatography (HPLC) equipped with a refractive index detector (RID) and photodiode array detector (PDA). One milliliter of fermentation broth was sampled every four days from the bioreactors. The samples were centrifuged at 12,000 rpm for 20 minutes, and the supernatant was filtered through 0.22 µm membranes. An analytical method was followed by Sluiter (2008) for sugar measurement. A Biorad Aminex HPX-87H column (Hercules, California, United States) was used as the analytical column, and a 5 mM H_2SO_4 solution as the mobile phase. During the HPLC analysis, the oven temperature was controlled to 60 ℃ and the flow rate

at 0.6 ml/min. The CDM and PHA yields were also measured every four days before fed-batch feeding. The CDM yield was determined as the mass of CDM grown per mass of total sugars consumed, g VS/g total sugar. Similarly, the PHA yield was calculated by the mass of PHA accumulated per mass of total sugars consumed, g VS/g total sugar.

6.3.5 Statistical analysis

The fed-batch fermentations were conducted in duplicate. Each assay's mean and standard deviation (SD) were calculated for the duplicates. The values were reported as the mean ± standard deviation. One-way Analysis of Variance (ANOVA) was performed for each of the two feedstocks to determine the significance of the differences among the studied parameters with changes in time. The Tukey test was performed for pairwise comparisons. One-way ANOVA was chosen since the hydrolyzed DLP resulted in inhibition leading to the bioreactor being only operated for 16 days compared to 24 days for the hydrolyzed whey permeate. GraphPad Prism 10 was used for the data analysis of the experiments.

6.4 Results and discussion

6.4.1 Effects of fed-batch feeding with hydrolyzed DLP and whey permeate on cell growth

Figure 6.2 displays the fed-batch *H. mediterranei* growth with hydrolyzed DLP at 4-day intervals. The reactor turned a dense pink color after 4 days, with the initial feeding indicating successful cell cultivation. The cell culture remained the dense pink color on day 8 (i.e., 4 days after the second feeding). However, the culture then turned a browner color on day 12, after the third feeding, indicating that the culture may be inhibited. The reactor became darker on the next 4 days up to day 16, signaling more inhibition may be occurring. Figure 6.3 shows the corresponding fed-batch cultivation of the archaea with hydrolyzed whey permeate at 4 days intervals. After 4 days, the cell culture became a dense pink color indicating successful cultivation. However, unlike the hydrolyzed DLP, the culture remained the same pink

color until day 24. This color difference between the two hydrolyzed cheese byproducts demonstrated that more inhibition might occur with hydrolyzed DLP than hydrolyzed whey permeate.

Figure 6.4 shows the cell growth with time for the fed-batch bioreactor with hydrolyzed DLP and whey permeate feedstock. The OD increased during the first 6 days for the hydrolyzed DLP, reaching a high on days 6 and 7 near 16.0. The OD then steadily decreased until the end of the fermentation to around 5.0, which matched what was visibly observed with the bioreactor losing its pink color past day 8. The hydrolyzed DLP resulted in a different OD trend from the hydrolyzed DLP. The hydrolyzed whey permeate OD increased to day 11, reaching a peak near 21.5. The OD remained reasonably constant from day 12 to day 24 in the range of 17.0-21.0. This nearly constant OD with the hydrolyzed whey permeate aligned with the consistent pink color of the bioreactor observed throughout the fermentation.

a)  b)  c)  d)  e) 

Figure 6.2 Fed-batch bioreactor with hydrolyzed DLP feedstock at various times: a) day 0; b) day 4; c) day 8; d) day 12; e) day 16.

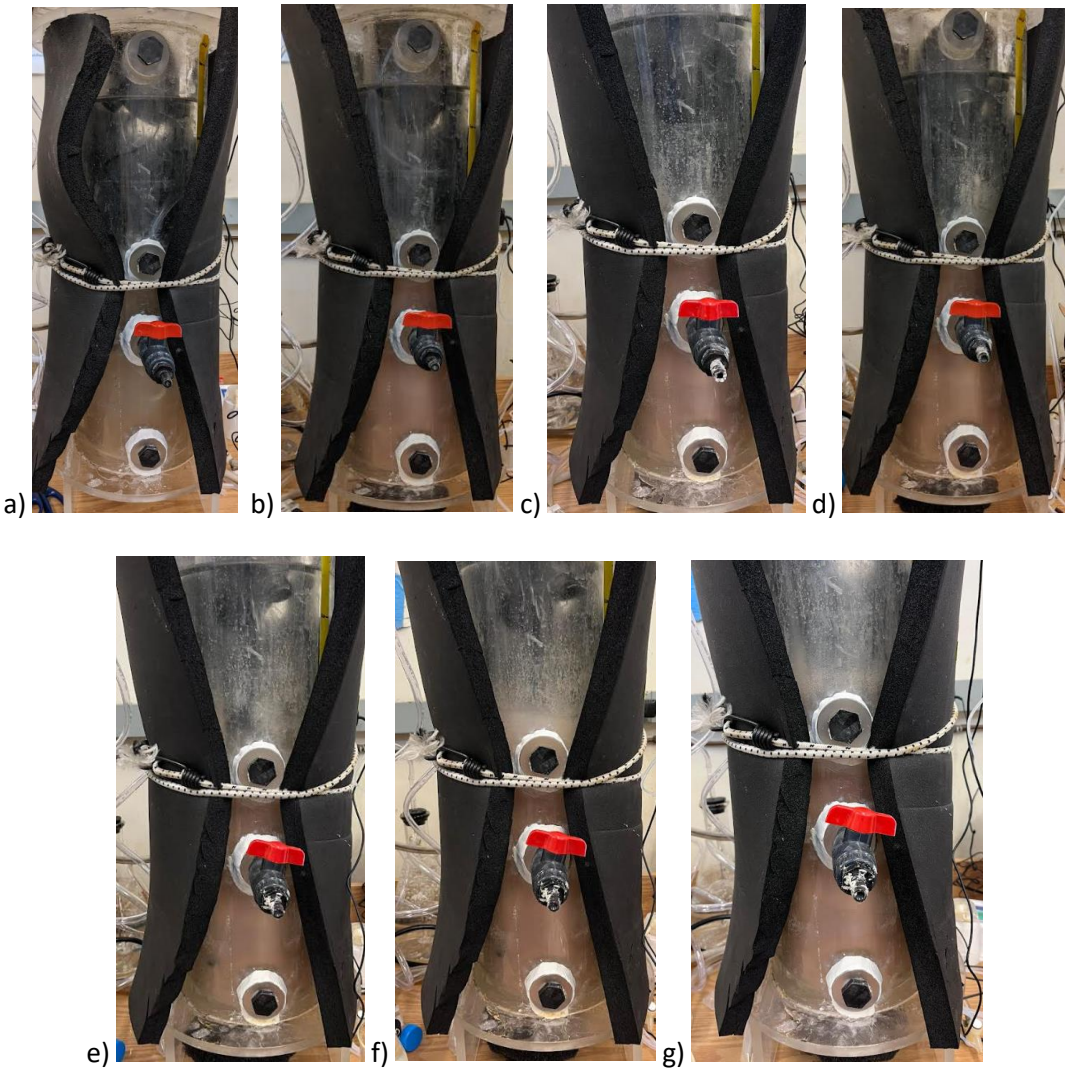

Figure 6.3 Fed-batch bioreactor with hydrolyzed whey permeate feedstock at various times: a) day 0; b) day 4; c) day 8; d) day 12; e) day 16; f) day 20; g) day 24.

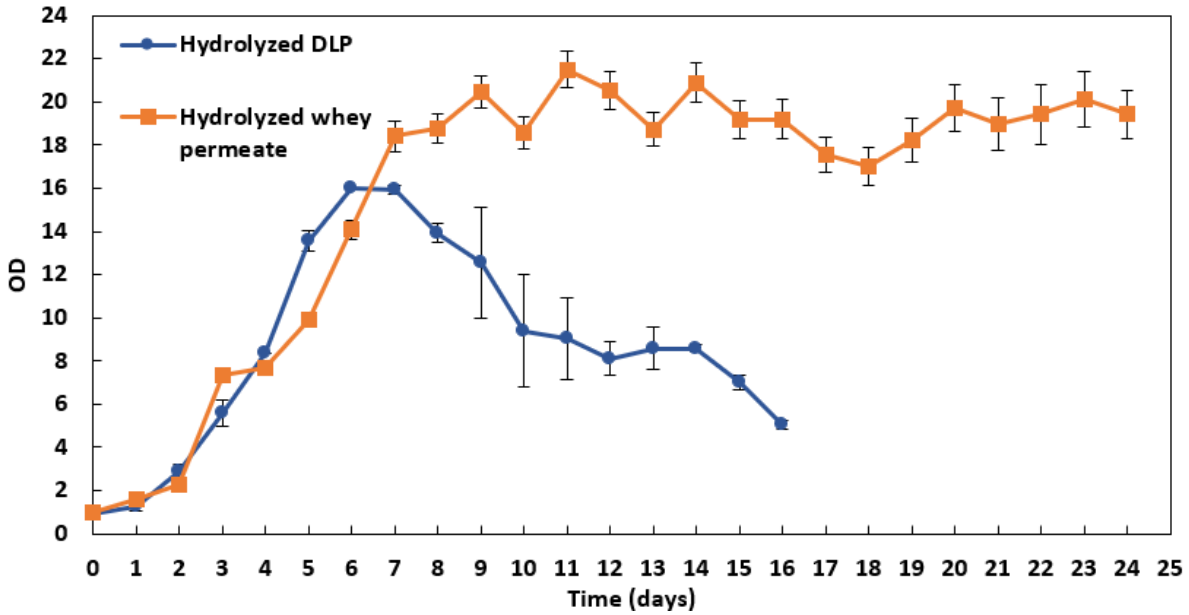

Figure 6.4 Growth of *H. mediterranei* cells over time with hydrolyzed DLP and whey permeate.

Y-error bars are standard deviations.

Figure 6.5 shows the final cell dry mass (CDM) concentrations and cell dry mass yields measured every four days before feeding. The yields were calculated based on the total sugars consumed up to the respective time point. One-way ANOVA demonstrated that the final CDM concentrations of the different time points of the hydrolyzed DLP and whey permeate fed-batch feedings were significantly different (hydrolyzed DLP p-value = 0.0008) (hydrolyzed whey peremate p-value < 0.0001), and the Tukey test was performed for pairwise comparisons. The CDM concentrations agreed well with the respective OD measurements. After the first four days of fermentation, the hydrolyzed DLP CDM concentration was 3.5 ± 0.2 g VS/l. Then on day 8, after the second feeding, the CDM concentration significantly increased (p-value = 0.0044) to 5.2 ± 0.2 g VS/l. The hydrolyzed DLP CDM concentration on day 8 was approximately 25% more than the final CDM concentration achieved with a single batch feeding of 10 g total sugar/l in Chapter 5. The hydrolyzed DLP CDM concentration significantly decreased (p-value = 0.0210) from day 8

to day 16 to 2.3 g ± 0.0 g VS/l, indicating inhibition was present. The hydrolyzed whey permeate CDM concentration significantly increased (p-value = 0.0008) from day 4 at 2.8 g ± 0.2 VS/l to day 8 at 6.0 ± 0.2 g VS/l, and significantly increased (p-value = 0.0083) from day 8 to day 12 at 8.0 ± 0.0 g VS/l. From days 16 to 24, there was no significant difference (days 16 and 20 p-value = 0.9972) (days 20 and 24 p-value > 0.9999) for the hydrolyzed whey permeate CDM concentrations near 8.0 g VS/l. The CDM concentration on day 12 was approximately 20% more than the final CDM concentration achieved with a single batch feeding of 30 g total sugar/l in Chapter 5. As in Chapter 5, more inhibition appeared to occur with the hydrolyzed DLP than the hydrolyzed whey permeate. This difference may be due to DLP containing other constituents, such as Maillard reaction products, that can form when processing whey permeate with hig-temperature evaporation steps (Božanić et al., 2014) and can be inhibitory to microorganisms (Einarsson et al., 1983; Einarsson & Eklund, 1988).

One-way ANOVA demonstrated that the CDM yields of the different time points of the hydrolyzed DLP and whey permeate fed-batch feedings were significantly different (hydrolyzed DLP p-value < 0.0001) (hydrolyzed whey peremate p-value < 0.0001), and the Tukey test was performed for pairwise comparisons. The hydrolyzed DLP and whey permeate CDM yields were the highest on day 4 at 0.48 ± 0.02 and 0.39 ± 0.01 g VS/g total sugar, respectively. The hydrolyzed DLP CDM yield significantly decreased (p-value = 0.0092) from day 4 to day 8 (0.35 ± 0.02 g VS/g total sugar) and continued to decrease with time. The hydrolyzed whey permeate CDM yields were not significantly different (days 4 and 8 p-value = 0.8720) (days 8 and 12 p-value = 0.9987) from days 4 to 12, indicating that the sugars consumed with the first three feedings were similarly utilized for CDM growth. The hydrolyzed whey permeate CDM yield significantly decreased (p-value < 0.0001) from days 12 to 24. The decrease in CDM over time with the two hydrolyzed cheese byproducts suggested less carbon was being diverted to cell growth and PHA accumulation in the later part of the fermentations.

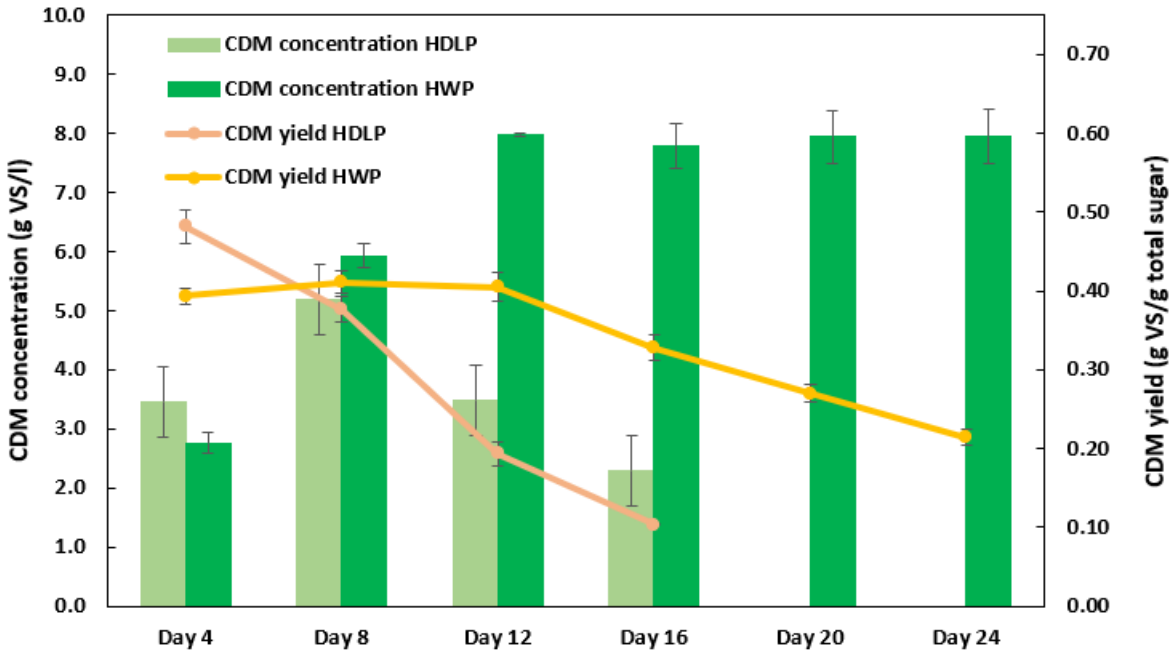

Figure 6.5 Fed-batch *H. mediterranei* cell dry mass (CDM) concentration and yield with hydrolyzed DLP (HDLP) and whey permeate (HWP). Y-error bars are standard deviations.

6.4.2 Effects of fed-batch feeding with hydrolyzed DLP and whey permeate on PHA production and accumulation

Figure 6.6 displays the analogous PHA concentrations and yields measured every four days. The PHA yields were also calculated based on the cumulative sugars consumed from day 0 to the day of measurement. One-way ANOVA demonstrated that the final PHA concentrations of the different time points of the hydrolyzed DLP and whey permeate fed-batch feedings were significantly different (hydrolyzed DLP p-value = 0.0034) (hydrolyzed whey peremate p-value < 0.0001), and the Tukey test was performed for pairwise comparisons. The PHA concentration followed a similar trend to what was observed for CDM concentration. The hydrolyzed DLP PHA concentration significantly increased (p-value = 0.0090) from 1.5 ± 0.2 g VS/l on day 4 to 3.1 ± 0.3 g VS/l on day 8. The maximum PHA concentration that

was achieved with the fed-batch bioreactor on day 8 was approximately 50% more than the single-batch feeding of 10 g total sugar/l in Chapter 5. The increases in CDM and PHA concentration observed with fed-batch feeding compared to batch feeding was due to being able to load 10 g total sugar/l more before inhibition occurred. The hydrolyzed DLP PHA concentration, like CDM, then significantly decreased (p-value = 0.0029) from day 8 to 16 to 0.9 ± 0.0 g VS/l. For the hydrolyzed whey permeate, the PHA concentration significantly increased (p-value < 0.0001) from 1.4 ± 0.1 g VS/l on day 4 to 3.5 ± 0.1 g VS/l on day 8, and significantly increased (p-value = 0.0005) from days 8 to 12 at 4.8 ± 0.3 g VS/l. The PHA concentrations from days 12 to 24 were not significantly different (days 12 and 16 p-value = 0.2522) (days 16 and 20 p-value = 0.9994) (days 20 and 24 p-value = 0.5363) and remained near 5.0 g VS/l. The fed-batch bioreactor operation with hydrolyzed whey permeate, and three 10 g total sugar/l feedings resulted in approximately 20% more PHA than the single batch feeding of 30 g total sugar/l in Chapter 5. This difference between feeding strategies may be due to decreased substrate inhibition and more favorable conditions for PHA accumulation with fed-batch feeding.

The hydrolyzed DLP PHA yield was 0.21 ± 0.02 g VS/g total sugar on days 4 and 8 and were not significantly different (p-value = 0.3863). This result indicated that the sugar consumed by *H. mediterranei* led to similar PHA accumulation for the first two feedings. The PHA yield then decreased with the following two feedings to ≤ 0.12 g VS/g total sugar when *H. mediterranei* inhibition appeared to be present. The PHA yield significantly increased (p-value = 0.0197) from days 4 to 8, 0.21 ± 0.01 to 0.25 ± 0.01 g VS/g total sugar, respectively, for the hydrolyzed whey permeate. The hydrolyzed whey permeate PHA yields of days 8 and 12 were not significantly different (p-value = 0.9859) suggesting that sugar consumption on these days led to similar PHA production. The hydrolyzed whey permeate PHA yield then steadily declined to 0.13 ± 0.00 g VS/g total sugar on day 24, signifying that the additional sugar fed was not going towards PHA accumulation and potentially was going towards maintenance energy. The PHA yields obtained in the

study were similar to the value determined by Koller et al. (2007a) for fed-batch culturing *H. mediterranei* with hydrolyzed cheese byproduct whey at 0.29 g PHA/g whey sugar. The slightly lower PHA yield in this study may be due to Koller et al. (2007a) applying yeast extract as a nitrogen and phosphorus source at 5 g/l and not considering the PHA production from the yeast extract that contained approximately 40% carbon.

Figure 6.7 shows the *H. mediterranei* PHA contents with hydrolyzed DLP and whey permeate every four days of fed-batch feeding. One-way ANOVA demonstrated that the final PHA concentrations of the different time points of the hydrolyzed DLP fed-batch feedings were significantly different (p-value = 0.0095). However, the whey permeate fed-batch feedings were not significantly different (p-value = 0.0666). The Tukey test was performed for pairwise comparisons of the hydrolyzed DLP PHA contents on the different days. The hydrolyzed DLP PHA content increased from 0.43 ± 0.02 g VS/g VS on day 4 to 0.60 ± 0.03 g VS/g VS on day 8. The hydrolyzed PHA content on day 8 was significantly greater (p-value = 0.230) than on day 4, indicating more PHA accumulation occurred with the second feeding. In contrast the hydrolyzed whey permeate PHA contents were consistent throughout the operation of the fed-batch bioreactor in the range of 0.51-0.65 g VS/g VS.

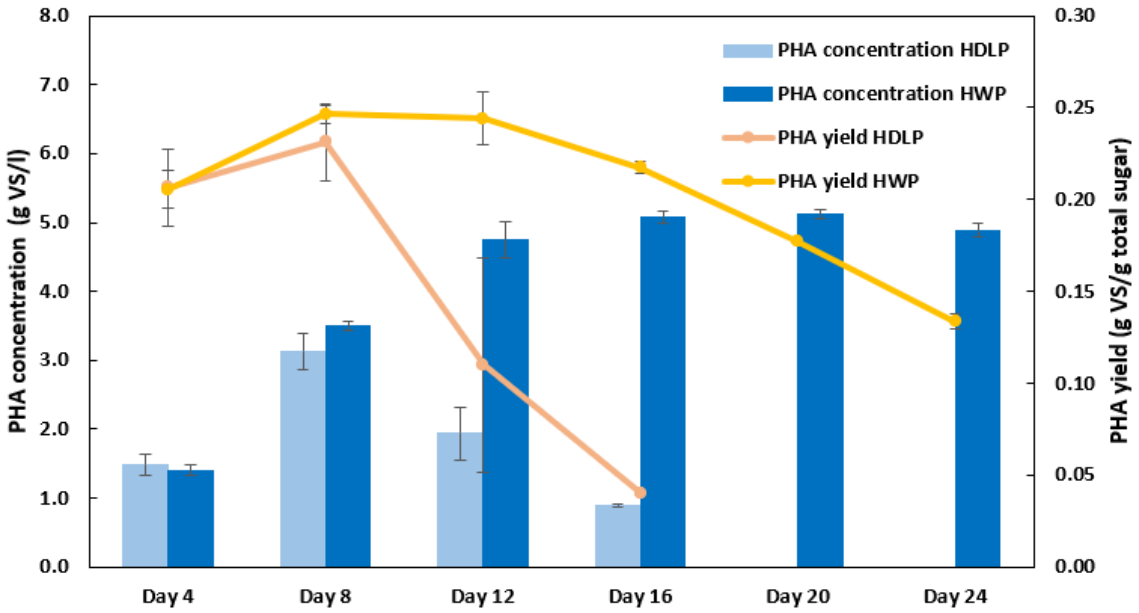

Figure 6.6 Fed-batch *H. mediterranei* PHA concentration and yield with hydrolyzed DLP (HDLP) and whey permeate (HWP). Y-error bars are standard deviations.

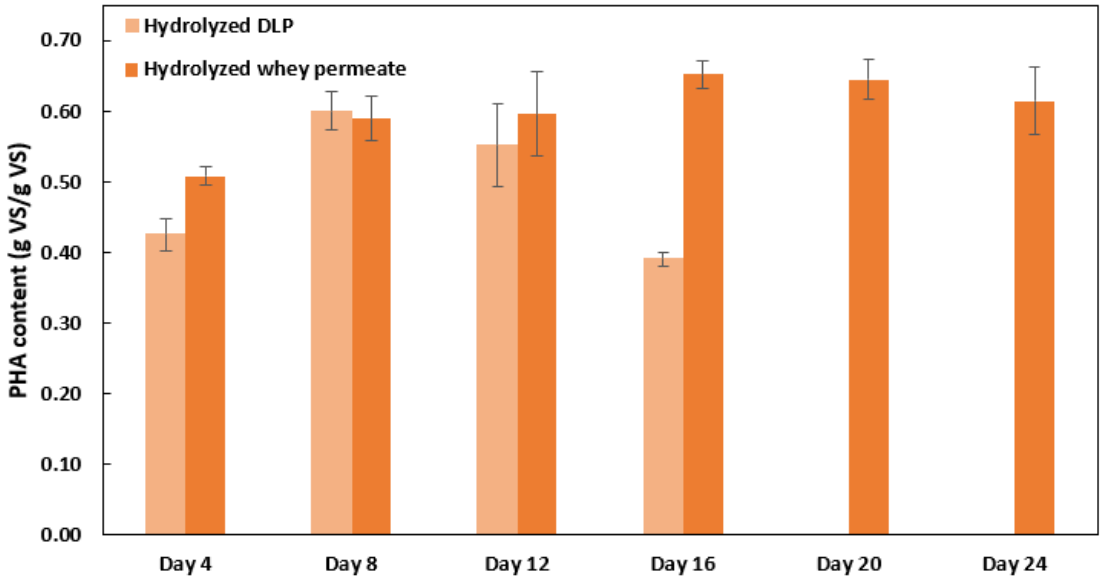

Figure 6.7 Fed-batch *H. mediterranei* PHA content with hydrolyzed DLP and whey permeate. Y-error bars are standard deviations.

6.4.3 Effects of fed-batch feeding with hydrolyzed DLP and whey permeate on sugar consumption

Figures 6.8 and 6.9 show the sugar consumption during fed-batch bioreactor operation with hydrolyzed DLP and whey permeate, respectively. Glucose consumption was higher than galactose consumption for all feeding times with both feedstocks, which aligned with what was observed in previous chapters. For the hydrolyzed DLP, the total sugar consumption was approximately 65% for the first two feedings when the culture was a dense pink color and growing. The sugar consumption then declined with the last two feedings corresponding to when the culture appeared inhibited, as indicated by a loss of the pink color of the reactor and a decrease in OD, CDM, and PHA concentration. For the hydrolyzed whey permeate, the total sugar consumption was reasonably consistent in the range of 56%-68% throughout the fermentation. This result aligned with the culture being active throughout the entire fermentation and not exhibiting inhibition like the hydrolyzed DLP.

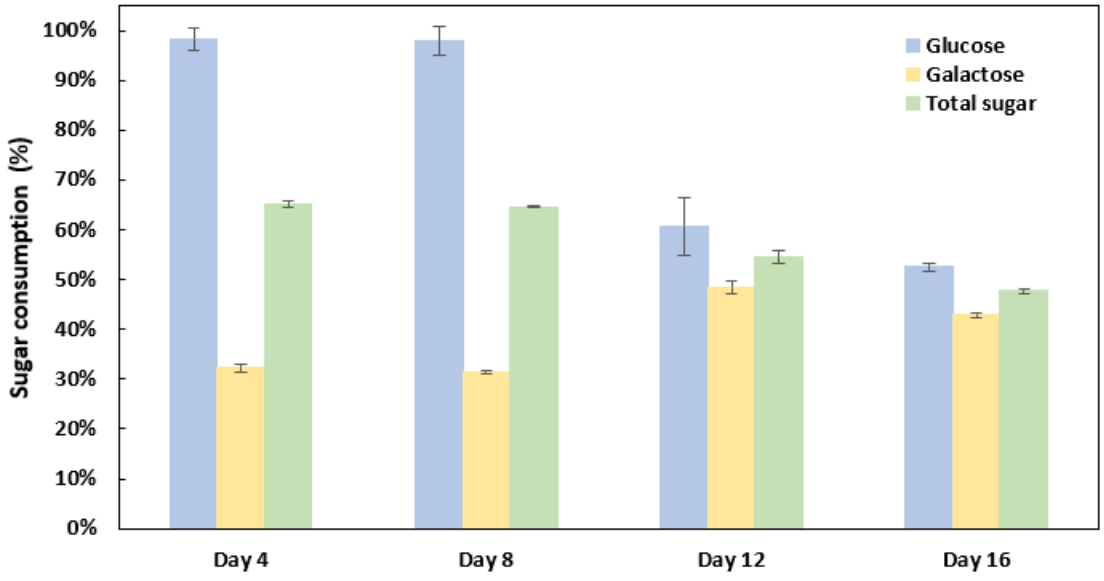

Figure 6.8 Fed-batch *H. mediterranei* sugar consumption with hydrolyzed DLP.

Y-error bars are standard deviations.

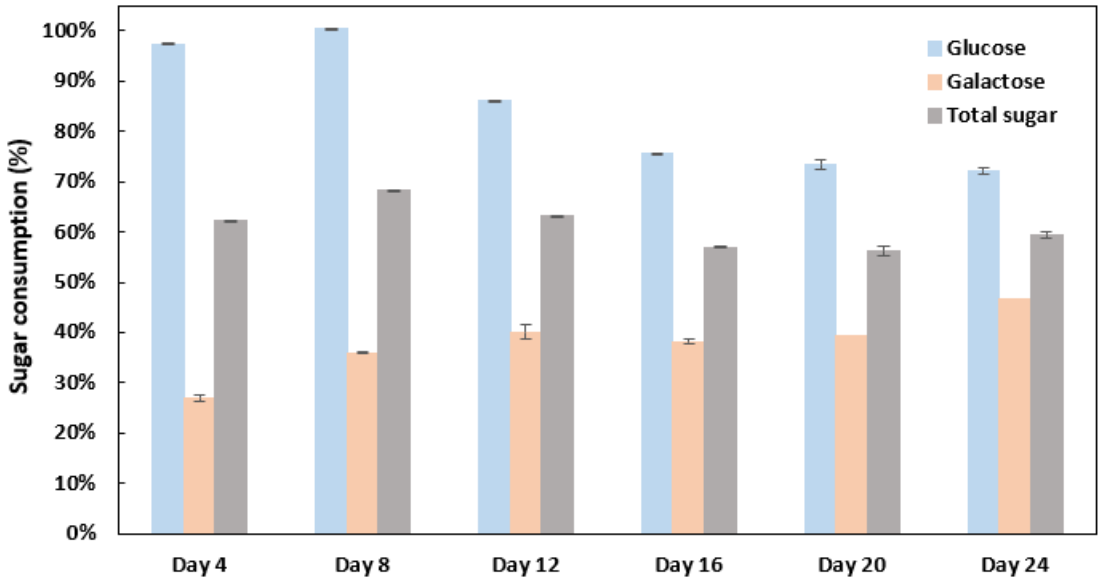

Figure 6.9 Fed-batch *H. mediterranei* sugar consumption with hydrolyzed whey permeate.

Y-error bars are standard deviations.

6.5 Conclusions

Fed-batch cultivation of *H. mediterranei* was studied using hydrolyzed DLP and whey permeate feeding with a concentration of 10 g total sugar/l and a feeding time of four days. Hydrolyzed whey permeate resulted in an approximately 20% increase in PHA production with three feedings compared to the single batch loading of 30 g total sugar/l in Chapter 5. Hydrolyzed whey permeate PHA yields remained nearly constant, with the first three feedings indicating that the sugar consumed was equivalently diverted toward PHA production. A final PHA concentration of 3.1 ± 0.3 g VS/l was achieved for the hydrolyzed DLP, approximately 50% more than with the single batch loading in Chapter 5 due to the additional second feeding of sugars. However, inhibition appeared to occur past the second feeding as the CDM and PHA concentration decreased. It appears that considerably more inhibition occurs with hydrolyzed DLP than with hydrolyzed whey permeate. This inhibition difference may be due to reaction products, such as

Maillard products, that form during the processing of whey permeate into DLP and can be inhibitory towards other microorganisms. In further research, higher loadings of hydrolyzed whey permeate with fed-batch bioreactor operation could be applied since minimal inhibition of the culture appeared to occur with six feedings of the feedstock. However, a loading limit where substrate inhibition starts to occur is expected, like for batch loading in Chapter 5; therefore, research is needed to determine where this fed-batch loading limit occurs. Additional research on the inhibition that occurs with hydrolyzed DLP could also be studied, including removing Maillard reaction products to decrease inhibition potentially. The research in the study can help commercialize the cheese byproduct PHA process, increase the global PHA production capacity, grow the dairy market, and improve sustainability in the dairy and plastic industries.

Chapter 7. Continuous *H. mediterranei* and PHA Production with Hydrolyzed DLP

7.1 Abstract

Conventional plastics pose numerous environmental issues, including being derived from unsustainable raw materials, littering terrestrial and oceanic environments, and producing large amounts of greenhouse gas emissions. Polyhydroxyalkanoates (PHA) are polyesters produced naturally from numerous microorganisms that can replace traditional plastics in many applications, such as packaging, films, and cutlery. Researchers have demonstrated that PHA can be produced economically with cheese byproduct delactosed permeate (DLP) and PHA producer *Haloferax mediterranei* (*H. mediterranei*). In Chapters 5 and 6, batch and fed-batch feeding strategies resulted in *H. mediterranei* substrate inhibition at low loadings of more than 10 g total sugar/l. A continuous stirred tank reactor (CSTR) can reduce substrate inhibition by diluting the feed contents with the bioreactor's working volume. Additionally, cheese makers produce DLP continuously, and abnormal conditions commonly occur in an industrial setting making continuous feeding a seemingly good fit with the cheese byproduct. In this study, a 6 L continuous stirred tank reactor (CSTR) with a 5 L working volume was operated with hydrolyzed DLP feedstock at two hydraulic retention times (HRT) of 10 and 20 days. The 10-day HRT bioreactor was fed hydrolyzed DLP at an organic loading rate (OLR) of 2.5 g total sugar/l/day. The bioreactor reached a steady-state after approximately 1.5 HRTs. The steady-state cell dry mass concentration, PHA concentration, and PHA content were 6.1 g VS/l, 4.0 g VS/l, and 0.66 g VS/g VS, respectively. The cell dry mass and PHA yields were 0.26 and 0.18 g VS/g total sugar, respectively. However, the culture then became unstable after 22 days of continuous feeding. The cell dry mass and PHA concentration decreased as the substrate concentration increased, indicating that cell washout occurred. The 20-day CSTR was operated at different OLRs of hydrolyzed DLP at 1.25, 1.5, and 2 g total sugar/l/day. A stable culture was maintained for 130 days with hydrolyzed DLP, with > 94% of the sugar substrate consumed. With the OLR of 1.25 g total sugar/l/day, a steady-state cell dry mass concentration, PHA concentration, and PHA content of 6.6 g VS/l,

2.1 g VS/l, and 0.32 g VS/g VS/g VS, respectively, was observed after 2 HRTs. The cell dry mass and PHA yields during this apparent steady-state were 0.27 g and 0.08 g VS/g total sugar, respectively. However, a decline in PHA production appeared to occur after 26 days of continuous feeding, similar in timing when the 10-day HRT CSTR also experienced issues. The 20-day HRT CSTR culture appearance changed after 30 days of continuous feeding, losing its typical dense pink color characteristic of the archaea. Although a stable culture was present, the archaea appeared to be inhibited, and unfavorable conditions of the bioreactor appeared to be present for PHA production. Therefore, continuous feeding with hydrolyzed DLP for *H. mediterranei* PHA production may pose numerous challenges at these HRTs and OLRs.

Key Words

Polyhydroxyalkanoates, *Haloferax mediterranei*, delactosed permeate, continuous stirred tank reactor

7.2 Introduction

It is estimated that over 120 million tons of whey are produced annually worldwide (Nikodinovic-Runic et al., 2013). Only about half of the whey is processed into a useful form for human or animal consumption, with the rest ending up as waste material (Nikodinovic-Runic et al., 2013), contributing to an estimated 150 million tons of CO_2-e/year (United Nations Environment Programme, 2021). Cheese byproducts used for animal feed are often considered wasteful and inefficient since these products contain less energy and protein than plant-based livestock feeds (Alexander, 2018). Furthermore, although some cheese manufacturers can create food ingredients such as whey protein concentrates and lactose powder from these byproducts (Byylund, 2015), market limitations and capital cost investments prevent all cheese manufacturer coproducts from being utilized for animal or human consumption (Liang et al., 2009; Oliveira et al., 2019). For cheese manufacturers who produce whey and lactose products, crystallization restrictions limit the amount of lactose that can be recovered as food products (Oliveira et

al., 2019). As a result, one-third of the lactose remains as a byproduct, delactosed permeate (DLP), typically sold as low-value animal feed or disposed of as waste (Liang et al., 2009). Researchers have focused on using whey and whey byproducts for mineral-enriched salt substitutes, lactose-enriched food streams, lactic acid for food or biomaterial applications, and bioethanol substrates. However, the commercial success of these applications is meager as these proposed products require further costly processing that does not outweigh the revenue created (Oliveira et al., 2019). Alternatively, the lactose could be converted to bioderived and biodegradable bioplastics. These bioplastics could replace unsustainable petroleum-based plastics that generate large amounts of CO_2-e emissions, be a value-added product for the cheese industry, and lead to a circular economy.

Polyhydroxyalkanoates (PHA) are bioderived biodegradable bioplastics with similar properties to thermoplastics (Madison & Huisman, 1999). PHAs can aerobically and anaerobically biodegrade at ambient temperatures in terrestrial and ocean environments (Hegde et al., 2021; Meereboer et al., 2020). This allows improperly discarded PHA products to have minimal environmental impacts (Meereboer et al., 2020). PHAs can be used in various applications, including plastic bags, packaging film, food containers, disposable cutlery, 3D printing material, and medical sutures (Bugnicourt et al., 2014; Raza et al., 2018). Numerous microorganisms can produce PHA, which is stored intracellularly as an energy reserve (Bernard, 2014). In particular, *Haloferax mediterranei* (*H. mediterranei*), appears to be an exceptional fit for PHA production from cheese byproducts (Koller, 2018). This pairing is due to *H. mediterranei* is an extreme halophile that grows in up to 20% high salinity environments (Ferre-Guell & Winterburn, 2018). This salt tolerance allows easy incorporation of waste or byproducts since common contaminants, such as *Bacillus Cereus*, cannot survive the harsh saline environment (Amaro et al., 2019; Koller et al., 2011). Therefore, costly sterility steps such as high-temperature exposure, ultraviolet radiation, or antibiotics are not required before fermentation (Amaro et al., 2019). The salts contained in DLP can also be beneficial

nutrients for *H. mediterranei* growth (Rodriguez-Valera et al., 1980). Intracellular PHA extraction can occur via simple water addition, causing cell lysis from osmotic shock rather than using expensive chlorine-based chemicals that are often environmentally malign (Amaro et al., 2019). Additionally, *H. mediterranei* produces a valuable form of PHA, poly(3-hydroxybutyrate-co-3-hydroxyvalerate) (PHBV), that can be used to create food packaging film, bags, or containers (Bugnicourt et al., 2014; Raza et al., 2018; Reddy et al., 2003).

Previous chapters utilized batch and fed-batch feeding strategies. In Chapter 5, hydrolyzed DLP substrate inhibition was demonstrated to occur at low loadings of greater than 10 g total sugar/l. Similarly, in Chapter 6, fed-batch feeding of hydrolyzed DLP only allowed two feedings of 10 g total sugar/l total, resulting in marginal PHA production improvements. Although these modes of feeding are easy to apply for small-scale PHA production experiments, they may not be ideal at the industrial scale due to the low substrate loadings required to prevent substrate inhibition. At an industrial scale, batch feeding could lead to increased capital costs from larger required bioreactors and downstream processing equipment (Wang et al., 2021). Alternatively, continuous feeding could be applied by operating a continuous stirred tank reactor (CSTR). Theoretically, CSTRs offer potential benefits of higher volumetric productivity due to no downtime, more consistent product quality, and higher feed loadings that can be applied, saving water and reducing reactor size (Koller & Muhr, 2014). DLP is typically produced continuously at large-scale cheese factories making continuous PHA fermentation a good process fit at the industrial scale (Byylund, 2015). Additionally, upset conditions common for upstream processes in cheese and whey factories, such as increased loadings (Byylund, 2015), can be better managed with a CSTR due to the dilution of the feed in the reactor volume (Koller & Muhr, 2014). A common downside of a CSTR is microbial contamination (Koller & Muhr, 2014). However, since *H. mediterranei* is cultivated in a high-saline environment, these salt conditions should prevent the growth of common contaminants (Amaro et al., 2019; Koller, 2018).

Although continuous feeding of dairy byproduct substrates appears to be a good fit for PHA production and cheese byproducts, to my knowledge no research has been conducted on this topic. Moreover, minimal research has been conducted cultivating *H. mediterranei* in a CSTR with any substrate (Amaro et al., 2019; Bugnicourt et al., 2014; Koller, 2018; Koller & Braunegg, 2015). In early research studying the growth of *H. mediterranei* by Lillo and Rodriguez-Valera (1990), continuous production of the archaea was studied with a 20 g/l glucose substrate loading supplemented with 5 g/l yeast extract. A CSTR with a working volume of 1.5L was studied at 5 different dilution rates (0.02, 0.04, 0.06, 0.08, and 0.10 h^{-1}). The authors found that the dilution rate of 0.02 h^{-1} resulted in the highest PHA concentration of 1.5 g/l and PHA content of 0.43 g PHA/g cell dry mass with PHA production decreasing with increased dilution rate. A 0.10 h^{-1}dilution rate resulted in cell washout with no cell mass and PHA measured in the bioreactor. With the 0.02 h^{-1} dilution rate, the researchers found that the culture remained stable and monoclonal for three months. Therefore, continuous feeding of hydrolyzed DLP may be a feasible feeding strategy that can increase PHA production.

This study aimed to apply a continuous feeding of hydrolyzed DLP with PHA producer *H. mediterranei.* The task of this study was to evaluate the performance of a continuously stirred tank reactor (CSTR) at different hydraulic retention times (HRTs) to observe if a stable culture can be achieved.

7.3 Materials and methods

7.3.1 Delactosed permeate collection and pretreatment

Delactosed permeate (DLP) was collected from the lactose plant of Hilmar Cheese Company, Hilmar, California. *H. mediterranei* cannot directly consume the lactose present in DLP (Koller et al., 2007a). Therefore, an enzymatic hydrolysis step was applied to convert the disaccharide lactose into monosaccharides glucose and galactose that the archaea can consume. Centrifugation pretreatment was

conducted before hydrolysis, as described in Chapter 3, with a bench-top centrifuge (Heraeus Multifuge X1R Thermo Scientific, Waltham, Massachusetts) at 5,000 rpm for 1 hour. After centrifugation, the liquid DLP was decanted off the top of the buckets leaving the remaining solids settled on the bottom. As described in Chapter 3, lactase enzyme Nola Fit 5550 (Chris Hansen, Hoersholm, Denmark) was loaded at 0.25 g of lactase enzyme per g of lactose, and the DLP with enzyme was incubator for 12 hours at 40 ℃ and continuous agitation at 180 rpm. The hydrolyzed DLP was used as feedstock for subsequent fermentations.

7.3.2 PHA production with hydrolyzed DLP and continuous feeding

7.3.2.1 *H. mediterranei* cultivation and media preparation

Halophilic archaeon *H. mediterranei* (ATCC 33500) was utilized as the microbial PHA producer. The active inoculum was prepared according to the procedures described in Chapter 3. Minimum salt media (MSM) with 1% v/v SL-6, as stated in Chapter 3, was used as the base for the media. Ammonium chloride was added to the media as a supplementary nitrogen source to give a constant C/N ratio of 8. The hydrolyzed DLP possessed adequate phosphorus; therefore, no phosphorus supplementation was needed. Sodium bicarbonate was utilized as a buffer to prevent pH swings. The pH was controlled to 7.0 ± 0.2 with 3 M hydrochloric acid and 3 M sodium hydroxide using a Bluelab pH controller (Tauranga, Gisborne, New Zealand). The CSTR was a 6 L bioreactor with a 5 L working volume. The CSTR was initially loaded with 10 g total sugar/l from the hydrolyzed DLP and operated in batch mode to grow an initial culture and prevent overloading the reactor. Hydrolyzed DLP media containing 25, 30, and 40 g total sugar/l were applied for the feed for continuous bioreactor operation. The bioreactor's temperature was controlled to 37 ± 1.0 ℃ using a water bath and jacket that enclosed the bioreactor. Forced air was supplied to the bioreactor through two polytube lines connected to a compressed air line. The air was pre-humified by passing through two 2 L Erlenmeyer flasks containing water to prevent water loss and

salinity changes to the bioreactor. The airflow rate was controlled using manually adjustable rotameters. The dissolved oxygen (DO) was measured with a YSI ProSolo optical dissolved oxygen meter (Yellow Spring, Ohio, USA) and adjusted daily to 20%-40% of saturation level, which was shown by Wang (2022) to provide adequate oxygen for *H. mediterranei* cultivation. Magrabar food-grade antifoam (Morton Grove, Illinois, USA) was added as needed to the bioreactor to prevent excessive foaming of the reactor.

7.3.2.2 PHA production from CSTR at an HRT of 10 days

The bioreactor was first operated in batch mode for 14 days until the stationary phase was reached to grow an initial culture and prevent overloading and cell washout. The bioreactor had an effective volume of 5 L and was initially loaded with hydrolyzed DLP media at 10 g total sugar/l. After 14 days, the continuous operation began at an organic loading rate (OLR) of 2.5 g total sugar/l/day. Hydrolyzed DLP media containing 25 g total sugar/l was fed and a hydraulic rendition time (HRT) of 10 days was applied. The bioreactor reached steady-state near 1.5 HRTs of continuous feeding as defined when the cell dry mass concentration, PHA concentration, and PHA content values differed by less than +/- 5%. The fermentation was stopped after 26 days of continuous operation when the culture became unstable and cell washout appeared to have occurred.

7.3.2.3 PHA production from CSTR at an HRT of 20 days

Since the 10-day HRT CSTR experiment resulted in an unstable culture and cell washout, the HRT was increased to 20 days to help prevent cell washout by reducing the dilution rate and daily biomass loss from the CSTR effluent. The initial hydrolyzed DLP feedstock loading was 10 g total sugar/l for batch operation, like for the 10-day HRT CSTR. The bioreactor was operated batchwise for 6 days to ensure the exponential growth phase rather than in the stationary phase where the culture may be less active. Then, the bioreactor was continuously fed at an OLR of 1.25 g total sugar/l/day. The bioreactor reached the

steady-state condition after 1 HRT again defined when the cell dry mass concentration, PHA concentration, and PHA content values differed by less than +/- 5%. The OLR was then increased to 1.5 g total sugar/l/day on day 28 by increasing the feed loading to 30 g total sugar/l. This OLR was applied until day 48 as the culture steadily began to lose its pink color and appeared to become unhealthy.

Substrate inhibition appeared to be occurring from the loss of the pink color characteristic of the archaea. Therefore, attempts were conducted to recover the bioreactor culture. MSM with no carbon source was fed to the reactor at the same rate as the hydrolyzed DLP feedings from days 43-45 to dilute the fermentation broth and potentially reduce substrate inhibition. Hydrolyzed DLP feedings were then continued at an OLR of 1.5 g total sugar/l/day for 6 days to provide a carbon source for *H. mediterranei* growth. However, after these efforts to reduce inhibition, the culture did not regain its pink, which led to trialing further dilution of the bioreactor to attempt to alleviate the potential inhibition. One-third of the fermentation broth was removed and replaced with MSM containing no carbon source on day 51. The OLR of 1.5 g total sugar/l/day was then resumed to observe if the culture removed would grow back once hydrolyzed DLP was fed. The hydrolyzed DLP OLR was increased to 2 g total sugar/l/day on day 72 by increasing the feed loading to 40 g total sugar/l after a steady-state condition was achieved with the OLR of 1.5 g total sugar/l/day. The hydrolyzed DLP OLR of 2 g total sugar/l/day was fed until a steady-state condition was reached. The feed was then switched to MSM with 40 g glucose/l at the same OLR of 2 g total sugar/l/day on day 90 to determine if the glucose substrate could reduce inhibition. The glucose media was fed for 40 days (2 HRTs) to allow sufficient turnover of the bioreactor. The CSTR study was concluded after only marginal improvements with the glucose feedstock occurred. The 20-day HRT CSTR was operated for 130 days.

7.3.2.4 Study of the CSTR at an HRT of 20 days inhibited culture

Flask studies were conducted when the bioreactor became less visibly pink and appeared to have declining health to observe if the *H. mediterranei* culture was viable outside of the CSTR. After feeding the bioreactor MSM without a carbon source from days 43-45, as described previously, the effluent of the CSTR on day 45 was used as inoculum for 250 ml flask batch fermentations with a working volume of 130 ml. Three conditions were tested, diluting the effluent with one-third MSM by volume, diluting the effluent with one-half MSM by volume, and inoculating an MSM media that contained 10 g glucose/l as a carbon source. The glucose media was supplemented with ammonium chloride to give a C/N ratio of 8, dihydrogen potassium phosphate to give a C/P of 35, and a 5 g/l loading of complex nutrient source yeast extract (same glucose media used in Chapter 4). On day 47 of continuous feeding, the effluent was collected as inoculum for a 10 g total sugar/l hydrolyzed DLP feedstock (same hydrolyzed DLP media used for CSTR start-up). The 10 g glucose/l media study was conducted again with CSTR effluent from day 55 of continuous feeding to verify the results of the first glucose study. All flasks were grown in a shaker incubator with the same conditions used in previous Chapters 3-5, with the temperature controlled to 37 °C and the agitation at 180 rpm. The diluted flasks were conducted singularly, and the glucose and hydrolyzed DLP flasks were in duplicate. The fermentations were ended when the stationary phase was reached after 240-360 hours.

7.3.3 Determination of cell dry mass and PHA concentration and yield, PHA content, and sugar consumption

The cell growth of the CSTR studies was measured by sampling 1 ml of fermentation broth daily throughout the fermentation. The samples' optical density (OD) was measured at 520 nm, as described by Huang et al. (2016). The final cell dry mass (CDM) was measured as the fermentation broth's volatile solids (VS) at the end of cell cultivation and following standard methods and the procedure outlined in

Chapter 3 (American Public Health Association, 2012). The PHA was extracted following methods stated in Chapter 3 based on a method described by Escalona et al. (1996) with modifications and measured as VS with the same standard method used for CDM. The PHA content was calculated from the measured CDM and PHA VS as the percentage of PHA of the total CDM (g VS PHA/g VS CDM). The glucose and galactose were measured with high-performance liquid chromatography (HPLC) following a method by Sluiter (2008) outlined in previous chapters. The CDM concentration, PHA concentration, and sugar consumption were measured every other day from the CSTR effluent. The cell dry mass yield was determined as the mass of CDM grown divided by the mass of total sugars consumed, g VS/g total sugar. Similarly, the PHA yield was calculated by the mass of PHA accumulated divided by the total sugars consumed, g VS/g total sugar.

7.3.4 Statistical analysis

The 10-day and 20-day CSTR studies were conducted singularly. The steady-state parameters were reported as the mean ± standard deviation. One-way Analysis of Variance (ANOVA) was performed to determine the significance of the differences among steady-state parameters achieved with the various OLR conditions of the 20-day HRT CSTR. The data analysis of the study was completed with GraphPad Prism 10 software.

7.4 Results and discussion

7.4.1 Continuous stirred tank reactor with 10-day hydraulic retention time and hydrolyzed DLP feed

7.4.1.1 Effects of 10-day HRT continuous feeding of hydrolyzed DLP on cell growth

Figure 7.1 shows the 10-day HRT CSTR bioreactor after 20 and 24 days of continuous feeding. After two HRTs (20 days) of continuous feeding, the bioreactor possessed a bright pink color (Figure 7.1a), which is typical of a healthy *H. mediterranei* culture from carotenoid production (W. Chen et al., 2015).

However, after 24 days of continuous operation, the culture became visibly less pink and started to become browner (Figure 7.1b). This change in the color of the bioreactor indicated that the culture may be inhibited, and cell growth was declining. Additionally, a considerable amount of thick stable foam was being produced from the fermentation broth, possibly caused by the archaeal cells starting to lyse.

Figure 7.2 shows the cell growth curve or OD versus time for the CSTR operated at a 10-day HRT. A slight decrease in OD was observed for the first two days of continuous feeding, most likely due to an initial lag phase and cell washout where the cells being removed from the effluent exceeded the growth of new cells. The OD then increased on day 3 as the culture started to consume the new sugars at higher rates introduced in the feed. Exponential growth occurred from days 3 to 16, with the OD increasing from 7.0 to 21.9. A near-constant OD was then observed from days 16 to 22 in the range of 21.9-23.3, indicating that a steady-state condition was achieved with the specific growth rate equaling the dilution rate. However, the OD rapidly decreased to 14.7 on day 24 and 11.2 on day 26, indicating that inhibition and cell washout was occurring, e.g., the dilution rate was greater than the specific growth rate. This decrease in OD coincided with a noticeable color change of the bioreactor contents, transitioning from a bright pink color to a dull brownish-pink hue.

a) 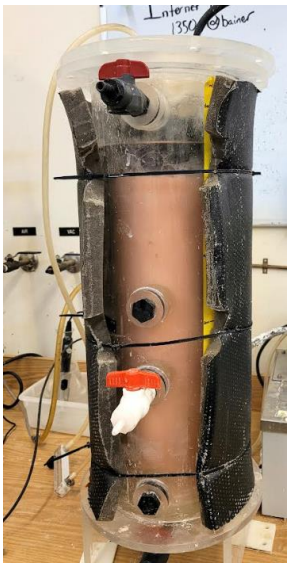 b) 

Figure 7.1 6 L bioreactor operated with continuous feeding at a 10-day hydraulic retention time and hydrolyzed DLP feed: a) day 20 of continuous feeding; b) day 24 of continuous feeding.

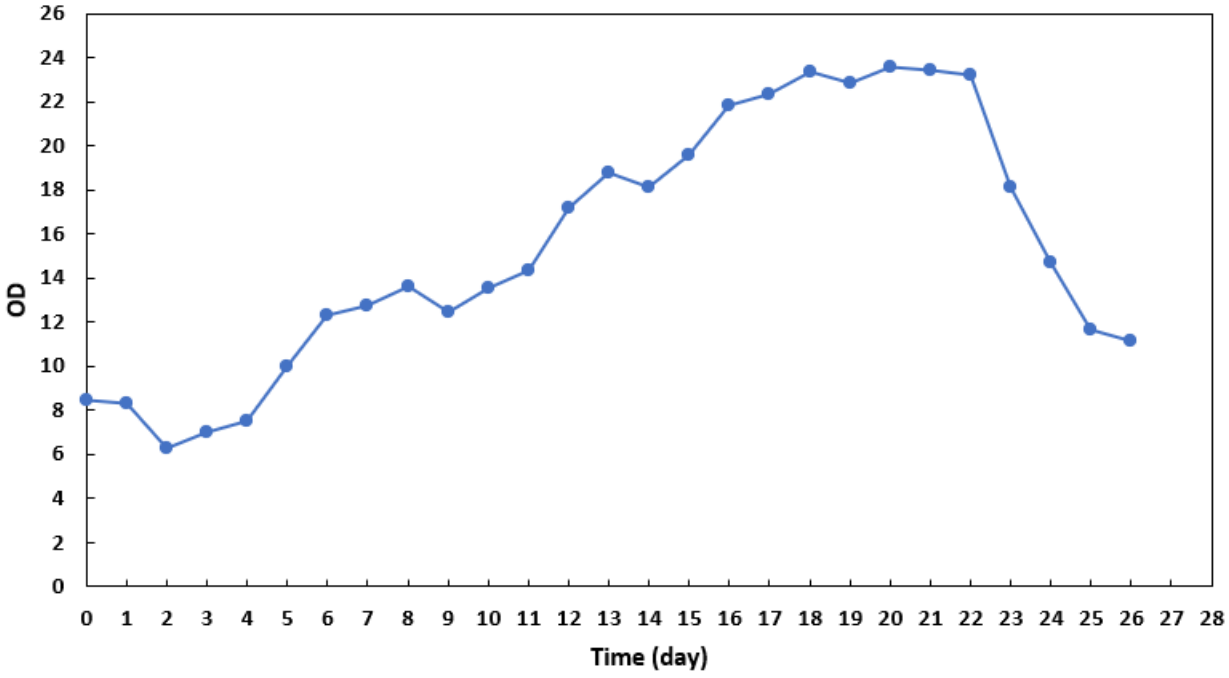

Figure 7.2 Cell growth of *H. mediterranei* in the CSTR fed with hydrolyzed DLP at an HRT of 10-days over time.

7.4.1.2 Effects of 10-day HRT continuous feeding of hydrolyzed DLP on cell mass and PHA production

Figure 7.3 displays the cell dry mass (CDM) concentration, PHA concentration, and PHA content during the 10-day HRT CSTR operation. The CDM agreed well with the cell growth time profile. For the same reasons stated for the OD, an initial decrease in CDM concentration occurred during the first two days of continuous operation, with the CDM concentration decreasing from 3.1 g VS/l at the start of continuous feeding to 2.4 g VS/l on day 2. The CDM concentration then steadily increased from day 2 to 16 to 6.1 g VS/l. A constant CDM concentration of 6.0 ± 0.0 g VS/l was observed from days 16 to 22, indicating that a steady-state was achieved with the CSTR. The steady-state CDM concentration was higher than that obtained by Lillo and Rodriguez-Valera (1990) when operating a CSTR with a loading of 20 g/l glucose and an HRT of 50 hours of 3.6 g VS/l. This difference may be due to several factors, including the use of hydrolyzed DLP, which was shown to result in greater cell growth than glucose in Chapter 3, a longer HRT that was applied in this study, a higher substrate loading used with the hydrolyzed DLP, and Lillo and Rodriguez-Valera (1990) grew *H. mediterranei* with a phosphorus limitation. The CDM concentration then decreased to 4.4 g VS/l from day 22 to 26, indicating cell washout was occurring. The inhibition observed after 22 days of bioreactor operation may be due to prolonged exposure to high-heat reaction compounds such as Maillard products (Kuechel, 2017) that can be inhibitory to microorganisms (Einarsson et al., 1983; Einarsson & Eklund, 1988). Although continuous feeding can reduce substrate inhibition by diluting the feed contents with the volume of the bioreactor (Koller & Muhr, 2014), potential inhibitory compounds such as Maillard reaction byproducts could accumulate in the CSTR at high concentrations if they are not being broken down. This accumulation of inhibitory compounds could lead to reduced cell growth rates and washout.

The PHA concentration followed a similar trend to the CDM concentration since *H. mediterranei* PHA production has been cited to be growth or partially growth-associated (Cui, 2017; Wang & Zhang,

2021). The PHA concentration was 1.9 g VS/l at the start of continuous feeding, declined on day 2 to a low of 1.6 g VS/l, and increased to 4.0 g VS/l on day 16. A near-constant PHA concentration at 4.0 ± 0.1 g VS/l was again observed from days 16 to 22 when the bioreactor appeared to reach a steady-state. The steady-state PHA concentration was more than double that Lillo and Rodriguez-Valera (1990) found with continuous feeding of 20 g/l glucose with a 50-hour HRT of 1.5 g PHA/l. The same reasons stated for the difference in CDM concentration can explain this PHA difference. The reasons include hydrolyzed DLP can result in higher PHA yields than glucose, as shown in Chapter 3, a longer HRT was applied, a 25% higher loading of hydrolyzed DLP was fed, and excess phosphorus was utilized rather than a deficiency in the study by Lillo and Rodriguez-Valera (1990). The PHA concentration then declined to 1.9 g VS/l on day 26, indicating cell washout. Differences in the rate of increase of CDM and PHA concentration were observed during the exponential cell growth phase from days 2 to 16. Although the PHA concentration increased at a similar rate to the CDM concentration from days 2 to 6, the PHA concentration increased at a lower rate than the CDM concentration from days 6 to 16. This result indicated that PHA production was becoming less favorable after 6 days of continuous feeding. The decrease in PHA accumulation after day 6 may be due to a lower sugar concentration in the bioreactor, as PHA production can be triggered by excess carbon in the environment for many PHA producers (Anderson & Dawes, 1990).

The PHA content exhibited a different trend than the CDM and PHA concentrations. The PHA content increased from 0.62 to 0.70 g VS/g VS in the first six days of continuous feeding, decreased to 0.64 g VS/g VS from days 6 to 8, and increased back to 0.71 g VS/g VS on day 10. The PHA content then decreased to 0.64 g VS/g VS on day 14, remaining consistent until day 22. The PHA content from days 16 to 22, where steady-state CDM and PHA concentrations were observed, was also nearly constant at 0.67 ± 0.02 g VS/g VS. The changes in the PHA content during initial continuous feeding may be due to the transient conditions of carbon in the environment that can affect PHA accumulation (Anderson & Dawes,

1990), the age of the cells (Wang & Zhang, 2021), and the differing consumption of glucose and galactose sugars with time that could lead to variance in PHA accumulation (Pais et al., 2016). The PHA content decreased to 0.43 ± 0.00 g VS/g VS by day 26. The decline in PHA content at the end of the fermentation suggests that the cells began to consume intracellular PHA, or PHA was lost if the cells had lysed.

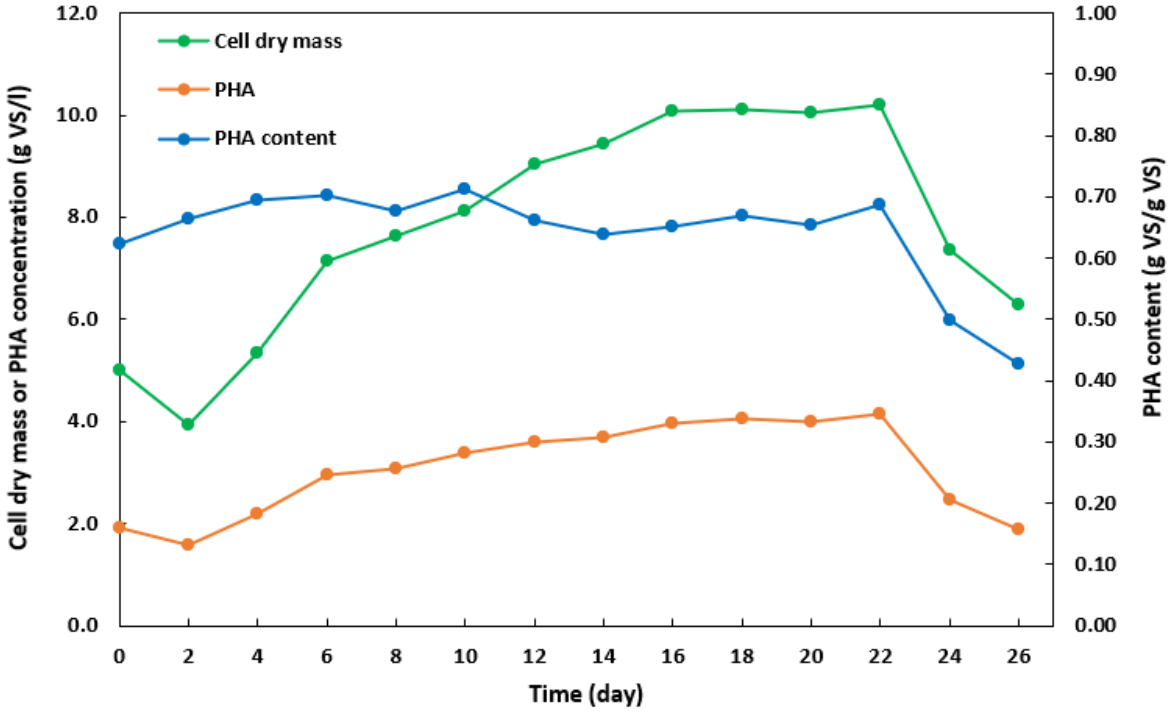

Figure 7.3 *H. mediterranei* cell dry mass concentration, PHA concentration, and PHA content with 10-day hydraulic retention time continuous feeding of hydrolyzed DLP.

7.4.1.3 Effects of 10-day HRT continuous feeding of hydrolyzed DLP on cell mass and PHA yield, and glucose and galactose consumption

Figure 7.4 shows the glucose and galactose concentrations during the operation of the CSTR at 10-day HRT. The glucose and galactose concentrations increased in the first 6 days of continuous feeding

from 1.1 to 1.7 g/l and 3.4 to 6.0 g/l, respectively. These sugar concentration increases were most likely due to the lag phase seen as the culture reacclimated to introducing a new carbon source. This initial increase in sugar concentration occurred at the same time when PHA content was also increasing, supporting the notion that the initial feeding of sugar may have contributed to the increase in PHA content observed. Similarly, after 6 days of continuous feeding, the galactose concentration decreased on day 8 by nearly 1.0 g/l, and the glucose concentration slightly decreased by 0.2 g/l, which aligns when the PHA content had a noticeable decline of 0.06 g VS/g VS. The galactose concentration then increased on day 10 to 6.1 g/l before slightly decreasing again on day 12 to 5.5 g/l, where it remained somewhat steady to day 20, around 5.0 g/l. The glucose concentration, however, remained much more constant during the fermentation and at low levels of < 1.5 g/l from days 0 to 18. The glucose and galactose concentrations during the observed steady-state CDM and PHA concentrations from days 16-22 were 1.5 ± 0.4 g/l and 5.2 ± 0.6 g/l, respectively. The reasonably constant sugar concentrations during this period may help explain the observed near constant PHA content, as PHA storage is related to carbon availability for many PHA producers (Anderson & Dawes, 1990). Both the glucose and galactose concentrations began to increase from days 18 to 26 from 1.5 to 8.7 g/l and 4.5 to 11.3 g/l, respectively. The bioreactor's sugar concentration increased earlier than when the CDM and PHA concentrations began to decrease after day 22. Therefore, the increase in sugar concentration by *H. mediterranei* was the first sign that cell washout was occurring.

The steady-state glucose and galactose consumption after continuous feedings were considered from days 16-20 as the glucose and galactose consumption decreased by ~15% from days 20 to 22. Likewise, the steady-state CDM and PHA yields were determined during this period. The steady-state glucose and galactose consumptions were 87% ± 4% and 61% ± 4%, respectively. It was expected that more glucose would be consumed than galactose since glucose is the preferred substrate by *H.*

mediterranei, as demonstrated in previous chapters and by other researchers (Bonete et al., 1996; Lillo & Rodriguez-Valera, 1990). The consumption of glucose and galactose was comparable to what was found with batch and fed-batch feeding in previous Chapters 3-6. The steady-state CDM and PHA yields were 0.31 ± 0.03 g VS/g total sugar and 0.22 ± 0.00 g VS/g total sugar, respectively. The CDM and PHA yields were greater than what Lillo and Rodriguez-Valera (1990) found with a 50-hour HRT with a 20 g/l glucose loading feed of 0.27 and 0.12 g/l, respectively. The difference in yields of this study and the one by Lillo and Rodriguez-Valera (1990) may be due to reasons stated previously for CDM and PHA concentrations. Figure 7.5 shows the steady-state cell dry mass, PHA, glucose, galactose concentrations, and percent PHA content. Figure 7.6 displays the steady-state PHA content, CDM yield, PHA yield, and glucose and galactose consumption.

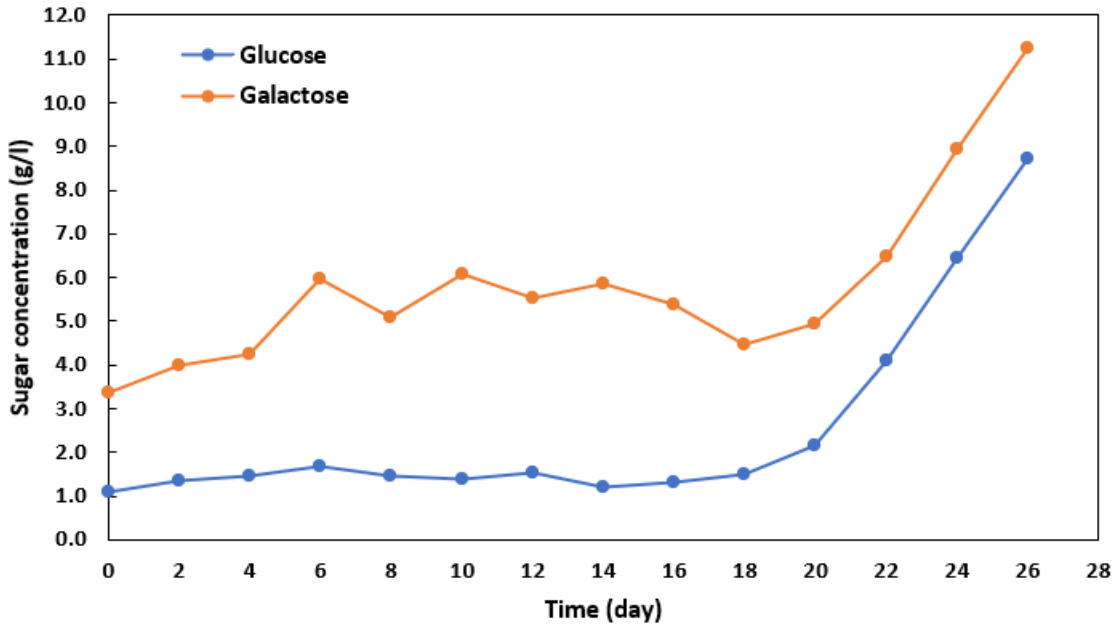

Figure 7.4 Glucose and galactose concentration with 10-day hydraulic retention time continuous feeding of hydrolyzed DLP.

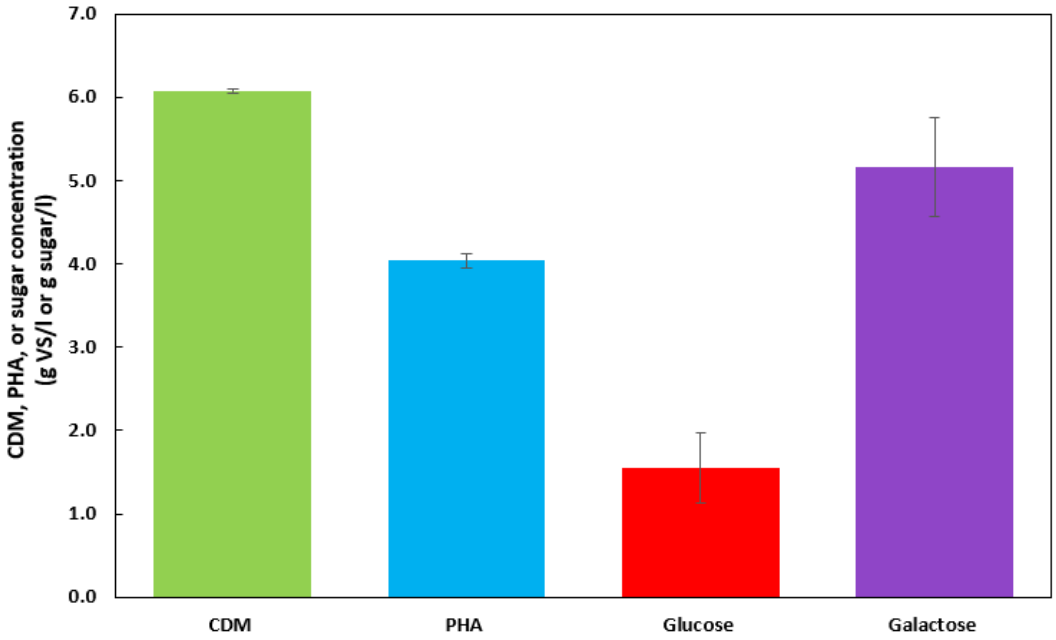

Figure 7.5 *H. mediterranei* steady-state cell dry mass (CDM), PHA, glucose, and galactose concentration with 10-day hydraulic retention time continuous feeding of hydrolyzed DLP. Y-error bars are standard deviations.

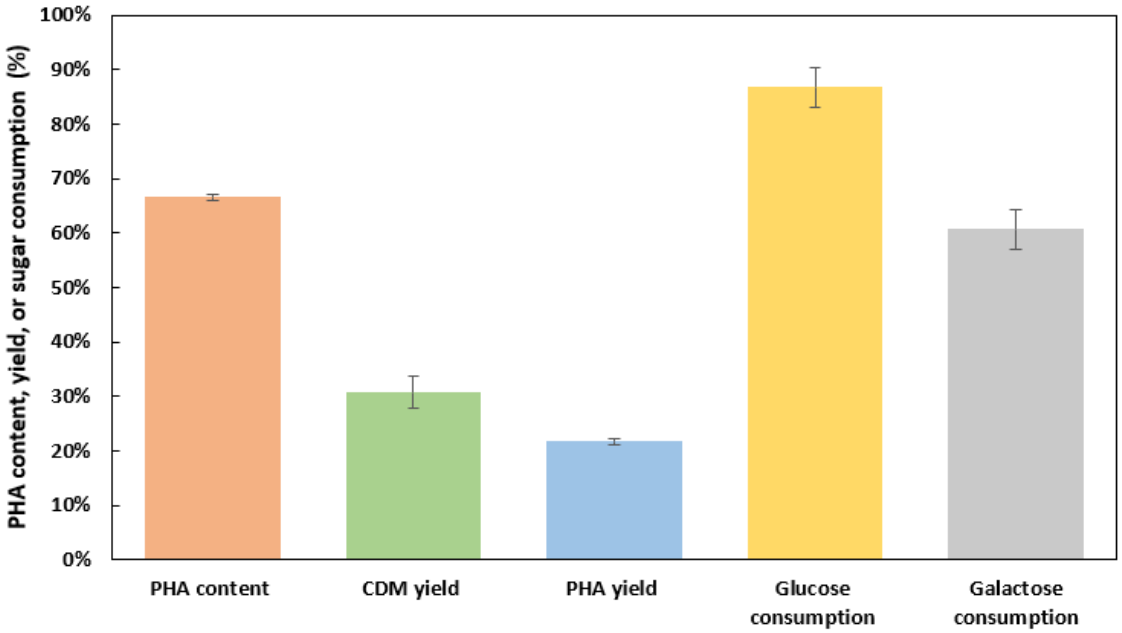

Figure 7.6 *H. mediterranei* steady-state PHA content, cell dry mass (CDM) yield, PHA yield, glucose and galactose consumption with 10-day hydraulic retention time continuous feeding of hydrolyzed DLP. Y-error bars are standard deviations.

7.4.2 Continuous stirred tank reactor with 20-day hydraulic retention time and hydrolyzed DLP feed

7.4.2.1 Effects of 20-day HRT continuous feeding of hydrolyzed DLP on cell growth

Figure 7.7 shows the 20-day CSTR bioreactor at various points in the fermentation from initial continuous feeding on day 0 to the end of an OLR of 2 g total sugar/l/day of glucose MSM on day 130. After 6 days of batch culturing, the bioreactor turned a dense pink color (Figure 7.7a), indicating successful growth, and a healthy culture was present to begin continuous feeding. The bioreactor was pink in color for the first 20 days of continuous operation, with a slight decline in intensity over time (Figures 7.7a-d). However, the pink pigment visually started to decrease in the next 30 days until the bioreactor became a yellow color (Figures 7.7e-g). The timing of the loss of the pink pigment was similar to when the 10-day HRT bioreactor was also observed to become less pink in color after 22 days of continuous operation. The bioreactor became pale yellow by day 40 (Figure 7.7f), potentially due to constituents present in the hydrolyzed DLP substrate and inhibition of *H. mediterranei*. The bioreactor increased in yellow color on day 50 after further feeding of hydrolyzed DLP feedstock (Figure 7.7g). The bioreactor became paler after one-third of the bioreactor fermentation broth was replaced with MSM containing no substrate on day 51 of continuous feeding (Figure 7.7h). The bioreactor slowly regained a yellow color after the feeding of hydrolyzed DLP resumed from days 52-90 (Figures 7.7h-k). However, the bioreactor did not regain its pink color characteristic of *H. mediterranei*, indicating that the dilution of the bioreactor with MSM did not recover the archaeal culture. After feeding an OLR of 2 g total sugar/l/day glucose MSM from days 90-130, the bioreactor again did not turn pink, indicating that the *H. mediterranei* culture did not fully recover

with the introduction of glucose substrate. Instead, the bioreactor remained a pale-yellow color even after operating for 2 HRT lengths (40 days) (Figures 7.7l-o).

Figure 7.8 shows the cell pellets separated from the fermentation broth by centrifugation during CDM concentration measurement. Vibrant pink cells were present after the initial batch operation of the bioreactor when continuous feeding began (Figure 7.8a). The cells became a darker pink after 20 days (Figure 7.8b), aligning with the bioreactor fermentation broth. After 40 days, the cell pellet was a darker brown-pink color (Figure 7.8c). The cell pellet at this time was considerably pinker than the bioreactor fermentation broth, which appeared to be a more yellow shade. Therefore, although it appeared that the bioreactor had lost *H. mediterranei* cells from a lack of observable pink color characteristic of the archaea, the *H. mediterranei* cells appeared to be present after centrifugation of the fermentation broth. The continuous feeding of hydrolyzed DLP for 40 days may have led to this color difference due to the accumulation of Maillard reaction byproducts and melanoidin browning pigments in DLP. At day 60, after diluting the bioreactor with MSM, the cells were pale yellow with only a slight observable pink hue (Figure 7.8d), matching the bioreactor color. By day 80, with the feeding of hydrolyzed DLP, the cell pellet had a more pronounced pink color but was overall a brown hue (Figure 7.8e). After feeding at an OLR of 2 g total sugar/l/day of glucose MSM, the cells became noticeably pinker on day 100 (Figure 7.8f). However, the bioreactor remained yellow in color, potentially due to the residual hydrolyzed DLP constituents that remained in the bioreactor. The color of the cell pellet remained fairly constant for the rest of the bioreactor operation with the glucose substrate. The cell pellets were observably pinker with glucose feeding than when operating the bioreactor with the hydrolyzed DLP feedstock. However, the pink color was less prominent than that observed in the first 30 days of bioreactor operation. Therefore, introducing glucose may have led to more *H. mediterranei* growth but at lower rates than observed during initial continuous feeding.

a) 

b) 

c) 
d) 

e) 
f) 
g) 
h) 

i)  j)  k)  l) 

m)  n)  o) 

Figure 7.7 20-day HRT CSTR with hydrolyzed DLP feed at various days during the fermentation: a) day 0; b) day 5; c) day 10; d) day 20; e) day 30; f) day 40; g) day 50; h) day 60; i) day 70; j) day 80; k) day 90; l) day 100; m) day 110; n) day 120; o) day 130.

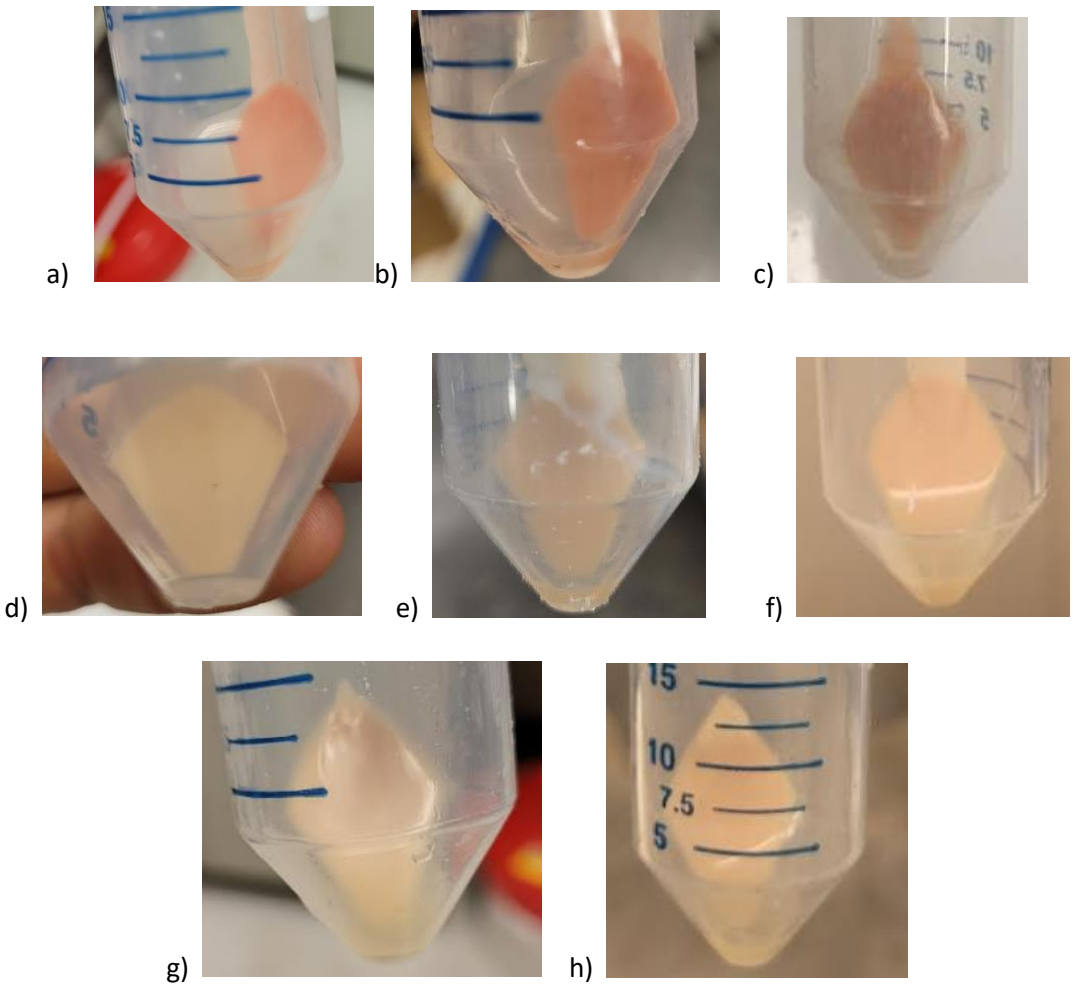

Figure 7.8 Cell pellets from 20-day HRT CSTR with hydrolyzed DLP feed for various days of reactor operation a) day 0; b) day 20; c) day 40; d) day 60; e) day 80; f) day 100; g) day 120; h) day 130.

Figure 7.9 displays the *H. mediterranei* cell growth curve measured by OD throughout continuous operation of the bioreactor. During the first 9 days of continuous feeding, the OD increased from 11.9 to 21.5, indicating successful cell growth of *H. mediterranei*. The OD then decreased during the following 3 days before increasing back to a similar OD of 21.7 on day 18. This OD trend may be due to the transient conditions that existed when starting continuous feeding before a steady-state was reached. The OD rapidly decreased the next two days to 17.0 on day 20 (1 HRT) of continuous feeding. The OD remained

at a near-constant value of 17.0, while feeding hydrolyzed DLP at a loading of 25 g/l to day 32, indicating a steady-state was achieved. After increasing the OLR to 1.5 g total sugar/l/day on day 32, the OD increased slightly to 17.5 on day 40. However, during this time, the bioreactor started to lose its pink color and become a yellow shade.

The OD decreased to 15.5 when MSM without substrate was fed on days 43-45 to observe if substrate inhibition could be reduced. When continuous feeding of hydrolyzed DLP resumed, the OD increased to 16.2 on day 51, demonstrating that the culture was still active. Although the OD increased after feeding hydrolyzed DLP, the OD did not reach previous values before diluting with MSM, indicating that the culture was becoming more inhibited over time. This result aligned with the bioreactor not increasing in pink color during the same period, which was expected if the *H. mediterranei* culture fully recovered. Therefore, one-third of the reactor fermentation media was removed and replaced with MSM to observe if less potential substrate inhibition would occur. The reactor dilution decreased the OD from 16.2 to 11.8 on days 51 to 52, respectively, which was the expected approximately one-third decrease. After resuming hydrolyzed DLP feeding at the OLR of 1.5 g total sugar/l/day, the OD increased to over 14.0 after 1 HRT (20 days). However, the OD did not increase to 16.0-17.0, where it was measured before reactor dilution. The culture during this time also became more brown-yellow than the archaea's natural pink color. Therefore, the culture appeared active but not at full health based the differences in bioreactor color and gradual decrease of OD from the beginning of continuous feeding. The pH continued to decrease with the pH controller continuing to apply sodium hydroxide during this timeframe, supporting that the culture was active since it is typical for *H. mediterranei* to produce organic acids during cell growth (Oren & Gurevich, 1994).

After the hydrolyzed DLP media OLR was increased to 2 g total sugars/l/day on day 72, the OD did not increase the first 15 days and remained near the range of 13.0-14.0. The OD then increased to 15.7 by day 90, indicating more cell mass growth occurred with the additional loading. The bioreactor, however, did not become pinker as expected, with the additional cell growth. With the glucose feeding at an OLR of 2 g total sugars/l/day starting on day 90, the OD increased to 18.1 after 15 days (1.5 HRT) and then declined rapidly over the next 5 days to 12.9. The OD remained fairly constant from 12.5-14.4 the last 20 days of bioreactor operation. Although the OD decreased with the glucose feeding, the cell pellets during the glucose feeding were noticeably pinker during glucose feeding, indicating more *H. mediterranei* grew.

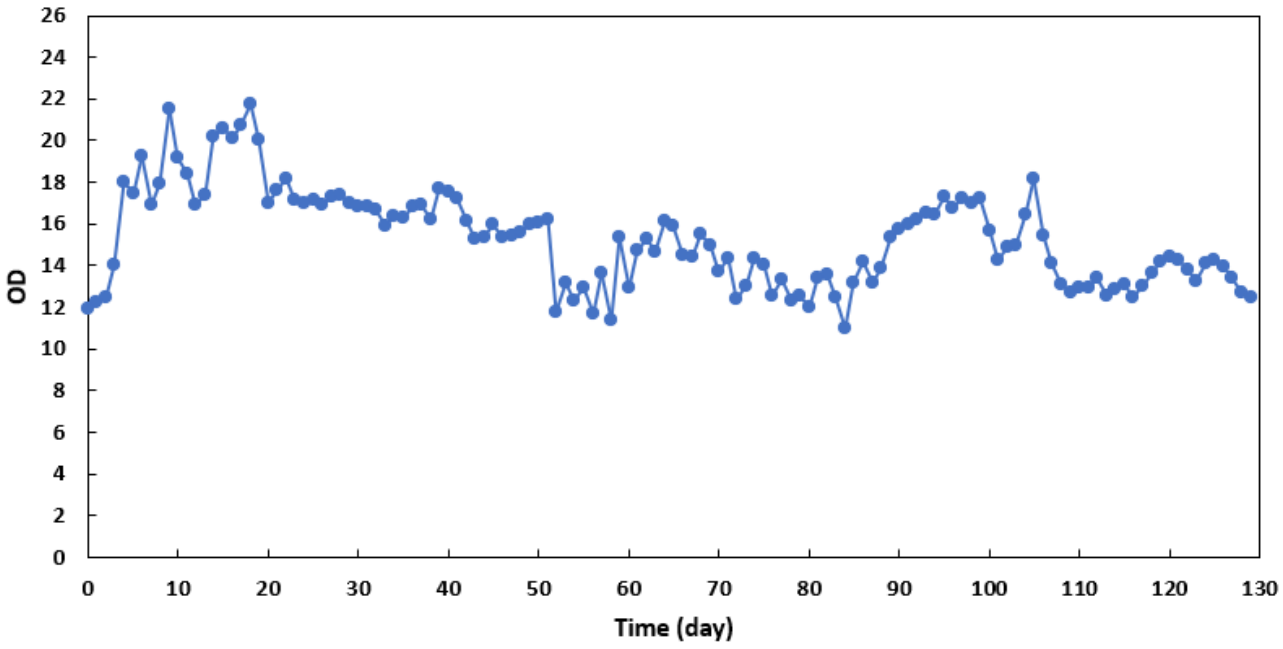

Figure 7.9 Cell growth of *H. mediterranei* in the CSTR fed with hydrolyzed DLP at an HRT of 20-days over time.

7.4.2.2 Effects of 20-day HRT continuous feeding of hydrolyzed DLP on cell dry mass and PHA yield, PHA content, and sugar consumption

Figure 7.10 shows the cell dry mass concentration, PHA concentration, and PHA content throughout the operation of the 20-day HRT CSTR from days 0 to 130. The CDM concentration, as expected, followed the same general trend as the OD. Furthermore, the maximum OD and CDM concentration occurred on day 18, a noticeable drop in OD and CDM concentration occurred on day 26, both the OD and CDM concentration decreased by the expected approximate one-third after the reactor was diluted with MSM on day 51, and a decline in OD and CDM occurred leading up to day 110. However, the OD and cell dry mass concentration relationship changed over time. In the first 60 days of bioreactor operation, the CDM concentration and OD ratio were near 0.42 that was similar to that cited by Huang et al. (2006). The CDM concentration to OD ratio increased closer to 0.48 until glucose was fed on day 90, where it decreased to approximately 0.42 again. This CDM to OD ratio change was likely due to the fermentation broth losing its pink color over time since the OD measurements were at a 520 nm wavelength in the red region of the visible spectrum. Even though the CDM to OD ratio changed during the fermentation, the OD still gave an adequate measurement of the changes in CDM concentration over time, as demonstrated by the OD and CDM concentrations following similar trends.

The CDM concentration increased in the first 18 days (near 1 HRT) of continuous feeding to a high of 8.0 g VS/l. The PHA concentration increased in the first 8 days (near 0.5 HRT) of continuous feeding to 3.8 ± 0.1 g VS/l and was nearly the same on day 18 at 3.7 ± 0.1 g VS/l when the high CDM concentration occurred. The PHA content followed a similar trend to the PHA concentration, increasing in the first 8 days to 0.50 g VS/g VS. From days 18 to 28, the PHA concentration decreased from 3.7 to 1.8 g VS/l, and the PHA content decreased from 0.46 to 0.27 g VS/g VS. The PHA concentration and content may have been the highest at the start of continuous feeding when more carbon was available in the environment, which

often triggers PHA accumulation by PHA producers (Anderson & Dawes, 1990). The CDM concentration, PHA concentration, and PHA content reached an approximate steady-state with the hydrolyzed DLP OLR of 1.25 g total sugar/l/day after 1 HRT (20 days) of continuous operation from days 22 to 26. The CDM concentration was 6.6 ± 0.1 g VS/l, the PHA concentration was 2.1 ± 0.2 g VS/l, and the PHA content was 0.32 ± 0.03 g VS/g VS/g VS during this apparent steady-state condition. Although the CDM concentration increased with the longer HRT from the first 10-day HRT CSTR experiment, as expected, the PHA concentration and PHA content were around half of what was found for the 10-day HRT CSTR. The lower PHA production with the 20-day HRT CSTR may be due to less favorable conditions for PHA accumulation, such as lower environmental carbon. The longer HRT may have also led to more PHA consumed by *H. mediterranei* since less substrate was available. The 20-day HRT CSTR conditions did not appear favorable for *H. mediterranei* PHA production at the applied HRT and OLR.

The steady-state CDM concentration (p-value = 0.0034), PHA concentration (p-value = 0.002), and PHA content (p-value < 0.0001) of the five OLR changes were significantly different. Therefore, further Tukey test pairwise comparisons were conducted. After the hydrolyzed DLP OLR was increased to 1.5 g total sugar/l/day, new steady-state values for the CDM concentration, PHA concentration, and PHA content were achieved after approximately 0.5 HRT (10 days) of continuous feeding from days 40 to 44. During this time, the CDM concentration was 7.1 ± 0.2 g VS/l, the PHA concentration was 2.0 ± 0.2 g VS/l, and the PHA content was 0.28 ± 0.02 g VS/g VS. Although the CDM concentration significantly increased (p-value = 0.0150), as expected, the PHA concentration was not significantly different (p-value = 0.9113) with the additional loading. The same reasons stated for the low PHA production of the 20-day HRT CSTR compared to the 10-day HRT CSTR of low carbon availability and potential PHA consumption may also explain the PHA not increasing as predicted with the additional loading. Sustained exposure to the hydrolyzed DLP that contains potentially inhibitory compounds, such as Maillard reaction byproducts, may

have caused inhibition of the culture. After diluting the bioreactor by one-third with MSM with no carbon source present on day 51, the CDM and PHA concentrations quickly decreased by approximately one-third, as expected from 7.3 and 2.0 g VS/l to 5.4 and 1.4 g VS/l, respectively. When feeding resumed with the hydrolyzed DLP media at an OLR of 1.5 g total sugar/l/day, a steady-state condition was achieved again after approximately 0.75 HRT (15 days) from days 66 to 72. The steady-state CDM concentration was 6.6 ± 0.1 g VS/l, the PHA concentration was 1.4 ± 0.1 g VS/l, and the PHA content was 0.21 ± 0.01 g VS/g VS during this period. The CDM and PHA concentrations were less than those with the previous operation with the OLR of 1.5 g total sugar/l/day before the MSM dilution. This result indicated that although the culture recovered after the MSM dilution, greater inhibition appeared to have occurred potentially due to prolonged exposure to the hydrolyzed DLP.

After increasing the hydrolyzed DLP OLR to 2 g total sugar/l/day on day 72, an approximate steady-state condition was achieved after 0.75 HRT from days 86 to 90. The steady-state CDM concentration, PHA concentration, and PHA content were 6.6 ± 0.2 g VS/l, 1.2 ± 0.1 g VS/l, and 0.19 ± 0.01 g VS/g VS, respectively. The CDM concentration was not significantly different (p-value > 0.9999) from the previous OLR of 1.5 g total sugar/l/day. The CDM concentration was expected to increase with the higher loading as more substrate was available to grow more cells. However, this anticipated result did not occur, demonstrating further inhibition of the culture. The PHA concentration was not significantly different (p-value = 0.7172) for the OLR of 2 g total sugar/l/day than the previous OLR of 1.5 g total sugar/l/day, which was also expected to increase with additional loading. The low PHA production suggested unfavorable conditions for PHA accumulation, potentially due to low environmental carbon and exposure to higher concentrations of hydrolyzed DLP.

After the feed was changed from hydrolyzed DLP to glucose substrate on day 90, the CDM, PHA concentration, and PHA content increased from days 96 to 102. A steady-state condition was observed after nearly 1 HRT for CDM concentration, PHA concentration, and PHA content from days 98 to 102 of 7.0 ± 0.2 g VS/l, 1.9 g ± 0.2 VS/l, and 0.28 ± 0.01 g VS/g VS, respectively. The glucose OLR of 2 g total sugar/l/day CDM concentration was not significantly different (p-value = 0.0655) from the hydrolyzed DLP OLR of 2 g total sugar/l/day. However, the PHA concentration was significantly greater (p-value = 0.0036) with the glucose OLR of 2 g total sugar/l/day than with the hydrolyzed DLP OLR of 2 g total sugar/l/day, and the PHA content was also significantly greater (p-value = 0.0012). Therefore, feeding glucose may have improved PHA production in the 20-day HRT CSTR compared to hydrolyzed DLP. The PHA increase may be due to removing potentially inhibitory compounds from the hydrolyzed DLP and adding glucose that *H. mediterranei* prefers over the galactose (Pais et al., 2016). The CDM and PHA concentration decreased to 5.4 g VS/l and 0.9 ± 0.0 g VS/l on day 130. The fermentation was concluded on day 130 of continuous feeding since the culture did not appear would fully recover after repeated attempts.

Table 7.1 summarizes the steady-state parameters achieved for the different OLR conditions. The steady-state CDM yield and PHA yield were 0.27 ± 0.01 g VS/g total sugar and 0.08 ± 0.01 g VS/total sugar with the initial hydrolyzed DLP OLR of 1.25 g/l. The CDM yield was comparable to what Lillo and Rodriguez (1990) found continuously feeding of 20 g/l of glucose at a dilution rate of 0.02 h^{-1} of 0.27 g VS/g glucose, and the PHA yield was also comparable at 0.12 g PHA/g glucose. The CSTR PHA yields of this study and by Lillo and Rodriguez (1990) were on the lower end of PHA yields reported with sugar substrates with *H. mediterranei* and batch cultivation of 0.07-0.33 g PHA/g (Don et al., 2006; Koller et al., 2007a, 2007b; Lillo & Rodriguez-Valera, 1990; Melanie et al., 2018; Rodriguez-Valera et al., 1991). The lower PHA yields from the CSTR compared to the batch bioreactor may be caused by reduced substrate concentrations that are

unfavorable for PHA production (Anderson & Dawes, 1990). Therefore, continuous feeding at these OLRs and HRTs with *H. mediterranei* may not be the optimal bioreactor operation strategy for PHA production.

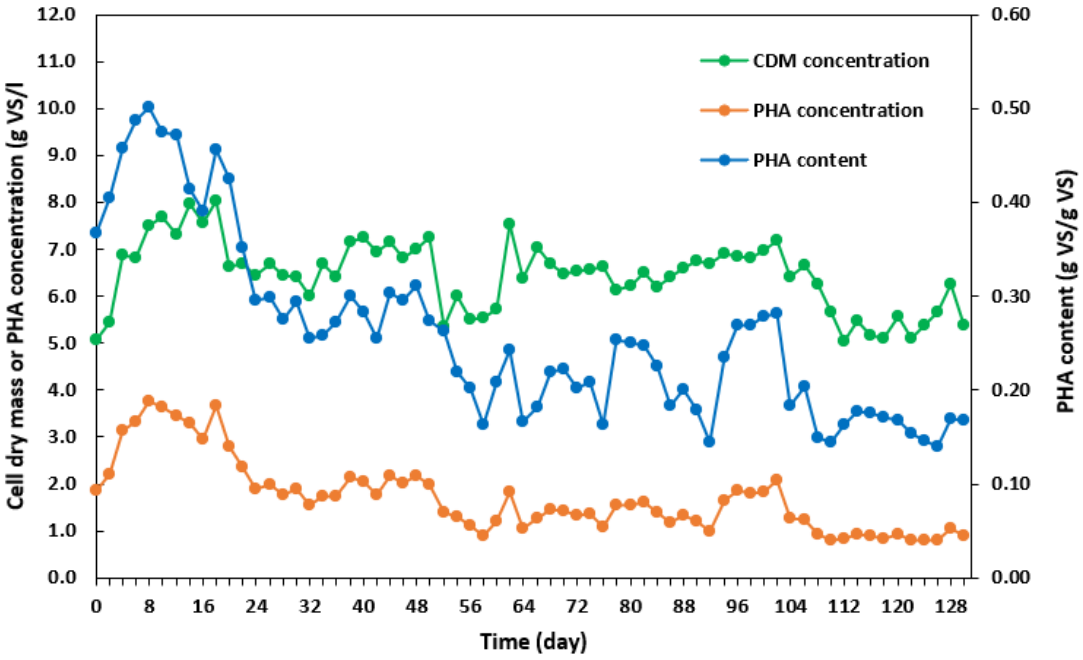

Figure 7.10 *H. mediterranei* cell dry mass (CDM) concentration, PHA concentration, and PHA content with 20-day hydraulic retention time continuous feeding of hydrolyzed DLP.

Table 7.1 *H. mediterranei* steady-state CDM concentration, PHA concentration, PHA content, CDM yield, PHA yield, total sugar concentration, and sugar consumption for the various loading conditions during the operation of the CSTR with hydrolyzed DLP and glucose at a 20-day HRT.

Loading	Steady state days	CDM concentration (g VS/l)	PHA concentration (g VS/l)	PHA content (g VS/g VS)	Total sugar concentration (g/l)	Total sugar consumption (%)	CDM yield (g VS/g total sugar)	PHA yield (g VS/g total sugar)
1.25 g/l/day hydrolyzed DLP	22-26	6.6 ± 0.1	2.1 ± 0.2	0.32 ± 0.03	0.1 ± 0.1	99.7 ± 0.0	0.27 ± 0.01	0.08 ± 0.01
1.5 g/l/day hydrolyzed DLP (before CSTR dilution)	40-44	7.1 ± 0.2	2.0 ± 0.2	0.28 ± 0.02	0.4 ± 0.1	99.8 ± 0.0	0.24 ± 0.01	0.07 ± 0.01
1.5 g/l/day hydrolyzed DLP (after CSTR dilution)	68-72	6.6 ± 0.1	1.4 ± 0.1	0.21 ± 0.01	0.4 ± 0.1	97.9 ± 0.7	0.22 ± 0.01	0.05 ± 0.00
2 g/l/day hydrolyzed DLP	86-90	6.6 ± 0.2	1.2 ± 0.1	0.19 ± 0.01	2.6 ± 0.5	94.4 ± 1.9	0.17 ± 0.01	0.03 ± 0.00
2 g/l/day glucose	98-102	7.0 ± 0.2	1.9 ± 0.2	0.28 ± 0.01	1.8 ± 0.7	96.4 ± 1.0	0.18 ± 0.01	0.05 ± 0.00

Figure 7.11 shows the sugar concentration of the 20-day HRT CSTR. At the beginning of continuous feeding on day 0, the initial glucose concentration was 0.0 g/l, and the galactose was 4.6 g/l. These sugar concentrations were similar to what was observed in Chapter 3 with hydrolyzed DLP feedstock and batch feeding, as *H. mediterranei* was shown to prefer glucose compared with galactose substrate. With 6 days of continuous feeding of hydrolyzed DLP, the galactose concentration decreased to 0.0 g/l. However, the glucose concentration unexpectedly increased to 4.8 g/l on day 6. The glucose concentration then started to decrease after all the galactose was consumed by day 6 to 0.0 g/l by day 14. The archaea culture continuing to consume galactose even though the preferred glucose sugar was present suggested that *H. mediterranei*'s glucose dehydrogenase enzyme, which is responsible for glucose and galactose metabolism (Bonete et al., 1996), may only metabolize one sugar at a time. It appears that once *H. mediterranei*'s glucose dehydrogenase switched to metabolizing galactose from glucose sugar during batch feeding, the enzyme continued to metabolize the galactose until it was depleted, then acclimated back to glucose. The 10-day HRT CSTR did not display this phenomenon, potentially due to the shorter HRT that was present and starting the continuous feeding after the stationary phase was reached. The glucose concentration remained low, < 2.5 g/l, from day 14 to 114, and the galactose concentration

remained < 1.5 g/l from day 4 to the end of the fermentation on day 130. The glucose and galactose sugar consumption were high, between 90%-100% from day 14 to 114. The galactose consumption was higher than observed in previous chapters at less than 70%, potentially due to the extended fermentation time with a 20-day HRT. After feeding with the glucose at an OLR of 2 g total sugar/l/day on day 90, the glucose concentration remained < 1.5 until day 106 and then increased to 4.5 g/l from day 108 to 130, coinciding with the decrease in CDM concentration.

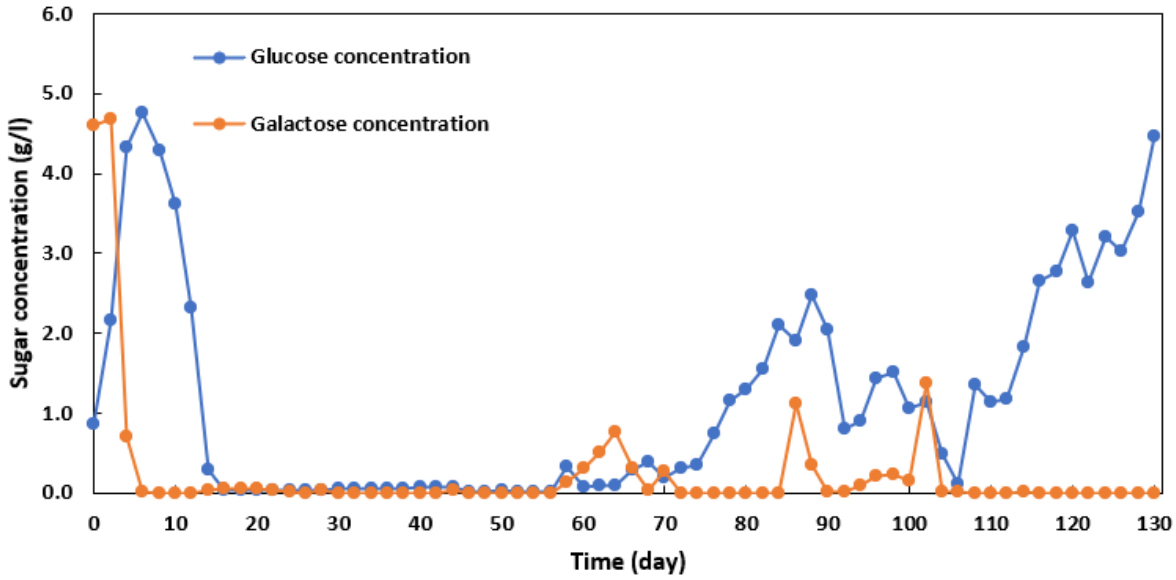

Figure 7.11 *H. mediterranei* glucose and galactose concentration with 20-day hydraulic retention time continuous feeding of hydrolyzed DLP.

7.4.3 Batch flasks inhibition studies

Batch flask fermentation experiments were conducted with CSTR effluent when the bioreactor appeared to be inhibited on day 45, as indicated by the loss of pink color characteristic of *H. mediterranei* and decline in OD. Figure 7.12 displays the batch cultures at the end of the fermentation. Figure 7.13

shows the cell growth curves. The flasks that were diluted with MSM by one-half (1/2 dilution) and one-third (1/3 dilution) without additional feeding did not change color considerably and remained yellow, indicating that no cell growth had occurred. The one-third dilution OD did not increase after 4 days of incubation, while the one-half dilution OD increased marginally by about 1.0. Initially, it was difficult to determine if substrate inhibition was occurring in these flasks. However, after measuring the sugar concentration by HPLC, the results of these diluted batches could be explained by the minimal sugars were present to allow further cell growth.

The flasks re-inoculated with MSM containing glucose or hydrolyzed DLP loading of 10 g total sugar/l turned dense pink, indicating a successful growth of *H. mediterranei* and that the culture was still active. Figure 7.14 shows the final CDM concentration, final PHA concentration, and PHA content of the batch culture grown with glucose and hydrolyzed DLP. The first culture grown on the glucose MSM media (Glucose 1) had a similar growth curve to the glucose batch cultures in Chapter 4, with the OD increasing to 11.0 after 10 days. The final CDM concentration was 4.1 ± 0.2 g VS/l, the final PHA concentration was 2.3 ± 0.2 g VS/l, and the PHA content was 0.57 ± 0.07 g VS/g VS. These values were comparable to those in Chapter 4 with the same glucose and yeast extract feedstock indicating that the archaea were still viable. The cultures grown with hydrolyzed DLP media (HDLP) also resulted in successful cell growth, with the OD increasing to 12.4 ± 0.2 by day 13. The final CDM concentration, PHA concentration, and PHA content were 4.7 ± 0.5 g VS/l, 2.5 ± 0.5 g VS/l, and 0.73 ± 0.02 g VS/g VS, respectively. The culture grew slightly slower than the hydrolyzed DLP flasks in Chapters 3 and 4. However, the final CDM concentration, PHA concentration, and PHA content were comparable.

These results demonstrated that the culture could still effectively consume hydrolyzed DLP as the substrate for cell growth and produce dense pink cells. Additionally, the results established that high PHA

contents could be achieved with the CSTR culture and hydrolyzed DLP feedstock. These findings suggested that the conditions of the CSTR were causing the low accumulation of PHA product rather than potential mutations to the culture that can occur with CSTR feeding (Koller & Braunegg, 2015) causing low PHA accumulation. The low sugar concentration of the CSTR and potential constituents in DLP, e.g., Maillard reaction products that are inhibitory to other microorganisms (Einarsson et al., 1983; Einarsson & Eklund, 1988), appear to be unfavorable for PHA production. The DLP compounds could accumulate with continuous feeding until a steady-state concentration was reached due to minimal or no consumption/breakdown of these constituents. In the second study, with glucose media (Glucose 2) collected 10 days later, the culture grew successfully again, obtaining a final OD of 7.6 after 10 days. In the second glucose study, the final CDM and PHA concentrations were 3.4 ± 0.3 g/l and 1.6 ± 0.3 g/l,respectively, significantly less (final CDM concentration p-value = 0.0111 and final PHA concentration p-value = 0.0348) than the previous glucose flasks. However, the PHA contents were not significantly different (p-value = 0.9242). These results suggested that the culture was becoming more inhibited over time, but the *H. mediterranei* culture was still viable.

a) 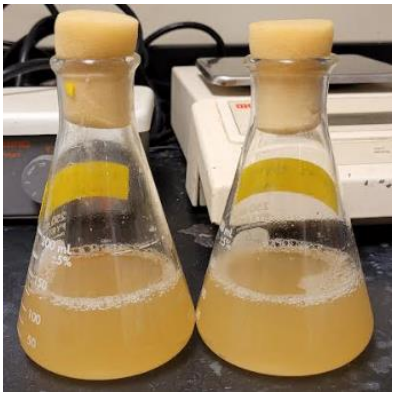 b) 

c)  d) 

Figure 7.12 *H. mediterranei* batch fermentations inoculated with CSTR effluent with: a) half-dilution (left) and one-third dilution (right); b) glucose and yeast extract feedstock; c) glucose and yeast extract feedstock and inoculum culture 10-days older; d) hydrolyzed DLP feedstock.

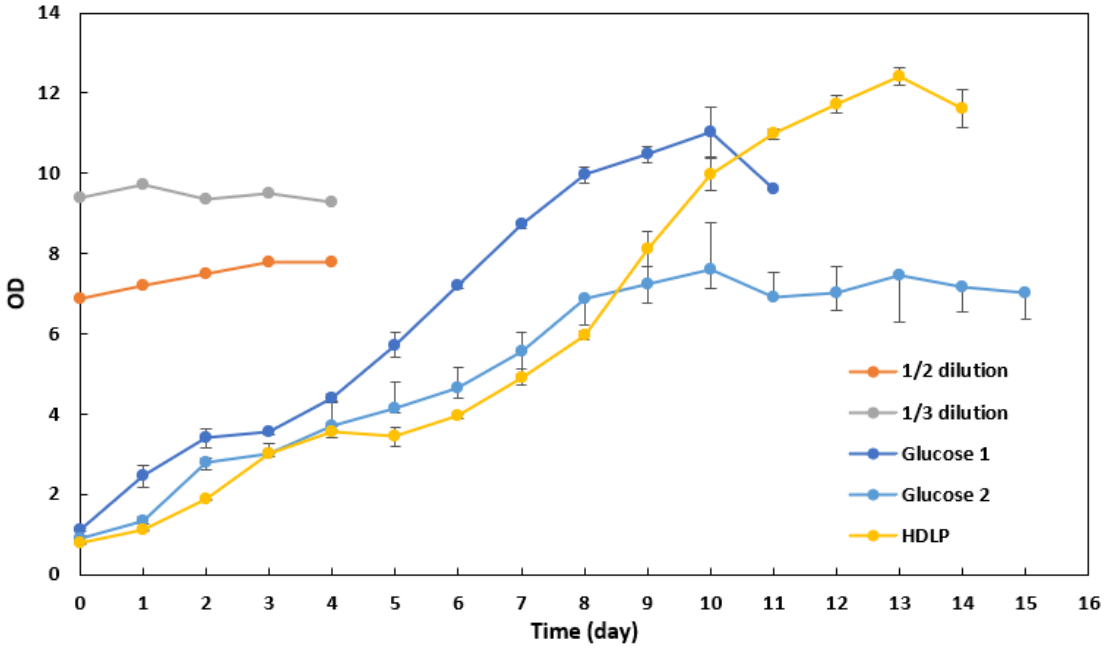

Figure 7.13 Growth of *H. mediterranei* cells over time with CSTR effluent inoculum and dilution with MSM, glucose feedstock, and hydrolyzed DLP (HDLP) feedstock. Y-error bars are standard deviations.

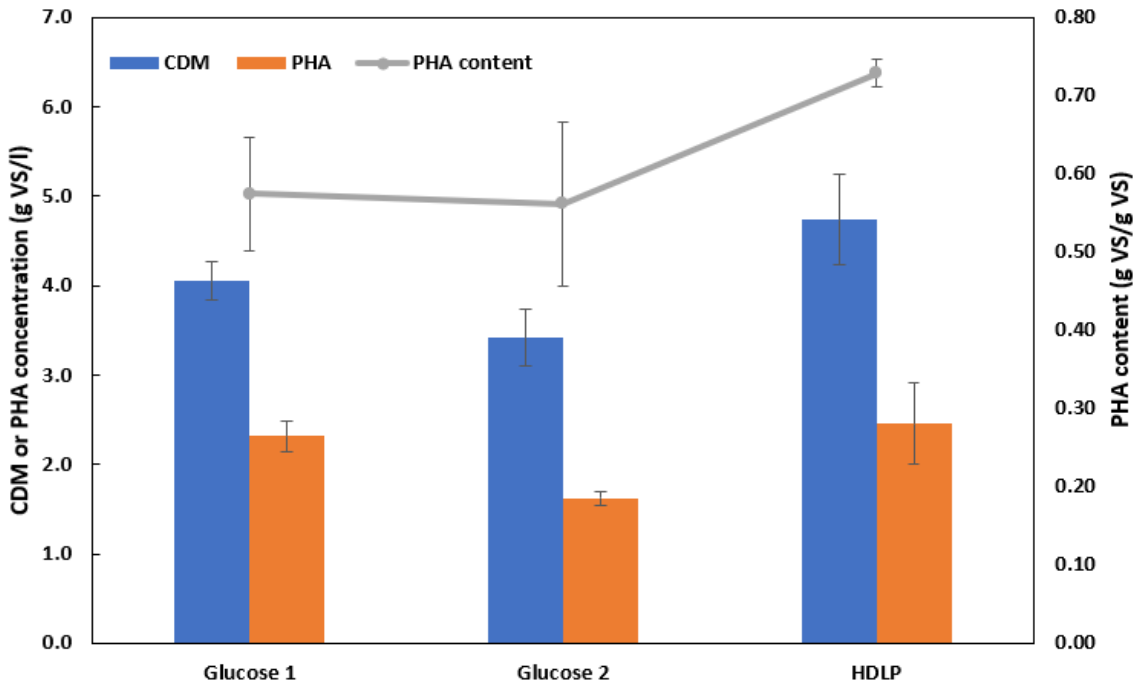

Figure 7.14 *H. mediterranei* final CDM concentration, final PHA concentration, and PHA content for culture inhibition flask experiments with CSTR effluent inoculum and dilution with glucose and hydrolyzed DLP feedstocks. Y-error bars are standard deviations.

7.5 Conclusions

A 20-day HRT CSTR feeding hydrolyzed DLP and glucose at an OLR of 1.25-2.0 g total sugar/l/day was successfully operated with a stable culture for 130 days. However, a shorter 10-day HRT CSTR fed hydrolyzed DLP at an OLR of 2.5 g total sugar/l/day resulted in an unstable culture and cell washout after 22 days of operation. Although the 20-day HRT CSTR maintained a stable culture for an extended period, the PHA yield of the bioreactor was lower than what was obtained with batch operation in previous chapters. The culture's physiology appeared to change over time with the 20-day HRT CSTR operation, losing its pink pigment and becoming more yellow-brown. The culture regained its dense pink color when inoculated in glucose and hydrolyzed DLP at a loading of 10 g total sugar/l with batch flask bioreactors.

These batch studies with CSTR effluent indicated that environmental pressures from the 20-day CSTR operation, such as low sugar concentration and exposure to potential inhibitory compounds e.g., Maillard reaction byproducts, were causing reversible changes to the culture since the culture was still viable in other sugar-containing feedstocks. Although a desirable high consumption of total sugars was achieved with the 20-day HRT CSTR, the low sugar concentrations appear to be a potential cause for the low PHA yield and content since PHA production typically occurs when carbon is in excess. Therefore, it may be challenging to optimize for both sugar consumption and PHA yield simultaneously. Batch and fed-batch feeding strategies may improve PHA yields compared to continuous feeding since the higher sugar concentrations initially present may improve PHA production. Despite the lack of improvements with continuous feeding of hydrolyzed DLP, the study provides valuable insights and data that could contribute to future research and improvements. Hydrolyzed whey permeate may give better results with continuous feeding since less inhibition appeared to be present than hydrolyzed DLP in Chapter 6. The results of this study can lead to the effective selection of feeding strategies for cheese byproducts, furthering the potential commercialization of the PHA process.

Chapter 8. Acclimation to Galactose by *Haloferax mediterranei* for Increased Cell Mass Growth and PHA Production

8.1 Abstract

Traditional plastics pose numerous environmental problems, including accumulating in landfills and littering the ocean, contributing to greenhouse gas emissions, and deriving from non-renewable resources. Polyhydroxyalkanoates (PHA) are a bioplastic that can replace traditional plastics in many applications that are highly biodegradable and bioderived from renewable resources. PHA can be produced economically from hydrolyzed cheese byproducts using *Haloferax mediterranei* (*H. mediterranei*). However, one downside of utilizing *H. mediterranei* and hydrolyzed cheese byproducts is that the galactose contained is often consumed at lower rates thanglucose. One method that can be applied to improve galactose consumption is to acclimate *H. mediterranei* to galactose substrate by growing the microorganism successively on the sugar. In this study, PHA yield was determined using *H. mediterranei,* which was grown for five consecutive batches with galactose as a substrate. With galactose acclimation, the final CDM concentration significantly increased with three batches, the specific growth rate with four batches, the final PHA concentration with five batches, and the galactose consumption with three batches (total galactose consumption), indicating successful galactose acclimation had occurred. The results of this study can assist in developing industrial-scale PHA production from hydrolyzed cheese byproducts by increasing the PHA yield from these feedstocks. The acclimation technique could also be applied to other substrates to improve *H. mediterranei* PHA yields.

Keywords: *Haloferax mediterranei*, galactose, polyhydroxyalkanoates, hydrolyzed cheese byproducts

8.2 Introduction

Haloferax mediterranei (*H. mediterranei*) is a polyhydroxyalkanoate (PHA) producer that can convert low-value cheese byproducts into profitable bioplastic. However, additional research is needed to commercialize this proposed bioplastic process to further decrease production costs and improve yields (Amaro et al., 2019). One of the limitations of *H. mediterranei* is its inability to directly consume cheese byproducts' main carbon source, lactose, at high rates (Amaro et al., 2019; Rodriguez-Valera et al., 1980). Therefore, an enzymatic hydrolysis step of the lactose is one common method used to convert the disaccharide into glucose and galactose that the organism can consume (Koller, 2015a; Koller et al., 2007a). One difficulty with the enzymatic pretreatment of cheese byproducts is that *H. mediterranei* prefers glucose over galactose, often leading to incomplete galactose consumption (Koller, 2015a; Pais et al., 2016). This result was observed in previous Chapters 3-6 with hydrolyzed cheese byproduct DLP and whey permeate, where less than 70% of the galactose was consumed compared to nearly 100% of the glucose. In Chapter 7, although galactose consumption was near 100% when operating the CSTR with a 20-day HRT, PHA yields were low.

Since hydrolyzed cheese byproducts contain half galactose as substrate, it is important to achieve complete consumption of the sugar and comparable PHA yields to glucose for more effective PHA production. *H. mediterranei*'s glucose dehydrogenase enzyme, whose primary function is metabolizing glucose, has a broad substrate specificity (Bonete et al., 1996). The promiscuous enzyme allows glucose and other aldose sugars to be metabolized as part of the modified Entner-Doudoroff pathway in halophilic archaea (Bonete et al., 1996), as shown in Figure 8.1 (Siebers & Schönheit, 2005). The enzyme can catalyze the oxidation of numerous sugars, including, D-xylose, D-galactose, and D-fucose, into their corresponding glyconates (Bonete et al., 1996). Bonete et al. (1996) measured the relative rates of enzymatic activity of the sugars when $NADP^+$ is used as a coenzyme compared to that of D-glucose (D-glucose enzymatic activity

defined as the 100% reference). The authors determined the relative rates of enzymatic activity to be 13% for D-galactose, 88% for D-xylose, and 18% for D-fucose. Therefore, although other sugars, such as xylose, can be metabolized at similar rates to glucose by *H. mediterranei*'s glucose dehydrogenase enzyme, galactose is metabolized considerably slower. This finding theoretically explains the lower galactose consumption compared to glucose observed in previous chapters and by other researchers (Pais et al., 2016).

Pais et al. (2016) improved *H. mediterranei* galactose consumption by supplementing SL-6 micronutrients to media containing equal concentrations of glucose and galactose derived from pure sugars and hydrolyzed cheese byproduct whey. The researchers compared SL-6 loadings of 0.0%, 0.1%, and 1.0% v/v. Galactose consumption increased relative to the SL-6 loading, with no consumption occurring for the control without SL-6 and the greatest galactose consumption occurring for the 1.0% v/v loading. The glucose consumption rate also increased with the addition of SL-6 but with no additional benefits noted for the higher 1.0% v/v than the 0.1% v/v loading. However, even with these improvements, Pais et al. (2016) only achieved around 60% galactose consumption. Therefore, more research is needed to further improve *H. mediterranei* galactose consumption. These experimental results suggested that micronutrients are critical for galactose consumption. Peire et al. (2002) demonstrated that micronutrients, such as zinc, are contained in *H. mediterranei*'s glucose dehydrogenase at two zinc ions per subunit, with some evidence to suggest that one zinc ion is essential for catalytic activity and the other is part of the enzyme's structure. The glucose dehydrogenase activity also depends on the divalent cations' presence (Bonete et al., 1996). Bonete et al. (1996) showed that the absence of such ions resulted in low enzymatic activity, and the addition of cations caused increased enzymatic activity. The supplementation of Mn^{2+} resulted in the greatest increase of enzymatic activity of the cations tested, less for Mg^{2+}, and the least for Ni^{2+}. These findings indicate why micronutrients may be crucial for *H.*

mediterranei's sugar metabolism and pose an explanation for the observations of Pais et al. (2016) with SL-6 supplementation. Other methods other than micronutrient addition could be employed to increase galactose consumption. One technique that could be applied is acclimating the *H. mediterranei* to galactose substrate with successive growth on the sugar, which has been demonstrated to be a feasible approach for increasing galactose consumption and cell mass growth rates for other microorganisms, such as yeasts (Cho et al., 2014; Keating et al., 2004).

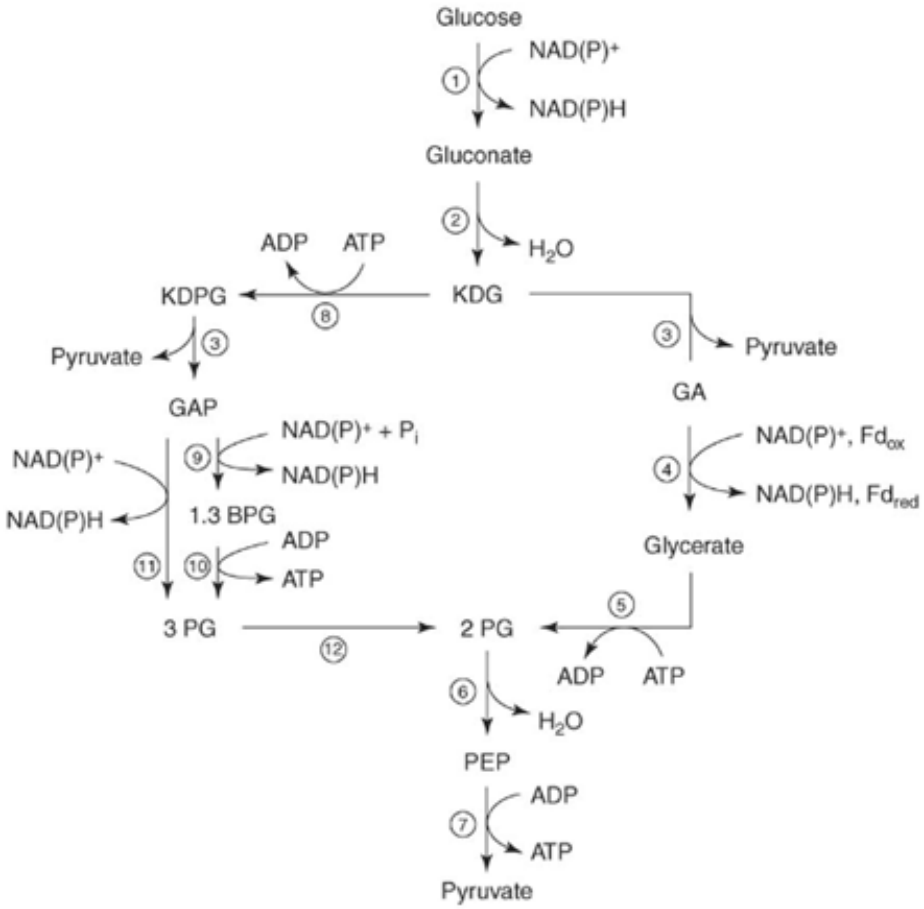

Figure 8.1

Figure 8.1 Modifications of the Entner–Doudoroff (ED) pathway in archaea (Siebers & Schönheit, 2005).

This study aimed to increase *H. mediterranei* and PHA production with galactose as a substrate. The tasks of this research were to: 1) determine the effect of the acclimation of *H. mediterranei* to galactose after growing multiple generations in batch reactors; and 2) quantify the potential increases in cell mass growth, PHA production, and sugar consumption.

8.3 Materials and methods

8.3.1 Microorganism and culture conditions with galactose media

Halophilic archaeon *H. mediterranei* (ATCC 33500) was used as the PHA producer in batch bioreactors. Two-hundred-milliliter Erlenmeyer flasks with a working volume of 130 ml were utilized as bioreactors. The flasks were placed in a shaker incubator (New Brunswick Scientific, C24KC refrigerated incubator shaker, Edison, New Jersey, United States) controlled to a temperature of 37℃ and agitation at 180 rpm like in previous Chapters 3-5. The fermentation was stopped when the culture had reached the stationary phase after 288 hours.

Galactose was used as a substrate at a loading of 10 g galactose/l. Five consecutive batches of *H. mediterranei* growth were carried out. The initial inoculum for the first fermentation batch was prepared following the procedures described in previous chapters. For the second through fifth batches, the cells from the previous fermentation were collected and used as inoculum for the subsequent batch. Therefore, each consecutive inoculum was derived from more parental generations of archaea grown on the galactose substrate. Minimum salt media (MSM) and 1% v/v SL-6 trace elements described previously in Chapter 3 were applied for adequate salinity and nutrients for growth. Ammonium chloride was added as a nitrogen source to give a constant C/N ratio of 8, which provided excess nitrogen (Cui, Shi, et al., 2017). Potassium dihydrogen phosphate was added to obtain a C/P ratio of 35, providing excess phosphorous (Melanie et al., 2018). Complex nutrient source yeast extract was also supplied at a loading

of 1 g/l. Sodium bicarbonate was added at a 2.5 g/l loading as a buffer, and 3 M NaOH and 3 M HCl were added twice daily to control the pH.

8.3.2 Determination of cell mass concentration and growth kinetics

Cell growth was monitored daily without disturbing the culture by sampling 1 ml of the fermentation broth daily. The optical density (OD) was measured, as an indicator of the cell concentration, at a wavelength of 520 nm in the red region of the visible light spectrum with a spectrophotometer (Hach, DR 2700 Loveland, Colorado, United States) as described by Huang et al. (2016). The cell growth rate was determined by analyzing the change in cell dry mass during the exponential growth phase (hours 0 to 96) and employing first-order growth kinetics as described in Chapter 7. The optical density (OD) measurements were converted to cell dry mass using the method described by Huang et al. (2016). The natural logarithm of the cell dry mass, ln(X), was plotted against time. The specific growth rate, μ, was estimated as the slope determined with linear regression using Microsoft Excel. As described in previous chapters, the final cell dry mass (CDM) was determined by measuring the fermentation broth volatile solids (VS) after 288 hours. A 20 ml sample of the fermentation broth was collected and centrifuged at 8,000 rpm for 30 minutes. The cell mass was washed with MSM solution twice, and the VS were measured with an oven and furnace following standard methods (American Public Health Association, 2012).

8.3.3 Extraction, purification, and quantification of PHA

PHA extraction was conducted following methods outlined by Escalona et al. (1996), with modifications described in previous chapters. A 20 ml fermentation broth sample was collected and centrifuged at 8,000 rpm for 30 minutes to separate the cell mass. The cell mass was then washed with a 0.1% sodium dodecyl-sulfate (SDS) and deionized (DI) water solution and subjected to vigorous vortexing for 2 minutes. The solution was incubated with the 0.1% SDS solution in a shaker incubator at 40℃ and

continuous agitation at 180 rpm for 12 hours. The sample was centrifuged again at the same rotation speed and time as before, and the cell pellet was washed twice with DI water. The PHA mass was measured as VS following the same standard methods for CDM (American Public Health Association, 2012). The measured CDM and PHA concentrations were used to determine the PHA content of the CDM, calculated as the percentage of PHA of the total CDM, and reported as g VS/g VS.

8.3.4 Measurement of sugars and determination of yields

The galactose sugar was measured at the end of the fermentation with high-performance liquid chromatography (HPLC) equipped with a refractive index detector (RID) and photodiode array detector (PDA), as described by Sluiter (2008). One milliliter of fermentation broth was sampled daily from the bioreactors. The samples were then centrifuged at 12,000 rpm for 20 minutes, and the supernatant was filtered through 0.22 µm membranes to remove suspended solids. A Biorad Aminex HPX-87H column (Hercules, California, United States) was used as the analytical column, and a 5 mM H2SO4 solution as the mobile phase. During the HPLC analysis, the oven temperature was controlled to 60 ℃ and the flow rate at 0.6 ml/min.

From the CDM measured results and galactose consumption, the CDM yield was determined as the mass of CDM grown divided by the mass of galactose consumed, reported as g VS/g galactose.

$$Y_{CDM} = \frac{\Delta m_{CDM}}{\Delta m_{galactose\ consumed}} \quad (8.1)$$

Similarly, the PHA yield was calculated as the mass of PHA accumulated divided by the mass of galactose that was consumed and reported as g VS/g galactose.

$$Y_{PHA} = \frac{\Delta m_{PHA}}{\Delta m_{galactose\ consumed}} \quad (8.2)$$

8.3.5 Statistical analysis

Experiments were conducted in triplicates, with each assay's mean and standard deviation (SD) calculated for the triplicates. The values were reported as the mean ± standard deviation. One-way Analysis of Variance (ANOVA) and the Tukey test for pairwise comparisons were performed to determine the significance of the differences among the studied parameters. GraphPad Prism 10 software was used for the experimental data analysis.

8.4 Results and discussion

8.4.1 Effects of galactose acclimation on cell dry mass yield and growth rate

Figure 8.2 shows the five batches of *H. mediterranei* grown with galactose as a substrate at the start and end of the fermentation. Initially, the flasks were opaque white from the salts and galactose sugar added to the media with a faint pink hue from the initial *H. mediterranei* inoculum. All flasks turned pink at the end of the fermentation, signifying that at least some archaea grew on galactose. However, the different batches at the stationary phase showed varying shades of pink. The resultant pink biomass was appreciably paler in the first two batches, where the color was off-white with a slight pink hue. The culture in the second batch visually appeared denser than the first batch, although the colors were similar. The greatest discrepancy in color between consecutive batches was observed between the second and third batches (Figure 8.3). After two generations of growing the culture on galactose, the culture was considerably denser pink, indicating that *H. mediterranei* may have improved cell growth with the galactose substrate. Additionally, the fourth and fifth batches (Figures 8.2d and e) possessed a more vibrant pink color typically observed when the microorganism is grown on glucose or hydrolyzed cheese byproduct substrates. This color difference could be explained by varying cell mass concentrations with the batches and potentially increased carotenoid production by *H. mediterranei* (W. Chen et al., 2015).

The increased pink color observed with successive batches grown with galactose was the first indication that *H. mediterranei* might acclimate to the galactose sugar.

a) 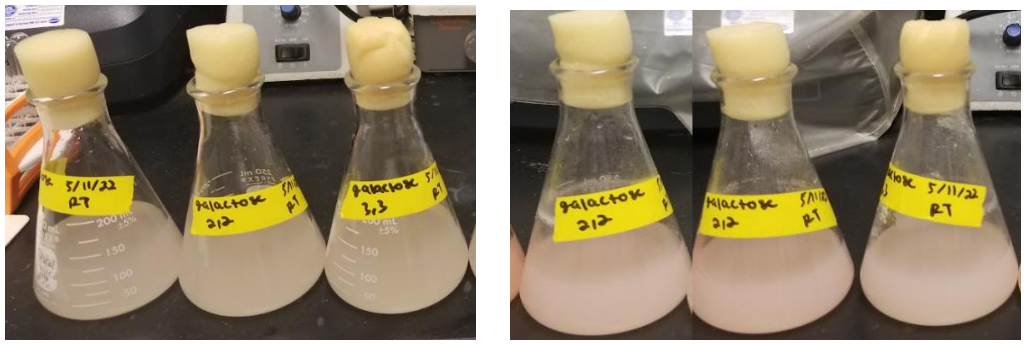

b) 

c) 

d) 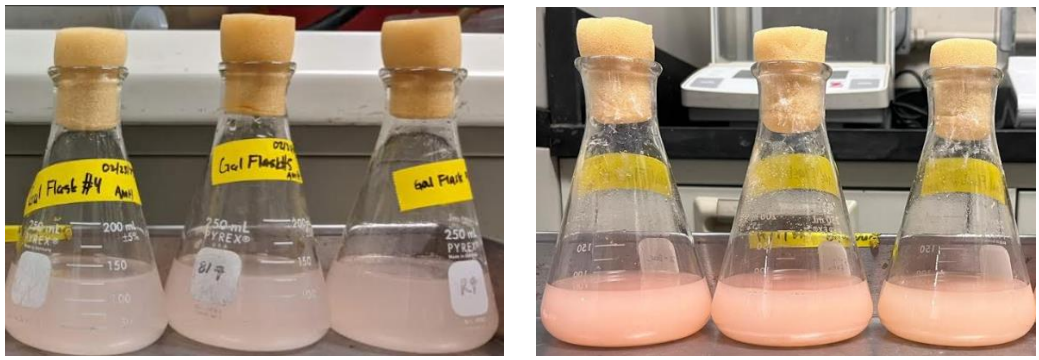

e) 

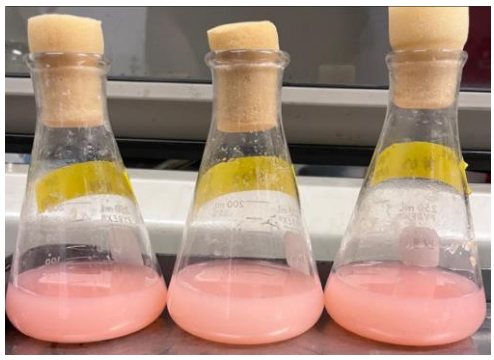

Figure 8.2 Change of the color of *H. mediterranei* grown on galactose for five successive batches: a) first batch; b) second batch; c) third batch; d) fourth batch; e) fifth batch. For the flask triplicates, the left is hour 0, and the right is the end of the fermentation hour 288 for each batch.

Figure 8.3 The color of *H. mediterranei* grown on galactose for two (left) and three (right) successive batches at the end of fermentation after 288 hours for each batch.

Figure 8.4 shows the cell growth time profiles for the five galactose batches as measured by optical density (OD). The first, second, and third batches exhibited a short lag phase during the first 24 hours of growth, but no lag phase was present for the later fourth and fifth batches. The first, second, and third batches then grew at similar growth rates up to 192 hours, with the second and third batches continuing to grow while the first batch reached the stationary phase. The growth rate of the second and third batches continued to be similar for the next 24 hours, from hours 192 to 216. However, after 216 hours, the third batch increased to a higher final OD than the second batch in the next 48 hours of growth. Both the second and third batches reached the stationary phase after 264 hours of growth. The fourth and fifth batches grew at higher rates than the first three batches and possessed similar ODs throughout the fermentation. The fourth and fifth batches reached the stationary phase at 216 hours, earlier than the first three batches. The final ODs of the first four batches increased for each successive batch. The first, second, third, fourth, and fifth batches' final ODs were 3.1 ± 0.1, 4.4 ± 0.1, 5.1 ± 0.1, and 6.1 ± 0.1 g VS/l, respectively. The fifth batch's final OD was almost identical to the fourth at 6.0 ± 0.2. The OD nearly doubled from the first to the fourth and fifth batches, demonstrating that the *H. mediterranei* culture was acclimating to the galactose substrate causing more cell growth.

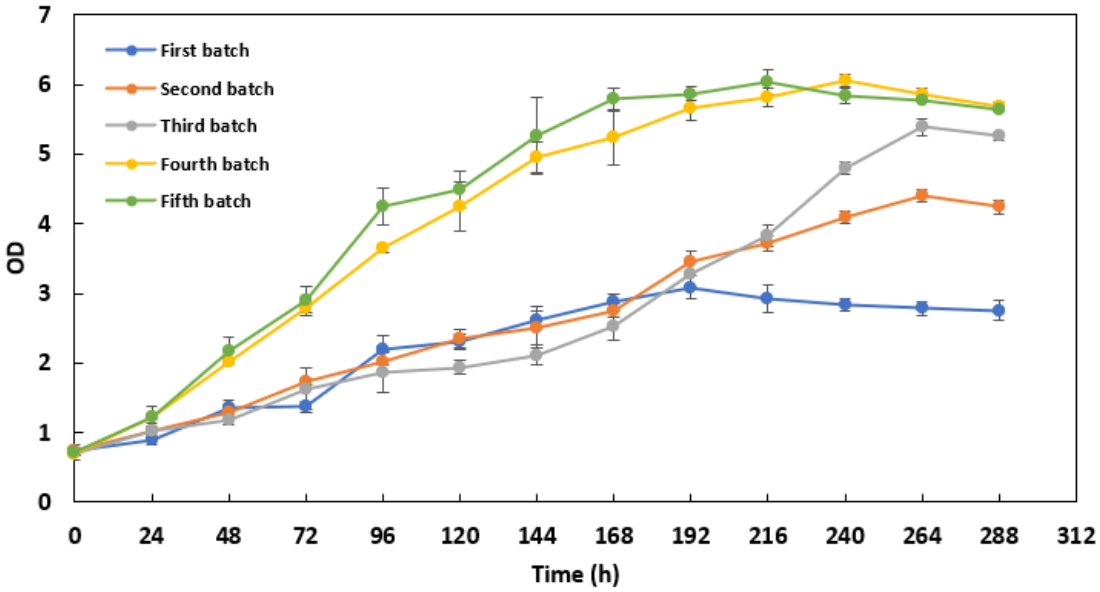

Figure 8.4 Cell growth of *H. mediterranei* over time successively grown with galactose substrate. Y-error bars are standard deviations.

Figure 8.5 displays the final cell dry mass (CDM) concentration and CDM yield for the different galactose batches. The final CDM concentration followed the final OD trend. One-way ANOVA showed that the final CDM concentrations of the five batches were significantly different (p-value < 0.0001), and the CDM yields were also significantly different (p-value = 0.0029). The Tukey test was conducted for further pairwise comparisons of the parameters. The final CDM concentration increased with successive generations, with the first batch, second, third, fourth, and fifth batch at 1.3 ± 0.1, 2.1 ± 0.1, 2.8 ± 0.1, 2.9 ± 0.1, and 3.0 ± 0.3 g VS/l, respectively. However, the difference in final CDM concentration between consecutive batches decreased with each batch. For example, the difference between the first and second batches was the greatest at 0.5 g VS/l and the least for the fourth and fifth batches at 0.1 g VS/l. This result indicated that more galactose acclimation improvements occurred with the earlier batches than with the later batches. Furthermore, the final CDM concentrations of the first and second batches were significantly different (p-value = 0.0033), and the second and third batches were also significantly different

(p-value = 0.0132). However, the third and fourth batches were not significantly (p-value = 0.8853) different; likewise, batches 4 and 5 were not significantly different (p-value = 0.9857). Therefore, it appears that galactose acclimation improved final CDM concentration up to three generations.

The CDM yield had a different trend from that observed for the final CDM concentration. The CDM yield of the first batch was 0.35 ± 0.02 g VS/g galactose, the greatest of the five batches. The first batch's CDM yield was significantly greater (p-value = 0.0279) than the second batch. The last four batches had similar CDM yield values of 0.25-0.28 g VS/g galactose, suggesting that galactose acclimation did not improve CDM yield. The yeast extract in the media may have caused the higher CDM yield in the first batch since the complex nutrient contained 40% carbon. In Chapter 4, yeast extract was demonstrated to result in high *H. mediterranei* CDM yields. Therefore, for the first batch, more of the total CDM may have been derived from yeast extract consumption than galactose leading to an apparent higher CDM yield.

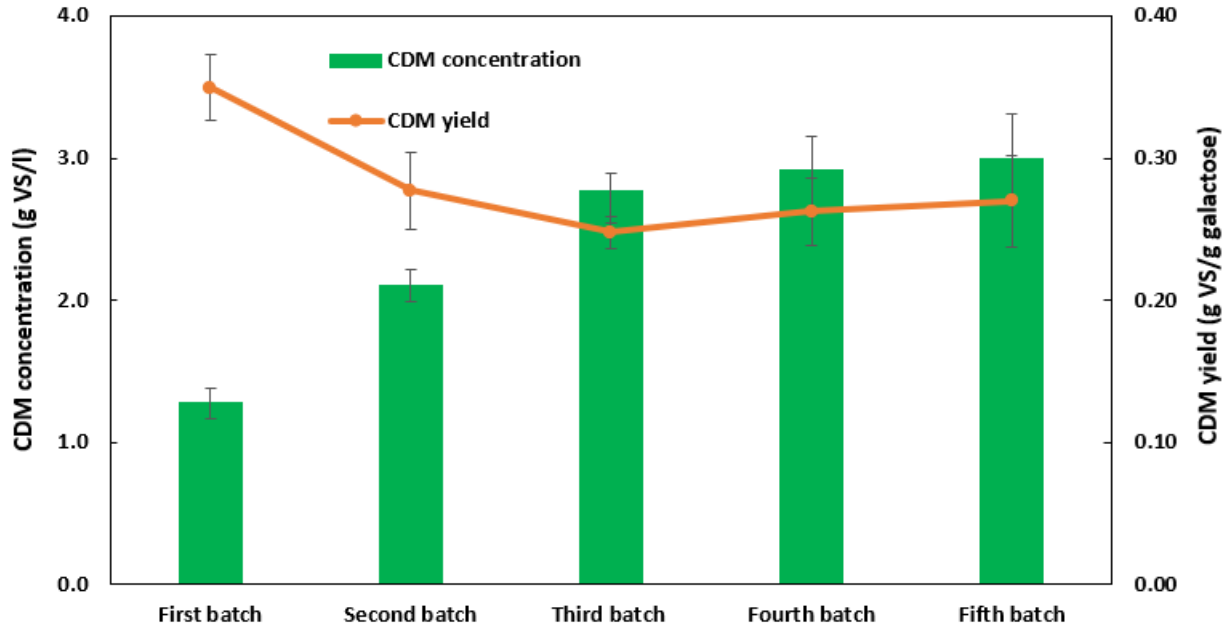

Figure 8.5 Final *H. mediterranei* cell dry mass (CDM) concentration and yield during the successive growth with galactose substrate. Y-error bars are standard deviations.

Figure 8.6 displays the specific growth rates from hours 0 to 96 of the five galactose batches. The specific growth rates followed a different trend than the final CDM concentrations and yields. One-way ANOVA demonstrated that the specific growth rates were significantly different (p-value < 0.0001), and the Tukey test was performed for pairwise comparisons. The growth rate of the first three batches were all near 0.010 h^{-1} and were not significantly different (first and second batches p-value = 0.9964) (second and third batches p value = 0.9964). An increase in the specific growth rate occurred from the third and fourth batches, where the parameter increased from 0.010 ± 0.002 to 0.017 ± 0.000 h^{-1}, and were significantly different (p-value = 0.0002). This result differed from what was found for the final CDM concentrations of the third and fourth batches, which were not significantly different. The fourth and fifth batches were not significantly different (p-value = 0.7275). Therefore, galactose acclimation improved the specific growth rate with 4 subsequent batches grown with the sugar.

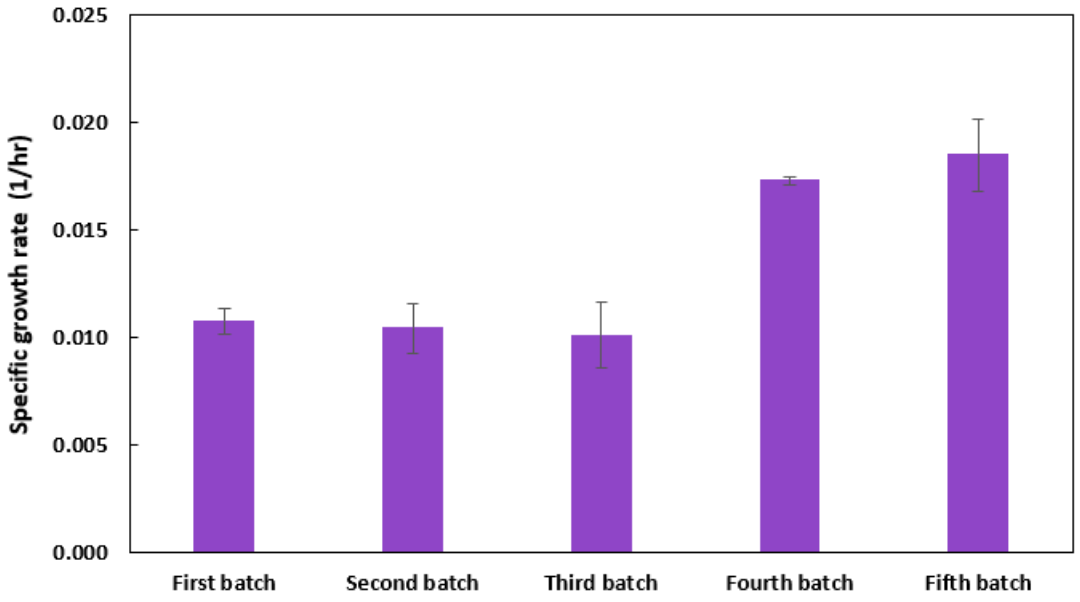

Figure 8.6 Specific growth rate of *H. mediterranei* cell dry mass (CDM) during the successive growth with galactose as a substrate. Y-error bars are standard deviations.

8.4.2 Effects of galactose acclimation on PHA accumulation and yield

Figure 8.7 shows the five galactose batches' final PHA concentrations and yields. One-way ANOVA demonstrated that the PHA concentrations were significantly different (p-value = 0.0002), and the PHA yields were also significantly different (p-value = 0.0004). The Tukey test was conducted for further pairwise comparisons of the parameters. As expected, the final PHA concentrations followed a similar trend as the final CDM concentrations since *H. mediterranei*'s PHA accumulation is growth associated (Cui, Zhang, et al., 2017; Wang & Zhang, 2021). As with the final CDM concentrations, the final PHA concentrations increased with each successive batch. The first, second, third, fourth, and fifth batches' final PHA concentrations were 0.7 ± 0.1, 1.2 ± 0.1, 1.4 ± 0.1, 1.5 ± 0.2, 1.7 ± 0.1 g VS/l, respectively. The greatest improvement in final PHA concentration occurred between the first and second batches, with an increase of 0.5 g VS/l. The final PHA concentration of the first batch was significantly greater (p-value = 0.0141) than in the second batch. A more moderate increase was present for PHA concentration from the second to the fifth batch of 0.5 g VS/l. The second and fourth batches were not significantly different (p = 0.3500). However, the second and fifth batches were significantly different (p-value = 0.0334). Therefore, obtaining statistically significant PHA concentration improvements after the second batch took three additional batches of *H. mediterranei* grown on galactose. Since PHA production did not significantly increase (p-value = 0.1988) from the third and fifth batches, further galactose acclimation was not pursued since it appeared that a plateau had occurred.

The PHA yield followed a different trend from the final PHA concentration but was similar to the CDM yield. The PHA yield was the greatest for the first batch at 0.22 ± 0.01 g VS/g galactose. The second batch's PHA yield was significantly lower (p-value = 0.0438) than the first batch at 0.17 ± 0.01 g VS/g galactose. The second and fifth batches were not significantly different (p-value = 0.7487) and nearly equivalent at approximately 0.16 g VS/g galactose. These results can most likely be explained by the same reason stated for CDM yield, where the effects of the yeast extract may be more pronounced in the first batch with less galactose consumption. The galactose PHA yield was in the range reported by other researchers who studied glucose substrate of 0.07-0.33 g PHA/g glucose. Therefore, *H. mediterranei* can effectively utilize galactose for PHA production.

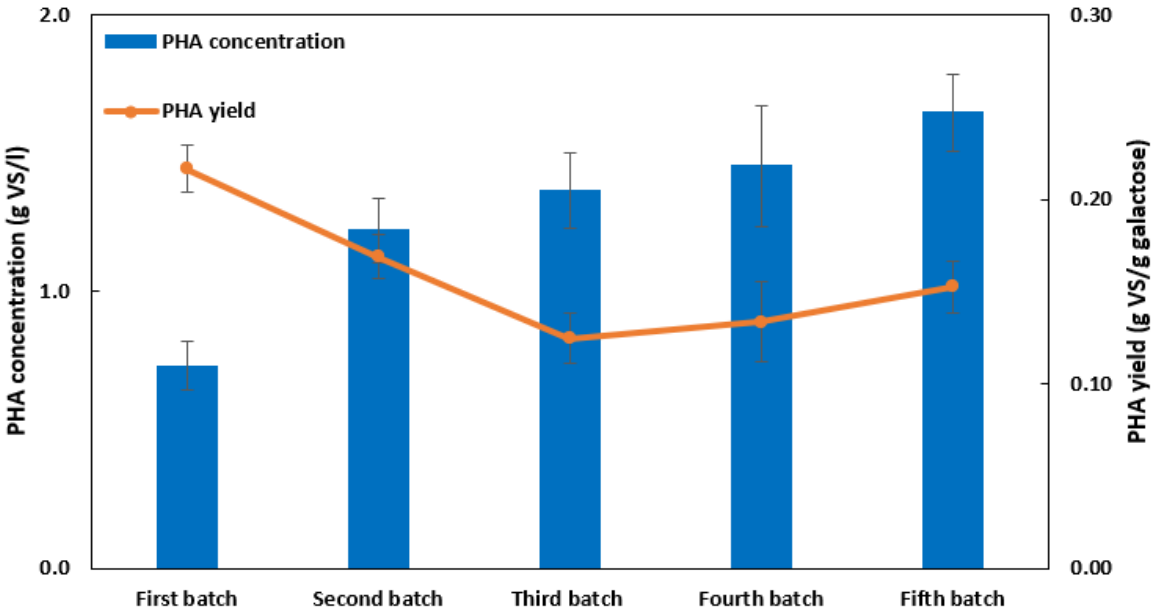

Figure 8.7 Final *H. mediterranei* PHA concentration and yield during the successive growth with galactose as a substrate. Y-error bars are standard deviations.

8.4.3 Effects of galactose acclimation on PHA content

PHA content is an important measurement to observe if the carbon consumed by *H. mediterranei* is diverted towards desirable PHA product compared with residual cell mass. Figure 8.8 shows the PHA content of the galactose acclimated batches. The PHA content followed a different trend from all the other measured parameters. The PHA content did not increase with subsequent batches grown on galactose and was steady between 0.49-0.57 g VS/g VS. One-way ANOVA analysis showed the PHA contents of the five batches were not significantly different (p-value = 0.0562). Therefore, there does not appear to be an improvement in PHA content with galactose acclimation. The PHA contents were on the upper-end range of PHA contents reported by other researchers with sugar-containing substrates 0.13-0.53 g PHA/g CDM (Don et al., 2006; Koller et al., 2007a, 2007b; Lillo & Rodriguez-Valera, 1990; Melanie et al., 2018; Pais et al., 2016), demonstrating that galactose can lead to effective PHA accumulation regardless of galactose acclimation. This result may be due to galactose being metabolized by the same pathways as glucose resulting in similar cell growth and PHA accumulation (Bonete et al., 1996).

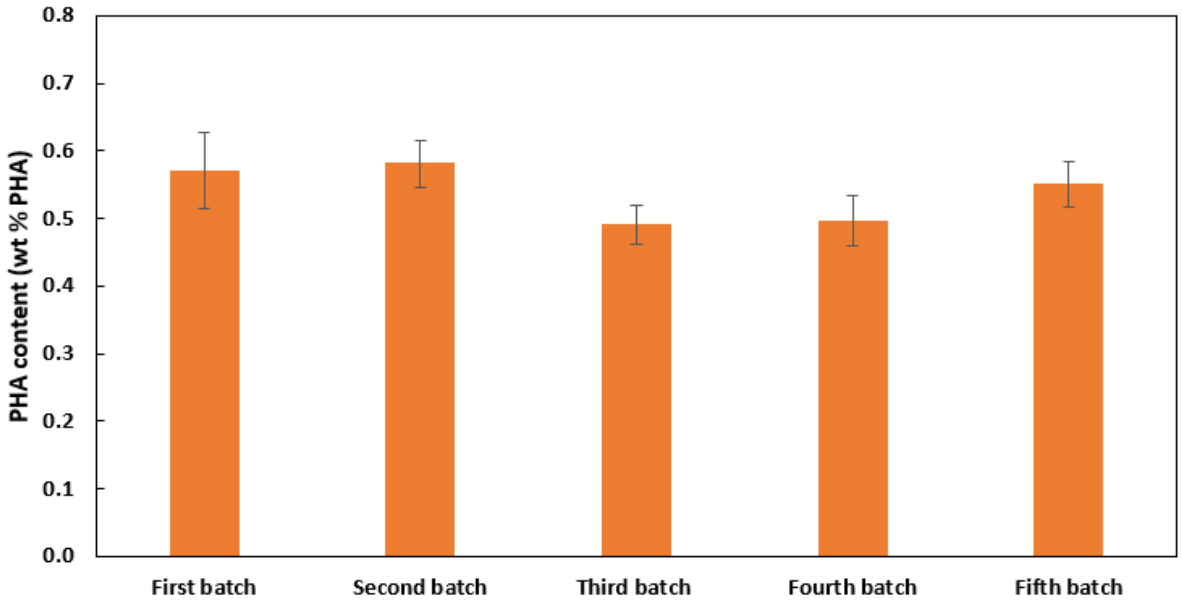

Figure 8.8 *H. mediterranei* PHA content successively grown with galactose substrate. Y-error bars are standard deviations.

8.4.4 Effects of galactose acclimation on galactose consumption

Figure 8.9 displays the galactose consumption for the different galactose acclimated batches. Little galactose consumption occurred for the first batch, inoculated with *H. mediterranei* previously grown on glucose, at 28% ± 3% of the initial galactose loading. Galactose consumption was higher for the second batch than the first at 65% ± 6%. Total galactose consumption occurred at 100% ± 0% for the last three batches. Therefore, these results suggest that substrate acclimation can improve galactose consumption in *H. mediterranei* and, after three generations, can lead to complete galactose consumption.

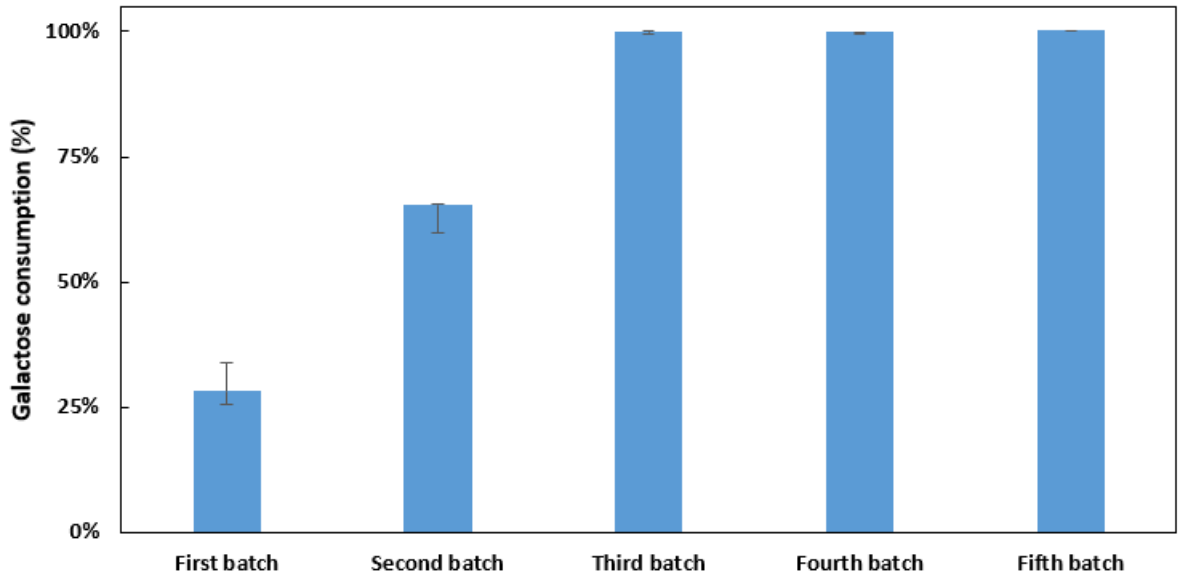

Figure 8.9 Galactose consumption by *H. mediterranei* successively grown with galactose substrate. Y-error bars are standard deviations.

8.5 Conclusions

Hydrolyzed cheese byproducts are one possible low-cost feedstock to convert into valuable PHA bioplastic. One common downside of applying these substrates is potentially lower galactose consumption than glucose leading to reduced yields and more expensive waste treatment processes. Therefore, increasing *H. mediterranei* galactose consumption is vital to improving the economics of utilizing these potential PHA substrates. *H. mediterranei* was acclimated to galactose by successive inoculation of the archaeal culture grown with galactose substrate for five batches. The final CDM concentration significantly increased with three batches, the specific growth rate with four batches, the final PHA concentration with five batches, and the galactose consumption with three batches (total galactose consumption). Further research by others could study if this acclimation technique could be used to improve other aldose sugars that *H. mediterranei's* glucose dehydrogenase enzyme can utilize, e.g., D-Xylose, D-Mannose, D-Fructose, D-Fucose, D-Glucosamine, and D-Ribose. The research can contribute towards making the proposed cheese byproduct to PHA bioplastic economic by increasing PHA production using the acclimated *H. mediterranei* galactose cultures. Further research is needed with hydrolyzed cheese byproducts to realize these potential benefits of galactose acclimated cultures.

Chapter 9. Conclusions and Future Research

Traditional plastics pose significant sustainability challenges due to their dependence on unsustainable petroleum sources, contribution to greenhouse gas emissions, and environmental waste accumulation due to their resistance to biodegradation. To achieve a sustainable future, it is imperative to explore alternative materials and adopt environmentally friendly practices in the production, usage, and disposal of plastics. Bioplastics offer a promising solution for replacing conventional plastics, as they possess key advantages such as biodegradability, net-zero carbon emissions, and a sustainable origin. Polyhydroxyalkanoates (PHA) is one bioplastic that is readily biodegradable and can replace thermoplastics in numerous applications. Although PHA is the fastest-growing bioplastic on the market, production costs, such as expensive feedstocks, limit its future growth unless a cost-effective feedstock can be utilized. Cheesemakers produce low-value byproducts in large quantities with high concentrations of fermentable sugars and other nutrients that could be used as feedstock for PHA production. The research goal was to develop an economic PHA production process utilizing cheese byproducts as a cost-effective feedstock. This research not only helps decrease the production cost of bioplastics but can also reduce the environmental impacts of traditional plastics and help further build a circular economy for the cheese industry.

This study aimed to devise and evaluate efficient and economically viable strategies for producing PHA utilizing cheese byproduct delactosed permeate (DLP). DLP pretreatment with centrifugation and enzymatic hydrolysis was established and optimized before the fermentation of the feedstock into PHA. *Haloferax mediterranei* (*H. mediterranei)* was used as the PHA producer and was demonstrated to give high PHA yields utilizing hydrolyzed DLP feedstock compared to other commonly studied sugar substrates such as glucose. Nitrogen source supplementation was further optimized to reduce PHA production costs while obtaining high PHA yields. The best feeding strategies of hydrolyzed DLP were established for PHA

production with *H. mediterranei*. Cheese byproduct, whey permeate, was also studied to assess the differences that may exist between the two comparable feedstocks. An acclimation technique was developed to increase the PHA yield with galactose sugar. The conclusions of the study are stated in the following sections.

9.1 Conclusions

9.1.1 Polyhydroxyalkanoate production by extreme halophile archaea *Haloferax mediterranei* using hydrolyzed delactosed permeate and synthetic sugar media

Centrifugation pretreatment of DLP was demonstrated to improve lactase hydrolysis efficiency and cell growth of *H. mediterranei* archaea. Lactase enzyme achieved a lactose hydrolysis efficiency of 92.5% at a loading of 0.025 g lactase/g lactose and shaking incubation at 40 ℃ for 12 hours with the centrifuged DLP. The centrifugation pretreatment and determined lactase hydrolysis loading, temperature, and timing were selected and applied in further studies. Hydrolyzed DLP was used as a feedstock for *H. mediterranei* and PHA production for the first time. Using hydrolyzed DLP as a feedstock, the archaea could give high PHA yields of 0.33 ± 0.01 g VS/g total sugar that exceeded yields obtained with glucose synthetic media. However, low galactose consumption by *H. mediterranei* was observed to decrease PHA production with this substrate. The study could help to commercialize the cheese byproduct PHA process, increase the global PHA production capacity, grow the dairy market, and improve sustainability in the dairy and plastic industries.

9.1.2 Effect of organic and inorganic nitrogen source on polyhydroxyalkanoates yields using delactosed permeate by extreme halophile archaea *Haloferax mediterranei*

Three hydrolyzed DLP media were tested in batch flask reactors supplemented with 5 g/l yeast extract, ammonium chloride, or an equal nitrogen loading of yeast extract and ammonium chloride. The

feedstock supplemented with ammonium chloride resulted in the highest PHA yield of 0.34 ± 0.03 g VS/g total sugar. The media containing ammonium chloride also gave the lowest PHA production costs of the feedstocks studied, approximately 8 times less than the sole yeast extract and 5 times less than the yeast extract and ammonium chloride nitrogen sources. Therefore, the ammonium chloride nitrogen source was selected for further studies.

9.1.3 Batch *H. mediterranei* and PHA production with hydrolyzed DLP and whey permeate

Hydrolyzed cheese byproducts, DLP and whey permeate, were tested at 4 different loadings of 10, 20, 30, and 40 g total sugar/l to determine the maximum substrate loading before inhibition occurred. The maximum loading for the hydrolyzed DLP and whey permeate were 10 and 30 g total sugar/l, respectively. The difference in maximum loading of the two hydrolyzed cheese byproducts indicated that inhibitory compounds were present at higher concentrations in the DLP compared to the whey permeate. It was postulated that high-heat reaction products that form during whey permeate processing to lactose powder and DLP, such as Maillard products, were potentially the cause since these compounds are inhibitory to other organisms. The maximum specific growth rate for *H. mediterranei* with hydrolyzed DLP and whey permeate were estimated and found to be similar for the two byproducts. These findings could assist in developing large-scale PHA production facilities utilizing cheese byproduct substrate.

9.1.4 Fed-batch *H. mediterranei* and PHA production using hydrolyzed delactosed permeate (DLP) and whey permeate

Fed-batch feeding of hydrolyzed DLP and whey permeate was conducted at a feeding rate of 10 g total sugar/l every 4 days to reduce substrate inhibition. A 50% increase in the final PHA concentration of the hydrolyzed DLP was achieved with the fed-batch operation and two feedings than with the single batch feeding due to the ability to load additional sugars. However, inhibition occurred past the first two

feedings, as indicated by a decline in the cell growth of the culture. The PHA production with hydrolyzed whey permeate increased with the first three feedings, resulting in a 20% increase in final PHA concentration compared to a single batch feeding of equivalent sugars. This difference was potentially due to reduced substrate inhibition effects and more favorable conditions for PHA accumulation with the fed-batch feeding. The hydrolyzed whey permeate fed-batch culture was not inhibited with further feedings like that fed with hydrolyzed DLP. This result further assured the findings of the batch reactor regarding the differences in substrate inhibition between the two cheese byproducts.

9.1.5 Continuous *H. mediterranei* and PHA production using hydrolyzed DLP

A continuous stirred tank reactor (CSTR) was operated feeding hydrolyzed DLP at two hydraulic retention times (HRT), 10 and 20 days. The 10-day HRT CSTR was operated at an organic loading rate (OLR) of 2.5 g total sugar/l/day, and the 20-day HRT CSTR was operated at OLRs of 1.25-2 g total sugar/l/day. The 10-day HRT CSTR initially gave comparable PHA yields to that of the batch and fed-batch operation. However, the reactor became unstable after 22 days of operation, potentially due to substrate inhibition. The 20-day HRT CSTR resulted in a stable culture for 130 days, but the PHA yields were low < 0.10 g VS/g total sugar and declined over time of operating the bioreactor. Therefore, continuous feeding of hydrolyzed DLP for PHA production with *H. mediterranei* was not recommended at these HRTs and substrate loadings.

9.1.6 Acclimation to galactose by *Haloferax mediterranei* for increased cell mass growth and PHA production

An acclimation technique was developed to increase the robustness of *H. mediterranei* archaea and PHA production with galactose substrate. The archaea was cultivated with galactose substrate for five consecutive batches to observe if galactose acclimation would occur. The final cell dry mass (CDM)

concentration of *H. mediterranei* significantly increased with three batches, the specific growth rate with four batches, the final PHA concentration with five batches, and the galactose consumption with three batches (total galactose consumption), indicating successful galactose acclimation had occurred. The research can potentially lead to improved PHA yields with galactose-containing feedstocks such as hydrolyzed cheese byproducts.

9.2 Future research

9.2.1 Identification of the cause of *H. mediterranei* substrate inhibition with hydrolyzed DLP feedstock

Hydrolyzed DLP inhibition was considerably greater than with the hydrolyzed whey permeate substrate for *H. mediterranei* in batch and fed-batch reactors. Additionally, continuous feeding of hydrolyzed DLP also showed apparent substrate inhibition. High-heat reaction products from processing whey permeate into lactose powder and hydrolyzed DLP was suggested as the potential cause, but further research is needed to prove this claim. Once the inhibitory compounds are identified, additional research should be conducted to develop a method to remove the source of inhibition and increase PHA yield with hydrolyzed DLP.

9.2.2 Testing hydrolyzed whey permeate with higher loadings with fed-batch or continuous feeding

Less inhibition was observed with hydrolyzed whey permeate in the batch and the fed-batch reactors. The hydrolyzed whey permeate fed-batch culture remained stable for 26 days with consistent PHA production. Therefore, higher loadings of hydrolyzed DLP could be applied with fed-batch reactor operation, resulting in greater cell densities. However, there would be a limit to this substrate loading, like what was observed with the batch loading experiment, and this maximum fed-batch loading should also be determined. Although continuous feeding resulted in low PHA yields with hydrolyzed DLP, whey permeate may allow shorter hydraulic retention times and improved yields due to less substrate

inhibition. Therefore, further research is needed with continuous feeding of whey permeate to determine if improved PHA production can occur.

9.2.3 Applying the galactose acclimated culture to hydrolyzed cheese byproduct feedstocks

Galactose acclimated *H. mediterranei* cultures, grown successively with the galactose substrate for 3-5 generations, should be studied with hydrolyzed cheese byproducts to observe if improvements in PHA yields can occur with these feedstocks. It needs to be determined if the galactose acclimated cultures will continue to consume galactose when glucose and galactose are both present or if glucose is the preferred sugar. Different inoculation strategies could be studied, including inoculating with standard glucose grown culture and the galactose acclimated culture to observe if both sugars can be consumed simultaneously. Alternatively, the galactose acclimated culture could be added later in the fermentation after all the glucose has been consumed to grow on the remaining galactose. These studies could lead to higher PHA production with hydrolyzed cheese byproducts and complete sugar consumption.

9.2.4 Alternative metabolic routes for lactose conversion to PHA

Enzymatic hydrolysis was utilized in this study to convert the lactose in cheese byproducts into glucose and galactose sugars that *H. mediterranei* can consume. Alternative routes exist to convert lactose into a carbon source that *H. mediterranei* can readily consume to eliminate lactase enzyme production costs. One route is the conversion of cheese byproduct lactose into lactic acid with a pre-fermentation step. The literature review showed that whey permeate, and DLP can be fermented with high yields into lactic acid that *H. mediterranei* can consume to produce PHA. However, to my knowledge, no research has integrated the two processes. Similarly, the cheese byproducts could be anaerobically digested, potentially with other food wastes, generating organic acids to produce PHA. Alternatively, metabolic engineering could be applied to allow *H. mediterranei* to grow and produce PHA directly from lactose

bypassing the pretreatment step. The alternative pathways of PHA production with *H. mediterranei* and cheese byproducts should be assessed with economic modeling to determine which mode offers the greatest economic return.

9.2.5 Life cycle assessment of the proposed cheese byproduct PHA process

The study focused on developing the fermentation process of cheese byproducts to PHA and did not evaluate the potential environmental benefits of the proposed method. A life cycle assessment (LCA) is needed to show the potential carbon emission benefits compared to traditional plastics and other bioplastics. The energy use of the proposed process would also need to be estimated to understand the carbon emissions associated with electrical and heating demands. The LCA should examine the carbon emission differences between DLP and whey permeate feedstocks, how the byproducts are currently disposed of, e.g., sold as animal feed, processed with a waste treatment system, or landfilled, and the end-of-life of the bioplastic, e.g., composted, anaerobically digested, or landfilled. The carbon emissions associated with the production of PHA from cheese byproducts should be compared to similar conventional plastics such as high-density polypropylene (HDPE) and common bioplastics such as polylactic acid (PLA).

References

Abbasi, M., Pokhrel, D., Coats, E. R., Guho, N. M., & McDonald, A. G. (2022). Effect of 3-Hydroxyvalerate Content on Thermal, Mechanical, and Rheological Properties of Poly(3-hydroxybutyrate-co-3-hydroxyvalerate) Biopolymers Produced from Fermented Dairy Manure. *Polymers*, *14*(19), Article 19. https://doi.org/10.3390/polym14194140

Abbott, S. (2010). Chemical Compatibility of Poly(Lactic Acid): A Practical Framework Using Hansen Solubility Parameters. In *Poly(Lactic Acid)* (pp. 83–95). John Wiley & Sons, Ltd. https://doi.org/10.1002/9780470649848.ch7

Ahn, W. S., Park, S. J., & Lee, S. Y. (2001). Production of poly(3-hydroxybutyrate) from whey by cell recycle fed-batch culture of recombinant Escherichia coli. *Biotechnology Letters*, *23*(3), 235–240. https://doi.org/10.1023/A:1005633418161

Al-Battashi, H. S., Annamalai, N., Sivakumar, N., Al-Bahry, S., Tripathi, B. N., Nguyen, Q. D., & Gupta, V. K. (2019). Lignocellulosic biomass (LCB): A potential alternative biorefinery feedstock for polyhydroxyalkanoates production. *Reviews in Environmental Science and Bio/Technology*, *18*(1), 183–205. https://doi.org/10.1007/s11157-018-09488-4

Albuquerque, M. G. E., Eiroa, M., Torres, C., Nunes, B. R., & Reis, M. A. M. (2007). Strategies for the development of a side stream process for polyhydroxyalkanoate (PHA) production from sugar cane molasses. *Journal of Biotechnology*, *130*(4), 411–421. https://doi.org/10.1016/j.jbiotec.2007.05.011

Alexander, P. (2018, November 28). One in six pints of milk thrown away each year, study shows. *The Guardian*. https://www.theguardian.com/environment/2018/nov/28/one-in-six-pints-of-milk-thrown-away-each-year-study-shows

Alibaba a. (2023). *Bulk Sugar Price—Alibaba.com*. https://www.alibaba.com/showroom/bulk-sugar-price.html

Alibaba b. (2023). *Best Price Industry Grade 99.5% Ammonium Chloride—Buy Price Of Ammonium Chloride,Dodecyl Dimethyl Benzyl Ammonium Chloride,Octyl Decyl Dimethyl Ammonium Chloride Product on Alibaba.com*. https://www.alibaba.com/product-detail/Ammonium-Chloride-Chloride-Ammonium-Chloride-Industrial_1600110918463.html?spm=a2700.galleryofferlist.normal_offer.d_image.b809fe5fC6wvax&s=p

Alibaba c. (2023). *Ammonium Sulfate for Fertilizer in Bulk—Alibaba.com*. https://www.alibaba.com/showroom/ammonium-sulfate.html

Almutairi, F. M., Monier, M., Alatawi, R. A. S., Alhawiti, A. S., Al-Rasheed, H. H., Almutairi, T. M., & Elsayed, N. H. (2022). Synthesis of photo-crosslinkable hydrogel membranes for entrapment of lactase enzyme. *Reactive and Functional Polymers*, *172*, 105159. https://doi.org/10.1016/j.reactfunctpolym.2022.105159

Alsafadi, D., & Al-Mashaqbeh, O. (2017). A one-stage cultivation process for the production of poly-3-(hydroxybutyrate-co-hydroxyvalerate) from olive mill wastewater by Haloferax mediterranei. *New Biotechnology*, *34*, 47–53. https://doi.org/10.1016/j.nbt.2016.05.003

Alsafadi, D., Al-Mashaqbeh, O., Mansour, A., & Alsaad, M. (2020). Optimization of nitrogen source supply for enhanced biosynthesis and quality of poly(3-hydroxybutyrate-co-3-hydroxyvalerate) by extremely halophilic archaeon Haloferax mediterranei. *MicrobiologyOpen*, *9*(8), e1055. https://doi.org/10.1002/mbo3.1055

Alsafadi, D., Ibrahim, M. I., Alamry, K. A., Hussein, M. A., & Mansour, A. (2020). Utilizing the crop waste of date palm fruit to biosynthesize polyhydroxyalkanoate bioplastics with favorable properties. *Science of The Total Environment*, *737*, 139716. https://doi.org/10.1016/j.scitotenv.2020.139716

Amaro, T. M. M. M., Rosa, D., Comi, G., & Iacumin, L. (2019). Prospects for the Use of Whey for Polyhydroxyalkanoate (PHA) Production. *Frontiers in Microbiology*, *10*. https://doi.org/10.3389/fmicb.2019.00992

American Public Health Association. (2012). *APHA, AWWA, WEF. Standard Methods for examination of water and wastewater.* (22nd ed.).

Anderson, A. J., & Dawes, E. A. (1990). Occurrence, metabolism, metabolic role, and industrial uses of bacterial polyhydroxyalkanoates. *Microbiological Reviews*, *54*(4), 450–472.

ATCC. (2022). *Haloferax mediterranei (Rodriguez-Valera et al.) Torreblanca et al. - 33500 | ATCC*. https://www.atcc.org/products/33500

Axelsson, H. (2010). Cell Separation, Centrifugation. In *Encyclopedia of Industrial Biotechnology* (pp. 1–21). American Cancer Society. https://doi.org/10.1002/9780470054581.eib203

Benavides, P. T., Lee, U., & Zarè-Mehrjerdi, O. (2020). Life cycle greenhouse gas emissions and energy use of polylactic acid, bio-derived polyethylene, and fossil-derived polyethylene. *Journal of Cleaner Production*, *277*, 124010. https://doi.org/10.1016/j.jclepro.2020.124010

Bernard, M. (2014). Industrial Potential of Polyhydroxyalkanoate Bioplastic: A Brief Review. *USURJ: University of Saskatchewan Undergraduate Research Journal*, *1*(1). https://doi.org/10.32396/usurj.v1i1.55

Berwig, K. H., Baldasso, C., & Dettmer, A. (2016). Production and characterization of poly(3-hydroxybutyrate) generated by Alcaligenes latus using lactose and whey after acid protein precipitation process. *Bioresource Technology*, *218*, 31–37. https://doi.org/10.1016/j.biortech.2016.06.067

Beucler, J., Drake, M., & Foegeding, E. A. (2005). Design of a Beverage from Whey Permeate. *Journal of Food Science*, *70*(4), S277–S285. https://doi.org/10.1111/j.1365-2621.2005.tb07203.x

Bhattacharyya, A., Saha, J., Haldar, S., Bhowmic, A., Mukhopadhyay, U. K., & Mukherjee, J. (2014). Production of poly-3-(hydroxybutyrate-co-hydroxyvalerate) by Haloferax mediterranei using rice-based ethanol stillage with simultaneous recovery and re-use of medium salts. *Extremophiles: Life Under Extreme Conditions*, *18*(2), 463–470. https://doi.org/10.1007/s00792-013-0622-9

Bomgardner, M. (2012, January 23). *Bioplastics Venture Is Off*. Chemical & Engineering News. https://cen.acs.org/articles/90/i4/Bioplastics-Venture-Off.html

Bonete, M.-J., Pire, C., Llorca, F. I., & Camacho, M. L. (1996). Glucose dehydrogenase from the halophilic Archaeon Haloferax mediterranei: Enzyme purification, characterisation and N-terminal sequence. *FEBS Letters*, *383*(3), 227–229. https://doi.org/10.1016/0014-5793(96)00235-9

Božanić, R., Barukčić, I., Lisak Jakopović, K., & Tratnik, L. (2014). Possibilities of Whey Utilisation. *Austin Journal of Nutrition and Food Science*, *2*.

Braunegg, G., Lefebvre, G., Renner, G., Zeiser, A., Haage, G., & Loidl-Lanthaler, K. (1995). Kinetics as a tool for polyhydroxyalkanoate production optimization. *Canadian Journal of Microbiology*, *41*(13), 239–248. https://doi.org/10.1139/m95-192

Bugnicourt, E., Cinelli, P., Lazzeri, A., & Alvarez, V. (2014). Polyhydroxyalkanoate (PHA): Review of synthesis, characteristics, processing and potential applications in packaging. *Express Polymer Letters*, *8*(11), 791–808. https://doi.org/10.3144/expresspolymlett.2014.82

Burrington, K., Schoenfuss, T., & Patel, S. (2014). *Technical Report: Coproducts of Milk and Whey Processing*. U.S. Dairy Export Council. https://www.usdairy.com/getmedia/96025c6a-f357-46ba-9be8-435f6450590b/coproducts%20milk%20report.pdf

Byrom, D. (1987). Polymer synthesis by microorganisms: Technology and economics. *Trends in Biotechnology*, *5*(9), 246–250. https://doi.org/10.1016/0167-7799(87)90100-4

Byylund, G. (2015, May 15). *WHEY PROCESSING*. Tetra Pak Dairy Processing Handbook. https://dairyprocessinghandbook.tetrapak.com/chapter/whey-processing

Calil, M., Fassina, C., & Rosa, D. (2021). Biodegradation behavior of PHBV films in a pilot-scale composting condition. *Mater Sci Eng*, *24*, 659–662.

Calo, P., de Miguel, T., Sieiro, C., Velazquez, J. b., & Villa, T. g. (1995). Ketocarotenoids in halobacteria: 3-hydroxy-echinenone and trans-astaxanthin. *Journal of Applied Bacteriology*, *79*(3), 282–285. https://doi.org/10.1111/j.1365-2672.1995.tb03138.x

Cao, X., & Harris, W. (2008). Carbonate and Magnesium Interactive Effect on Calcium Phosphate Precipitation. *Environmental Science & Technology*, *42*(2), 436–442. https://doi.org/10.1021/es0716709

Carbery, M., O'Connor, W., & Palanisami, T. (2018). Trophic transfer of microplastics and mixed contaminants in the marine food web and implications for human health. *Environment International*, *115*, 400–409. https://doi.org/10.1016/j.envint.2018.03.007

Chavan, S., Yadav, B., Tyagi, R. D., & Drogui, P. (2021). A review on production of polyhydroxyalkanoate (PHA) biopolyesters by thermophilic microbes using waste feedstocks. *Bioresource Technology*, *341*, 125900. https://doi.org/10.1016/j.biortech.2021.125900

Chen, G.-Q. (2009). A microbial polyhydroxyalkanoates (PHA) based bio- and materials industry. *Chemical Society Reviews*, *38*(8), 2434–2446. https://doi.org/10.1039/B812677C

Chen, W., Hsu, S., Lin, M.-T., & Hsu, Y. (2015). Mass production of C50 carotenoids by Haloferax mediterranei in using extruded rice bran and starch under optimal conductivity of brined medium. *Bioprocess and Biosystems Engineering*, *38*(12), 2361–2367. https://doi.org/10.1007/s00449-015-1471-y

Chen, Y., Cheng, J. J., & Creamer, K. S. (2008). Inhibition of anaerobic digestion process: A review. *Bioresource Technology*, *99*(10), 4044–4064. https://doi.org/10.1016/j.biortech.2007.01.057

Cho, H., Ra, C.-H., & Kim, S.-K. (2014). Ethanol Production from the Seaweed Gelidium amansii, Using Specific Sugar Acclimated Yeasts. *Journal of Microbiology and Biotechnology*, *24*(2), 264–269. https://doi.org/10.4014/jmb.1307.07054

Colombo, B., Pepè Sciarria, T., Reis, M., Scaglia, B., & Adani, F. (2016). Polyhydroxyalkanoates (PHAs) production from fermented cheese whey by using a mixed microbial culture. *Bioresource Technology*, *218*, 692–699. https://doi.org/10.1016/j.biortech.2016.07.024

Cózar, A., Echevarría, F., González-Gordillo, J. I., Irigoien, X., Úbeda, B., Hernández-León, S., Palma, Á. T., Navarro, S., García-de-Lomas, J., Ruiz, A., Fernández-de-Puelles, M. L., & Duarte, C. M. (2014). Plastic debris in the open ocean. *Proceedings of the National Academy of Sciences*, *111*(28), 10239. https://doi.org/10.1073/pnas.1314705111

Cui, Y.-W. (2017). Salinity effect on production of PHA and EPS by Haloferax mediterranei. *RSC Advances*, 9.

Cui, Y.-W., Shi, Y.-P., & Gong, X.-Y. (2017). Effects of C/N in the substrate on the simultaneous production of polyhydroxyalkanoates and extracellular polymeric substances by Haloferax mediterranei via kinetic model analysis. *RSC Advances*, *7*(31), 18953–18961. https://doi.org/10.1039/C7RA02131C

Cui, Y.-W., Zhang, H.-Y., Ji, S.-Y., & Wang, Z.-W. (2017). Kinetic Analysis of the Temperature Effect on Polyhydroxyalkanoate Production by Haloferax mediterranei in Synthetic Molasses Wastewater. *Journal of Polymers and the Environment*, *25*(2), 277–285. https://doi.org/10.1007/s10924-016-0807-2

Dahlqvist, A., Asp, N.-G., Burvall, A., & Rausing, H. (1977). Hydrolysis of lactose in milk and whey with minute amounts of lactase. *Journal of Dairy Research*, *44*(3), 541–548. https://doi.org/10.1017/S0022029900020495

Dam, B. V., Revallier-warffemius, J. G., & Dam-schermerhorn, L. C. V. (1950). Preparation of lactase from Saccharomyces fragilis. *Nederlandsch Melk- en Zuiveltijdschrift*, *4*(2), 96–114.

Dietrich, K., Dumont, M.-J., Del Rio, L. F., & Orsat, V. (2017). Producing PHAs in the bioeconomy—Towards a sustainable bioplastic. *Sustainable Production and Consumption*, *9*, 58–70. https://doi.org/10.1016/j.spc.2016.09.001

Dilkes-Hoffman, L. S., Lane, J. L., Grant, T., Pratt, S., Lant, P. A., & Laycock, B. (2018). Environmental impact of biodegradable food packaging when considering food waste. *Journal of Cleaner Production*, *180*, 325–334. https://doi.org/10.1016/j.jclepro.2018.01.169

Dionisi, D., Carucci, G., Papini, M. P., Riccardi, C., Majone, M., & Carrasco, F. (2005). Olive oil mill effluents as a feedstock for production of biodegradable polymers. *Water Research*, *39*(10), 2076–2084. https://doi.org/10.1016/j.watres.2005.03.011

Dobroth, Z. T., Hu, S., Coats, E. R., & McDonald, A. G. (2011). Polyhydroxybutyrate synthesis on biodiesel wastewater using mixed microbial consortia. *Bioresource Technology*, *102*(3), 3352–3359. https://doi.org/10.1016/j.biortech.2010.11.053

Don, T.-M., Chen, C. W., & Chan, T.-H. (2006). Preparation and characterization of poly(hydroxyalkanoate) from the fermentation of Haloferax mediterranei. *Journal of Biomaterials Science, Polymer Edition*, *17*(12), 1425–1438. https://doi.org/10.1163/156856206778937208

Dosuky, A. S., Nasr, F. N., Yousef, E. T. A., & Barakat, O. S. (2019). BIO-PRODUCTION OF LACTIC ACID FROM SALTED WHEY AND WHEY PERMEATE. *Plant Archives*, *Vol. 19,*(Supplement 2), 793–798.

Einarsson, H., & Eklund, T. (1988). Inhibitory mechanisms of Maillard reaction products. *Microbios*, *53*, 27–36.

Einarsson, H., Snygg, B. G., & Eriksson, C. (1983). Inhibition of bacterial growth by Maillard reaction products. *Journal of Agricultural and Food Chemistry*, *31*(5), 1043–1047. https://doi.org/10.1021/jf00119a031

Escalona, A. M., Varela, F. R., & Gomis, A. M. (1996). *Procedure for extraction of polyhydroxyalkanoates from halophilic bacteria which contain them* (United States Patent US5536419A). https://patents.google.com/patent/US5536419A/en

Esclapez, J., Bravo-Barrales, G., Bautista, V., Pire, C., Camacho, M., & Bonete, M. J. (2014). Effects of nitrogen sources on the nitrate assimilation in Haloferax mediterranei: Growth kinetics and transcriptomic analysis. *FEMS Microbiology Letters*, *350*(2), 168–174. https://doi.org/10.1111/1574-6968.12325

European Bioplastics. (2021). Market. *European Bioplastics e.V.* https://www.european-bioplastics.org/market/

European Bioplastics. (2023). Market. *European Bioplastics e.V.* https://www.european-bioplastics.org/market/

Fang, C.-J., Ku, K.-L., Lee, M.-H., & Su, N.-W. (2010). Influence of nutritive factors on C50 carotenoids production by Haloferax mediterranei ATCC 33500 with two-stage cultivation. *Bioresource Technology*, *101*(16), 6487–6493. https://doi.org/10.1016/j.biortech.2010.03.044

Ferre-Guell, A., & Winterburn, J. (2018). Biosynthesis and Characterization of Polyhydroxyalkanoates with Controlled Composition and Microstructure. *Biomacromolecules*, *19*(3), 996–1005. https://doi.org/10.1021/acs.biomac.7b01788

Finocchiaro, T., Olson, N. F., & Richardson, T. (1980). Use of immobilized lactase in milk systems. *Advances in Biochemical Engineering, Volume 15*, 71–88. https://doi.org/10.1007/3540096868_3

Fox, P. F. (Ed.). (1997). *Advanced Dairy Chemistry Volume 3: Lactose, water, salts and vitamins*. Springer US. https://doi.org/10.1007/978-1-4757-4409-5

Fradinho, J. C., Oehmen, A., & Reis, M. A. M. (2014). Photosynthetic mixed culture polyhydroxyalkanoate (PHA) production from individual and mixed volatile fatty acids (VFAs): Substrate preferences and co-substrate uptake. *Journal of Biotechnology*, *185*, 19–27. https://doi.org/10.1016/j.jbiotec.2014.05.035

Fradinho, J., Reis, M., & Oehmen, A. (2016). Beyond feast and famine: Selecting a PHA accumulating photosynthetic mixed culture in a permanent feast regime. *Water Research*, *105*. https://doi.org/10.1016/j.watres.2016.09.022

Gänzle, M. G., Haase, G., & Jelen, P. (2008). Lactose: Crystallization, hydrolysis and value-added derivatives. *International Dairy Journal*, *18*(7), 685–694. https://doi.org/10.1016/j.idairyj.2008.03.003

Geyer, R., Jambeck, J. R., & Law, K. L. (2017). Production, use, and fate of all plastics ever made. *Science Advances*, *3*(7), e1700782. https://doi.org/10.1126/sciadv.1700782

Ghaly, A. E., & Kamal, M. A. (2004). Submerged yeast fermentation of acid cheese whey for protein production and pollution potential reduction. *Water Research*, *38*(3), 631–644. https://doi.org/10.1016/j.watres.2003.10.019

Ghosh, S., Gnaim, R., Greiserman, S., Fadeev, L., Gozin, M., & Golberg, A. (2019). Macroalgal biomass subcritical hydrolysates for the production of polyhydroxyalkanoate (PHA) by Haloferax mediterranei. *Bioresource Technology*, *271*, 166–173. https://doi.org/10.1016/j.biortech.2018.09.108

Guo, Q., & Crittenden, J. C. (2011). An energy analysis of polylactic acid (PLA) produced from corn grain and corn stover integrated system. *Proceedings of the 2011 IEEE International Symposium on Sustainable Systems and Technology*, 1–5. https://doi.org/10.1109/ISSST.2011.5936897

Han, J., Hou, J., Zhang, F., Ai, G., Li, M., Cai, S., Liu, H., Wang, L., Wang, Z., Zhang, S., Cai, L., Zhao, D., Zhou, J., & Xiang, H. (2013). Multiple Propionyl Coenzyme A-Supplying Pathways for Production of the Bioplastic Poly(3-Hydroxybutyrate-co-3-Hydroxyvalerate) in Haloferax mediterranei. *Applied and Environmental Microbiology*, *79*(9), 2922–2931. https://doi.org/10.1128/AEM.03915-12

Harju, M., Kallioinen, H., & Tossavainen, O. (2012). Lactose hydrolysis and other conversions in dairy products: Technological aspects. *International Dairy Journal*, *22*(2), 104–109. https://doi.org/10.1016/j.idairyj.2011.09.011

Hegde, S., Diaz, C. A., Dell, E. M., Trabold, T. A., & Lewis, C. L. (2021a). Investigation of process parameters on the anaerobic digestion of a poly(hydroxyalkonate) film. *European Polymer Journal*, *148*, 110349. https://doi.org/10.1016/j.eurpolymj.2021.110349

Holmes, P. A. (1985). Applications of PHB - a microbially produced biodegradable thermoplastic. *Physics in Technology*, *16*(1), 32. https://doi.org/10.1088/0305-4624/16/1/305

Huang, T.-Y., Duan, K.-J., Huang, S.-Y., & Chen, C. W. (2006). Production of polyhydroxyalkanoates from inexpensive extruded rice bran and starch by Haloferax mediterranei. *Journal of Industrial Microbiology & Biotechnology*, *33*(8), 701–706. https://doi.org/10.1007/s10295-006-0098-z

Jambeck, J. R., Geyer, R., Wilcox, C., Siegler, T. R., Perryman, M., Andrady, A., Narayan, R., & Law, K. L. (2015). Plastic waste inputs from land into the ocean. *Science*, *347*(6223), 768. https://doi.org/10.1126/science.1260352

Joyce, C. (2018). *PHA: plastic the way nature intended? | Cambridge Consultants*. https://www.cambridgeconsultants.com/insights/bioplastics-pha-whitepaper

Kamilah, H., Tsuge, T., Yang, T. A., & Sudesh, K. (2013). Waste cooking oil as substrate for biosynthesis of poly(3-hydroxybutyrate) and poly(3-hydroxybutyrate-co-3-hydroxyhexanoate): Turning waste into a value-added product. *Malaysian Journal of Microbiology*, 51–59.

Keating, J. D., Robinson, J., Bothast, R. J., Saddler, J. N., & Mansfield, S. D. (2004). Characterization of a unique ethanologenic yeast capable of fermenting galactose. *Enzyme and Microbial Technology*, *35*(2), 242–253. https://doi.org/10.1016/j.enzmictec.2004.04.015

Khanna, S., & Srivastava, A. K. (2005). Statistical media optimization studies for growth and PHB production by Ralstonia eutropha. *Process Biochemistry*, *40*(6), 2173–2182. https://doi.org/10.1016/j.procbio.2004.08.011

Kiselev, E. G., Demidenko, A. V., Zhila, N. O., Shishatskaya, E. I., & Volova, T. G. (2022). Sugar Beet Molasses as a Potential C-Substrate for PHA Production by Cupriavidus necator. *Bioengineering*, *9*(4), Article 4. https://doi.org/10.3390/bioengineering9040154

Koller, M. (2015a). Recycling of Waste Streams of the Biotechnological Poly(hydroxyalkanoate) Production by *Haloferax mediterranei* on Whey. *International Journal of Polymer Science*, *2015*, 1–8. https://doi.org/10.1155/2015/370164

Koller, M. (2017). Production of Polyhydroxyalkanoate (PHA) Biopolyesters by Extremophiles. *MOJ Polymer Science*, *1*(2). https://doi.org/10.15406/mojps.2017.01.00011

Koller, M. (2018). A Review on Established and Emerging Fermentation Schemes for Microbial Production of Polyhydroxyalkanoate (PHA) Biopolyesters. *Fermentation*, *4*(2), Article 2. https://doi.org/10.3390/fermentation4020030

Koller, M. (2015b, March 3). *Recycling of Waste Streams of the Biotechnological Poly(hydroxyalkanoate) Production by Haloferax mediterranei on Whey* [Research Article]. International Journal of Polymer Science; Hindawi. https://doi.org/10.1155/2015/370164

Koller, M., Bona, R., Hermann, C., Horvat, P., Martinz, J., Neto, J., Pereira, L., Varila, P., & Braunegg, G. (2005). Biotechnological production of poly(3-hydroxybutyrate) with Wautersia eutropha by application of green grass juice and silage juice as additional complex substrates. *Biocatalysis and Biotransformation*, *23*(5), 329–337. https://doi.org/10.1080/10242420500292252

Koller, M., & Braunegg, G. (2015). Potential and Prospects of Continuous Polyhydroxyalkanoate (PHA) Production. *Bioengineering*, *2*(2), Article 2. https://doi.org/10.3390/bioengineering2020094

Koller, M., Hesse, P., Bona, R., Kutschera, C., Atlić, A., & Braunegg, G. (2007a). Biosynthesis of High Quality Polyhydroxyalkanoate Co- and Terpolyesters for Potential Medical Application by the Archaeon Haloferax mediterranei. *Macromolecular Symposia*, *253*(1), 33–39. https://doi.org/10.1002/masy.200750704

Koller, M., Hesse, P., Bona, R., Kutschera, C., Atlić, A., & Braunegg, G. (2007b). Potential of Various Archae- and Eubacterial Strains as Industrial Polyhydroxyalkanoate Producers from Whey. *Macromolecular Bioscience*, *7*(2), 218–226. https://doi.org/10.1002/mabi.200600211

Koller, M., Hesse, P., Salerno, A., Reiterer, A., & Braunegg, G. (2011). A viable antibiotic strategy against microbial contamination in biotechnological production of polyhydroxyalkanoates from surplus whey. *Biomass and Bioenergy*, *35*(1), 748–753. https://doi.org/10.1016/j.biombioe.2010.10.008

Koller, M., & Muhr, A. (2014). Continuous Production Mode as a Viable Process-Engineering Tool for Efficient Poly(hydroxyalkanoate) (PHA) Bio-Production. *Chem. Biochem. Eng. Q.*, 13.

Korkakaki, E., van Loosdrecht, M. C. M., & Kleerebezem, R. (2017). Impact of phosphate limitation on PHA production in a feast-famine process. *Water Research*, *126*, 472–480. https://doi.org/10.1016/j.watres.2017.09.031

Kourmentza, C., Plácido, J., Venetsaneas, N., Burniol-Figols, A., Varrone, C., Gavala, H. N., & Reis, M. A. M. (2017). Recent Advances and Challenges towards Sustainable Polyhydroxyalkanoate (PHA) Production. *Bioengineering*, *4*(2), Article 2. https://doi.org/10.3390/bioengineering4020055

Kovalcik, A., Kucera, D., Matouskova, P., Pernicova, I., Obruca, S., Kalina, M., Enev, V., & Marova, I. (2018). Influence of removal of microbial inhibitors on PHA production from spent coffee grounds employing Halomonas halophila. *Journal of Environmental Chemical Engineering*, *6*(2), 3495–3501. https://doi.org/10.1016/j.jece.2018.05.028

Kuechel, A. F. (2017). *Lactose Polymerization to Polylactose: Furthering Our Understanding for Commercialization.* UNIVERSITY OF MINNESOTA.

Kumar, P., Ray, S., & Kalia, V. C. (2016). Production of co-polymers of polyhydroxyalkanoates by regulating the hydrolysis of biowastes. *Bioresource Technology*, *200*, 413–419. https://doi.org/10.1016/j.biortech.2015.10.045

Kushwaha, S. C., Gochnauer, M. B., Kushner, D. J., & Kates, M. (1974). Pigments and isoprenoid compounds in extremely and moderately halophilic bacteria. *Canadian Journal of Microbiology*, *20*(2), 241–245. https://doi.org/10.1139/m74-038

Lappa, I. K., Papadaki, A., Kachrimanidou, V., Terpou, A., Koulougliotis, D., Eriotou, E., & Kopsahelis, N. (2019). Cheese Whey Processing: Integrated Biorefinery Concepts and Emerging Food Applications. *Foods*, *8*(8), Article 8. https://doi.org/10.3390/foods8080347

Leentvaar, J., & Rebhun, M. (1982). Effect of magnesium and calcium precipitation on coagulation-flocculation with lime. *Water Research*, *16*(5), 655–662. https://doi.org/10.1016/0043-1354(82)90087-2

Li, D., Lv, L., Chen, J.-C., & Chen, G.-Q. (2017). Controlling microbial PHB synthesis via CRISPRi. *Applied Microbiology and Biotechnology*, *101*(14), 5861–5867. https://doi.org/10.1007/s00253-017-8374-6

Liang, B., Bund, R., & Hartel, R. (2009). Effect of composition on moisture sorption of delactosed permeate. *International Dairy Journal - INT DAIRY J*, *19*, 630–636. https://doi.org/10.1016/j.idairyj.2009.04.010

Lillo, J. G., & Rodriguez-Valera, F. (1990). Effects of Culture Conditions on Poly(beta-Hydroxybutyric Acid) Production by Haloferax mediterranei. *Applied and Environmental Microbiology*, *56*(8), 2517–2521. https://doi.org/10.1128/AEM.56.8.2517-2521.1990

Lim, S. W., Kansedo, J., Tan, I. S., Tan, Y. H., Nandong, J., Lam, M. K., & Ongkudon, C. M. (2023). Microbial valorization of oil-based substrates for polyhydroxyalkanoates (PHA) production – Current strategies, status, and perspectives. *Process Biochemistry*, *130*, 715–733. https://doi.org/10.1016/j.procbio.2023.05.013

Liu, H., Kumar, V., Jia, L., Sarsaiya, S., Kumar, D., Juneja, A., Zhang, Z., Sindhu, R., Binod, P., Bhatia, S. K., & Awasthi, M. K. (2021). Biopolymer poly-hydroxyalkanoates (PHA) production from apple industrial waste residues: A review. *Chemosphere*, *284*, 131427. https://doi.org/10.1016/j.chemosphere.2021.131427

Maddipati, P., Atiyeh, H. K., Bellmer, D. D., & Huhnke, R. L. (2011). Ethanol production from syngas by Clostridium strain P11 using corn steep liquor as a nutrient replacement to yeast extract. *Bioresource Technology*, *102*(11), 6494–6501. https://doi.org/10.1016/j.biortech.2011.03.047

Madison, L. L., & Huisman, G. W. (1999). Metabolic Engineering of Poly(3-Hydroxyalkanoates): From DNA to Plastic. *MICROBIOL. MOL. BIOL. REV.*, *63*, 33.

Mai, T. H. A., Tran, V. N., & Le, V. V. M. (2013). Biochemical studies on the immobilized lactase in the combined alginate–carboxymethyl cellulose gel. *Biochemical Engineering Journal*, *74*, 81–87. https://doi.org/10.1016/j.bej.2013.03.003

Mango Materials. (2022). *Mango Materials Innovation*. Mango Materials. https://www.mangomaterials.com/innovation/

Market Data Forecast. (2022, January). *Polyhydroxyalkanoate Market | Share, Growth, Size | 2022 to 2027*. Market Data Forecast. http://www.marketdataforecast.com/

Matarredona, L., Camacho, M., Zafrilla, B., Bravo-Barrales, G., Esclapez, J., & Bonete, M.-J. (2021). The Survival of Haloferax mediterranei under Stressful Conditions. *Microorganisms*, *9*(2), 336. https://doi.org/10.3390/microorganisms9020336

Md. Din, M. F., Mohanadoss, P., Ujang, Z., van Loosdrecht, M., Yunus, S. M., Chelliapan, S., Zambare, V., & Olsson, G. (2012). Development of Bio-PORec® system for polyhydroxyalkanoates (PHA) production and its storage in mixed cultures of palm oil mill effluent (POME). *Bioresource Technology*, *124*, 208–216. https://doi.org/10.1016/j.biortech.2012.08.036

Meereboer, K. W., Misra, M., & Mohanty, A. K. (2020). Review of recent advances in the biodegradability of polyhydroxyalkanoate (PHA) bioplastics and their composites. *Green Chemistry*, *22*(17), 5519–5558. https://doi.org/10.1039/D0GC01647K

Melanie, S., Winterburn, J. B., School of Chemical Engineering and Analytical Science, The University of Manchester, M13 9PL, United Kingdom, Devianto, H., & Department of Chemical Engineering, Faculty of Industrial Technology, Institut Teknologi Bandung, Jalan Ganesa No. 10, Bandung 40132, Indonesia. (2018). Production of Biopolymer Polyhydroxyalkanoates (PHA) by Extreme Halophilic Marine Archaea Haloferax mediterranei in Medium with Varying Phosphorus Concentration. *Journal of Engineering and Technological Sciences*, *50*(2), 255–271. https://doi.org/10.5614/j.eng.technol.sci.2017.50.2.7

Miller, J. J., & Brand, J. C. (1980). Enzymic lactose hydrolysis. *Food Technol. Aust.; (Australia)*, *32:3*. https://www.osti.gov/etdeweb/biblio/5203706

Mitra, R., Xu, T., Xiang, H., & Han, J. (2020). Current developments on polyhydroxyalkanoates synthesis by using halophiles as a promising cell factory. *Microbial Cell Factories*, *19*(1), 86. https://doi.org/10.1186/s12934-020-01342-z

Mudenur, C., Mondal, K., Singh, U., & Katiyar, V. (2019). Production of Polyhydroxyalkanoates and Its Potential Applications. In V. Katiyar, R. Gupta, & T. Ghosh (Eds.), *Advances in Sustainable Polymers: Processing and Applications* (pp. 131–164). Springer. https://doi.org/10.1007/978-981-32-9804-0_7

Munir, S., Iqbal, S., & Jamil, N. (2015). *Polyhydroxyalkanoates (PHA) Production using Paper Mill Wastewater as Carbon Source in Comparison with Glucose*.

Naor, A., Lapierre, P., Mevarech, M., Papke, R. T., & Gophna, U. (2012). Low species barriers in halophilic archaea and the formation of recombinant hybrids. *Current Biology: CB*, *22*(15), 1444–1448. https://doi.org/10.1016/j.cub.2012.05.056

Nath, A., Dixit, M., Bandiya, A., Chavda, S., & Desai, A. J. (2008). Enhanced PHB production and scale up studies using cheese whey in fed batch culture of Methylobacterium sp. ZP24. *Bioresource Technology*, *99*(13), 5749–5755. https://doi.org/10.1016/j.biortech.2007.10.017

Nielsen, C., Rahman, A., Rehman, A. U., Walsh, M. K., & Miller, C. D. (2017). Food waste conversion to microbial polyhydroxyalkanoates. *Microbial Biotechnology*, *10*(6), 1338–1352. https://doi.org/10.1111/1751-7915.12776

Nieto, J. J., Ventosa, A., & Ruiz-Berraquero, F. (1987). Susceptibility of Halobacteria to Heavy Metals. *Applied and Environmental Microbiology*, *53*(5), 1199–1202. https://doi.org/10.1128/aem.53.5.1199-1202.1987

Nikodinovic-Runic, J., Guzik, M., Kenny, S. T., Babu, R., Werker, A., & O Connor, K. E. (2013). Chapter Four—Carbon-Rich Wastes as Feedstocks for Biodegradable Polymer (Polyhydroxyalkanoate) Production Using Bacteria. In S. Sariaslani & G. M. Gadd (Eds.), *Advances in Applied Microbiology* (Vol. 84, pp. 139–200). Academic Press. https://doi.org/10.1016/B978-0-12-407673-0.00004-7

Obuchi, S., & Ogawa, S. (2010). Packaging and Other Commercial Applications. In *Poly(Lactic Acid)* (pp. 457–467). John Wiley & Sons, Ltd. https://doi.org/10.1002/9780470649848.ch28

Oliveira, D., Puri, R., Fenelon, M. A., & O'Mahony, J. A. (2019). Delactosed permeate as a dairy processing co-product with major potential value: A review. *International Journal of Food Science & Technology*, *54*(4), 999–1008. https://doi.org/10.1111/ijfs.14064

Oren, A., & Gurevich, P. (1994). Production of d-lactate, acetate, and pyruvate from glycerol in communities of halophilic archaea in the Dead Sea and in saltern crystallizer ponds. *FEMS Microbiology Ecology*, *14*(2), 147–155. https://doi.org/10.1111/j.1574-6941.1994.tb00101.x

Pais, J., Serafim, L. S., Freitas, F., & Reis, M. A. M. (2016). Conversion of cheese whey into poly(3-hydroxybutyrate-co-3-hydroxyvalerate) by Haloferax mediterranei. *New Biotechnology*, *33*(1), 224–230. https://doi.org/10.1016/j.nbt.2015.06.001

Panesar, P. S., Panesar, R., Singh, R. S., Kennedy, J. F., & Kumar, H. (2006). Microbial production, immobilization and applications of β-D-galactosidase. *Journal of Chemical Technology & Biotechnology*, *81*(4), 530–543. https://doi.org/10.1002/jctb.1453

Pantazaki, A. A., Papaneophytou, C. P., Pritsa, A. G., Liakopoulou-Kyriakides, M., & Kyriakidis, D. A. (2009). Production of polyhydroxyalkanoates from whey by Thermus thermophilus HB8. *Process Biochemistry*, *44*(8), 847–853. https://doi.org/10.1016/j.procbio.2009.04.002

Pire, C., Martínez-Espinosa, R. M., Pérez-Pomares, F., Esclapez, J., & Bonete, M. J. (2014). Ferredoxin-dependent glutamate synthase: Involvement in ammonium assimilation in Haloferax mediterranei. *Extremophiles*, *18*(1), 147–159. https://doi.org/10.1007/s00792-013-0606-9

Poli, A., Di Donato, P., Abbamondi, G. R., & Nicolaus, B. (2011). Synthesis, Production, and Biotechnological Applications of Exopolysaccharides and Polyhydroxyalkanoates by Archaea. *Archaea*, *2011*, e693253. https://doi.org/10.1155/2011/693253

Poontawee, R., & Limtong, S. (2020). Feeding Strategies of Two-Stage Fed-Batch Cultivation Processes for Microbial Lipid Production from Sugarcane Top Hydrolysate and Crude Glycerol by the Oleaginous Red Yeast Rhodosporidiobolus fluvialis. *Microorganisms*, *8*(2), 151. https://doi.org/10.3390/microorganisms8020151

Popescu, L., Bulgaru, V., & Siminiuc, R. (2021). Effect of Temperature, pH and Amount of Enzyme Used in the Lactose Hydrolysis of Milk. *Food and Nutrition Sciences*, *12*(12), Article 12. https://doi.org/10.4236/fns.2021.1212091

Qian, J., Zhu, L., Zhang, J., & Whitehouse, R. S. (2007). Comparison of different nucleating agents on crystallization of poly(3-hydroxybutyrate-co-3-hydroxyvalerates). *Journal of Polymer Science Part B: Polymer Physics*, *45*(13), 1564–1577. https://doi.org/10.1002/polb.21157

Raho, S., Carofiglio, V. E., Montemurro, M., Miceli, V., Centrone, D., Stufano, P., Schioppa, M., Pontonio, E., & Rizzello, C. G. (2020). Production of the Polyhydroxyalkanoate PHBV from Ricotta Cheese Exhausted Whey by Haloferax mediterranei Fermentation. *Foods*, *9*(10), Article 10. https://doi.org/10.3390/foods9101459

Raza, Z. A., Abid, S., & Banat, I. M. (2018). Polyhydroxyalkanoates: Characteristics, production, recent developments and applications. *International Biodeterioration & Biodegradation*, *126*, 45–56. https://doi.org/10.1016/j.ibiod.2017.10.001

Reddy, C. S. K., Ghai, R., Rashmi, & Kalia, V. C. (2003). Polyhydroxyalkanoates: An overview. *Bioresource Technology*, *87*(2), 137–146. https://doi.org/10.1016/S0960-8524(02)00212-2

Reis, M. A. M., Serafim, L. S., Lemos, P. C., Ramos, A. M., Aguiar, F. R., & Van Loosdrecht, M. C. M. (2003). Production of polyhydroxyalkanoates by mixed microbial cultures. *Bioprocess and Biosystems Engineering*, *25*(6), 377–385. https://doi.org/10.1007/s00449-003-0322-4

Richmond, M. L., Gray, J. I., & Stine, C. M. (1981). Beta-Galactosidase: Review of Recent Research Related to Technological Application, Nutritional Concerns, and Immobilization1. *Journal of Dairy Science*, *64*(9), 1759–1771. https://doi.org/10.3168/jds.S0022-0302(81)82764-6

Rivera-Briso, A. L., & Serrano-Aroca, Á. (2018). Poly(3-Hydroxybutyrate-co-3-Hydroxyvalerate): Enhancement Strategies for Advanced Applications. *Polymers*, *10*(7), 732. https://doi.org/10.3390/polym10070732

Robinson, J. L., Pyzyna, B., Atrasz, R. G., Henderson, C. A., Morrill, K. L., Burd, A. M., DeSoucy, E., Fogleman, R. E., Naylor, J. B., Steele, S. M., Elliott, D. R., Leyva, K. J., & Shand, R. F. (2005). Growth Kinetics of Extremely Halophilic Archaea (Family Halobacteriaceae) as Revealed by Arrhenius Plots. *Journal of Bacteriology*, *187*(3), 923–929. https://doi.org/10.1128/JB.187.3.923-929.2005

Rodriguez-Valera, F., Juez, G., & Kushner, D. J. (1983). Halobacterium mediterranei spec, nov., a New Carbohydrate-Utilizing Extreme Halophile. *Systematic and Applied Microbiology*, *4*(3), 369–381. https://doi.org/10.1016/S0723-2020(83)80021-6

Rodriguez-Valera, F., Lillo, J. A. G., Antón, J., & Meseguer, I. (1991). Biopolymer Production by Haloferax Mediterranei. In F. Rodriguez-Valera (Ed.), *General and Applied Aspects of Halophilic Microorganisms* (pp. 373–380). Springer US. https://doi.org/10.1007/978-1-4615-3730-4_45

Rodriguez-Valera, F., Ruiz-Berraquero, F., & Ramos-Cormenzana, A. (1980). SHORT COMMUNICATION Isolation of Extremely Halophilic Bacteria Able to Grow in Defined Inorganic Media with Single Carbon Sources. *Microbiology*, *119*(2), 535–538. https://doi.org/10.1099/00221287-119-2-535

Roland-Holst, D. (2013). *Bioplastics in California: Economic Assessment of Market Conditions for PHA/PHB Bioplastics Produced from Waste Methane*. 82.

Roland-Holst, D., Triolo, R., Heft-Neal, S., & Bayrami, B. (2013). *Contractor's Report Produced Under Contract By:* 82.

Rossi, V., Cleeve-Edwards, N., & Lundquist, L. (2015). Life cycle assessment of end-of-life options for two biodegradable packaging materials: Sound application of the European waste hierarchy. *Journal of Cleaner Production*, *86*, 132–145. https://doi.org/10.1016/j.jclepro.2014.08.049

Scott, H. (2020, October 15). *Chris Hansen Lactase Interview* [Telephone].

Sharifzadeh, M., Najafpour, G., Z, L., Tabandeh, F., Younesi, H., H, I., & Khodabandeh, M. (2010). Optimization PHAs production from dairy industry wastewater (cheese whey) by Azohydromonas lata DSMZ 1123. *Iranica Journal of Energy and Environment (IJEE)*, *1*.

Shieber, J. (2020). *YC graduate Genecis Bioindustries turns food waste into compostable plastics | TechCrunch*. https://techcrunch.com/2020/03/16/yc-graduate-genecis-bioindustries-turns-food-waste-into-compostable-plastics/

Siebers, B., & Schönheit, P. (2005). Unusual pathways and enzymes of central carbohydrate metabolism in Archaea. *Current Opinion in Microbiology*, *8*(6), 695–705. https://doi.org/10.1016/j.mib.2005.10.014

Simó-Cabrera, L., García-Chumillas, S., Hagagy, N., Saddiq, A., Tag, H., Selim, S., AbdElgawad, H., Arribas Agüero, A., Monzó Sánchez, F., Cánovas, V., Pire, C., & Martínez-Espinosa, R. M. (2021). Haloarchaea as Cell Factories to Produce Bioplastics. *Marine Drugs*, *19*(3), Article 3. https://doi.org/10.3390/md19030159

Sluiter, A. (2008). Determination of Sugars, Byproducts, and Degradation Products in Liquid Fraction Process Samples: Laboratory Analytical Procedure (LAP); Issue Date: 12/08/2006. *Technical Report*, 14.

Smet, M. J. D. (1983). Characterization of Intracellular Inclusions Formed by Pseudomonas oleovorans During Growth on Octane. *J. BACTERIOL.*, *154*, 9.

Smith, S. T., Metzger, L., & Drake, M. A. (2016). Evaluation of whey, milk, and delactosed permeates as salt substitutes. *Journal of Dairy Science*, *99*(11), 8687–8698. https://doi.org/10.3168/jds.2016-10904

Suriyamongkol, P., Weselake, R., Narine, S., Moloney, M., & Shah, S. (2007). Biotechnological approaches for the production of polyhydroxyalkanoates in microorganisms and plants—A

review. *Biotechnology Advances*, *25*(2), 148-175.https://doi.org/10.1016/j.biotechadv.2006.11.007

Szacherska, K., Oleskowicz-Popiel, P., Ciesielski, S., & Mozejko-Ciesielska, J. (2021). Volatile Fatty Acids as Carbon Sources for Polyhydroxyalkanoates Production. *Polymers*, *13*(3), Article 3. https://doi.org/10.3390/polym13030321

Tejayadi, S., & Cheryan, M. (1995). Lactic acid from cheese whey permeate. Productivity and economics of a continuous membrane bioreactor. *Applied Microbiology and Biotechnology*, *43*(2), 242–248. https://doi.org/10.1007/BF00172819

Ten, E., Jiang, L., Zhang, J., & Wolcott, M. P. (2015). 3—Mechanical performance of polyhydroxyalkanoate (PHA)-based biocomposites. In M. Misra, J. K. Pandey, & A. K. Mohanty (Eds.), *Biocomposites* (pp. 39–52). Woodhead Publishing. https://doi.org/10.1016/B978-1-78242-373-7.00008-1

Tian, L., Li, H., Song, X., Ma, L., & Li, Z.-J. (2022). Production of polyhydroxyalkanoates by a novel strain of Photobacterium using soybean oil and corn starch. *Journal of Environmental Chemical Engineering*, *10*(5), 108342. https://doi.org/10.1016/j.jece.2022.108342

TianAn Biopolyme. (2022). *TianAn Biopolymer: Nature's Eco-Friendly Solution*. http://www.tianan-enmat.com/#

Tolhurst, L. (2016). FROM DAIRY 'WASTE' TO PROFITS. *La Chimica E L'Industria*, *98*.

United Nations Environment Programme. (2021). *|Food Loss Reduction CoP| Food and Agriculture Organization of the United Nations*. https://www.fao.org/platform-food-loss-waste/resources/detail/en/c/1378978/

US EPA, O. (1996). *Method 200.7: Determination of Metals and Trace Elements in Water and Wastes by Inductively Coupled Plasma-Atomic Emission Spectrometry* [Data and Tools].

https://www.epa.gov/esam/method-2007-determination-metals-and-trace-elements-water-and-wastes-inductively-coupled

US EPA, O. (2017, September 12). *Plastics: Material-Specific Data* [Collections and Lists]. US EPA. https://www.epa.gov/facts-and-figures-about-materials-waste-and-recycling/plastics-material-specific-data

USDA. (2023). *Nitrogen Interactive | Cost Comparison Example*. https://scienceofagriculture.org/nitrogen/fertilizer/fertilizer-comparison-01.html

Valentino, F., Karabegovic, L., Majone, M., Morgan-Sagastume, F., & Werker, A. (2015). Polyhydroxyalkanoate (PHA) storage within a mixed-culture biomass with simultaneous growth as a function of accumulation substrate nitrogen and phosphorus levels. *Water Research*, *77*, 49–63. https://doi.org/10.1016/j.watres.2015.03.016

Vandi, L.-J., Chan, C., Werker, A., Richardson, D., Laycock, B., & Pratt, S. (2018). Wood-PHA Composites: Mapping Opportunities. *Polymers*, *10*, 751. https://doi.org/10.3390/polym10070751

Wallner, E., Haage, G., Bona, R., Schellauf, F., & Braunegg, G. (2001). The Production of Poly-3-hydroxybutyrate-co-3-hydroxyvalerate with Pseudomonas cepacia ATCC 17759 on Various Carbon Sources. In E. Chiellini, H. Gil, G. Braunegg, J. Buchert, P. Gatenholm, & M. van der Zee (Eds.), *Biorelated Polymers: Sustainable Polymer Science and Technology* (pp. 139–145). Springer US. https://doi.org/10.1007/978-1-4757-3374-7_12

Wang, K. (2021). *The pretreatment and utilization of four types of real-world feedstocks for PHBV production by H. mediterranei*.

Wang, K. (2022). *Bioprocess Development for Production of Polyhydroxyalkanoates from Organic Feedstocks* [UC Davis]. https://escholarship.org/uc/item/4p52w2gk

Wang, K., Hobby, A., Chen, Y., & Chio, A. (2021). *Techno-economic Analysis on An Industrial-scale Production System of Biodegradable Plastics from Cheese By-products by Haloferax mediterranei*. https://doi.org/10.13031/aim.202100227

Wang, K., & Zhang, R. (2021). *Production of Polyhydroxyalkanoates (PHA) by Haloferax mediterranei from Food Waste Derived Nutrients for Biodegradable Plastic Applications*. *31*(2), 338–347. https://doi.org/10.4014/jmb.2008.08057

Williams, T. J., Allen, M. A., Liao, Y., Raftery, M. J., & Cavicchioli, R. (2019). Sucrose Metabolism in Haloarchaea: Reassessment Using Genomics, Proteomics, and Metagenomics. *Applied and Environmental Microbiology*, *85*(6), e02935-18. https://doi.org/10.1128/AEM.02935-18

Wong, H. H., & Lee, S. Y. (1998). Poly-(3-hydroxybutyrate) production from whey by high-density cultivation of recombinant Escherichia coli. *Applied Microbiology and Biotechnology*, *50*(1), 30–33. https://doi.org/10.1007/s002530051252

Yadav, B., Chavan, S., Atmakuri, A., Tyagi, R. D., & Drogui, P. (2020). A review on recovery of proteins from industrial wastewaters with special emphasis on PHA production process: Sustainable circular bioeconomy process development. *Bioresource Technology*, *317*, 124006. https://doi.org/10.1016/j.biortech.2020.124006

Yield10 Bio. (2022). *PHA Biopolymers Development & Applications | Yield10 Bio*. https://www.yield10bio.com/commitment/pha-biopolymers

Yoong Kit, L., Show, P.-L., Lan, J., Loh, S. H.-S., Lam, H., & Ling, T. (2017). Economic and environmental analysis of PHAs production process. *Clean Technologies and Environmental Policy*, *19*. https://doi.org/10.1007/s10098-017-1377-2

Zadow, J. G. (1984). Lactose: Properties and Uses. *Journal of Dairy Science*, *67*(11), 2654–2679. https://doi.org/10.3168/jds.S0022-0302(84)81625-2

Zadow, J. G. (2012). *Whey and Lactose Processing*. Springer Science & Business Media.

Zhang, J., Reddy, J., Buckland, B., & Greasham, R. (2003). Toward consistent and productive complex media for industrial fermentations: Studies on yeast extract for a recombinant yeast fermentation process. *Biotechnology and Bioengineering*, *82*(6), 640–652. https://doi.org/10.1002/bit.10608

Zheng, J., & Suh, S. (2019). Strategies to reduce the global carbon footprint of plastics. *Nature Climate Change*, *9*(5), Article 5. https://doi.org/10.1038/s41558-019-0459-z

Appendices

Appendix A. Chapter 3 statistical analysis reports

Table A.1 Unpaired t-test for final CDM concentration of hydrolyzed DLP with and without centrifugation (as illustrated in Figure 3.6).

Table Analyzed	Unpaired t-test
Column B	HDLP w centrifugation CDM
vs.	vs.
Column A	HDLP w/o centrifugation CDM
Unpaired t test	
P value	0.0152
P value summary	*
Significantly different (P < 0.05)?	Yes
One- or two-tailed P value?	Two-tailed
t, df	t=8.008, df=2

Table A.2 Unpaired t-test for final PHA concentration of hydrolyzed DLP with and without centrifugation (as illustrated in Figure 3.6).

Table Analyzed	Unpaired t-test
Column B	HDLP w centrifugation PHA
vs.	vs.
Column A	HDLP w/o centrifugation PHA
Unpaired t test	
P value	0.0371
P value summary	*
Significantly different (P < 0.05)?	Yes
One- or two-tailed P value?	Two-tailed
t, df	t=5.049, df=2

Table A.3 Unpaired t-test PHA content of hydrolyzed DLP with and without centrifugation (as illustrated in Figure 3.6).

Table Analyzed	Unpaired t-test
Column B	HDLP w centrifugation PHA content
vs.	vs.
Column A	HDLP w/o centrifugation PHA content
Unpaired t test	
P value	0.1982
P value summary	ns
Significantly different (P < 0.05)?	No
One- or two-tailed P value?	Two-tailed
t, df	t=1.897, df=2

Table A.4 One-way ANOVA and pairwise Tukey test for final CDM concentration with sugar feedstocks, hydrolyzed DLP, glucose, galactose, and glucose and galactose (as illustrated in Figure 3.9).

Table Analyzed	One-way ANOVA
Data sets analyzed	A-D
ANOVA summary	
F	624.5
P value	<0.0001
P value summary	****
Significant diff. among means (P < 0.05)?	Yes
R squared	0.9957

Number of families	1							
Number of comparisons per family	6							
Alpha	0.05							
Tukey's multiple comparisons test	**Mean Diff.**	**95.00% CI of diff.**	**Below threshold?**	**Summary**	**Adjusted P Value**			
Hydrolyzed DLP CDM vs. Glucose CDM	0.6200	0.4145 to 0.8255	Yes	****	<0.0001	A-B		
Hydrolyzed DLP CDM vs. Galactose CDM	2.627	2.421 to 2.832	Yes	****	<0.0001	A-C		
Hydrolyzed DLP CDM vs. Glucose + galactose CDM	0.7433	0.5379 to 0.9488	Yes	****	<0.0001	A-D		
Glucose CDM vs. Galactose CDM	2.007	1.801 to 2.212	Yes	****	<0.0001	B-C		
Glucose CDM vs. Glucose + galactose CDM	0.1233	-0.08213 to 0.3288	No	ns	0.2917	B-D		
Galactose CDM vs. Glucose + galactose CDM	-1.883	-2.089 to -1.678	Yes	****	<0.0001	C-D		
Test details	**Mean 1**	**Mean 2**	**Mean Diff.**	**SE of diff.**	**n1**	**n2**	**q**	**DF**
Hydrolyzed DLP CDM vs. Glucose CDM	3.913	3.293	0.6200	0.06416	3	3	13.67	8
Hydrolyzed DLP CDM vs. Galactose CDM	3.913	1.287	2.627	0.06416	3	3	57.90	8
Hydrolyzed DLP CDM vs. Glucose + galactose CDM	3.913	3.170	0.7433	0.06416	3	3	16.38	8
Glucose CDM vs. Galactose CDM	3.293	1.287	2.007	0.06416	3	3	44.23	8
Glucose CDM vs. Glucose + galactose CDM	3.293	3.170	0.1233	0.06416	3	3	2.718	8
Galactose CDM vs. Glucose + galactose CDM	1.287	3.170	-1.883	0.06416	3	3	41.51	8

Table A.5 One-way ANOVA and pairwise Tukey test for CDM yield with sugar feedstocks, hydrolyzed DLP, glucose, galactose, and glucose and galactose (as illustrated in Figure 3.9).

Table Analyzed	One-way ANOVA
Data sets analyzed	A-D
ANOVA summary	
F	122.5
P value	<0.0001
P value summary	****
Significant diff. among means (P < 0.05)?	Yes
R squared	0.9787

Number of families	1							
Number of comparisons per family	6							
Alpha	0.05							
Tukey's multiple comparisons test	**Mean Diff.**	**95.00% CI of diff.**	**Below threshold?**	**Summary**	**Adjusted P Value**			
Hydrolyzed DLP CDM yield vs. Glucose CDM yield	0.1733	0.1300 to 0.2167	Yes	****	<0.0001	A-B		
Hydrolyzed DLP CDM yield vs. Galactose CDM yield	0.1567	0.1133 to 0.2000	Yes	****	<0.0001	A-C		
Hydrolyzed DLP CDM yield vs. Glucose + galactose CDM yield	-0.03333	-0.07669 to 0.01003	No	ns	0.1417	A-D		
Glucose CDM yield vs. Galactose CDM yield	-0.01667	-0.06003 to 0.02669	No	ns	0.6263	B-C		
Glucose CDM yield vs. Glucose + galactose CDM yield	-0.2067	-0.2500 to -0.1633	Yes	****	<0.0001	B-D		
Galactose CDM yield vs. Glucose + galactose CDM yield	-0.1900	-0.2334 to -0.1466	Yes	****	<0.0001	C-D		
Test details	**Mean 1**	**Mean 2**	**Mean Diff.**	**SE of diff.**	**n1**	**n2**	**q**	**DF**
Hydrolyzed DLP CDM yield vs. Glucose CDM yield	0.4933	0.3200	0.1733	0.01354	3	3	18.10	8
Hydrolyzed DLP CDM yield vs. Galactose CDM yield	0.4933	0.3367	0.1567	0.01354	3	3	16.36	8
Hydrolyzed DLP CDM yield vs. Glucose + galactose CDM yield	0.4933	0.5267	-0.03333	0.01354	3	3	3.482	8
Glucose CDM yield vs. Galactose CDM yield	0.3200	0.3367	-0.01667	0.01354	3	3	1.741	8
Glucose CDM yield vs. Glucose + galactose CDM yield	0.3200	0.5267	-0.2067	0.01354	3	3	21.59	8
Galactose CDM yield vs. Glucose + galactose CDM yield	0.3367	0.5267	-0.1900	0.01354	3	3	19.84	8

Table A.6 One-way ANOVA and pairwise Tukey test for final PHA concentration with sugar feedstocks, hydrolyzed DLP, glucose, galactose, and glucose and galactose (as illustrated in Figure 3.10).

Table Analyzed	One-way ANOVA
Data sets analyzed	A-D
ANOVA summary	
F	288.0
P value	<0.0001
P value summary	****
Significant diff. among means (P < 0.05)?	Yes
R squared	0.9908

Number of families	1							
Number of comparisons per family	6							
Alpha	0.05							
Tukey's multiple comparisons test	**Mean Diff.**	**95.00% CI of diff.**	**Below threshold?**	**Summary**	**Adjusted P Value**			
Hydrolyzed DLP PHA vs. Glucose PHA	0.2600	0.03878 to 0.4812	Yes	*	0.0229	A-B		
Hydrolyzed DLP PHA vs. Galactose PHA	1.840	1.619 to 2.061	Yes	****	<0.0001	A-C		
Hydrolyzed DLP PHA vs. Glucose + galactose PHA	0.3767	0.1554 to 0.5979	Yes	**	0.0027	A-D		
Glucose PHA vs. Galactose PHA	1.580	1.359 to 1.801	Yes	****	<0.0001	B-C		
Glucose PHA vs. Glucose + galactose PHA	0.1167	-0.1046 to 0.3379	No	ns	0.3881	B-D		
Galactose PHA vs. Glucose + galactose PHA	-1.463	-1.685 to -1.242	Yes	****	<0.0001	C-D		
Test details	**Mean 1**	**Mean 2**	**Mean Diff.**	**SE of diff.**	**n1**	**n2**	**q**	**DF**
Hydrolyzed DLP PHA vs. Glucose PHA	2.573	2.313	0.2600	0.06908	3	3	5.323	8
Hydrolyzed DLP PHA vs. Galactose PHA	2.573	0.7333	1.840	0.06908	3	3	37.67	8
Hydrolyzed DLP PHA vs. Glucose + galactose PHA	2.573	2.197	0.3767	0.06908	3	3	7.711	8
Glucose PHA vs. Galactose PHA	2.313	0.7333	1.580	0.06908	3	3	32.35	8
Glucose PHA vs. Glucose + galactose PHA	2.313	2.197	0.1167	0.06908	3	3	2.388	8
Galactose PHA vs. Glucose + galactose PHA	0.7333	2.197	-1.463	0.06908	3	3	29.96	8

Table A.7 One-way ANOVA and pairwise Tukey test for PHA yield with sugar feedstocks, hydrolyzed DLP, glucose, galactose, and glucose and galactose (as illustrated in Figure 3.10).

Table Analyzed	One-way ANOVA
Data sets analyzed	A-D
ANOVA summary	
F	40.80
P value	<0.0001
P value summary	****
Significant diff. among means (P < 0.05)?	Yes
R squared	0.9387

Number of families	1							
Number of comparisons per family	6							
Alpha	0.05							
Tukey's multiple comparisons test	**Mean Diff.**	**95.00% CI of diff.**	**Below threshold?**	**Summary**	**Adjusted P Value**			
Hydrolyzed DLP PHA yield vs. Glucose PHA yield	0.09667	0.03442 to 0.1589	Yes	**	0.0048	A-B		
Hydrolyzed DLP PHA yield vs. Galactose PHA yield	0.1233	0.06109 to 0.1856	Yes	**	0.0010	A-C		
Hydrolyzed DLP PHA yield vs. Glucose + galactose PHA yield	-0.06667	-0.1289 to -0.004424	Yes	*	0.0363	A-D		
Glucose PHA yield vs. Galactose PHA yield	0.02667	-0.03558 to 0.08891	No	ns	0.5481	B-C		
Glucose PHA yield vs. Glucose + galactose PHA yield	-0.1633	-0.2256 to -0.1011	Yes	***	0.0001	B-D		
Galactose PHA yield vs. Glucose + galactose PHA yield	-0.1900	-0.2522 to -0.1278	Yes	****	<0.0001	C-D		
Test details	**Mean 1**	**Mean 2**	**Mean Diff.**	**SE of diff.**	**n1**	**n2**	**q**	**DF**
Hydrolyzed DLP PHA yield vs. Glucose PHA yield	0.3333	0.2367	0.09667	0.01944	3	3	7.034	8
Hydrolyzed DLP PHA yield vs. Galactose PHA yield	0.3333	0.2100	0.1233	0.01944	3	3	8.974	8
Hydrolyzed DLP PHA yield vs. Glucose + galactose PHA yield	0.3333	0.4000	-0.06667	0.01944	3	3	4.851	8
Glucose PHA yield vs. Galactose PHA yield	0.2367	0.2100	0.02667	0.01944	3	3	1.940	8
Glucose PHA yield vs. Glucose + galactose PHA yield	0.2367	0.4000	-0.1633	0.01944	3	3	11.88	8
Galactose PHA yield vs. Glucose + galactose PHA yield	0.2100	0.4000	-0.1900	0.01944	3	3	13.82	8

Table A.8 One-way ANOVA and pairwise Tukey test for PHA content with sugar feedstocks, hydrolyzed DLP, glucose, galactose, and glucose and galactose (as illustrated in Figure 3.11).

Table Analyzed	One-way ANOVA
Data sets analyzed	A-D
ANOVA summary	
F	8.824
P value	0.0064
P value summary	**
Significant diff. among means (P < 0.05)?	Yes
R squared	0.7679

Number of families	1							
Number of comparisons per family	6							
Alpha	0.05							
Tukey's multiple comparisons test	**Mean Diff.**	**95.00% CI of diff.**	**Below threshold?**	**Summary**	**Adjusted P Value**			
Hydrolyzed DLP PHA content vs. Glucose PHA content	-0.04667	-0.1391 to 0.04578	No	ns	0.4219	A-B		
Hydrolyzed DLP PHA content vs. Galactose PHA content	0.08667	-0.005777 to 0.1791	No	ns	0.0663	A-C		
Hydrolyzed DLP PHA content vs. Glucose + galactose content	-0.03667	-0.1291 to 0.05578	No	ns	0.6043	A-D		
Glucose PHA content vs. Galactose PHA content	0.1333	0.04089 to 0.2258	Yes	**	0.0074	B-C		
Glucose PHA content vs. Glucose + galactose content	0.01000	-0.08244 to 0.1024	No	ns	0.9847	B-D		
Galactose PHA content vs. Glucose + galactose content	-0.1233	-0.2158 to -0.03089	Yes	*	0.0116	C-D		
Test details	**Mean 1**	**Mean 2**	**Mean Diff.**	**SE of diff.**	**n1**	**n2**	**q**	**DF**
Hydrolyzed DLP PHA content vs. Glucose PHA content	0.6567	0.7033	-0.04667	0.02887	3	3	2.286	8
Hydrolyzed DLP PHA content vs. Galactose PHA content	0.6567	0.5700	0.08667	0.02887	3	3	4.246	8
Hydrolyzed DLP PHA content vs. Glucose + galactose content	0.6567	0.6933	-0.03667	0.02887	3	3	1.796	8
Glucose PHA content vs. Galactose PHA content	0.7033	0.5700	0.1333	0.02887	3	3	6.532	8
Glucose PHA content vs. Glucose + galactose content	0.7033	0.6933	0.01000	0.02887	3	3	0.4899	8
Galactose PHA content vs. Glucose + galactose content	0.5700	0.6933	-0.1233	0.02887	3	3	6.042	8

Appendix B. Chapter 4 statistical analysis reports

Table B.1 One-way ANOVA and pairwise Tukey test for final CDM concentration with hydrolyzed DLP supplemented with yeast extract (YE) and ammonium chloride (NH_4Cl), and glucose and supplemented with yeast extract (as illustrated in Figure 4.7).

Table Analyzed	One-way ANOVA
Data sets analyzed	A-D
ANOVA summary	
F	23.28
P value	0.0054
P value summary	**
Significant diff. among means (P < 0.05)?	Yes
R squared	0.9458

Number of families	1							
Number of comparisons per family	6							
Alpha	0.05							
Tukey's multiple comparisons test	**Mean Diff.**	**95.00% CI of diff.**	**Below threshold?**	**Summary**	**Adjusted P Value**			
HDLP+YE CDM vs. HDLP+YE+NH_4Cl CDM	0.5400	-0.09654 to 1.177	No	ns	0.0832	A-B		
HDLP+YE CDM vs. HDLP+NH_4Cl CDM	1.220	0.5835 to 1.857	Yes	**	0.0050	A-C		
HDLP+YE CDM vs. Glucose+YE CDM	0.2100	-0.4265 to 0.8465	No	ns	0.5871	A-D		
HDLP+YE+NH_4Cl CDM vs. HDLP+NH_4Cl CDM	0.6800	0.04346 to 1.317	Yes	*	0.0403	B-C		
HDLP+YE+NH_4Cl CDM vs. Glucose+YE CDM	-0.3300	-0.9665 to 0.3065	No	ns	0.2894	B-D		
HDLP+NH_4Cl CDM vs. Glucose+YE CDM	-1.010	-1.647 to -0.3735	Yes	*	0.0102	C-D		
Test details	**Mean 1**	**Mean 2**	**Mean Diff.**	**SE of diff.**	**n1**	**n2**	**q**	**DF**
HDLP+YE CDM vs. HDLP+YE+NH_4Cl CDM	5.955	5.415	0.5400	0.1564	2	2	4.884	4
HDLP+YE CDM vs. HDLP+NH_4Cl CDM	5.955	4.735	1.220	0.1564	2	2	11.03	4
HDLP+YE CDM vs. Glucose+YE CDM	5.955	5.745	0.2100	0.1564	2	2	1.899	4
HDLP+YE+NH_4Cl CDM vs. HDLP+NH_4Cl CDM	5.415	4.735	0.6800	0.1564	2	2	6.150	4
HDLP+YE+NH_4Cl CDM vs. Glucose+YE CDM	5.415	5.745	-0.3300	0.1564	2	2	2.985	4
HDLP+NH_4Cl CDM vs. Glucose+YE CDM	4.735	5.745	-1.010	0.1564	2	2	9.135	4

Table B.2 One-way ANOVA and pairwise Tukey test for CDM yield with hydrolyzed DLP supplemented with yeast extract (YE) and ammonium chloride (NH_4Cl), and glucose and supplemented with yeast extract (as illustrated in Figure 4.7).

Table Analyzed	One-way ANOVA
Data sets analyzed	A-D
ANOVA summary	
F	58.18
P value	0.0009
P value summary	***
Significant diff. among means (P < 0.05)?	Yes
R squared	0.9776

Number of families	1							
Number of comparisons per family	6							
Alpha	0.05							
Tukey's multiple comparisons test	**Mean Diff.**	**95.00% CI of diff.**	**Below threshold?**	**Summary**	**Adjusted P Value**			
HDLP+YE CDM yield vs. HDLP+YE+NH_4Cl CDM yield	-0.05500	-0.1338 to 0.02383	No	ns	0.1442	A-B		
HDLP+YE CDM yield vs. HDLP+NH_4Cl CDM yield	-0.2050	-0.2838 to -0.1262	Yes	**	0.0016	A-C		
HDLP+YE CDM yield vs. Glucose+YE CDM yield	0.03000	-0.04883 to 0.1088	No	ns	0.4911	A-D		
HDLP+YE+NH_4Cl CDM yield vs. HDLP+NH_4Cl CDM yield	-0.1500	-0.2288 to -0.07117	Yes	**	0.0052	B-C		
HDLP+YE+NH_4Cl CDM yield vs. Glucose+YE CDM yield	0.08500	0.006168 to 0.1638	Yes	*	0.0391	B-D		
HDLP+NH_4Cl CDM yield vs. Glucose+YE CDM yield	0.2350	0.1562 to 0.3138	Yes	***	0.0009	C-D		
Test details	**Mean 1**	**Mean 2**	**Mean Diff.**	**SE of diff.**	**n1**	**n2**	**q**	**DF**
HDLP+YE CDM yield vs. HDLP+YE+NH_4Cl CDM yield	0.4200	0.4750	-0.05500	0.01936	2	2	4.017	4
HDLP+YE CDM yield vs. HDLP+NH_4Cl CDM yield	0.4200	0.6250	-0.2050	0.01936	2	2	14.97	4
HDLP+YE CDM yield vs. Glucose+YE CDM yield	0.4200	0.3900	0.03000	0.01936	2	2	2.191	4
HDLP+YE+NH_4Cl CDM yield vs. HDLP+NH_4Cl CDM yield	0.4750	0.6250	-0.1500	0.01936	2	2	10.95	4
HDLP+YE+NH_4Cl CDM yield vs. Glucose+YE CDM yield	0.4750	0.3900	0.08500	0.01936	2	2	6.208	4
HDLP+NH_4Cl CDM yield vs. Glucose+YE CDM yield	0.6250	0.3900	0.2350	0.01936	2	2	17.16	4

Table B.3 One-way ANOVA and pairwise Tukey test for final PHA concentration with hydrolyzed DLP supplemented with yeast extract (YE) and ammonium chloride (NH_4Cl), and glucose and supplemented with yeast extract (as illustrated in Figure 4.8).

Table Analyzed	One-way ANOVA
Data sets analyzed	A-D
ANOVA summary	
F	17.71
P value	0.0090
P value summary	**
Significant diff. among means (P < 0.05)?	Yes
R squared	0.9300

Number of families	1							
Number of comparisons per family	6							
Alpha	0.05							
Tukey's multiple comparisons test	**Mean Diff.**	**95.00% CI of diff.**	**Below threshold?**	**Summary**	**Adjusted P Value**			
HDLP+YE PHA vs. HDLP+YE+NH_4Cl PHA	0.1800	-0.5337 to 0.8937	No	ns	0.7454	A-B		
HDLP+YE PHA vs. HDLP+NH_4Cl PHA	0.9400	0.2263 to 1.654	Yes	*	0.0198	A-C		
HDLP+YE PHA vs. Glucose+YE PHA	1.025	0.3113 to 1.739	Yes	*	0.0146	A-D		
HDLP+YE+NH_4Cl PHA vs. HDLP+NH_4Cl PHA	0.7600	0.04629 to 1.474	Yes	*	0.0408	B-C		
HDLP+YE+NH_4Cl PHA vs. Glucose+YE PHA	0.8450	0.1313 to 1.559	Yes	*	0.0286	B-D		
HDLP+NH_4Cl PHA vs. Glucose+YE PHA	0.08500	-0.6287 to 0.7987	No	ns	0.9585	C-D		
Test details	**Mean 1**	**Mean 2**	**Mean Diff.**	**SE of diff.**	**n1**	**n2**	**q**	**DF**
HDLP+YE PHA vs. HDLP+YE+NH_4Cl PHA	3.445	3.265	0.1800	0.1753	2	2	1.452	4
HDLP+YE PHA vs. HDLP+NH_4Cl PHA	3.445	2.505	0.9400	0.1753	2	2	7.582	4
HDLP+YE PHA vs. Glucose+YE PHA	3.445	2.420	1.025	0.1753	2	2	8.268	4
HDLP+YE+NH_4Cl PHA vs. HDLP+NH_4Cl PHA	3.265	2.505	0.7600	0.1753	2	2	6.130	4
HDLP+YE+NH_4Cl PHA vs. Glucose+YE PHA	3.265	2.420	0.8450	0.1753	2	2	6.816	4
HDLP+NH_4Cl PHA vs. Glucose+YE PHA	2.505	2.420	0.08500	0.1753	2	2	0.6856	4

Table B.4 One-way ANOVA and pairwise Tukey test for PHA yield with hydrolyzed DLP supplemented with yeast extract (YE) and ammonium chloride (NH_4Cl), and glucose and supplemented with yeast extract (as illustrated in Figure 4.8).

Table Analyzed	One-way ANOVA
Data sets analyzed	A-D
ANOVA summary	
F	40.12
P value	0.0019
P value summary	**
Significant diff. among means (P < 0.05)?	Yes
R squared	0.9678

Number of families	1							
Number of comparisons per family	6							
Alpha	0.05							
Tukey's multiple comparisons test	**Mean Diff.**	**95.00% CI of diff.**	**Below threshold?**	**Summary**	**Adjusted P Value**			
HDLP+YE PHA yield vs. HDLP+YE+NH_4Cl PHA yield	-0.04500	-0.1125 to 0.02251	No	ns	0.1623	A-B		
HDLP+YE PHA yield vs. HDLP+NH_4Cl PHA yield	-0.09500	-0.1625 to -0.02749	Yes	*	0.0157	A-C		
HDLP+YE PHA yield vs. Glucose+YE PHA yield	0.08000	0.01249 to 0.1475	Yes	*	0.0285	A-D		
HDLP+YE+NH_4Cl PHA yield vs. HDLP+NH_4Cl PHA yield	-0.05000	-0.1175 to 0.01751	No	ns	0.1227	B-C		
HDLP+YE+NH_4Cl PHA yield vs. Glucose+YE PHA yield	0.1250	0.05749 to 0.1925	Yes	**	0.0057	B-D		
HDLP+NH_4Cl PHA yield vs. Glucose+YE PHA yield	0.1750	0.1075 to 0.2425	Yes	**	0.0016	C-D		
Test details	**Mean 1**	**Mean 2**	**Mean Diff.**	**SE of diff.**	**n1**	**n2**	**q**	**DF**
HDLP+YE PHA yield vs. HDLP+YE+NH_4Cl PHA yield	0.2450	0.2900	-0.04500	0.01658	2	2	3.838	4
HDLP+YE PHA yield vs. HDLP+NH_4Cl PHA yield	0.2450	0.3400	-0.09500	0.01658	2	2	8.102	4
HDLP+YE PHA yield vs. Glucose+YE PHA yield	0.2450	0.1650	0.08000	0.01658	2	2	6.822	4
HDLP+YE+NH_4Cl PHA yield vs. HDLP+NH_4Cl PHA yield	0.2900	0.3400	-0.05000	0.01658	2	2	4.264	4
HDLP+YE+NH_4Cl PHA yield vs. Glucose+YE PHA yield	0.2900	0.1650	0.1250	0.01658	2	2	10.66	4
HDLP+NH_4Cl PHA yield vs. Glucose+YE PHA yield	0.3400	0.1650	0.1750	0.01658	2	2	14.92	4

Table B.5 One-way ANOVA and pairwise Tukey test for PHA content with hydrolyzed DLP supplemented with yeast extract (YE) and ammonium chloride (NH_4Cl), and glucose and supplemented with yeast extract (as illustrated in Figure 4.9).

Table Analyzed	One-way ANOVA
Data sets analyzed	A-D
ANOVA summary	
F	22.87
P value	0.0056
P value summary	**
Significant diff. among means (P < 0.05)?	Yes
R squared	0.9449

Number of families	1							
Number of comparisons per family	6							
Alpha	0.05							
Tukey's multiple comparisons test	**Mean Diff.**	**95.00% CI of diff.**	**Below threshold?**	**Summary**	**Adjusted P Value**			
HDLP+YE PHA content vs. HDLP+YE+NH_4Cl PHA content	-0.03000	-0.1276 to 0.06762	No	ns	0.6325	A-B		
HDLP+YE PHA content vs. HDLP+NH_4Cl PHA content	0.04500	-0.05262 to 0.1426	No	ns	0.3623	A-C		
HDLP+YE PHA content vs. Glucose+YE PHA content	0.1550	0.05738 to 0.2526	Yes	*	0.0101	A-D		
HDLP+YE+NH_4Cl PHA content vs. HDLP+NH_4Cl PHA content	0.07500	-0.02262 to 0.1726	No	ns	0.1108	B-C		
HDLP+YE+NH_4Cl PHA content vs. Glucose+YE PHA content	0.1850	0.08738 to 0.2826	Yes	**	0.0053	B-D		
HDLP+NH_4Cl PHA content vs. Glucose+YE PHA content	0.1100	0.01238 to 0.2076	Yes	*	0.0338	C-D		
Test details	**Mean 1**	**Mean 2**	**Mean Diff.**	**SE of diff.**	**n1**	**n2**	**q**	**DF**
HDLP+YE PHA content vs. HDLP+YE+NH_4Cl PHA content	0.5750	0.6050	-0.03000	0.02398	2	2	1.769	4
HDLP+YE PHA content vs. HDLP+NH_4Cl PHA content	0.5750	0.5300	0.04500	0.02398	2	2	2.654	4
HDLP+YE PHA content vs. Glucose+YE PHA content	0.5750	0.4200	0.1550	0.02398	2	2	9.141	4
HDLP+YE+NH_4Cl PHA content vs. HDLP+NH_4Cl PHA content	0.6050	0.5300	0.07500	0.02398	2	2	4.423	4
HDLP+YE+NH_4Cl PHA content vs. Glucose+YE PHA content	0.6050	0.4200	0.1850	0.02398	2	2	10.91	4
HDLP+NH_4Cl PHA content vs. Glucose+YE PHA content	0.5300	0.4200	0.1100	0.02398	2	2	6.487	4

Appendix C. Chapter 5 statistical analysis reports

Table C.1 Two-way ANOVA and pairwise Tukey test for final cell dry mass (CDM) concentration of batch loading study (as illustrated in Figure 5.5).

Table Analyzed	Grouped: Two-way ANOVA (three data sets)				
Two-way ANOVA	Ordinary				
Alpha	0.05				
Source of Variation	**% of total variation**	**P value**	**P value summary**	**Significant?**	
Interaction	33.03	<0.0001	****	Yes	
Row Factor	11.01	<0.0001	****	Yes	
Column Factor	54.15	<0.0001	****	Yes	
ANOVA table	**SS**	**DF**	**MS**	**F (DFn, DFd)**	**P value**
Interaction	16.69	6	2.781	F (6, 12) = 36.52	P<0.0001
Row Factor	5.560	3	1.853	F (3, 12) = 24.34	P<0.0001
Column Factor	27.35	2	13.68	F (2, 12) = 179.6	P<0.0001
Residual	0.9139	12	0.07615		
Data summary					
Number of columns (Column Factor)	3				
Number of rows (Row Factor)	4				
Number of values	24				

Compare cell means with others in its row and its column					
Number of families	7				
Number of comparisons per row family	3				
Number of comparisons per column family	6				
Alpha	0.05				
Tukey's multiple comparisons test	**Mean Diff.**	**95.00% CI of diff.**	**Below threshold?**	**Summary**	**Adjusted P Value**
10					
HDLP CDM vs. HWP CDM	0.3250	-0.4112 to 1.061	No	ns	0.4879
HDLP CDM vs. Glucose CDM	0.7400	0.003775 to 1.476	Yes	*	0.0488
HWP CDM vs. Glucose CDM	0.4150	-0.3212 to 1.151	No	ns	0.3236
20					
HDLP CDM vs. HWP CDM	-2.770	-3.506 to -2.034	Yes	****	<0.0001
HDLP CDM vs. Glucose CDM	-2.370	-3.106 to -1.634	Yes	****	<0.0001
HWP CDM vs. Glucose CDM	0.4000	-0.3362 to 1.136	No	ns	0.3482
30					
HDLP CDM vs. HWP CDM	-4.230	-4.966 to -3.494	Yes	****	<0.0001
HDLP CDM vs. Glucose CDM	-1.915	-2.651 to -1.179	Yes	****	<0.0001
HWP CDM vs. Glucose CDM	2.315	1.579 to 3.051	Yes	****	<0.0001
40					
HDLP CDM vs. HWP CDM	-3.675	-4.411 to -2.939	Yes	****	<0.0001
HDLP CDM vs. Glucose CDM	-0.3200	-1.056 to 0.4162	No	ns	0.4980
HWP CDM vs. Glucose CDM	3.355	2.619 to 4.091	Yes	****	<0.0001

HDLP CDM					
10 vs. 20	2.225	1.406 to 3.044	Yes	****	<0.0001
10 vs. 30	2.090	1.271 to 2.909	Yes	****	<0.0001
10 vs. 40	2.675	1.856 to 3.494	Yes	****	<0.0001
20 vs. 30	-0.1350	-0.9543 to 0.6843	No	ns	0.9600
20 vs. 40	0.4500	-0.3693 to 1.269	No	ns	0.3990
30 vs. 40	0.5850	-0.2343 to 1.404	No	ns	0.2017
HWP CDM					
10 vs. 20	-0.8700	-1.689 to -0.05070	Yes	*	0.0364
10 vs. 30	-2.465	-3.284 to -1.646	Yes	****	<0.0001
10 vs. 40	-1.325	-2.144 to -0.5057	Yes	**	0.0021
20 vs. 30	-1.595	-2.414 to -0.7757	Yes	***	0.0004
20 vs. 40	-0.4550	-1.274 to 0.3643	No	ns	0.3900
30 vs. 40	1.140	0.3207 to 1.959	Yes	**	0.0066
Glucose CDM					
10 vs. 20	-0.8850	-1.704 to -0.06570	Yes	*	0.0331
10 vs. 30	-0.5650	-1.384 to 0.2543	No	ns	0.2249
10 vs. 40	1.615	0.7957 to 2.434	Yes	***	0.0004
20 vs. 30	0.3200	-0.4993 to 1.139	No	ns	0.6619
20 vs. 40	2.500	1.681 to 3.319	Yes	****	<0.0001
30 vs. 40	2.180	1.361 to 2.999	Yes	****	<0.0001

Table C.2 Two-way ANOVA and pairwise Tukey test for cell dry mass (CDM) yield of batch loading study (as illustrated in Figure 5.5).

Table Analyzed	Grouped: Two-way ANOVA (three data sets)				
Two-way ANOVA	Ordinary				
Alpha	0.05				
Source of Variation	**% of total variation**	**P value**	**P value summary**	**Significant?**	
Interaction	15.26	<0.0001	****	Yes	
Row Factor	74.65	<0.0001	****	Yes	
Column Factor	8.779	<0.0001	****	Yes	
ANOVA table	**SS**	**DF**	**MS**	**F (DFn, DFd)**	**P value**
Interaction	0.08074	6	0.01346	F (6, 12) = 23.24	P<0.0001
Row Factor	0.3950	3	0.1317	F (3, 12) = 227.4	P<0.0001
Column Factor	0.04646	2	0.02323	F (2, 12) = 40.11	P<0.0001
Residual	0.006950	12	0.0005792		
Data summary					
Number of columns (Column Factor)	3				
Number of rows (Row Factor)	4				
Number of values	24				

Compare cell means with others in its row and its column					
Number of families	7				
Number of comparisons per row family	3				
Number of comparisons per column family	6				
Alpha	0.05				
Tukey's multiple comparisons test	**Mean Diff.**	**95.00% CI of diff.**	**Below threshold?**	**Summary**	**Adjusted P Value**
10					
HDLP CDM yield vs. HWP CDM yield	0.1300	0.06580 to 0.1942	Yes	***	0.0004
HDLP CDM yield vs. Glucose CDM yield	0.2550	0.1908 to 0.3192	Yes	****	<0.0001
HWP CDM yield vs. Glucose CDM yield	0.1250	0.06080 to 0.1892	Yes	***	0.0006
20					
HDLP CDM yield vs. HWP CDM yield	-0.1650	-0.2292 to -0.1008	Yes	****	<0.0001
HDLP CDM yield vs. Glucose CDM yield	-0.08000	-0.1442 to -0.01580	Yes	*	0.0155
HWP CDM yield vs. Glucose CDM yield	0.08500	0.02080 to 0.1492	Yes	*	0.0107
30					
HDLP CDM yield vs. HWP CDM yield	-0.1250	-0.1892 to -0.06080	Yes	***	0.0006
HDLP CDM yield vs. Glucose CDM yield	-0.02000	-0.08420 to 0.04420	No	ns	0.6917
HWP CDM yield vs. Glucose CDM yield	0.1050	0.04080 to 0.1692	Yes	**	0.0025
40					
HDLP CDM yield vs. HWP CDM yield	-0.1150	-0.1792 to -0.05080	Yes	**	0.0012
HDLP CDM yield vs. Glucose CDM yield	-0.005000	-0.06920 to 0.05920	No	ns	0.9765
HWP CDM yield vs. Glucose CDM yield	0.1100	0.04580 to 0.1742	Yes	**	0.0017

HDLP CDM yield					
10 vs. 20	0.4400	0.3686 to 0.5114	Yes	****	<0.0001
10 vs. 30	0.4500	0.3786 to 0.5214	Yes	****	<0.0001
10 vs. 40	0.5100	0.4386 to 0.5814	Yes	****	<0.0001
20 vs. 30	0.01000	-0.06145 to 0.08145	No	ns	0.9748
20 vs. 40	0.07000	-0.001449 to 0.1414	No	ns	0.0555
30 vs. 40	0.06000	-0.01145 to 0.1314	No	ns	0.1117
HWP CDM yield					
10 vs. 20	0.1450	0.07355 to 0.2164	Yes	***	0.0003
10 vs. 30	0.1950	0.1236 to 0.2664	Yes	****	<0.0001
10 vs. 40	0.2650	0.1936 to 0.3364	Yes	****	<0.0001
20 vs. 30	0.05000	-0.02145 to 0.1214	No	ns	0.2150
20 vs. 40	0.1200	0.04855 to 0.1914	Yes	**	0.0016
30 vs. 40	0.07000	-0.001449 to 0.1414	No	ns	0.0555
Glucose CDM yield					
10 vs. 20	0.1050	0.03355 to 0.1764	Yes	**	0.0044
10 vs. 30	0.1750	0.1036 to 0.2464	Yes	****	<0.0001
10 vs. 40	0.2500	0.1786 to 0.3214	Yes	****	<0.0001
20 vs. 30	0.07000	-0.001449 to 0.1414	No	ns	0.0555
20 vs. 40	0.1450	0.07355 to 0.2164	Yes	***	0.0003
30 vs. 40	0.07500	0.003551 to 0.1464	Yes	*	0.0387

Table C.3 Two-way ANOVA and pairwise Tukey test for final PHA concentration of batch loading study (as illustrated in Figure 5.6).

Table Analyzed	Grouped: Two-way ANOVA (three data sets)				
Two-way ANOVA	Ordinary				
Alpha	0.05				
Source of Variation	**% of total variation**	**P value**	**P value summary**	**Significant?**	
Interaction	17.40	<0.0001	****	Yes	
Row Factor	4.029	0.0013	**	Yes	
Column Factor	76.99	<0.0001	****	Yes	
ANOVA table	**SS**	**DF**	**MS**	**F (DFn, DFd)**	**P value**
Interaction	4.741	6	0.7901	F (6, 12) = 22.03	P<0.0001
Row Factor	1.098	3	0.3659	F (3, 12) = 10.21	P=0.0013
Column Factor	20.98	2	10.49	F (2, 12) = 292.5	P<0.0001
Residual	0.4303	12	0.03586		
Data summary					
Number of columns (Column Factor)	3				
Number of rows (Row Factor)	4				
Number of values	24				

Compare cell means with others in its row and its column					
Number of families	7				
Number of comparisons per row family	3				
Number of comparisons per column family	6				
Alpha	0.05				
Tukey's multiple comparisons test	**Mean Diff.**	**95.00% CI of diff.**	**Below threshold?**	**Summary**	**Adjusted P Value**
10					
HDLP PHAvs. HWP PHA	-0.1400	-0.6452 to 0.3652	No	ns	0.7455
HDLP PHAvs. Glucose PHA	0.7500	0.2448 to 1.255	Yes	**	0.0050
HWP PHA vs. Glucose PHA	0.8900	0.3848 to 1.395	Yes	**	0.0014
20					
HDLP PHAvs. HWP PHA	-2.130	-2.635 to -1.625	Yes	****	<0.0001
HDLP PHAvs. Glucose PHA	-0.2500	-0.7552 to 0.2552	No	ns	0.4113
HWP PHA vs. Glucose PHA	1.880	1.375 to 2.385	Yes	****	<0.0001
30					
HDLP PHAvs. HWP PHA	-2.670	-3.175 to -2.165	Yes	****	<0.0001
HDLP PHAvs. Glucose PHA	0.1650	-0.3402 to 0.6702	No	ns	0.6677
HWP PHA vs. Glucose PHA	2.835	2.330 to 3.340	Yes	****	<0.0001
40					
HDLP PHAvs. HWP PHA	-2.580	-3.085 to -2.075	Yes	****	<0.0001
HDLP PHAvs. Glucose PHA	0.1050	-0.4002 to 0.6102	No	ns	0.8462
HWP PHA vs. Glucose PHA	2.685	2.180 to 3.190	Yes	****	<0.0001

HDLP PHA					
10 vs. 20	0.8850	0.3228 to 1.447	Yes	**	0.0026
10 vs. 30	0.6150	0.05280 to 1.177	Yes	*	0.0308
10 vs. 40	1.190	0.6278 to 1.752	Yes	***	0.0002
20 vs. 30	-0.2700	-0.8322 to 0.2922	No	ns	0.5081
20 vs. 40	0.3050	-0.2572 to 0.8672	No	ns	0.4091
30 vs. 40	0.5750	0.01280 to 1.137	Yes	*	0.0445
HWP PHA					
10 vs. 20	-1.105	-1.667 to -0.5428	Yes	***	0.0004
10 vs. 30	-1.915	-2.477 to -1.353	Yes	****	<0.0001
10 vs. 40	-1.250	-1.812 to -0.6878	Yes	***	0.0001
20 vs. 30	-0.8100	-1.372 to -0.2478	Yes	**	0.0051
20 vs. 40	-0.1450	-0.7072 to 0.4172	No	ns	0.8683
30 vs. 40	0.6650	0.1028 to 1.227	Yes	*	0.0194
Glucose PHA					
10 vs. 20	-0.1150	-0.6772 to 0.4472	No	ns	0.9278
10 vs. 30	0.03000	-0.5322 to 0.5922	No	ns	0.9985
10 vs. 40	0.5450	-0.01720 to 1.107	No	ns	0.0585
20 vs. 30	0.1450	-0.4172 to 0.7072	No	ns	0.8683
20 vs. 40	0.6600	0.09780 to 1.222	Yes	*	0.0203
30 vs. 40	0.5150	-0.04720 to 1.077	No	ns	0.0766

Table C.4 Two-way ANOVA and pairwise Tukey test for PHA yield of batch loading study (as illustrated in Figure 5.6).

Table Analyzed	Grouped: Two-way ANOVA (three data sets)				
Two-way ANOVA	Ordinary				
Alpha	0.05				
Source of Variation	**% of total variation**	**P value**	**P value summary**	**Significant?**	
Interaction	12.34	<0.0001	****	Yes	
Row Factor	50.26	<0.0001	****	Yes	
Column Factor	35.60	<0.0001	****	Yes	
ANOVA table	**SS**	**DF**	**MS**	**F (DFn, DFd)**	**P value**
Interaction	0.02167	6	0.003611	F (6, 12) = 13.76	P<0.0001
Row Factor	0.08825	3	0.02942	F (3, 12) = 112.1	P<0.0001
Column Factor	0.06250	2	0.03125	F (2, 12) = 119.0	P<0.0001
Residual	0.003150	12	0.0002625		
Data summary					
Number of columns (Column Factor)	3				
Number of rows (Row Factor)	4				
Number of values	24				

Compare cell means with others in its row and its column					
Number of families	7				
Number of comparisons per row family	3				
Number of comparisons per column family	6				
Alpha	0.05				
Tukey's multiple comparisons test	**Mean Diff.**	**95.00% CI of diff.**	**Below threshold?**	**Summary**	**Adjusted P Value**
10					
HDLP PHA yield vs. HWP PHA yield	0.03000	-0.01322 to 0.07322	No	ns	0.1951
HDLP PHA yield vs. Glucose PHA yield	0.1750	0.1318 to 0.2182	Yes	****	<0.0001
HWP PHA yield vs. Glucose PHA yield	0.1450	0.1018 to 0.1882	Yes	****	<0.0001
20					
HDLP PHA yield vs. HWP PHA yield	-0.1250	-0.1682 to -0.08178	Yes	****	<0.0001
HDLP PHA yield vs. Glucose PHA yield	0.02000	-0.02322 to 0.06322	No	ns	0.4566
HWP PHA yield vs. Glucose PHA yield	0.1450	0.1018 to 0.1882	Yes	****	<0.0001
30					
HDLP PHA yield vs. HWP PHA yield	-0.07500	-0.1182 to -0.03178	Yes	**	0.0016
HDLP PHA yield vs. Glucose PHA yield	0.04500	0.001776 to 0.08822	Yes	*	0.0412
HWP PHA yield vs. Glucose PHA yield	0.1200	0.07678 to 0.1632	Yes	****	<0.0001
40					
HDLP PHA yield vs. HWP PHA yield	-0.08000	-0.1232 to -0.03678	Yes	***	0.0009
HDLP PHA yield vs. Glucose PHA yield	0.01000	-0.03322 to 0.05322	No	ns	0.8136
HWP PHA yield vs. Glucose PHA yield	0.09000	0.04678 to 0.1332	Yes	***	0.0003

HDLP PHA yield					
10 vs. 20	0.2050	0.1569 to 0.2531	Yes	****	<0.0001
10 vs. 30	0.2050	0.1569 to 0.2531	Yes	****	<0.0001
10 vs. 40	0.2550	0.2069 to 0.3031	Yes	****	<0.0001
20 vs. 30	0.000	-0.04810 to 0.04810	No	ns	>0.9999
20 vs. 40	0.05000	0.001898 to 0.09810	Yes	*	0.0408
30 vs. 40	0.05000	0.001898 to 0.09810	Yes	*	0.0408
HWP PHA yield					
10 vs. 20	0.05000	0.001898 to 0.09810	Yes	*	0.0408
10 vs. 30	0.1000	0.05190 to 0.1481	Yes	***	0.0002
10 vs. 40	0.1450	0.09690 to 0.1931	Yes	****	<0.0001
20 vs. 30	0.05000	0.001898 to 0.09810	Yes	*	0.0408
20 vs. 40	0.09500	0.04690 to 0.1431	Yes	***	0.0004
30 vs. 40	0.04500	-0.003102 to 0.09310	No	ns	0.0694
Glucose PHA yield					
10 vs. 20	0.05000	0.001898 to 0.09810	Yes	*	0.0408
10 vs. 30	0.07500	0.02690 to 0.1231	Yes	**	0.0028
10 vs. 40	0.09000	0.04190 to 0.1381	Yes	***	0.0006
20 vs. 30	0.02500	-0.02310 to 0.07310	No	ns	0.4441
20 vs. 40	0.04000	-0.008102 to 0.08810	No	ns	0.1162
30 vs. 40	0.01500	-0.03310 to 0.06310	No	ns	0.7919

Table C.5 Two-way ANOVA and pairwise Tukey test for PHA content of batch loading (as illustrated in Figure 5.7).

Table Analyzed	Grouped: Two-way ANOVA (three data sets)				
Two-way ANOVA	Ordinary				
Alpha	0.05				
Source of Variation	**% of total variation**	**P value**	**P value summary**	**Significant?**	
Interaction	11.25	0.0354	*	Yes	
Row Factor	6.033	0.0463	*	Yes	
Column Factor	76.01	<0.0001	****	Yes	
ANOVA table	**SS**	**DF**	**MS**	**F (DFn, DFd)**	**P value**
Interaction	0.05196	6	0.008660	F (6, 12) = 3.352	P=0.0354
Row Factor	0.02787	3	0.009289	F (3, 12) = 3.596	P=0.0463
Column Factor	0.3511	2	0.1756	F (2, 12) = 67.96	P<0.0001
Residual	0.03100	12	0.002583		
Data summary					
Number of columns (Column Factor)	3				
Number of rows (Row Factor)	4				
Number of values	24				

Compare cell means with others in its row and its column					
Number of families	7				
Number of comparisons per row family	3				
Number of comparisons per column family	6				
Alpha	0.05				
Tukey's multiple comparisons test	**Mean Diff.**	**95.00% CI of diff.**	**Below threshold?**	**Summary**	**Adjusted P Value**
10					
HDLP PHA content vs. HWP PHA content	-0.08000	-0.2156 to 0.05560	No	ns	0.2937
HDLP PHA content vs. Glucose PHA content	0.1050	-0.03060 to 0.2406	No	ns	0.1390
HWP PHA content vs. Glucose PHA content	0.1850	0.04940 to 0.3206	Yes	**	0.0088
20					
HDLP PHA content vs. HWP PHA content	-0.08500	-0.2206 to 0.05060	No	ns	0.2552
HDLP PHA content vs. Glucose PHA content	0.2800	0.1444 to 0.4156	Yes	***	0.0004
HWP PHA content vs. Glucose PHA content	0.3650	0.2294 to 0.5006	Yes	****	<0.0001
30					
HDLP PHA content vs. HWP PHA content	0.05500	-0.08060 to 0.1906	No	ns	0.5424
HDLP PHA content vs. Glucose PHA content	0.3800	0.2444 to 0.5156	Yes	****	<0.0001
HWP PHA content vs. Glucose PHA content	0.3250	0.1894 to 0.4606	Yes	****	<0.0001
40					
HDLP PHA content vs. HWP PHA content	-0.04500	-0.1806 to 0.09060	No	ns	0.6593
HDLP PHA content vs. Glucose PHA content	0.1750	0.03940 to 0.3106	Yes	*	0.0125
HWP PHA content vs. Glucose PHA content	0.2200	0.08440 to 0.3556	Yes	**	0.0026

HDLP PHA content					
10 vs. 20	-0.1200	-0.2709 to 0.03090	No	ns	0.1384
10 vs. 30	-0.2100	-0.3609 to -0.05910	Yes	**	0.0066
10 vs. 40	-0.1250	-0.2759 to 0.02590	No	ns	0.1181
20 vs. 30	-0.09000	-0.2409 to 0.06090	No	ns	0.3327
20 vs. 40	-0.005000	-0.1559 to 0.1459	No	ns	0.9996
30 vs. 40	0.08500	-0.06590 to 0.2359	No	ns	0.3785
HWP PHA content					
10 vs. 20	-0.1250	-0.2759 to 0.02590	No	ns	0.1181
10 vs. 30	-0.07500	-0.2259 to 0.07590	No	ns	0.4805
10 vs. 40	-0.09000	-0.2409 to 0.06090	No	ns	0.3327
20 vs. 30	0.05000	-0.1009 to 0.2009	No	ns	0.7612
20 vs. 40	0.03500	-0.1159 to 0.1859	No	ns	0.8995
30 vs. 40	-0.01500	-0.1659 to 0.1359	No	ns	0.9906
Glucose PHA content					
10 vs. 20	0.05500	-0.09590 to 0.2059	No	ns	0.7064
10 vs. 30	0.06500	-0.08590 to 0.2159	No	ns	0.5923
10 vs. 40	-0.05500	-0.2059 to 0.09590	No	ns	0.7064
20 vs. 30	0.01000	-0.1409 to 0.1609	No	ns	0.9971
20 vs. 40	-0.1100	-0.2609 to 0.04090	No	ns	0.1885
30 vs. 40	-0.1200	-0.2709 to 0.03090	No	ns	0.1384

Table C.6 Unpaired t-test for final cell dry mass (CDM) concentration of 6 L batch bioreactor (as illustrated in Figure 5.11).

Table Analyzed	t-test
Column B	20 g/l HDLP CDM
vs.	vs.
Column A	10 g/l HDLP CDM
Unpaired t test	
P value	0.0057
P value summary	**
Significantly different (P < 0.05)?	Yes
One- or two-tailed P value?	Two-tailed
t, df	t=13.16, df=2

Table C.7 Unpaired for t-test final PHA concentration of 6 L batch bioreactor (as illustrated in Figure 5.11).

Table Analyzed	t-test
Column B	20 g/l HDLP PHA
vs.	vs.
Column A	10 g/l HDLP PHA
Unpaired t test	
P value	0.0169
P value summary	*
Significantly different (P < 0.05)?	Yes
One- or two-tailed P value?	Two-tailed
t, df	t=7.586, df=2

Table C.8 Unpaired t-test for cell dry mass (CDM) yield of 6 L batch bioreactor study (as illustrated in Figure 5.12).

Table Analyzed	t-test
Column B	20 g/l HDLP CDM yield
vs.	vs.
Column A	10 g/l HDLP CDM yield
Unpaired t test	
P value	0.0028
P value summary	**
Significantly different (P < 0.05)?	Yes
One- or two-tailed P value?	Two-tailed
t, df	t=18.78, df=2

Table C.9 Unpaired t-test for PHA yield of 6 L batch bioreactor study (as illustrated in Figure 5.12).

Table Analyzed	t-test
Column B	20 g/l HDLP PHA yield
vs.	vs.
Column A	10 g/l HDLP PHA yield
Unpaired t test	
P value	0.0012
P value summary	**
Significantly different (P < 0.05)?	Yes
One- or two-tailed P value?	Two-tailed
t, df	t=29.00, df=2

Table C.10 Unpaired t-test for PHA yield of 6 L batch bioreactor study (as illustrated in Figure 5.12).

Table Analyzed	t-test
Column B	20 g/l HDLP PHA
vs.	vs.
Column A	10 g/l HDLP PHA
Unpaired t test	
P value	0.0434
P value summary	*
Significantly different (P < 0.05)?	Yes
One- or two-tailed P value?	Two-tailed
t, df	t=4.642, df=2

Appendix D. Chapter 6 statistical analysis reports

Table D.1 One-way ANOVA and pairwise Tukey test for final CDM concentrations with fed-batch bioreactor operation and hydrolyzed DLP feed at different days (as illustrated in Figure 6.5).

Table Analyzed	One-way ANOVA
Data sets analyzed	A-D
ANOVA summary	
F	62.99
P value	0.0008
P value summary	***
Significant diff. among means (P < 0.05)?	Yes
R squared	0.9793

Number of families	1							
Number of comparisons per family	6							
Alpha	0.05							
Tukey's multiple comparisons test	**Mean Diff.**	**95.00% CI of diff.**	**Below threshold?**	**Summary**	**Adjusted P Value**			
HDLP day 4 CDM vs. HDLP day 8 CDM	-1.725	-2.591 to -0.8593	Yes	**	0.0044	A-B		
HDLP day 4 CDM vs. HDLP day 12 CDM	-0.03000	-0.8957 to 0.8357	No	ns	0.9988	A-C		
HDLP day 4 CDM vs. HDLP day 16 CDM	1.175	0.3093 to 2.041	Yes	*	0.0178	A-D		
HDLP day 8 CDM vs. HDLP day 12 CDM	1.695	0.8293 to 2.561	Yes	**	0.0047	B-C		
HDLP day 8 CDM vs. HDLP day 16 CDM	2.900	2.034 to 3.766	Yes	***	0.0006	B-D		
HDLP day 12 CDM vs. HDLP day 16 CDM	1.205	0.3393 to 2.071	Yes	*	0.0163	C-D		
Test details	**Mean 1**	**Mean 2**	**Mean Diff.**	**SE of diff.**	**n1**	**n2**	**q**	**DF**
HDLP day 4 CDM vs. HDLP day 8 CDM	3.465	5.190	-1.725	0.2127	2	2	11.47	4
HDLP day 4 CDM vs. HDLP day 12 CDM	3.465	3.495	-0.03000	0.2127	2	2	0.1995	4
HDLP day 4 CDM vs. HDLP day 16 CDM	3.465	2.290	1.175	0.2127	2	2	7.814	4
HDLP day 8 CDM vs. HDLP day 12 CDM	5.190	3.495	1.695	0.2127	2	2	11.27	4
HDLP day 8 CDM vs. HDLP day 16 CDM	5.190	2.290	2.900	0.2127	2	2	19.29	4
HDLP day 12 CDM vs. HDLP day 16 CDM	3.495	2.290	1.205	0.2127	2	2	8.013	4

Table D.2 One-way ANOVA and pairwise Tukey test for CDM yield with fed-batch bioreactor operation and hydrolyzed DLP feed at different days (as illustrated in Figure 6.5).

Table Analyzed	One-way ANOVA
Data sets analyzed	A-D
ANOVA summary	
F	221.4
P value	<0.0001
P value summary	****
Significant diff. among means (P < 0.05)?	Yes
R squared	0.9940

Number of families	1							
Number of comparisons per family	6							
Alpha	0.05							
Tukey's multiple comparisons test	**Mean Diff.**	**95.00% CI of diff.**	**Below threshold?**	**Summary**	**Adjusted P Value**			
HDLP day 4 CDM yield vs. HDLP day 8 CDM yield	0.1100	0.04249 to 0.1775	Yes	**	0.0092	A-B		
HDLP day 4 CDM yield vs. HDLP day 12 CDM yield	0.2950	0.2275 to 0.3625	Yes	***	0.0002	A-C		
HDLP day 4 CDM yield vs. HDLP day 16 CDM yield	0.3850	0.3175 to 0.4525	Yes	****	<0.0001	A-D		
HDLP day 8 CDM yield vs. HDLP day 12 CDM yield	0.1850	0.1175 to 0.2525	Yes	**	0.0013	B-C		
HDLP day 8 CDM yield vs. HDLP day 16 CDM yield	0.2750	0.2075 to 0.3425	Yes	***	0.0003	B-D		
HDLP day 12 CDM yield vs. HDLP day 16 CDM yield	0.09000	0.02249 to 0.1575	Yes	*	0.0190	C-D		
Test details	**Mean 1**	**Mean 2**	**Mean Diff.**	**SE of diff.**	**n1**	**n2**	**q**	**DF**
HDLP day 4 CDM yield vs. HDLP day 8 CDM yield	0.4850	0.3750	0.1100	0.01658	2	2	9.381	4
HDLP day 4 CDM yield vs. HDLP day 12 CDM yield	0.4850	0.1900	0.2950	0.01658	2	2	25.16	4
HDLP day 4 CDM yield vs. HDLP day 16 CDM yield	0.4850	0.1000	0.3850	0.01658	2	2	32.83	4
HDLP day 8 CDM yield vs. HDLP day 12 CDM yield	0.3750	0.1900	0.1850	0.01658	2	2	15.78	4
HDLP day 8 CDM yield vs. HDLP day 16 CDM yield	0.3750	0.1000	0.2750	0.01658	2	2	23.45	4
HDLP day 12 CDM yield vs. HDLP day 16 CDM yield	0.1900	0.1000	0.09000	0.01658	2	2	7.675	4

Table D.3 One-way ANOVA and pairwise Tukey test for final PHA concentrations with fed-batch bioreactor operation and hydrolyzed DLP feed at different days (as illustrated in Figure 6.6).

Table Analyzed	One-way ANOVA
Data sets analyzed	A-D
ANOVA summary	
F	29.57
P value	0.0034
P value summary	**
Significant diff. among means (P < 0.05)?	Yes
R squared	0.9569

Number of families	1							
Number of comparisons per family	6							
Alpha	0.05							
Tukey's multiple comparisons test	**Mean Diff.**	**95.00% CI of diff.**	**Below threshold?**	**Summary**	**Adjusted P Value**			
HDLP day 4 PHA vs. HDLP day 8 PHA	-1.640	-2.639 to -0.6414	Yes	**	0.0090	A-B		
HDLP day 4 PHA vs. HDLP day 12 PHA	-0.4550	-1.454 to 0.5436	No	ns	0.3699	A-C		
HDLP day 4 PHA vs. HDLP day 16 PHA	0.5850	-0.4136 to 1.584	No	ns	0.2220	A-D		
HDLP day 8 PHA vs. HDLP day 12 PHA	1.185	0.1864 to 2.184	Yes	*	0.0284	B-C		
HDLP day 8 PHA vs. HDLP day 16 PHA	2.225	1.226 to 3.224	Yes	**	0.0029	B-D		
HDLP day 12 PHA vs. HDLP day 16 PHA	1.040	0.04140 to 2.039	Yes	*	0.0438	C-D		
Test details	**Mean 1**	**Mean 2**	**Mean Diff.**	**SE of diff.**	**n1**	**n2**	**q**	**DF**
HDLP day 4 PHA vs. HDLP day 8 PHA	1.480	3.120	-1.640	0.2453	2	2	9.455	4
HDLP day 4 PHA vs. HDLP day 12 PHA	1.480	1.935	-0.4550	0.2453	2	2	2.623	4
HDLP day 4 PHA vs. HDLP day 16 PHA	1.480	0.8950	0.5850	0.2453	2	2	3.373	4
HDLP day 8 PHA vs. HDLP day 12 PHA	3.120	1.935	1.185	0.2453	2	2	6.832	4
HDLP day 8 PHA vs. HDLP day 16 PHA	3.120	0.8950	2.225	0.2453	2	2	12.83	4
HDLP day 12 PHA vs. HDLP day 16 PHA	1.935	0.8950	1.040	0.2453	2	2	5.996	4

Table D.4 One-way ANOVA and pairwise Tukey test for PHA yield with fed-batch bioreactor operation and hydrolyzed DLP feed at different days (as illustrated in Figure 6.6).

Table Analyzed	One-way ANOVA
Data sets analyzed	A-D
ANOVA summary	
F	58.00
P value	0.0009
P value summary	***
Significant diff. among means (P < 0.05)?	Yes
R squared	0.9775

Number of families	1							
Number of comparisons per family	6							
Alpha	0.05							
Tukey's multiple comparisons test	**Mean Diff.**	**95.00% CI of diff.**	**Below threshold?**	**Summary**	**Adjusted P Value**			
HDLP day 4 PHA yield vs. HDLP day 8 PHA yield	-0.03000	-0.09751 to 0.03751	No	ns	0.3863	A-B		
HDLP day 4 PHA yield vs. HDLP day 12 PHA yield	0.09500	0.02749 to 0.1625	Yes	*	0.0157	A-C		
HDLP day 4 PHA yield vs. HDLP day 16 PHA yield	0.1650	0.09749 to 0.2325	Yes	**	0.0020	A-D		
HDLP day 8 PHA yield vs. HDLP day 12 PHA yield	0.1250	0.05749 to 0.1925	Yes	**	0.0057	B-C		
HDLP day 8 PHA yield vs. HDLP day 16 PHA yield	0.1950	0.1275 to 0.2625	Yes	**	0.0010	B-D		
HDLP day 12 PHA yield vs. HDLP day 16 PHA yield	0.07000	0.002493 to 0.1375	Yes	*	0.0445	C-D		
Test details	**Mean 1**	**Mean 2**	**Mean Diff.**	**SE of diff.**	**n1**	**n2**	**q**	**DF**
HDLP day 4 PHA yield vs. HDLP day 8 PHA yield	0.2050	0.2350	-0.03000	0.01658	2	2	2.558	4
HDLP day 4 PHA yield vs. HDLP day 12 PHA yield	0.2050	0.1100	0.09500	0.01658	2	2	8.102	4
HDLP day 4 PHA yield vs. HDLP day 16 PHA yield	0.2050	0.04000	0.1650	0.01658	2	2	14.07	4
HDLP day 8 PHA yield vs. HDLP day 12 PHA yield	0.2350	0.1100	0.1250	0.01658	2	2	10.66	4
HDLP day 8 PHA yield vs. HDLP day 16 PHA yield	0.2350	0.04000	0.1950	0.01658	2	2	16.63	4
HDLP day 12 PHA yield vs. HDLP day 16 PHA yield	0.1100	0.04000	0.07000	0.01658	2	2	5.970	4

Table D.5 One-way ANOVA and pairwise Tukey test for PHA content with fed-batch bioreactor operation and hydrolyzed whey permeate feed at different days (as illustrated in Figure 6.7).

Table Analyzed	One-way ANOVA
Data sets analyzed	A-D
ANOVA summary	
F	17.16
P value	0.0095
P value summary	**
Significant diff. among means (P < 0.05)?	Yes
R squared	0.9279

Number of families	1							
Number of comparisons per family	6							
Alpha	0.05							
Tukey's multiple comparisons test	**Mean Diff.**	**95.00% CI of diff.**	**Below threshold?**	**Summary**	**Adjusted P Value**			
HDLP day 4 PHA content vs. HDLP day 8 PHA content	-0.1750	-0.3138 to -0.03620	Yes	*	0.0230	A-B		
HDLP day 4 PHA content vs. HDLP day 12 PHA content	-0.1250	-0.2638 to 0.01380	No	ns	0.0695	A-C		
HDLP day 4 PHA content vs. HDLP day 16 PHA content	0.03500	-0.1038 to 0.1738	No	ns	0.7454	A-D		
HDLP day 8 PHA content vs. HDLP day 12 PHA content	0.05000	-0.08880 to 0.1888	No	ns	0.5284	B-C		
HDLP day 8 PHA content vs. HDLP day 16 PHA content	0.2100	0.07120 to 0.3488	Yes	*	0.0121	B-D		
HDLP day 12 PHA content vs. HDLP day 16 PHA content	0.1600	0.02120 to 0.2988	Yes	*	0.0313	C-D		
Test details	**Mean 1**	**Mean 2**	**Mean Diff.**	**SE of diff.**	**n1**	**n2**	**q**	**DF**
HDLP day 4 PHA content vs. HDLP day 8 PHA content	0.4250	0.6000	-0.1750	0.03410	2	2	7.259	4
HDLP day 4 PHA content vs. HDLP day 12 PHA content	0.4250	0.5500	-0.1250	0.03410	2	2	5.185	4
HDLP day 4 PHA content vs. HDLP day 16 PHA content	0.4250	0.3900	0.03500	0.03410	2	2	1.452	4
HDLP day 8 PHA content vs. HDLP day 12 PHA content	0.6000	0.5500	0.05000	0.03410	2	2	2.074	4
HDLP day 8 PHA content vs. HDLP day 16 PHA content	0.6000	0.3900	0.2100	0.03410	2	2	8.710	4
HDLP day 12 PHA content vs. HDLP day 16 PHA content	0.5500	0.3900	0.1600	0.03410	2	2	6.636	4

Table D.6 One-way ANOVA and pairwise Tukey test for final CDM concentrations with fed-batch bioreactor operation and hydrolyzed whey permeate feed at different days (as illustrated in Figure 6.5).

Table Analyzed	One-way ANOVA
Data sets analyzed	A-F
ANOVA summary	
F	71.68
P value	<0.0001
P value summary	****
Significant diff. among means (P < 0.05)?	Yes
R squared	0.9835

Number of families	1					
Number of comparisons per family	15					
Alpha	0.05					
Tukey's multiple comparisons test	**Mean Diff.**	**95.00% CI of diff.**	**Below threshold?**	**Summary**	**Adjusted P Value**	
HWP day 4 CDM vs. HWP day 8 CDM	-3.170	-4.566 to -1.774	Yes	***	0.0008	A-B
HWP day 4 CDM vs. HWP day 12 CDM	-5.220	-6.616 to -3.824	Yes	****	<0.0001	A-C
HWP day 4 CDM vs. HWP day 16 CDM	-5.025	-6.421 to -3.629	Yes	****	<0.0001	A-D
HWP day 4 CDM vs. HWP day 20 CDM	-5.175	-6.571 to -3.779	Yes	****	<0.0001	A-E
HWP day 4 CDM vs. HWP day 24 CDM	-5.200	-6.596 to -3.804	Yes	****	<0.0001	A-F
HWP day 8 CDM vs. HWP day 12 CDM	-2.050	-3.446 to -0.6542	Yes	**	0.0083	B-C
HWP day 8 CDM vs. HWP day 16 CDM	-1.855	-3.251 to -0.4592	Yes	*	0.0137	B-D
HWP day 8 CDM vs. HWP day 20 CDM	-2.005	-3.401 to -0.6092	Yes	**	0.0093	B-E
HWP day 8 CDM vs. HWP day 24 CDM	-2.030	-3.426 to -0.6342	Yes	**	0.0088	B-F
HWP day 12 CDM vs. HWP day 16 CDM	0.1950	-1.201 to 1.591	No	ns	0.9907	C-D
HWP day 12 CDM vs. HWP day 20 CDM	0.04500	-1.351 to 1.441	No	ns	>0.9999	C-E
HWP day 12 CDM vs. HWP day 24 CDM	0.02000	-1.376 to 1.416	No	ns	>0.9999	C-F
HWP day 16 CDM vs. HWP day 20 CDM	-0.1500	-1.546 to 1.246	No	ns	0.9972	D-E
HWP day 16 CDM vs. HWP day 24 CDM	-0.1750	-1.571 to 1.221	No	ns	0.9943	D-F
HWP day 20 CDM vs. HWP day 24 CDM	-0.02500	-1.421 to 1.371	No	ns	>0.9999	E-F

Table D.7 One-way ANOVA and pairwise Tukey test for CDM yield with fed-batch bioreactor operation and hydrolyzed whey permeate feed at different days (as illustrated in Figure 6.5).

Table Analyzed	One-way ANOVA
Data sets analyzed	A-F
ANOVA summary	
F	68.32
P value	<0.0001
P value summary	****
Significant diff. among means (P < 0.05)?	Yes
R squared	0.9827

Number of families	1					
Number of comparisons per family	15					
Alpha	0.05					
Tukey's multiple comparisons test	**Mean Diff.**	**95.00% CI of diff.**	**Below threshold?**	**Summary**	**Adjusted P Value**	
HWP day 4 CDM yield vs. HWP day 8 CDM yield	-0.01500	-0.07010 to 0.04010	No	ns	0.8720	A-B
HWP day 4 CDM yield vs. HWP day 12 CDM yield	-0.01000	-0.06510 to 0.04510	No	ns	0.9717	A-C
HWP day 4 CDM yield vs. HWP day 16 CDM yield	0.06500	0.009902 to 0.1201	Yes	*	0.0241	A-D
HWP day 4 CDM yield vs. HWP day 20 CDM yield	0.1250	0.06990 to 0.1801	Yes	***	0.0008	A-E
HWP day 4 CDM yield vs. HWP day 24 CDM yield	0.1800	0.1249 to 0.2351	Yes	***	0.0001	A-F
HWP day 8 CDM yield vs. HWP day 12 CDM yield	0.005000	-0.05010 to 0.06010	No	ns	0.9987	B-C
HWP day 8 CDM yield vs. HWP day 16 CDM yield	0.08000	0.02490 to 0.1351	Yes	**	0.0088	B-D
HWP day 8 CDM yield vs. HWP day 20 CDM yield	0.1400	0.08490 to 0.1951	Yes	***	0.0004	B-E
HWP day 8 CDM yield vs. HWP day 24 CDM yield	0.1950	0.1399 to 0.2501	Yes	****	<0.0001	B-F
HWP day 12 CDM yield vs. HWP day 16 CDM yield	0.07500	0.01990 to 0.1301	Yes	*	0.0122	C-D
HWP day 12 CDM yield vs. HWP day 20 CDM yield	0.1350	0.07990 to 0.1901	Yes	***	0.0005	C-E
HWP day 12 CDM yield vs. HWP day 24 CDM yield	0.1900	0.1349 to 0.2451	Yes	****	<0.0001	C-F
HWP day 16 CDM yield vs. HWP day 20 CDM yield	0.06000	0.004902 to 0.1151	Yes	*	0.0346	D-E
HWP day 16 CDM yield vs. HWP day 24 CDM yield	0.1150	0.05990 to 0.1701	Yes	**	0.0013	D-F
HWP day 20 CDM yield vs. HWP day 24 CDM yield	0.05500	-9.848e-005 to 0.1101	No	ns	0.0504	E-F

Table D.8 One-way ANOVA and pairwise Tukey test for final PHA concentrations with fed-batch bioreactor operation and hydrolyzed whey permeate feed at different days (as illustrated in Figure 6.6).

Table Analyzed	One-way ANOVA
Data sets analyzed	A-F
ANOVA summary	
F	254.9
P value	<0.0001
P value summary	****
Significant diff. among means (P < 0.05)?	Yes
R squared	0.9953

Number of families	1					
Number of comparisons per family	15					
Alpha	0.05					
Tukey's multiple comparisons test	**Mean Diff.**	**95.00% CI of diff.**	**Below threshold?**	**Summary**	**Adjusted P Value**	
HWP day 4 PHA vs. HWP day 8 PHA	-2.085	-2.600 to -1.570	Yes	****	<0.0001	A-B
HWP day 4 PHA vs. HWP day 12 PHA	-3.345	-3.860 to -2.830	Yes	****	<0.0001	A-C
HWP day 4 PHA vs. HWP day 16 PHA	-3.670	-4.185 to -3.155	Yes	****	<0.0001	A-D
HWP day 4 PHA vs. HWP day 20 PHA	-3.710	-4.225 to -3.195	Yes	****	<0.0001	A-E
HWP day 4 PHA vs. HWP day 24 PHA	-3.480	-3.995 to -2.965	Yes	****	<0.0001	A-F
HWP day 8 PHA vs. HWP day 12 PHA	-1.260	-1.775 to -0.7454	Yes	***	0.0005	B-C
HWP day 8 PHA vs. HWP day 16 PHA	-1.585	-2.100 to -1.070	Yes	***	0.0001	B-D
HWP day 8 PHA vs. HWP day 20 PHA	-1.625	-2.140 to -1.110	Yes	***	0.0001	B-E
HWP day 8 PHA vs. HWP day 24 PHA	-1.395	-1.910 to -0.8804	Yes	***	0.0003	B-F
HWP day 12 PHA vs. HWP day 16 PHA	-0.3250	-0.8396 to 0.1896	No	ns	0.2522	C-D
HWP day 12 PHA vs. HWP day 20 PHA	-0.3650	-0.8796 to 0.1496	No	ns	0.1787	C-E
HWP day 12 PHA vs. HWP day 24 PHA	-0.1350	-0.6496 to 0.3796	No	ns	0.8869	C-F
HWP day 16 PHA vs. HWP day 20 PHA	-0.04000	-0.5546 to 0.4746	No	ns	0.9994	D-E
HWP day 16 PHA vs. HWP day 24 PHA	0.1900	-0.3246 to 0.7046	No	ns	0.6929	D-F
HWP day 20 PHA vs. HWP day 24 PHA	0.2300	-0.2846 to 0.7446	No	ns	0.5363	E-F

Test details	**Mean 1**	**Mean 2**	**Mean Diff.**	**SE of diff.**	**n1**	**n2**	**q**	**DF**
HWP day 4 PHA vs. HWP day 8 PHA	1.410	3.495	-2.085	0.1293	2	2	22.81	6
HWP day 4 PHA vs. HWP day 12 PHA	1.410	4.755	-3.345	0.1293	2	2	36.59	6
HWP day 4 PHA vs. HWP day 16 PHA	1.410	5.080	-3.670	0.1293	2	2	40.14	6
HWP day 4 PHA vs. HWP day 20 PHA	1.410	5.120	-3.710	0.1293	2	2	40.58	6
HWP day 4 PHA vs. HWP day 24 PHA	1.410	4.890	-3.480	0.1293	2	2	38.06	6
HWP day 8 PHA vs. HWP day 12 PHA	3.495	4.755	-1.260	0.1293	2	2	13.78	6
HWP day 8 PHA vs. HWP day 16 PHA	3.495	5.080	-1.585	0.1293	2	2	17.34	6
HWP day 8 PHA vs. HWP day 20 PHA	3.495	5.120	-1.625	0.1293	2	2	17.77	6
HWP day 8 PHA vs. HWP day 24 PHA	3.495	4.890	-1.395	0.1293	2	2	15.26	6
HWP day 12 PHA vs. HWP day 16 PHA	4.755	5.080	-0.3250	0.1293	2	2	3.555	6
HWP day 12 PHA vs. HWP day 20 PHA	4.755	5.120	-0.3650	0.1293	2	2	3.992	6
HWP day 12 PHA vs. HWP day 24 PHA	4.755	4.890	-0.1350	0.1293	2	2	1.477	6
HWP day 16 PHA vs. HWP day 20 PHA	5.080	5.120	-0.04000	0.1293	2	2	0.4375	6
HWP day 16 PHA vs. HWP day 24 PHA	5.080	4.890	0.1900	0.1293	2	2	2.078	6
HWP day 20 PHA vs. HWP day 24 PHA	5.120	4.890	0.2300	0.1293	2	2	2.516	6

Table D.9 PHA yield with fed-batch bioreactor operation and hydrolyzed whey permeate feed at different days. One-way ANOVA and pairwise Tukey test (as illustrated in Figure 6.6).

Table Analyzed	One-way ANOVA
Data sets analyzed	A-F
ANOVA summary	
F	50.60
P value	<0.0001
P value summary	****
Significant diff. among means (P < 0.05)?	Yes
R squared	0.9768

Number of families	1					
Number of comparisons per family	15					
Alpha	0.05					
Tukey's multiple comparisons test	**Mean Diff.**	**95.00% CI of diff.**	**Below threshold?**	**Summary**	**Adjusted P Value**	
HWP day 4 PHA yield vs. HWP day 8 PHA yield	-0.04000	-0.07250 to -0.007505	Yes	*	0.0197	A-B
HWP day 4 PHA yield vs. HWP day 12 PHA yield	-0.03500	-0.06750 to -0.002505	Yes	*	0.0363	A-C
HWP day 4 PHA yield vs. HWP day 16 PHA yield	-0.01000	-0.04250 to 0.02250	No	ns	0.8124	A-D
HWP day 4 PHA yield vs. HWP day 20 PHA yield	0.02500	-0.007495 to 0.05750	No	ns	0.1367	A-E
HWP day 4 PHA yield vs. HWP day 24 PHA yield	0.07000	0.03750 to 0.1025	Yes	**	0.0011	A-F
HWP day 8 PHA yield vs. HWP day 12 PHA yield	0.005000	-0.02750 to 0.03750	No	ns	0.9859	B-C
HWP day 8 PHA yield vs. HWP day 16 PHA yield	0.03000	-0.002495 to 0.06250	No	ns	0.0694	B-D
HWP day 8 PHA yield vs. HWP day 20 PHA yield	0.06500	0.03250 to 0.09750	Yes	**	0.0016	B-E
HWP day 8 PHA yield vs. HWP day 24 PHA yield	0.1100	0.07750 to 0.1425	Yes	****	<0.0001	B-F
HWP day 12 PHA yield vs. HWP day 16 PHA yield	0.02500	-0.007495 to 0.05750	No	ns	0.1367	C-D
HWP day 12 PHA yield vs. HWP day 20 PHA yield	0.06000	0.02750 to 0.09250	Yes	**	0.0025	C-E
HWP day 12 PHA yield vs. HWP day 24 PHA yield	0.1050	0.07250 to 0.1375	Yes	***	0.0001	C-F
HWP day 16 PHA yield vs. HWP day 20 PHA yield	0.03500	0.002505 to 0.06750	Yes	*	0.0363	D-E
HWP day 16 PHA yield vs. HWP day 24 PHA yield	0.08000	0.04750 to 0.1125	Yes	***	0.0005	D-F
HWP day 20 PHA yield vs. HWP day 24 PHA yield	0.04500	0.01250 to 0.07750	Yes	*	0.0112	E-F

Test details	**Mean 1**	**Mean 2**	**Mean Diff.**	**SE of diff.**	**n1**	**n2**	**q**	**DF**
HWP day 4 PHA yield vs. HWP day 8 PHA yield	0.2050	0.2450	-0.04000	0.008165	2	2	6.928	6
HWP day 4 PHA yield vs. HWP day 12 PHA yield	0.2050	0.2400	-0.03500	0.008165	2	2	6.062	6
HWP day 4 PHA yield vs. HWP day 16 PHA yield	0.2050	0.2150	-0.01000	0.008165	2	2	1.732	6
HWP day 4 PHA yield vs. HWP day 20 PHA yield	0.2050	0.1800	0.02500	0.008165	2	2	4.330	6
HWP day 4 PHA yield vs. HWP day 24 PHA yield	0.2050	0.1350	0.07000	0.008165	2	2	12.12	6
HWP day 8 PHA yield vs. HWP day 12 PHA yield	0.2450	0.2400	0.005000	0.008165	2	2	0.8660	6
HWP day 8 PHA yield vs. HWP day 16 PHA yield	0.2450	0.2150	0.03000	0.008165	2	2	5.196	6
HWP day 8 PHA yield vs. HWP day 20 PHA yield	0.2450	0.1800	0.06500	0.008165	2	2	11.26	6
HWP day 8 PHA yield vs. HWP day 24 PHA yield	0.2450	0.1350	0.1100	0.008165	2	2	19.05	6
HWP day 12 PHA yield vs. HWP day 16 PHA yield	0.2400	0.2150	0.02500	0.008165	2	2	4.330	6
HWP day 12 PHA yield vs. HWP day 20 PHA yield	0.2400	0.1800	0.06000	0.008165	2	2	10.39	6
HWP day 12 PHA yield vs. HWP day 24 PHA yield	0.2400	0.1350	0.1050	0.008165	2	2	18.19	6
HWP day 16 PHA yield vs. HWP day 20 PHA yield	0.2150	0.1800	0.03500	0.008165	2	2	6.062	6
HWP day 16 PHA yield vs. HWP day 24 PHA yield	0.2150	0.1350	0.08000	0.008165	2	2	13.86	6
HWP day 20 PHA yield vs. HWP day 24 PHA yield	0.1800	0.1350	0.04500	0.008165	2	2	7.794	6

Table D.10 One-way ANOVA and pairwise Tukey test for PHA content with fed-batch bioreactor operation and hydrolyzed whey permeate feed at different days (as illustrated in Figure 6.7).

Table Analyzed	One-way ANOVA
Data sets analyzed	A-F
ANOVA summary	
F	3.823
P value	0.0666
P value summary	ns
Significant diff. among means (P < 0.05)?	No
R squared	0.7611

Number of families	1					
Number of comparisons per family	15					
Alpha	0.05					
Tukey's multiple comparisons test	**Mean Diff.**	**95.00% CI of diff.**	**Below threshold?**	**Summary**	**Adjusted P Value**	
HWP day 4 PHA content vs. HWP day 8 PHA content	-0.08000	-0.2320 to 0.07198	No	ns	0.3946	A-B
HWP day 4 PHA content vs. HWP day 12 PHA content	-0.08500	-0.2370 to 0.06698	No	ns	0.3444	A-C
HWP day 4 PHA content vs. HWP day 16 PHA content	-0.1450	-0.2970 to 0.006983	No	ns	0.0608	A-D
HWP day 4 PHA content vs. HWP day 20 PHA content	-0.1400	-0.2920 to 0.01198	No	ns	0.0700	A-E
HWP day 4 PHA content vs. HWP day 24 PHA content	-0.1050	-0.2570 to 0.04698	No	ns	0.1941	A-F
HWP day 8 PHA content vs. HWP day 12 PHA content	-0.005000	-0.1570 to 0.1470	No	ns	>0.9999	B-C
HWP day 8 PHA content vs. HWP day 16 PHA content	-0.06500	-0.2170 to 0.08698	No	ns	0.5743	B-D
HWP day 8 PHA content vs. HWP day 20 PHA content	-0.06000	-0.2120 to 0.09198	No	ns	0.6408	B-E
HWP day 8 PHA content vs. HWP day 24 PHA content	-0.02500	-0.1770 to 0.1270	No	ns	0.9812	B-F
HWP day 12 PHA content vs. HWP day 16 PHA content	-0.06000	-0.2120 to 0.09198	No	ns	0.6408	C-D
HWP day 12 PHA content vs. HWP day 20 PHA content	-0.05500	-0.2070 to 0.09698	No	ns	0.7078	C-E
HWP day 12 PHA content vs. HWP day 24 PHA content	-0.02000	-0.1720 to 0.1320	No	ns	0.9929	C-F
HWP day 16 PHA content vs. HWP day 20 PHA content	0.005000	-0.1470 to 0.1570	No	ns	>0.9999	D-E
HWP day 16 PHA content vs. HWP day 24 PHA content	0.04000	-0.1120 to 0.1920	No	ns	0.8856	D-F
HWP day 20 PHA content vs. HWP day 24 PHA content	0.03500	-0.1170 to 0.1870	No	ns	0.9285	E-F

Test details	**Mean 1**	**Mean 2**	**Mean Diff.**	**SE of diff.**	**n1**	**n2**	**q**	**DF**
HWP day 4 PHA content vs. HWP day 8 PHA content	0.5100	0.5900	-0.08000	0.03819	2	2	2.963	6
HWP day 4 PHA content vs. HWP day 12 PHA content	0.5100	0.5950	-0.08500	0.03819	2	2	3.148	6
HWP day 4 PHA content vs. HWP day 16 PHA content	0.5100	0.6550	-0.1450	0.03819	2	2	5.370	6
HWP day 4 PHA content vs. HWP day 20 PHA content	0.5100	0.6500	-0.1400	0.03819	2	2	5.185	6
HWP day 4 PHA content vs. HWP day 24 PHA content	0.5100	0.6150	-0.1050	0.03819	2	2	3.888	6
HWP day 8 PHA content vs. HWP day 12 PHA content	0.5900	0.5950	-0.005000	0.03819	2	2	0.1852	6
HWP day 8 PHA content vs. HWP day 16 PHA content	0.5900	0.6550	-0.06500	0.03819	2	2	2.407	6
HWP day 8 PHA content vs. HWP day 20 PHA content	0.5900	0.6500	-0.06000	0.03819	2	2	2.222	6
HWP day 8 PHA content vs. HWP day 24 PHA content	0.5900	0.6150	-0.02500	0.03819	2	2	0.9258	6
HWP day 12 PHA content vs. HWP day 16 PHA content	0.5950	0.6550	-0.06000	0.03819	2	2	2.222	6
HWP day 12 PHA content vs. HWP day 20 PHA content	0.5950	0.6500	-0.05500	0.03819	2	2	2.037	6
HWP day 12 PHA content vs. HWP day 24 PHA content	0.5950	0.6150	-0.02000	0.03819	2	2	0.7407	6
HWP day 16 PHA content vs. HWP day 20 PHA content	0.6550	0.6500	0.005000	0.03819	2	2	0.1852	6
HWP day 16 PHA content vs. HWP day 24 PHA content	0.6550	0.6150	0.04000	0.03819	2	2	1.481	6
HWP day 20 PHA content vs. HWP day 24 PHA content	0.6500	0.6150	0.03500	0.03819	2	2	1.296	6

Appendix E. Chapter 7 statistical analysis reports

Table E.1 One-way ANOVA and pairwise Tukey test for final CDM concentrations using 20-day HRT CSTR with hydrolyzed DLP feed at different organic loading rates (as illustrated in Table 7.1).

Table Analyzed	Col: One-way ANOVA
Data sets analyzed	A-E
ANOVA summary	
F	8.156
P value	0.0034
P value summary	**
Significant diff. among means (P < 0.05)?	Yes
R squared	0.7654

Number of families	1							
Number of comparisons per family	10							
Alpha	0.05							
Tukey's multiple comparisons test	**Mean Diff.**	**95.00% CI of diff.**	**Below threshold?**	**Summary**	**Adjusted P Value**			
25 g/l CDM vs. 30 g/l 1 CDM	-0.5267	-0.9526 to -0.1007	Yes	*	0.0150	A-B		
25 g/l CDM vs. 30 g/l 2 CDM	0.01667	-0.4093 to 0.4426	No	ns	>0.9999	A-C		
25 g/l CDM vs. 40 g/l CDM	0.003333	-0.4226 to 0.4293	No	ns	>0.9999	A-D		
25 g/l CDM vs. 40 g/l glucose CDM	-0.4000	-0.8260 to 0.02595	No	ns	0.0682	A-E		
30 g/l 1 CDM vs. 30 g/l 2 CDM	0.5433	0.1174 to 0.9693	Yes	*	0.0124	B-C		
30 g/l 1 CDM vs. 40 g/l CDM	0.5300	0.1040 to 0.9560	Yes	*	0.0145	B-D		
30 g/l 1 CDM vs. 40 g/l glucose CDM	0.1267	-0.2993 to 0.5526	No	ns	0.8589	B-E		
30 g/l 2 CDM vs. 40 g/l CDM	-0.01333	-0.4393 to 0.4126	No	ns	>0.9999	C-D		
30 g/l 2 CDM vs. 40 g/l glucose CDM	-0.4167	-0.8426 to 0.009285	No	ns	0.0559	C-E		
40 g/l CDM vs. 40 g/l glucose CDM	-0.4033	-0.8293 to 0.02262	No	ns	0.0655	D-E		
Test details	**Mean 1**	**Mean 2**	**Mean Diff.**	**SE of diff.**	**n1**	**n2**	**q**	**DF**
25 g/l CDM vs. 30 g/l 1 CDM	6.587	7.113	-0.5267	0.1294	3	3	5.755	10
25 g/l CDM vs. 30 g/l 2 CDM	6.587	6.570	0.01667	0.1294	3	3	0.1821	10
25 g/l CDM vs. 40 g/l CDM	6.587	6.583	0.003333	0.1294	3	3	0.03642	10
25 g/l CDM vs. 40 g/l glucose CDM	6.587	6.987	-0.4000	0.1294	3	3	4.371	10
30 g/l 1 CDM vs. 30 g/l 2 CDM	7.113	6.570	0.5433	0.1294	3	3	5.937	10
30 g/l 1 CDM vs. 40 g/l CDM	7.113	6.583	0.5300	0.1294	3	3	5.791	10
30 g/l 1 CDM vs. 40 g/l glucose CDM	7.113	6.987	0.1267	0.1294	3	3	1.384	10
30 g/l 2 CDM vs. 40 g/l CDM	6.570	6.583	-0.01333	0.1294	3	3	0.1457	10
30 g/l 2 CDM vs. 40 g/l glucose CDM	6.570	6.987	-0.4167	0.1294	3	3	4.553	10
40 g/l CDM vs. 40 g/l glucose CDM	6.583	6.987	-0.4033	0.1294	3	3	4.407	10

Table E.2 One-way ANOVA and pairwise Tukey test for final PHA concentrations using 20-day HRT CSTR with hydrolyzed DLP feed at different organic loading rates (as illustrated in Table 7.1).

Table Analyzed	Col: One-way ANOVA
Data sets analyzed	A-E
ANOVA summary	
F	15.96
P value	0.0002
P value summary	***
Significant diff. among means (P < 0.05)?	Yes
R squared	0.8646

Number of families	1							
Number of comparisons per family	10							
Alpha	0.05							
Tukey's multiple comparisons test	**Mean Diff.**	**95.00% CI of diff.**	**Below threshold?**	**Summary**	**Adjusted P Value**			
25 g/l PHA vs. 30 g/l 1 PHA	0.08667	-0.3560 to 0.5293	No	ns	0.9639	A-B		
25 g/l PHA vs. 30 g/l 2 PHA	0.6767	0.2340 to 1.119	Yes	**	0.0036	A-C		
25 g/l PHA vs. 40 g/l PHA	0.8467	0.4040 to 1.289	Yes	***	0.0007	A-D		
25 g/l PHA vs. 40 g/l glucose PHA	0.1700	-0.2726 to 0.6126	No	ns	0.7172	A-E		
30 g/l 1 PHA vs. 30 g/l 2 PHA	0.5900	0.1474 to 1.033	Yes	**	0.0093	B-C		
30 g/l 1 PHA vs. 40 g/l PHA	0.7600	0.3174 to 1.203	Yes	**	0.0015	B-D		
30 g/l 1 PHA vs. 40 g/l glucose PHA	0.08333	-0.3593 to 0.5260	No	ns	0.9685	B-E		
30 g/l 2 PHA vs. 40 g/l PHA	0.1700	-0.2726 to 0.6126	No	ns	0.7172	C-D		
30 g/l 2 PHA vs. 40 g/l glucose PHA	-0.5067	-0.9493 to -0.06403	Yes	*	0.0239	C-E		
40 g/l PHA vs. 40 g/l glucose PHA	-0.6767	-1.119 to -0.2340	Yes	**	0.0036	D-E		
Test details	**Mean 1**	**Mean 2**	**Mean Diff.**	**SE of diff.**	**n1**	**n2**	**q**	**DF**
25 g/l PHA vs. 30 g/l 1 PHA	2.087	2.000	0.08667	0.1345	3	3	0.9113	10
25 g/l PHA vs. 30 g/l 2 PHA	2.087	1.410	0.6767	0.1345	3	3	7.115	10
25 g/l PHA vs. 40 g/l PHA	2.087	1.240	0.8467	0.1345	3	3	8.903	10
25 g/l PHA vs. 40 g/l glucose PHA	2.087	1.917	0.1700	0.1345	3	3	1.788	10
30 g/l 1 PHA vs. 30 g/l 2 PHA	2.000	1.410	0.5900	0.1345	3	3	6.204	10
30 g/l 1 PHA vs. 40 g/l PHA	2.000	1.240	0.7600	0.1345	3	3	7.991	10
30 g/l 1 PHA vs. 40 g/l glucose PHA	2.000	1.917	0.08333	0.1345	3	3	0.8762	10
30 g/l 2 PHA vs. 40 g/l PHA	1.410	1.240	0.1700	0.1345	3	3	1.788	10
30 g/l 2 PHA vs. 40 g/l glucose PHA	1.410	1.917	-0.5067	0.1345	3	3	5.328	10
40 g/l PHA vs. 40 g/l glucose PHA	1.240	1.917	-0.6767	0.1345	3	3	7.115	10

Table E.3 One-way ANOVA and pairwise Tukey test for final PHA content using 20-day HRT CSTR with hydrolyzed DLP feed at different organic loading rates (as illustrated in Table 7.1).

Table Analyzed	Col: One-way ANOVA
Data sets analyzed	A-E
ANOVA summary	
F	23.65
P value	<0.0001
P value summary	****
Significant diff. among means (P < 0.05)?	Yes
R squared	0.9044

Number of families	1							
Number of comparisons per family	10							
Alpha	0.05							
Tukey's multiple comparisons test	**Mean Diff.**	**95.00% CI of diff.**	**Below threshold?**	**Summary**	**Adjusted P Value**			
25 g/l PHA content vs. 30 g/l 1 PHA content	0.04000	-0.01051 to 0.09051	No	ns	0.1424	A-B		
25 g/l PHA content vs. 30 g/l 2 PHA content	0.1033	0.05282 to 0.1538	Yes	***	0.0004	A-C		
25 g/l PHA content vs. 40 g/l PHA content	0.1300	0.07949 to 0.1805	Yes	****	<0.0001	A-D		
25 g/l PHA content vs. 40 g/l glucose PHA content	0.04000	-0.01051 to 0.09051	No	ns	0.1424	A-E		
30 g/l 1 PHA content vs. 30 g/l 2 PHA content	0.06333	0.01282 to 0.1138	Yes	*	0.0138	B-C		
30 g/l 1 PHA content vs. 40 g/l PHA content	0.09000	0.03949 to 0.1405	Yes	**	0.0012	B-D		
30 g/l 1 PHA content vs. 40 g/l glucose PHA content	0.000	-0.05051 to 0.05051	No	ns	>0.9999	B-E		
30 g/l 2 PHA content vs. 40 g/l PHA content	0.02667	-0.02384 to 0.07718	No	ns	0.4555	C-D		
30 g/l 2 PHA content vs. 40 g/l glucose PHA content	-0.06333	-0.1138 to -0.01282	Yes	*	0.0138	C-E		
40 g/l PHA content vs. 40 g/l glucose PHA content	-0.09000	-0.1405 to -0.03949	Yes	**	0.0012	D-E		
Test details	**Mean 1**	**Mean 2**	**Mean Diff.**	**SE of diff.**	**n1**	**n2**	**q**	**DF**
25 g/l PHA content vs. 30 g/l 1 PHA content	0.3167	0.2767	0.04000	0.01535	3	3	3.686	10
25 g/l PHA content vs. 30 g/l 2 PHA content	0.3167	0.2133	0.1033	0.01535	3	3	9.522	10
25 g/l PHA content vs. 40 g/l PHA content	0.3167	0.1867	0.1300	0.01535	3	3	11.98	10
25 g/l PHA content vs. 40 g/l glucose PHA content	0.3167	0.2767	0.04000	0.01535	3	3	3.686	10
30 g/l 1 PHA content vs. 30 g/l 2 PHA content	0.2767	0.2133	0.06333	0.01535	3	3	5.836	10
30 g/l 1 PHA content vs. 40 g/l PHA content	0.2767	0.1867	0.09000	0.01535	3	3	8.293	10
30 g/l 1 PHA content vs. 40 g/l glucose PHA content	0.2767	0.2767	0.000	0.01535	3	3	0.000	10
30 g/l 2 PHA content vs. 40 g/l PHA content	0.2133	0.1867	0.02667	0.01535	3	3	2.457	10
30 g/l 2 PHA content vs. 40 g/l glucose PHA content	0.2133	0.2767	-0.06333	0.01535	3	3	5.836	10
40 g/l PHA content vs. 40 g/l glucose PHA content	0.1867	0.2767	-0.09000	0.01535	3	3	8.293	10

Table E.4 Unpaired t-test for final CDM concentration using 20-day HRT CSTR effluent as inoculum at different times with glucose feedstock (as illustrated in Table Figure 7.14).

Table Analyzed	Unpaired t-test
Column B	Glucose 2 CDM
vs.	vs.
Column A	Glucose 1 CDM
Unpaired t test	
P value	0.0111
P value summary	*
Significantly different (P < 0.05)?	Yes
One- or two-tailed P value?	Two-tailed
t, df	t=9.400, df=2

Table E.5 Unpaired t-test for final PHA concentration using 20-day HRT CSTR effluent as inoculum at different times with glucose feedstock (as illustrated in Figure 7.14).

Table Analyzed	Unpaired t-test
Column B	Glucose 2 PHA
vs.	vs.
Column A	Glucose 1 PHA
Unpaired t test	
P value	0.0348
P value summary	*
Significantly different (P < 0.05)?	Yes
One- or two-tailed P value?	Two-tailed
t, df	t=5.217, df=2

Table E.6 Unpaired t-test for PHA content using 20-day HRT CSTR effluent as inoculum at different times with glucose feedstock (as illustrated in Figure 7.14).

Table Analyzed	Unpaired t-test
Column B	Glucose 2 PHA content
vs.	vs.
Column A	Glucose 1 PHA content
Unpaired t test	
P value	0.9242
P value summary	ns
Significantly different (P < 0.05)?	No
One- or two-tailed P value?	Two-tailed
t, df	t=0.1075, df=2

Appendix F. Chapter 8 statistical analysis reports

Table F.1 One-way ANOVA and pairwise Tukey test for final cell dry mass (CDM) concentration during the successive growth with galactose substrate (as illustrated in Figure 8.5).

Table Analyzed	One-way ANOVA
Data sets analyzed	A-E
ANOVA summary	
F	40.64
P value	<0.0001
P value summary	****
Significant diff. among means (P < 0.05)?	Yes
R squared	0.9421

Number of families	1					
Number of comparisons per family	10					
Alpha	0.05					
Tukey's multiple comparisons test	**Mean Diff.**	**95.00% CI of diff.**	**Below threshold?**	**Summary**	**Adjusted P Value**	
First batch CDM vs. Second batch CDM	-0.8200	-1.348 to -0.2918	Yes	**	0.0033	A-B
First batch CDM vs. Third batch CDM	-1.487	-2.015 to -0.9585	Yes	****	<0.0001	A-C
First batch CDM vs. Fourth batch CDM	-1.633	-2.162 to -1.105	Yes	****	<0.0001	A-D
First batch CDM vs. Fifth batch CDM	-1.713	-2.242 to -1.185	Yes	****	<0.0001	A-E
Second batch CDM vs. Third batch CDM	-0.6667	-1.195 to -0.1385	Yes	*	0.0132	B-C
Second batch CDM vs. Fourth batch CDM	-0.8133	-1.342 to -0.2851	Yes	**	0.0034	B-D
Second batch CDM vs. Fifth batch CDM	-0.8933	-1.422 to -0.3651	Yes	**	0.0017	B-E
Third batch CDM vs. Fourth batch CDM	-0.1467	-0.6749 to 0.3815	No	ns	0.8853	C-D
Third batch CDM vs. Fifth batch CDM	-0.2267	-0.7549 to 0.3015	No	ns	0.6342	C-E
Fourth batch CDM vs. Fifth batch CDM	-0.08000	-0.6082 to 0.4482	No	ns	0.9857	D-E

Test details	**Mean 1**	**Mean 2**	**Mean Diff.**	**SE of diff.**	**n1**	**n2**	**q**	**DF**
First batch CDM vs. Second batch CDM	1.287	2.107	-0.8200	0.1605	3	3	7.225	10
First batch CDM vs. Third batch CDM	1.287	2.773	-1.487	0.1605	3	3	13.10	10
First batch CDM vs. Fourth batch CDM	1.287	2.920	-1.633	0.1605	3	3	14.39	10
First batch CDM vs. Fifth batch CDM	1.287	3.000	-1.713	0.1605	3	3	15.10	10
Second batch CDM vs. Third batch CDM	2.107	2.773	-0.6667	0.1605	3	3	5.874	10
Second batch CDM vs. Fourth batch CDM	2.107	2.920	-0.8133	0.1605	3	3	7.167	10
Second batch CDM vs. Fifth batch CDM	2.107	3.000	-0.8933	0.1605	3	3	7.871	10
Third batch CDM vs. Fourth batch CDM	2.773	2.920	-0.1467	0.1605	3	3	1.292	10
Third batch CDM vs. Fifth batch CDM	2.773	3.000	-0.2267	0.1605	3	3	1.997	10
Fourth batch CDM vs. Fifth batch CDM	2.920	3.000	-0.08000	0.1605	3	3	0.7049	10

Table F.2 One-way ANOVA and pairwise Tukey test for cell dry mass (CDM) yield during the successive growth with galactose substrate (as illustrated in Figure 8.5).

Table Analyzed	One-way ANOVA
Data sets analyzed	A-E
ANOVA summary	
F	8.539
P value	0.0029
P value summary	**
Significant diff. among means (P < 0.05)?	Yes
R squared	0.7735

Number of families	1					
Number of comparisons per family	10					
Alpha	0.05					
Tukey's multiple comparisons test	**Mean Diff.**	**95.00% CI of diff.**	**Below threshold?**	**Summary**	**Adjusted P Value**	
First batch CDM yield vs. Second batch CDM yield	0.07333	0.007512 to 0.1392	Yes	*	0.0279	A-B
First batch CDM yield vs. Third batch CDM yield	0.1067	0.04085 to 0.1725	Yes	**	0.0024	A-C
First batch CDM yield vs. Fourth batch CDM yield	0.09000	0.02418 to 0.1558	Yes	**	0.0079	A-D
First batch CDM yield vs. Fifth batch CDM yield	0.08333	0.01751 to 0.1492	Yes	*	0.0130	A-E
Second batch CDM yield vs. Third batch CDM yield	0.03333	-0.03249 to 0.09915	No	ns	0.4927	B-C
Second batch CDM yield vs. Fourth batch CDM yield	0.01667	-0.04915 to 0.08249	No	ns	0.9141	B-D
Second batch CDM yield vs. Fifth batch CDM yield	0.01000	-0.05582 to 0.07582	No	ns	0.9855	B-E
Third batch CDM yield vs. Fourth batch CDM yield	-0.01667	-0.08249 to 0.04915	No	ns	0.9141	C-D
Third batch CDM yield vs. Fifth batch CDM yield	-0.02333	-0.08915 to 0.04249	No	ns	0.7692	C-E
Fourth batch CDM yield vs. Fifth batch CDM yield	-0.006667	-0.07249 to 0.05915	No	ns	0.9969	D-E

Test details	**Mean 1**	**Mean 2**	**Mean Diff.**	**SE of diff.**	**n1**	**n2**	**q**	**DF**
First batch CDM yield vs. Second batch CDM yield	0.3533	0.2800	0.07333	0.02000	3	3	5.185	10
First batch CDM yield vs. Third batch CDM yield	0.3533	0.2467	0.1067	0.02000	3	3	7.542	10
First batch CDM yield vs. Fourth batch CDM yield	0.3533	0.2633	0.09000	0.02000	3	3	6.364	10
First batch CDM yield vs. Fifth batch CDM yield	0.3533	0.2700	0.08333	0.02000	3	3	5.893	10
Second batch CDM yield vs. Third batch CDM yield	0.2800	0.2467	0.03333	0.02000	3	3	2.357	10
Second batch CDM yield vs. Fourth batch CDM yield	0.2800	0.2633	0.01667	0.02000	3	3	1.179	10
Second batch CDM yield vs. Fifth batch CDM yield	0.2800	0.2700	0.01000	0.02000	3	3	0.7071	10
Third batch CDM yield vs. Fourth batch CDM yield	0.2467	0.2633	-0.01667	0.02000	3	3	1.179	10
Third batch CDM yield vs. Fifth batch CDM yield	0.2467	0.2700	-0.02333	0.02000	3	3	1.650	10
Fourth batch CDM yield vs. Fifth batch CDM yield	0.2633	0.2700	-0.006667	0.02000	3	3	0.4714	10

Table F.3 One-way ANOVA and pairwise Tukey test for specific growth rate during the successive growth with galactose substrate (as illustrated in Figure 8.6).

Table Analyzed	One-way ANOVA
Data sets analyzed	A-E
ANOVA summary	
F	36.20
P value	<0.0001
P value summary	****
Significant diff. among means (P < 0.05)?	Yes
R squared	0.9354

Number of families	1					
Number of comparisons per family	10					
Alpha	0.05					
Tukey's multiple comparisons test	**Mean Diff.**	**95.00% CI of diff.**	**Below threshold?**	**Summary**	**Adjusted P Value**	
First batch u vs. Second batch u	0.0003333	-0.002839 to 0.003505	No	ns	0.9964	A-B
First batch u vs. Third batch u	0.0006667	-0.002505 to 0.003839	No	ns	0.9538	A-C
First batch u vs. Fourth batch u	-0.006500	-0.009672 to -0.003328	Yes	***	0.0004	A-D
First batch u vs. Fifth batch u	-0.007700	-0.01087 to -0.004528	Yes	****	<0.0001	A-E
Second batch u vs. Third batch u	0.0003333	-0.002839 to 0.003505	No	ns	0.9964	B-C
Second batch u vs. Fourth batch u	-0.006833	-0.01001 to -0.003661	Yes	***	0.0003	B-D
Second batch u vs. Fifth batch u	-0.008033	-0.01121 to -0.004861	Yes	****	<0.0001	B-E
Third batch u vs. Fourth batch u	-0.007167	-0.01034 to -0.003995	Yes	***	0.0002	C-D
Third batch u vs. Fifth batch u	-0.008367	-0.01154 to -0.005195	Yes	****	<0.0001	C-E
Fourth batch u vs. Fifth batch u	-0.001200	-0.004372 to 0.001972	No	ns	0.7275	D-E

Test details	**Mean 1**	**Mean 2**	**Mean Diff.**	**SE of diff.**	**n1**	**n2**	**q**	**DF**
First batch u vs. Second batch u	0.01080	0.01047	0.0003333	0.0009638	3	3	0.4891	10
First batch u vs. Third batch u	0.01080	0.01013	0.0006667	0.0009638	3	3	0.9782	10
First batch u vs. Fourth batch u	0.01080	0.01730	-0.006500	0.0009638	3	3	9.538	10
First batch u vs. Fifth batch u	0.01080	0.01850	-0.007700	0.0009638	3	3	11.30	10
Second batch u vs. Third batch u	0.01047	0.01013	0.0003333	0.0009638	3	3	0.4891	10
Second batch u vs. Fourth batch u	0.01047	0.01730	-0.006833	0.0009638	3	3	10.03	10
Second batch u vs. Fifth batch u	0.01047	0.01850	-0.008033	0.0009638	3	3	11.79	10
Third batch u vs. Fourth batch u	0.01013	0.01730	-0.007167	0.0009638	3	3	10.52	10
Third batch u vs. Fifth batch u	0.01013	0.01850	-0.008367	0.0009638	3	3	12.28	10
Fourth batch u vs. Fifth batch u	0.01730	0.01850	-0.001200	0.0009638	3	3	1.761	10

Table F.4 One-way ANOVA and pairwise Tukey test for final PHA concentration during the successive growth with galactose substrate (as illustrated in Figure 8.7).

Table Analyzed	One-way ANOVA
Data sets analyzed	A-E
ANOVA summary	
F	16.70
P value	0.0002
P value summary	***
Significant diff. among means (P < 0.05)?	Yes
R squared	0.8698

Number of families	1					
Number of comparisons per family	10					
Alpha	0.05					
Tukey's multiple comparisons test	**Mean Diff.**	**95.00% CI of diff.**	**Below threshold?**	**Summary**	**Adjusted P Value**	
First batch PHA vs. Second batch PHA	-0.4900	-0.8823 to -0.09770	Yes	*	0.0141	A-B
First batch PHA vs. Third batch PHA	-0.6300	-1.022 to -0.2377	Yes	**	0.0025	A-C
First batch PHA vs. Fourth batch PHA	-0.7233	-1.116 to -0.3310	Yes	***	0.0009	A-D
First batch PHA vs. Fifth batch PHA	-0.9133	-1.306 to -0.5210	Yes	***	0.0001	A-E
Second batch PHA vs. Third batch PHA	-0.1400	-0.5323 to 0.2523	No	ns	0.7652	B-C
Second batch PHA vs. Fourth batch PHA	-0.2333	-0.6256 to 0.1590	No	ns	0.3500	B-D
Second batch PHA vs. Fifth batch PHA	-0.4233	-0.8156 to -0.03103	Yes	*	0.0334	B-E
Third batch PHA vs. Fourth batch PHA	-0.09333	-0.4856 to 0.2990	No	ns	0.9299	C-D
Third batch PHA vs. Fifth batch PHA	-0.2833	-0.6756 to 0.1090	No	ns	0.1988	C-E
Fourth batch PHA vs. Fifth batch PHA	-0.1900	-0.5823 to 0.2023	No	ns	0.5322	D-E

Test details	**Mean 1**	**Mean 2**	**Mean Diff.**	**SE of diff.**	**n1**	**n2**	**q**	**DF**
First batch PHA vs. Second batch PHA	0.7333	1.223	-0.4900	0.1192	3	3	5.813	10
First batch PHA vs. Third batch PHA	0.7333	1.363	-0.6300	0.1192	3	3	7.474	10
First batch PHA vs. Fourth batch PHA	0.7333	1.457	-0.7233	0.1192	3	3	8.582	10
First batch PHA vs. Fifth batch PHA	0.7333	1.647	-0.9133	0.1192	3	3	10.84	10
Second batch PHA vs. Third batch PHA	1.223	1.363	-0.1400	0.1192	3	3	1.661	10
Second batch PHA vs. Fourth batch PHA	1.223	1.457	-0.2333	0.1192	3	3	2.768	10
Second batch PHA vs. Fifth batch PHA	1.223	1.647	-0.4233	0.1192	3	3	5.022	10
Third batch PHA vs. Fourth batch PHA	1.363	1.457	-0.09333	0.1192	3	3	1.107	10
Third batch PHA vs. Fifth batch PHA	1.363	1.647	-0.2833	0.1192	3	3	3.361	10
Fourth batch PHA vs. Fifth batch PHA	1.457	1.647	-0.1900	0.1192	3	3	2.254	10

Table F.5 One-way ANOVA and pairwise Tukey test for PHA yield during the successive growth with galactose substrate (as illustrated in Figure 8.7).

Table Analyzed	One-way ANOVA
Data sets analyzed	A-E
ANOVA summary	
F	14.15
P value	0.0004
P value summary	***
Significant diff. among means (P < 0.05)?	Yes
R squared	0.8499

Number of families	1					
Number of comparisons per family	10					
Alpha	0.05					
Tukey's multiple comparisons test	**Mean Diff.**	**95.00% CI of diff.**	**Below threshold?**	**Summary**	**Adjusted P Value**	
First batch PHA yield vs. Second batch PHA yield	0.04667	0.001170 to 0.09216	Yes	*	0.0438	A-B
First batch PHA yield vs. Third batch PHA yield	0.09333	0.04784 to 0.1388	Yes	***	0.0004	A-C
First batch PHA yield vs. Fourth batch PHA yield	0.08333	0.03784 to 0.1288	Yes	***	0.0009	A-D
First batch PHA yield vs. Fifth batch PHA yield	0.06333	0.01784 to 0.1088	Yes	**	0.0070	A-E
Second batch PHA yield vs. Third batch PHA yield	0.04667	0.001170 to 0.09216	Yes	*	0.0438	B-C
Second batch PHA yield vs. Fourth batch PHA yield	0.03667	-0.008830 to 0.08216	No	ns	0.1329	B-D
Second batch PHA yield vs. Fifth batch PHA yield	0.01667	-0.02883 to 0.06216	No	ns	0.7487	B-E
Third batch PHA yield vs. Fourth batch PHA yield	-0.01000	-0.05550 to 0.03550	No	ns	0.9462	C-D
Third batch PHA yield vs. Fifth batch PHA yield	-0.03000	-0.07550 to 0.01550	No	ns	0.2650	C-E
Fourth batch PHA yield vs. Fifth batch PHA yield	-0.02000	-0.06550 to 0.02550	No	ns	0.6147	D-E

Test details	**Mean 1**	**Mean 2**	**Mean Diff.**	**SE of diff.**	**n1**	**n2**	**q**	**DF**
First batch PHA yield vs. Second batch PHA yield	0.2167	0.1700	0.04667	0.01382	3	3	4.774	10
First batch PHA yield vs. Third batch PHA yield	0.2167	0.1233	0.09333	0.01382	3	3	9.548	10
First batch PHA yield vs. Fourth batch PHA yield	0.2167	0.1333	0.08333	0.01382	3	3	8.525	10
First batch PHA yield vs. Fifth batch PHA yield	0.2167	0.1533	0.06333	0.01382	3	3	6.479	10
Second batch PHA yield vs. Third batch PHA yield	0.1700	0.1233	0.04667	0.01382	3	3	4.774	10
Second batch PHA yield vs. Fourth batch PHA yield	0.1700	0.1333	0.03667	0.01382	3	3	3.751	10
Second batch PHA yield vs. Fifth batch PHA yield	0.1700	0.1533	0.01667	0.01382	3	3	1.705	10
Third batch PHA yield vs. Fourth batch PHA yield	0.1233	0.1333	-0.01000	0.01382	3	3	1.023	10
Third batch PHA yield vs. Fifth batch PHA yield	0.1233	0.1533	-0.03000	0.01382	3	3	3.069	10
Fourth batch PHA yield vs. Fifth batch PHA yield	0.1333	0.1533	-0.02000	0.01382	3	3	2.046	10

Table F.6 One-way ANOVA and pairwise Tukey test for PHA content during the successive growth with galactose substrate (as illustrated in Figure 8.8).

Table Analyzed	One-way ANOVA
Data sets analyzed	A-E
ANOVA summary	
F	3.323
P value	0.0562
P value summary	ns
Significant diff. among means (P < 0.05)?	No
R squared	0.5707

Number of families	1					
Number of comparisons per family	10					
Alpha	0.05					
Tukey's multiple comparisons test	**Mean Diff.**	**95.00% CI of diff.**	**Below threshold?**	**Summary**	**Adjusted P Value**	
First batch PHA content vs. Second batch PHA content	-0.01000	-0.1164 to 0.09636	No	ns	0.9977	A-B
First batch PHA content vs. Third batch PHA content	0.08000	-0.02636 to 0.1864	No	ns	0.1725	A-C
First batch PHA content vs. Fourth batch PHA content	0.07333	-0.03303 to 0.1797	No	ns	0.2313	A-D
First batch PHA content vs. Fifth batch PHA content	0.02000	-0.08636 to 0.1264	No	ns	0.9687	A-E
Second batch PHA content vs. Third batch PHA content	0.09000	-0.01636 to 0.1964	No	ns	0.1089	B-C
Second batch PHA content vs. Fourth batch PHA content	0.08333	-0.02303 to 0.1897	No	ns	0.1483	B-D
Second batch PHA content vs. Fifth batch PHA content	0.03000	-0.07636 to 0.1364	No	ns	0.8796	B-E
Third batch PHA content vs. Fourth batch PHA content	-0.006667	-0.1130 to 0.09969	No	ns	0.9995	C-D
Third batch PHA content vs. Fifth batch PHA content	-0.06000	-0.1664 to 0.04636	No	ns	0.3963	C-E
Fourth batch PHA content vs. Fifth batch PHA content	-0.05333	-0.1597 to 0.05303	No	ns	0.5015	D-E

Test details	**Mean 1**	**Mean 2**	**Mean Diff.**	**SE of diff.**	**n1**	**n2**	**q**	**DF**
First batch PHA content vs. Second batch PHA content	0.5700	0.5800	-0.01000	0.03232	3	3	0.4376	10
First batch PHA content vs. Third batch PHA content	0.5700	0.4900	0.08000	0.03232	3	3	3.501	10
First batch PHA content vs. Fourth batch PHA content	0.5700	0.4967	0.07333	0.03232	3	3	3.209	10
First batch PHA content vs. Fifth batch PHA content	0.5700	0.5500	0.02000	0.03232	3	3	0.8752	10
Second batch PHA content vs. Third batch PHA content	0.5800	0.4900	0.09000	0.03232	3	3	3.938	10
Second batch PHA content vs. Fourth batch PHA content	0.5800	0.4967	0.08333	0.03232	3	3	3.647	10
Second batch PHA content vs. Fifth batch PHA content	0.5800	0.5500	0.03000	0.03232	3	3	1.313	10
Third batch PHA content vs. Fourth batch PHA content	0.4900	0.4967	-0.006667	0.03232	3	3	0.2917	10
Third batch PHA content vs. Fifth batch PHA content	0.4900	0.5500	-0.06000	0.03232	3	3	2.626	10
Fourth batch PHA content vs. Fifth batch PHA content	0.4967	0.5500	-0.05333	0.03232	3	3	2.334	10